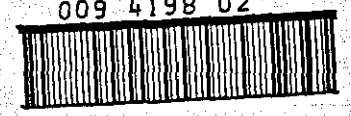

Characterisation and use of Radiotracers in Studies of Inflammatory Tissue and Opioid Binding Sites.

by

Andrew John Lawrence

A Doctoral Thesis submitted in partial fulfilment of the requirements for the award of Doctor of Philosophy of Loughborough University of Technology.

April 1990

Characterisation and use of Radiotracers in Studies of Inflammatory Tissue and Opioid Binding Sites.

By Andrew John Lawrence.

Key Words: Imaging, Technetium, Porphyrin, [3H] Opioids, Opioid binding sites, Receptors.

The thesis is presented in two parts, part one concerns the synthesis and biodistribution of technetium-porphyrin complexes: A series of compounds with the general formula TcO(Porhyrin)OAc and TcO(Phthalocyanine)OPh have been synthesised via a novel route. The starting material comprised NH_4TcO_4 with acetic acid for the porphyrin and phenol for the phthalocyanine. The compounds have been characterised both qualitatively and quantitatively by infra-red, ultra-violet and mass spectrommetry. Thin layer chromatography (tlc) and electrophoresis have also been employed to further analyse the complexes. Preliminary biodistribution studies have been performed in a model of inflamed tissue. The results suggest that the labelled porphyrins are capable of imaging such tissue. One of the complexes was tested for an ability to accumulate in, and image tumours, however this proved unsuccessful.

Part two concerns the properties of opioid agonist and antagonist binding: A number of opioid antagonists, reportedly selective for a single type of opioid receptor have been characterised in terms of binding profiles at all three opioid sites, namely μ-, δ- and κ-. The binding assays were performed in buffers of differing ionic strength. The compounds norbinaltorphimine, naltrindole and 16-methylcyprenorphine displayed a shift to higher affinity in more physiologically relevant conditions. The reasons for this are discussed in terms of possible intrinsic activity. The antagonists which proved to be selective were further utilised to improve the understanding of opioid binding sites. The unselective radioligand [3H]diprenorphine was employed to label opioid binding sites in both rat and guinea-pig brain. In rat brain, the μ-binding component appeared non-homogeneous to both μ-agonists and antagonists. These findings are discussed in terms of subtypes or different affinity states of the μ-binding site which might exist under the assay conditions. Similarly in guinea-pig brain different binding site affinity states were observed being particularly apparent at μ- and δ-sites by comparison of agonist (DAGOL, DPDPE) and antagonist (CTOP, naltrindole) binding. The κ-site population appeared to be more homogeneous both by competition assay and also in saturation assays. Possible κ-receptor heterogeneity was further studied in the guinea-pig ileum myenteric plexus longitudinal muscle preparation. Four κ-agonists, namely ethylketocyclazocine, U69593, ICI 204448 and dynorphin (1-13) were compared. Schild analysis was performed using naloxone as an antagonist and the results suggest that dynorphin (1-13) may be acting at a different receptor to the other compounds.

CONTENTS

PART ONE:

THE SYNTHESIS AND BIODISTRIBUTION OF TECHNETIUM PORPHYRIN COMPLEXES

LIST OF ABBREVIATIONS

Part One :

OEP	=	1,2,3,4,5,6,7,8–octaethylporphyrin
Pc	=	phthalocyanine
PPIX	=	protoporphyrin IX
TPP	=	α,β,γ,δ–tetraphenylporphyrin
$TPPS_2$	=	α,β,γ,δ–tetraphenylporphyrin disulphonate
t.l.c.	=	thin layer chromatography

Part Two :

ADP	=	adenosine diphosphate
Aib	=	aminoisobutyric acid
C.N.S.	=	central nervous system
CTOP	=	D–Phe–Cys–Tyr–D–Trp–Orn–Thr–Pen–Thr
DADLE	=	Tyr–D–Ala–Gly–Phe–D–Leu
DAGOL	=	Tyr–D–Ala–Gly–MePhe–Gly–ol
DPDPE	=	Tyr–D–Pen–Gly–Phe–D–Pen
EKC	=	ethylketocyclazocine
GPMPLM	=	guinea–pig ileum myenteric plexus longitudinal muscle
GppNHp	=	5'–guanylylimidodiphosphate sodium salt
G protein	=	guanine nucleotide–binding regulatory protein
GTP	=	guanosine triphosphate
NorBNI	=	norbinaltorphimine
Tris	=	(Tris(hydroxymethyl)aminomethane

ACKNOWLEDGEMENTS

I would like to express my gratitude to the following:

Part One:

My supervisor, Dr. J. R. Thornback for his help throughout the project.

Dr. G. D. Zanelli, from the C.R.C. Northwick Park Hospital, without whom the biodistribution studies would have been impossible.

Technical staff for their assistance.

Part Two:

My supervisor, Dr. J. R. Traynor for his help, encouragement and friendship throughout.

Stuart, Diane, Tim and David for companionship in the laboratory. Technical staff for their assistance.

Last but not least Mike and Julie for printing this thesis.

To mum and dad with love,
and to Carol for sharing her life with me.

PART ONE

The Synthesis and Biodistribution of Technetium–Porphyrin Complexes

INTRODUCTION.

1.1 Properties of Technetium-99.

Technetium is a 2nd. row transition element in group VIIa of the Periodic Table, situated in between manganese and rhenium.

Technetium and rhenium are chemically very similar and differ considerably from manganese, despite similarities in the stoichiometries of a few compounds (such as the series MnO_4^-, TcO_4^-, ReO_4^- and the metal carbonyls) [1]. The most stable and characteristic oxidation state for manganese is the II state, for which the chemistry is mainly that of the high-spin Mn^{2+} cation. Technetium and rhenium have little cationic chemistry, form few compounds in the II oxidation state, and have extensive chemistry in the IV and especially V states. The TcO_4^- and ReO_4^- ions are much less oxidising than MnO_4^-. A characteristic of ReIII in its halides is the formation of metal-metal bonds, technetium also does this to some extent whereas Mn forms no such compounds at all.

Technetium has the electronic configuration $1s^2 2s^2 p^6 3s^2 p^6 d^{10} 4s^2 p^6 d^5 5s^2$ and as previously mentioned can exist in various oxidation states (-I to +VII) which represent degrees of electron density:-

low oxidation state - high electron density
high oxidation state - low electron density

To stabilise a low oxidation state use a 'soft' ligand capable of spreading the electron charge for example phosphines, cyanides, isonitriles (π-acid ligands). Conversely to stabilise a high oxidation state use a 'hard'

ligand possessing lone pair electrons or a formal negative charge such as O, Cl^-.

1.2 Tc-99m Radiopharmaceuticals.

Tc-99m is the main radionuclide of choice for diagnostic nuclear medicine [2] due to the following 5 properties:-

1. It has a half-life of 6.02 hours which permits diagnosis over a reasonable period of time without administering an unnecessarily high radiation dose to the patient.

2. The photon energy peak of 142KeV is suited to today's γ-cameras which operate best between 100-200KeV.

3. Generator technology means that Tc-99m is readily available in a sterile solution and in a chemically useful state.

4. Technetium has several oxidation states and stereochemistries available giving a broad and varied co-ordination chemistry.

5. There is no α or β emission and radiation dose from the Tc-99 daughter is minimal.

From the above it is evident that technetium radiopharmaceuticals can contain the technetium in various oxidation states . Some examples are listed below:

1. **DMSA** : dimercaptosuccinic acid [3].

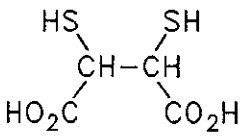

Figure 1. At low pH: TcIV renal imaging agent.
At high pH: TcV tumour imaging agent.

2. **DTPA** : diethyltriamine pentaacetic acid [4].

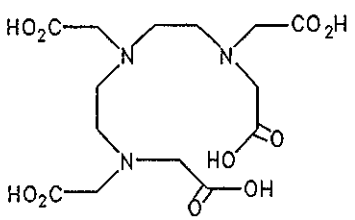

Figure 2. At low pH: TcV and TcIII.
At pH6: TcIV renal function agent.

These radiopharmaceuticals occur in the form of 'kits' where TcO_4^- in a sterile saline solution is introduced into a freeze-dried sample of ligand and reducing agent (usually SnII) whereupon a water soluble Tc complex is formed ready for injection. Tc-99m in the form of TcO_4^- is readily available from generators based on the decay of ^{99}Mo:-

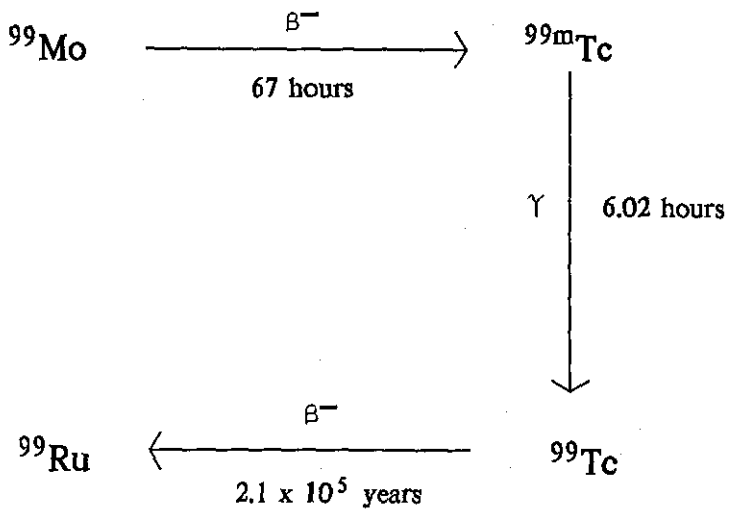

Figure 3.

The generator is basically a column of ammonium molybdate in powder form which, when eluted with saline, gives an isotonic sterile solution of ammonium pertechnetate in accordance with the above decay scheme.

An example of a Tc-99m labelled porphyrin as a radiopharmaceutical has been reported by Zanelli and co-workers [5], who have shown that [99mTc]TcO_4^- reacts with sulphonated tetraphenylporphyrins in citrate buffer with SnII as a reducing agent. This formulation accumulates the radioactivity in sites of inflamed tissue e.g. abscesses, but not in tumours. However, it has proven impossible to synthesise the longer lived Tc-99 complexes by this method.

1.3 Porphyrin Chemistry

1.3.1 Introduction

Porphyrins are of great interest as ligands in biological systems due to the unique nature of the coordination chemistry of these materials [6].

Changes or modification of general porphyrin metabolism are associated with cancer, drug metabolism and specific disease syndromes such as porphyria [7]. [The condition of porphyria results from a metabolic disorder in which porphyrin is retained in the tissue; it is always associated with an excess of porphyrin in the blood (porphyrinaemia) and in the urine (porphyrinuria). The symptoms may be precipitated by certain drugs e.g. sulphonamides. There are various forms of porphyria some of which are genetically determined for example congenital porphyria which is a rare, genetic, erythropoietic porphyria in which there is a defect of haem synthesis in erythrocytes.] Thus, the biological functions of metalloporphyrins have a great deal of importance. Most of the research into metalloporphyrins not only stems from interest in the biological systems to which they are related, but also from the search for new anti-cancer drugs and tumour localising agents [8].

Understanding of the porphyrin system has advanced appreciably in the last two decades [9], to the extent that almost every metal in the periodic table has been coordinated to a porphyrin [10].

1.3.2 Synthesis

There are four main synthetic routes available for the synthesis of metalloporphyrin complexes:-

1. Reaction of a porphyrin with a metallic salt (acetate, halide, oxide) in an acidic or basic medium [11], for example

$$\text{Copper acetate} + \text{porphyrin} \xrightarrow[\text{acetic acid}]{\Delta} \text{Cu(porph)}$$

2. Supplying the metal in the form of carbonyls, carbonyl halides or other organometallic compounds [12] for example

$$Tc_2(CO)_{10} + \text{porphyrin} \xrightarrow[\text{decalin}]{\Delta} (\text{Porph})Tc(CO)_3$$

3. The use of an acetylated complex as a source of metal [13].

4. Reaction in a medium of high dielectric constant such as phenol, N,N-DMF [14], for example

$$FeCl_2 + \text{Porphyrin} \xrightarrow[\text{DMF}]{\Delta} \text{Fe(Porph)Cl}$$

The major problem in the traditional metalloporphyrin syntheses is the difficulty in dissolving both the free porphyrin and the metallic salt simultaneously into the same solution under reactive conditions [11]. This is due to the fact that suitable solvents for the porphyrins in their un-ionised forms are generally poor solvents for simple metallic ions and vice versa. The solubility problem was overcome by using high dielectric solvents which are capable of dissolving both the free porphyrin and the metallic salt. It is general, rapid, convenient, usually gives high yields and requires no special reagents. This method was developed by Adler [14] for the preparation of a number of previously unknown metalloporphyrins such as Hf, Si, Zr, W porphyrins.

1.3.3 Group VIIa

Since technetium is in group VIIa it would be prudent to study known methods for the synthesis of other group VIIa porphyrin complexes before undertaking any major experimental work.

Buchler and Rohbock [15] reported the ability to make Re porphyrins by the reaction of Re_2O_7 with octaethylporphyrin (H_2OEP) in phenol. This yields two products, ReO[OEP](OPh) and the dimeric $[ReO(OEP)]_2O$. Boucher [16] described the synthesis of a Manganese III porphyrin by refluxing a mixture of the divalent metal acetate and porphyrin in glacial acetic acid.

Porphyrin complexes of technetium in high oxidation states have not previously been prepared although Tsutsui has synthesised from $Tc_2(CO)_{10}$ and the porphyrin, $Tc(CO)_3$(HPorph) and also a dimeric species $[Porph][Tc(CO)_3]_2$ which both have the technetium in the +I oxidation state [17]. Figure 4 shows that these complexes have the metal co-ordinated to only three of the N atoms of the porphyrin ring and hence the metal is out of the ring plane.

Figure 4a. (HPorph)$Tc(CO)_3$.

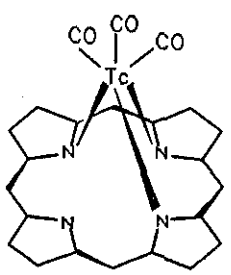

NB. Ring substitution and conjugation omitted for clarity.

Figure 4b. (Porph)[Tc(CO)$_3$]$_2$

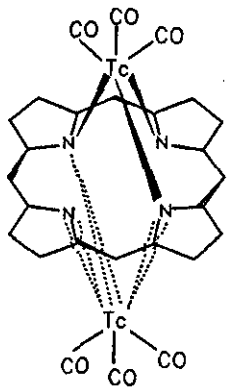

These are both prepared by refluxing $Tc_2(CO)_{10}$ and the porphyrin in decalin and the dimeric complex is obtained by heating two equivalents of the monomer which disproportionates to the dimer and free porphyrin.

1.3.4 Spectroscopy.

The study of porphyrins and metalloporphyrins is based mainly on qualitative and quantitative changes in electronic/optical spectra, since from the early days of study it was known that the parent molecule, or free-base, with two hydrogens in the centre, has a four-banded absorption spectrum distinctly different from the two-banded visible spectrum shown by most metal complexes and by the acid dication (figures 5 and 6) [18]. Therefore one can distinguish a free base type and a metal type spectrum. This difference arises from the fact that the two free-base hydrogens in the centre strongly reduce the conjugated ring symmetry from D_{4h} to D_{2h}, however within the class of metalloporphyrins changes in optical absorption are dependent on the ligands trans to each other in the centre of the ring [19]. All metalloporphyrins show the following characteristic spectra:-

1. **Q bands** : Two visible bands are seen between 500 and 600nm. The lower energy band (sometimes called α) is the electronic origin Q(0,0) of the lowest energy excitedsinglet state. The higher energy band (sometimes called β) includes a mode of vibrational excitation and is denoted Q(1,0) – it is actually a merging of several different vibrations. It was originally identified as a vibration on the basis of the relative constant energy gap between Q(1,0) and Q(0,0) [20]. The Q(1,0) band generally has a molar extinction coefficient in the narrow range of $1.2–2 \times 10^4 M^{-1}cm^{-1}$ [11].

2. **B bands :** An exceedingly intense band (sometimes called the Soret band) appears between 380 and 420nm. It is the origin B(0,0) of the second excited singlet state and has molar extinction generally from $2–4 \times 105 M^{-1}cm^{-1}$.

3. **N,L,M bands :** To the blue of the Soret band, metalloporphyrins generally show a weaker N band at ~325nm and an M band at ~215nm [21]. Between these they often show a weaker L band usually appearing as a shoulder on either the N or M band.

All of these bands are interpreted as (π,π^*) in origin and the Q,B nomenclature was originally given by Platt [20]. B implies a strongly allowed excited state and Q a quasi–allowed one. Later the N,L bands were identified in solution spectra [21] whereas the M band is only seen in vapour [22].

These are features of regular metalloporphyrins however the group VIIa tend to form irregular metalloporphyrin complexes known as hyperporphyrins because they show prominent extra absorption bands ($\varepsilon > 1000 M^{-1}cm^{-1}$) in the region $\lambda > 320$nm where normal metalloporphyrins show only Q,B and N (π,π^*) bands.

Figure 5.

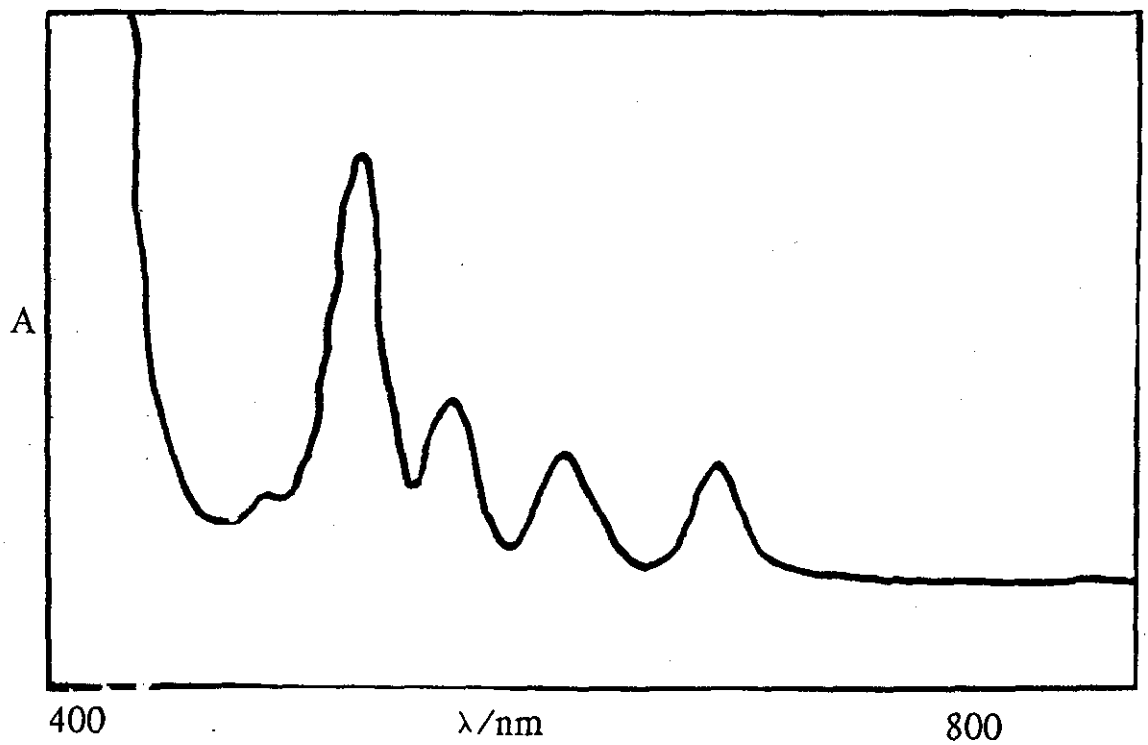

Absorbance (A) is in arbitrary units.

Figure 5 shows a magnification of the visible spectrum of H_2–TPP. This four banded spectrum is typical of free base porphyrins.

Figure 6.

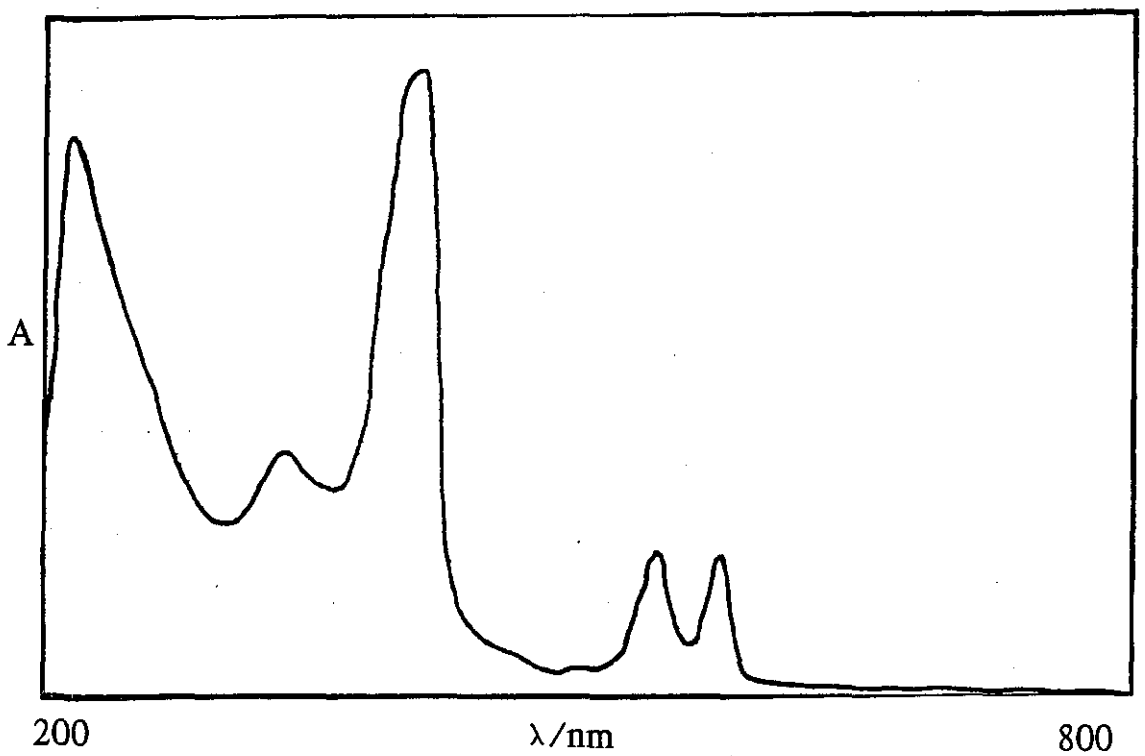

Absorbance (A) is in arbitrary units.

Figure 6. The electronic spectrum of H_4–OEP^{2+} showing the typically two–banded visible region as compared to the four–banded one of a free base porphyrin.

They are further classified into d-type hyperporphyrins which are found with transition metals in configurations of d^m, $1 \leq m \leq 6$, that have relatively stable lower oxidation states. These extra bands are attributed with somewhat uncertainty to charge transfer transitions. Another name for them is alloporphyrins since unlike the usual metalloporphyrins which are red to orange in solution, alloporphyrins are characteristically olive-green or brown [23]. Calvin and co-workers were the first to systematically study the optical spectra of the archetype d-type hyperporphyrin complex of Mn(III) [24]. These studies also included the oxidised and reduced porphyrins, Mn(IV), Mn(II). The spectra of (TPP)Mn(III)Cl has absorptions as follows:-

2 bands between 800-650nm.
2 bands in the normal metalloporphyrin region [Q(0,0) and Q(1,0)] ie 500-600nm.
1 band at ~450nm.
1 band at ~350nm.

The intensity ratio in between the latter two bands is quite variable depending on the metal and substituents on the porphyrin.

The porphyrin complexes of Cu(III), Mn(III), Mo(V), W(V) and Re(V) all show rather similar hyper absorption spectra and fit the pattern defined as d-type hyper quite well.

1.3.5 Medical Uses of Porphyrins.

Free base porphyrins are known to accumulate in tumours but the evidence for metalloporphyrins is not clear [25]. ^{111}In labelled porphyrins are known to accumulate in tumours but for metalloporphyrins there is little or no evidence of preferential tumour uptake [26].

As already mentioned in § 1.1 Zanelli and co-workers [5] have shown a Tc-99m labelled porphyrin to be a useful imaging agent for sites of inflammation such as in Crohn's disease. Hence there is plenty of scope for biological studies on novel technetoporphyrin complexes.

1.3.6 Porphyrins Chosen to Study.

The study undertaken was based mainly on three porphyrin molecules:-

a) 1,2,3,4,5,6,7,8,-octaethylporphyrin (H_2OEP).

This was first synthesised by Fischer in 1928 [27], and has the structure shown in figure 7.

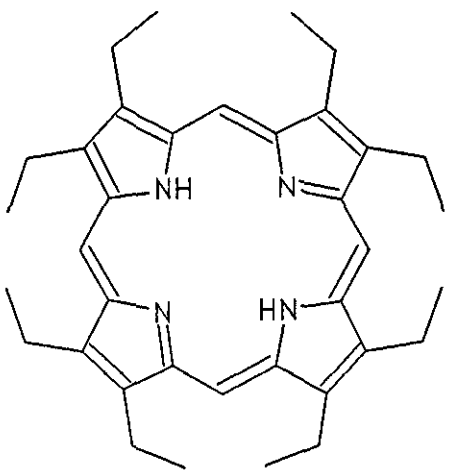

Figure 7: H_2OEP

This was chosen for 2 main reasons:-

i) It is structurally similar to the naturally occurring protoporphyrin IX (PPIX) which is the prosthetic group in the oxygen transport and storage pigments haemoglobin and myoglobin [28].

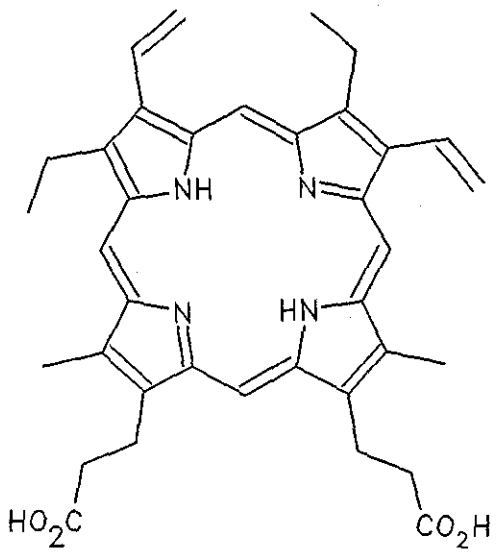

Figure 8: The structure of PPIX

ii) It is favoured for optical study since all porphyrins with eight alkyl groups on the exo pyrrole positions have essentially the same optical properties [29]. High symmetry is a prerequisite for an easy interpretation of spectra and a reduction of isomers produced in a model reaction of potential biochemical interest.

b) α,β,γ,δ-tetraphenylporphyrin (H2TPP).

The structure of H_2TPP is shown in figure 9.

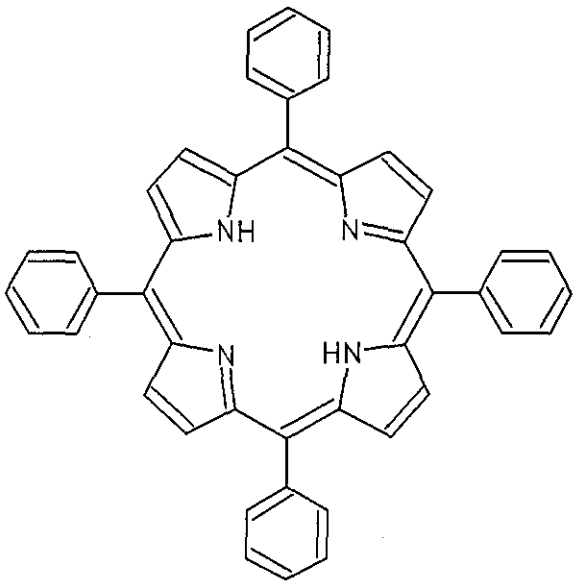

Figure 9: H_2TPP

This too is favoured for optical study since it has very characteristic absorption spectra and substitution of the phenyl rings in the para position have negligible or small effects on the absorption spectra.

c) α,β,γ,δ–tetraphenylporphyrin disulphonate (H_2TPPS_2).

This was chosen as a water soluble derivative of H_2TPP which would be better for a potential injectable preparation.

Also chosen to study was the porphyrin–like ring system of phthalocyanine (tetrazatetrabenz–porphyrin).

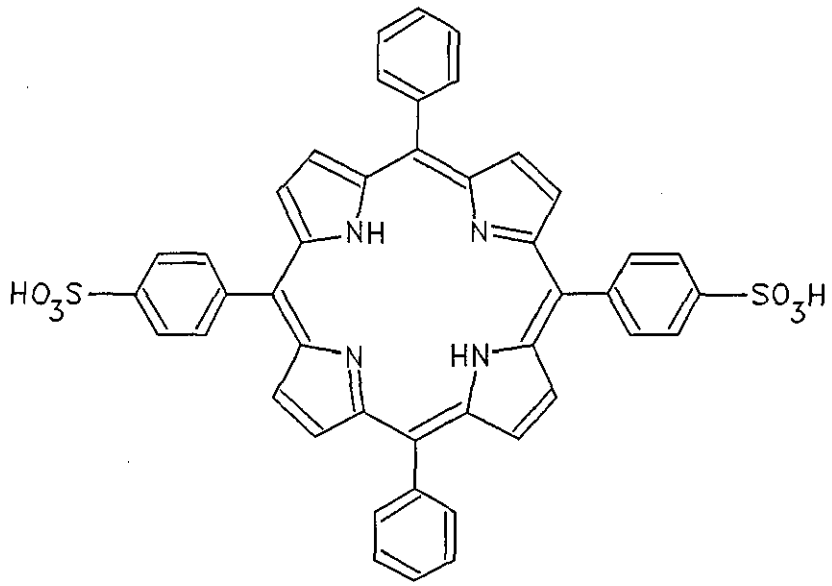

Figure 10: H_2TPPS_2

1.4 Phthalocyanine Chemistry.

Phthalocyanine is a tetrazatetrabenz-porphyrin and figure 11 shows its structural similarity with the aforementioned porphyrins.

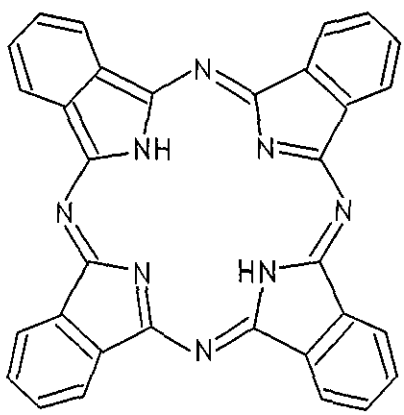

Figure 11: Phthalocyanine (PC)

The extremely high thermal stability, fastness to light, inertness to acids and alkalis, insolubility in most solvents, high dyeing power, purity and colour intensity has ensured the wide application of phthalocyanines in the paint, textile and paper industries as well as in chemical fibre and plastic dyeing processes [30].

1.4.2 Synthesis.

A specific feature of synthesising phthalocyanine complexes is that they are seldom obtained from an available phthalocyanine ligand. More often the complex is formed from molecular fragments of phthalocyanine, namely phthalonitrile, phthalimide, phthalic anhydride and other derivatives of o-phthalic acid in the presence of a metal ion source – chlorides, acetates, oxides of metals. For example [99Tc] Tetrasulphophthalocyanine has been prepared by the condensation of 3-sulphophthalic acid and pertechnetate in the presence of a reducing agent [31]. The [99mTc] analogue of this complex has also been synthesised by the same method and studied for tumour uptake properties [32].

Another method of obtaining metallophthalocyanine complexes is by recoil implantation, for example technetium and rhenium phthalocyanines have been synthesised by recoil implantation of isotopes generated by (d,xn) reactions induced by 40MeV deuteron irradiation with copper phthalocyanine [33].

1.4.3 Spectral Properties.

Like metalloporphyrins, metallophthalocyanines are best studied via characteristic optical spectra. Phthalocyanine complexes have a broadened

Soret (380–420nm) band due to underlying (n,π*) transitions and they also may have an extra band known as a C band at lower wavelengths (higher energy) than the N or L bands (250–350nm).

The optical absorption spectra of phthalocyanines as a function of the central metal have not had so much detailed study as the spectra of the porphyrins. In general metallo complexes that are regular as porphyrins are also regular as phthalocyanines, that is their visible and near UV spectra are principally (π,π*) in origin, with perhaps bridge (n,π*) contribution in the Soret (~350nm) region. Extra visible absorption bands are found in some of the same metallophthalocyanines, such as Mn(III), as shown in porphyrins.

1.5 The Aim of the Project.

The purpose of the project was to synthesise, starting from NH_4TcO_4, novel [99Tc] technetoporphyrin complexes with the technetium in a high oxidation state as opposed to those in the +I state reported by Tsutsui[17]. An advantage being the higher stability of high oxidation state technetium complexes as opposed to lower oxidation states. Most Tc-radiopharmaceuticals have the technetium in the V state. These complexes could then be characterised and determined unambiguously before the synthesis was repeated using [99mTc] to allow biological studies to be carried out.

EXPERIMENTAL.

2.1 Materials.

Octaethylporphyrin ($OEPH_2$) and phthalocyanine (PC) were purchased from Aldrich and used without further purification. Tetraphenylporphyrin (H_2TPP) was purchased from Sigma and used without further purification. Tetraphenylporphyrin disulphonate (H_2TPPS_2) was obtained as a gift from Dr. Zanelli at CRC, Northwick Park Hospital (Harrow). Solid [^{99}Tc] NH4TcO4 was obtained from Amersham International and recrystallised prior to use. [^{99m}Tc] NH_4TcO_4 was obtained from Amertec II generators kindly donated by Leicester Royal Infirmary's Radiopharmacy Dept. All other reagents were of laboratory grade from various manufacturers.

Thin layer chromatography plates (0.2mmx20cm) of Kieselgel 60 were purchased from Merck. Electronic spectra were measured on a Shimadzu UV-160 spectrophotometer while vibrational spectra were obtained using a Perkin-Elmer 257 spectrophotometer with the material dispersed in a KBr disc. FAB mass spectra were observed using a Varian-Mat 731 operating at 10kV and employing a matrix of thioglycerol/erythritol/dithioerythreitol.

Electrophoresis experiments were carried out using a Shandon Southern 602 chamber with a Volkam 400/100 power pack paper in phosphate buffer pH7, ran on 25cm strips of Whatman 3MM paper and the tests allowed to proceed for 2 hours at 300V.

2.2 Methods.

2.2.1 Porphyrin Complexes.

The complex octaethylporphyrinato(oxo)technetium(V)acetate was synthesised by the following method. This may be used to prepare a number of analogous complexes containing different porphyrins. [^{99}Tc] NH_4TcO_4 (8mg, 4.42×10^{-5} moles) and $OEPH_2$ (23.64mg, 4.42×10^{-5} moles) were added to glacial acetic acid (50ml) under a nitrogen atmosphere and the mixture refluxed for four hours. After cooling, the solution was reduced in volume to ca. 5ml and the mixture was chromatographed using CH_2Cl_2 as the eluting solvent.

The product appeared as a green band separate from unreacted $OEPH_2$ and protonated $OEPH_4^{2+}$. The complex was isolated from the Kieselgel 60 using ethanol. Evaporation of the ethanolic solution gave a green solid which can be recrystallised from a acetic acid / diethyl ether mixture with a yield ca. 40%.

2.2.2 Phthalocyanine Complexes.

An analogous [^{99}Tc] technetiumphthalocyanine complex to the previously mentioned porphyrin complexes is preparable by the following route.

[^{99}Tc] NH_4TcO_4 (8.3mg, 4.6×10^{-5} moles) and PC (23.6mg, 4.6×10^{-5} moles) were added to phenol (50ml) under a nitrogen atmosphere and the mixture refluxed for four hours. Following this the phenol was evaporated under gentle heating with nitrogen and the resulting solid was redissolved in an ethanol / water mixture. This allowed isolation of the product to be achieved

using a C18 Sep–Pak (reverse phase) in the normal manner. The product was isolated out of the Sep–Pak with ethanol in the form of a blue–green solution.

2.2.3 Redox Reactions.

Redox reactions were carried out on all of the complexes synthesised in the following manner. Firstly a drop of pyridine was added to ca. 5ml of an ethanolic solution of the complex under study, and the solution stirred for 30 minutes. Following this the electronic spectra was measured and then 5mg of sodium dithionite (reducing agent) was added to the solution and stirred for a further 30 minutes. Then the solution had the sodium dithionite filtered out, the electronic spectrum was measured again.

Also ran in parallel was purely a reduction of the complex solution by 5mg of sodium dithionite in the same manner as above.

These experiments were performed each time a particular batch of complex was made, with varying concentrations of complex, and can be quantified by studying peak height ratios.

Each time the experiments were performed a series of dilutions were made from 0.1 pyridine : 1 complex up to 50:1, and the results quantified in terms of peak height ratios.

2.2.4 Spectral Measurements.

2.2.4.1 Vibrational Spectra.

The vibrational spectra were measured with the material dispersed in a KBr disc using a Perkin-Elmer 257 spectrophotometer on a purely qualitative basis to observe any additional peaks in the complexes compared to free-base porphyrin.

2.2.4.2 Mass Spectra.

Mass spectra were carried out by a technician in the mass spectrometry department at Northwick Park Hospital using a Varian-Mat 731 operating at 10kV.

2.2.4.3 Electronic Spectra.

Electronic spectra were measured in ethanolic solutions using a Shimadzu UV-160. The solutions were obtained by scraping off the isolated band from the silica TLC plates and extracting the complex out of the silica with ethanol. Unless stated spectra are qualitative without calculated extinction coefficients, however quantification can be made in terms of peak height ratios. For each complex, peak height ratios remained constant on varying concentrations. Following the redox reactions the new peak height ratios also remained constant over a dilution range of up to 50:1. Absorbance below 300nm on spectra involving pyridine should be ignored due to possible interference caused by pyridine absorption and also instrumental error in lamp change over. The spectra reproduced in this report are photoenlargements of the originals obtained from the Shimadzu UV-160.

2.3 Biological Evaluation.

All of the animal work was carried out at CRC/MRC Northwick Park Hospital under the direct supervision of Dr. G. D. Zanelli who is responsible for all of the biodistribution data.

The biological models used were of two types:-

a) Male adult Sprague–Dawley rats with one abscessed rear leg – generated by turpentine influx.

b) Mice containing the CBA carcinoma NT.

These two models were chosen on the grounds already mentioned in § 1.3.5 (references [5] and [25]).

3. RESULTS AND DISCUSSION.

3.1 Octaethylporphyrin Studies.

Re_2O_7 has been shown to react with H_2OEP in phenol to give two complexes ReO(OEP)OPh and $[ReO(OEP)]_2O$ [15]. A similar reaction with NH_4TcO_4 gave only minute yields of a possibly analogous green complex, even after prolonged refluxing. The visible spectrum has a broad absorbance at 575nm with a shoulder on the main Soret band (364nm) at 456nm. Due to the poor yield further characterisation of this species proved impossible. However using glacial acetic acid as the solvent the reaction proceeds smoothly. A green product is obtained in high yield which is soluble in dichloromethane, benzene and appears neutral by electrophoresis. The electronic spectrum of the complex, measured using ethanol as the solvent, is reproduced in figure 12. It has two sharp absorptions at 499nm and 470nm, with a broad absorption at 617nm. This compares with the four banded visible spectrum of H_2OEP (622, 569, 532, 498nm) and the two banded one of H_4OEP^{2+} (569, 533nm) and is a typical metalloporphyrin spectrum. The Soret band of the complex is split in two with absorptions at 391 and 344nm, while those for the non-metallated porphyrins are at 404 and 405nm respectively.

The vibrational spectrum has absorptions typical of a metalloporphyrin and an additional absorption at $1604cm^{-1}$. This latter vibration is similar to those observed in other octaethylporphyrinatometalacetates [34]. Two absorptions at $962cm^{-1}$ and $918cm^{-1}$ are in the region typical of ν(Tc=O) [35] but an absolute assignment is impossible. ReO(OEP)F has ν(Re=O) at $953cm^{-1}$ [36] and the $962cm^{-1}$ absorption seems more probable.

Figure 12.

The electronic spectrum of the complex (OEP)TcO(OAc).

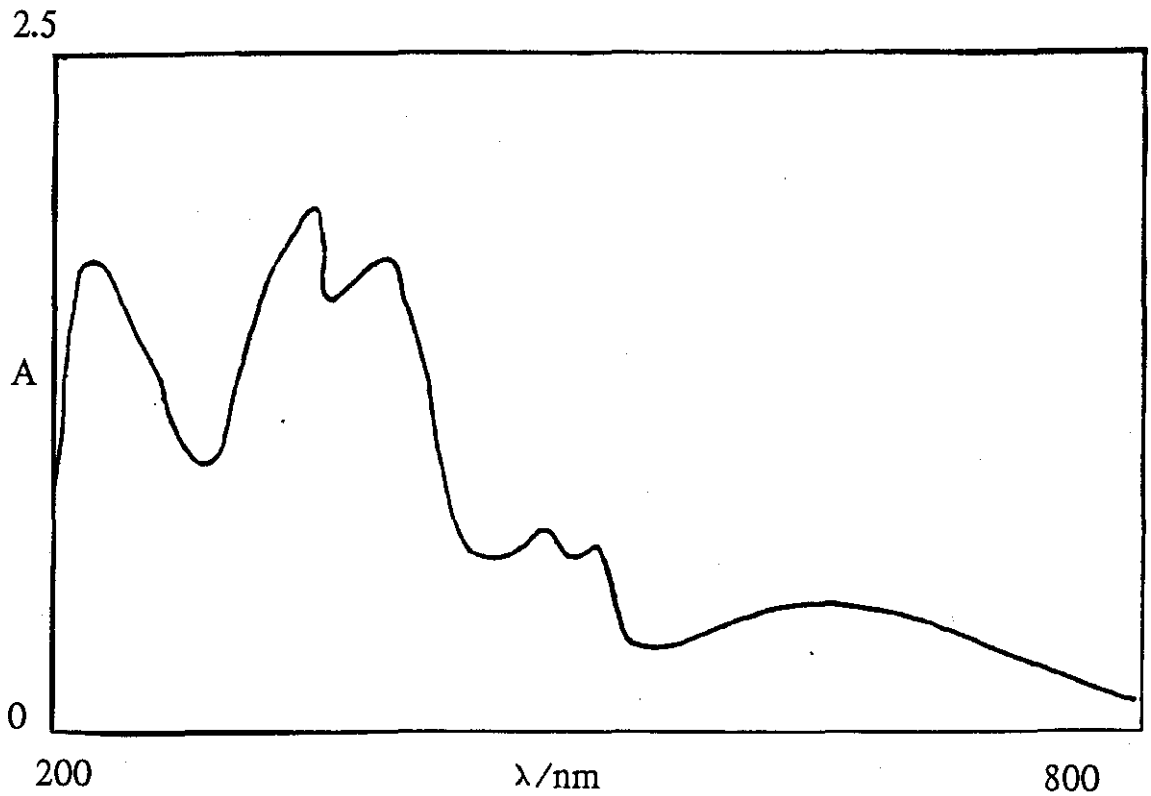

λ_{max}/nm	Σ /mol^{-1}dm^{3}cm^{-1}	λ_{max}/nm	Σ /mol^{-1}dm^{3}cm^{-1}
617	4.4x10^3	382	1.6x10^4
499	6.4x10^3	344	1.8x10^4
470	6.9x10^3		

These values are in accordance with previously reported rhenium complexes of OEP [34].

Figure 13: FAB^+ mass spectrum of the (OEP) Tc O(OAc) complex.

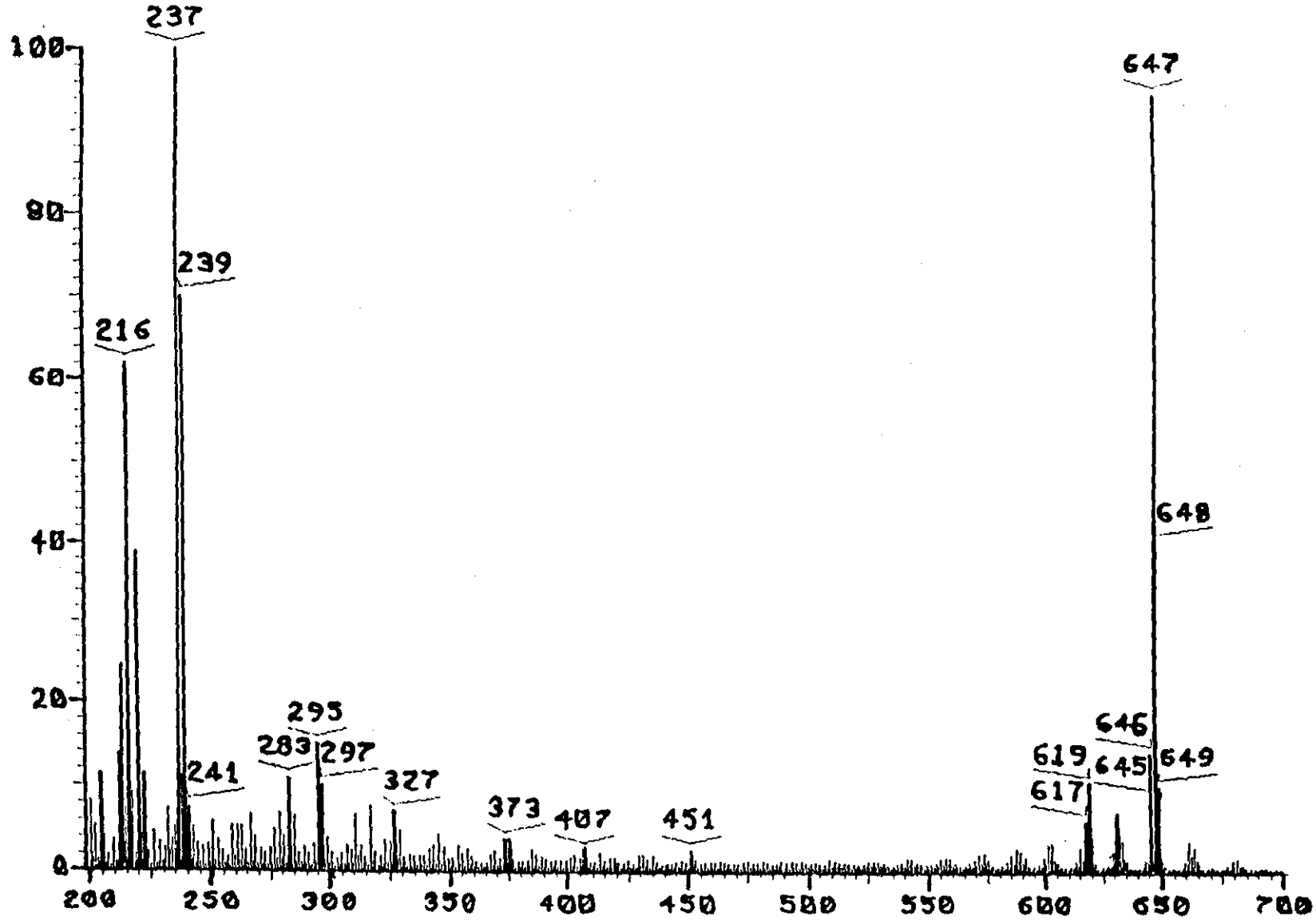
237
647
100
80
239
216
60
648
40
20
295
283
297
646
619
645
649
241
327
617
373
407
451
0
200
250
300
350
400
450
500
550
600
650
700

Figure 14.

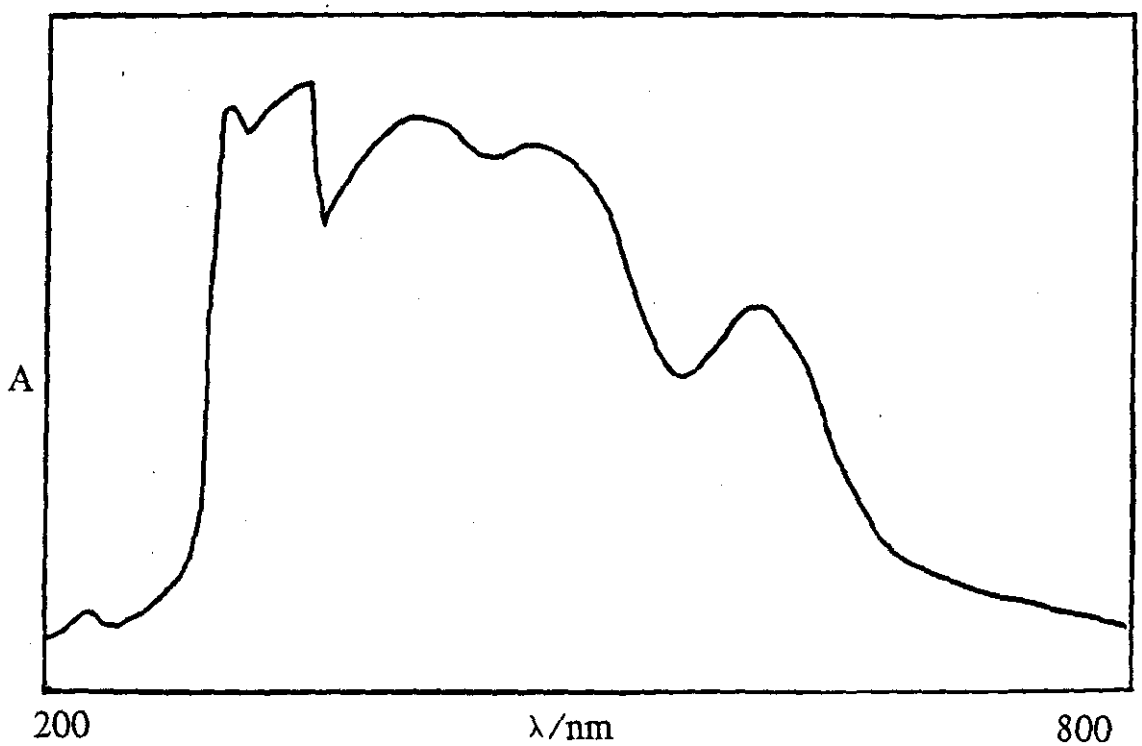

Absorbance (A) is in arbitrary units.

Figure 14 shows the effect on the UV/visible spectrum of the complex (OEP)TcO(OAc) caused by the addition of pyridine. Extinction coefficients are unknown, however dilution up to 1:50 causes no change in the ratio of peak heights.

Figure 15.

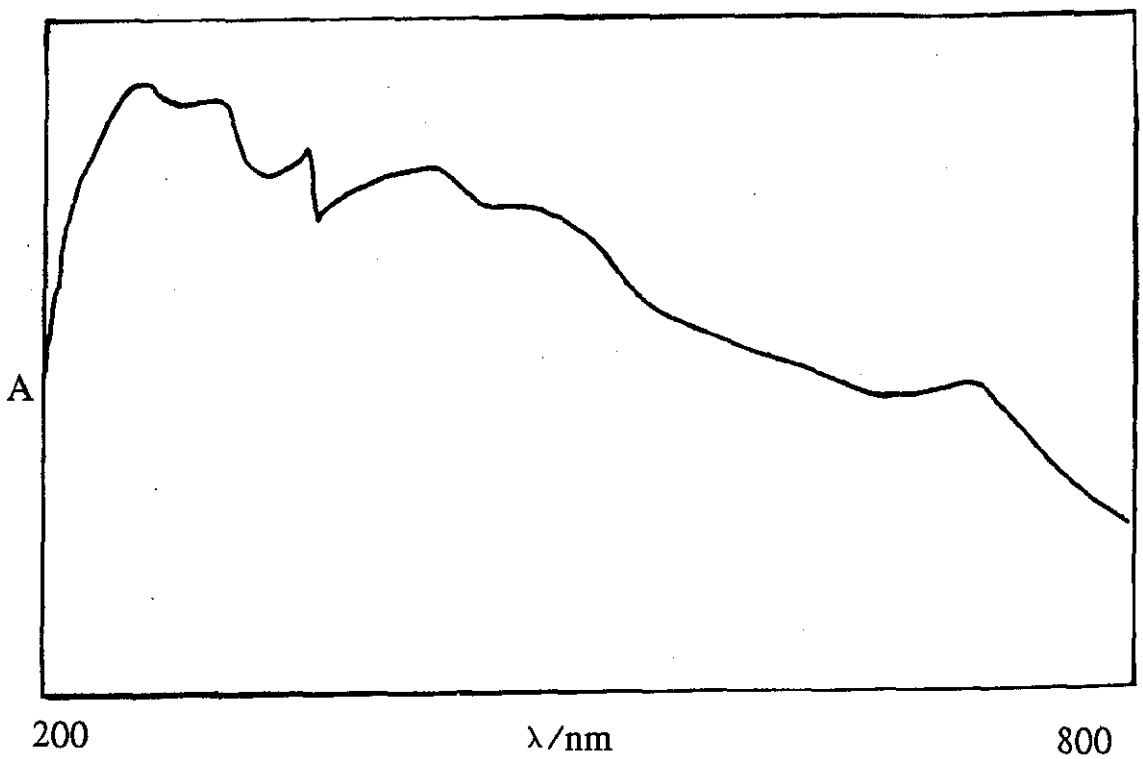

Absorbance (A) is in arbitrary units.

Figure 15 shows the change in the UV/visible spectrum of (OEP)TcO(OAc) caused by the addition of pyridine, followed by sodium dithionite reduction. Dilution up to 1:50 causes no change in the ratios of the peak heights.

Figure 16: FAB^+ mass spectrum of the product arising from the addition of pyridine and subsequent reduction of the (OEP) Tc O(OAc) complex.

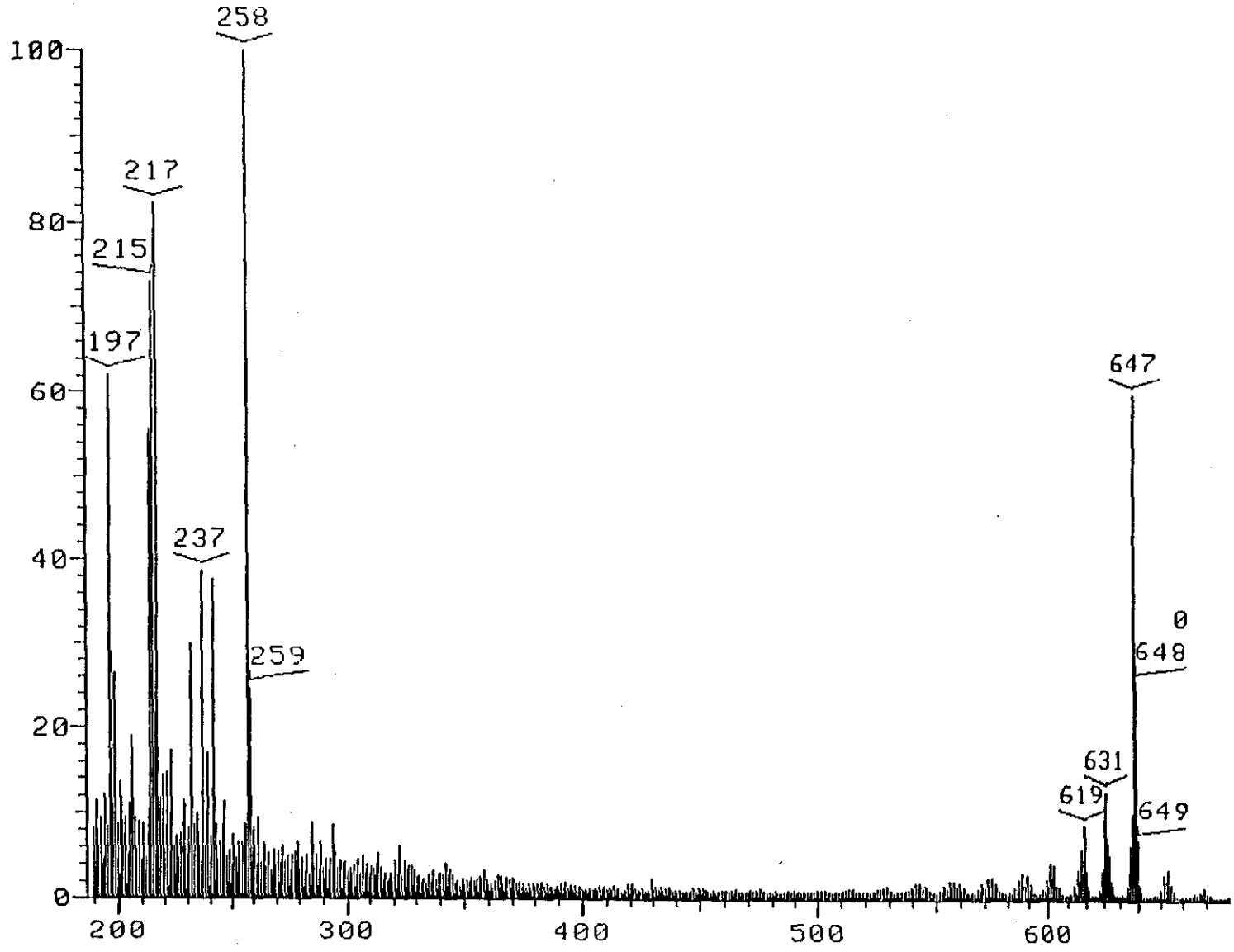
258
217
215
197
237
259
647
0
648
631
619
649
100
80
60
40
20
0
200
300
400
500
600

The FAB+ mass spectrum of the complex is reproduced in figure 13 and shows the major peak to be at m/z of 647, this corresponds to $[TcO(OEP)]^+$. In FAB+ mass spectrometry a parent ion $[M+H]^+$ is normally observed but in those technetium species with labile ligands trans to an oxo the major ion is usually $[M-L]^+$ where L is the trans ligand. Additionally the matrix employed is an acidic one and loss of acetic acid by protonation to give $[M-L]^+$ could occur. This appears to be the case for octaethylporphyrinato-(oxo)technetium (V) acetate. This complex may be used to synthesise a range of new technetium porphyrins and figure 14 shows the reaction of (OEP)TcO(OAc) with pyridine. The change in the visible spectrum was originally presumed to be indicative of ligand exchange of the trans acetate ligand. Further addition of sodium dithionite, (a reducing agent), caused additional changes to the visible spectrum figure 15, and an FAB+ mass spectrum (figure 16) shows this to be a reduction of the technetium oxo core to yield technetium (IV) or technetium (III) porphyrin. Furthermore, the mass spectrum shows no evidence of ligand exchange between the acetate and pyridine and from this one would conclude that the change in visible spectrum may be due to solvation by pyridine or that the complex in solid state is different to that in solution of pyridine. The reduction of the technetium oxo core is shown by the emergence of the peak at m/z 631 which is approximately 40% of the peak at m/z 647 and corresponds to $Tc(OEP)^+$. This peak is seen in the spectrum of (OEP)TcO(OAc) however it is less than 10% of the parent ion at m/z 647.

Therefore despite the fact that ligand exchange was not achieved, a reduction of the Tc=O core to yield different complexes was achieved.

Animal studies were performed on the complex (OEP)TcO(OAc) however solubility proved to be a problem due to the lipophilic nature of the complex. This was partially overcome by addition of a small amount of Tween 80 to act as a solubiliser.

The tests were carried out by Dr. G.D. Zanelli as follows:-

1ml of the complex in ethanol was diluted to 10ml with sterile saline to give approximately 100μCi/ml. Each of six male adult Sprague-Dawley rats with abscess in right hind leg were injected I.V. in the tail with 1ml and scanned on the γ-camera firstly in a dynamic mode, i.e. 1 minute frames for 30 minutes, and secondly in a static manner 45 minutes post injection.

The rats were then sacrificed at varying time intervals post injection from 24 minutes to 18 hours by cardiac puncture and removal of ca. 15.5ml of blood (average blood volume of these rats). Following sacrifice various organs were removed and counted to give separate organ values including liver, spleen, lungs, kidneys, heart, right leg, left leg and finally carcass. The legs were cut at mid-femur and counted in a bulk counter.

The standard was designated as 0.5% of the injected dose which gave an average of 13926 cpm and hence the activity injected is equivalent to 2,765,200 cpm. Results are shown in table 1, expressed as % of injected dose and also % whole body (cpm tissue/cpm total).

As can be seen from the table the activity tends to accumulate in the liver and lungs due to the high lipophilicity, however the right leg can be seen well on density boost (see photographs in figure 17).

Table 2 shows the ratio of right leg (abscess) : left leg (normal) for the various rats.

Table 1.

	Time of Sacrifice Post Injection.					
	24min	1hr.	4hrs.	6hrs.	8hrs.	18hrs.
Blood	0.66	0.24	0.77	0.2	0.36	0.41
	0.61	**0.18**	**0.67**	**0.19**	**0.32**	**0.46**
Liver	42.50	29.77	51.37	54.20	65.20	58.60
	38.90	**21.60**	**44.57**	**52.20**	**56.90**	**45.05**
Kidneys	0.64	0.34	0.98	1.21	1.29	1.01
	0.58	**0.25**	**0.85**	**1.17**	**1.13**	**1.12**
Lungs	39.01	23.03	21.82	17.02	10.20	11.96
	35.74	**16.71**	**18.94**	**16.39**	**8.91**	**13.28**
Heart	0.28	0.06	0.41	0.27	0.16	0.16
	0.25	**0.04**	**0.36**	**0.26**	**0.14**	**0.175**
Rt. leg	0.64	0.74	2.40	1.61	1.70	2.14
	0.59	**0.53**	**2.08**	**1.55**	**1.48**	**2.37**
L. leg	0.52	0.24	1.03	0.57	0.74	1.10
	0.48	**0.17**	**0.89**	**0.54**	**0.64**	**1.22**
Carcass	13.54	41.22	13.21	16.26	15.50	15.79
	12.38	**29.90**	**11.47**	**15.66**	**13.54**	**17.50**
Spleen	2.74	4.36	7.99	8.65	4.89	8.84
	2.50	**3.16**	**6.93**	**8.33**	**4.25**	**9.81**

% whole body.
% injected dose.

Table 2.

Time post injection.	Ratio of Rt. leg : Left leg.
24 min.	1.24
1 hour.	3.12
4 hours.	2.33
6 hours.	2.84
8 hours	2.30
18 hours.	1.95

As can be seen from the two tables the activity in the right leg with the abscess peaks between 1–4 hours and there is approximately 2½ times the activity in the abscessed leg compared to the normal leg.

Figure 17 shows a series of photographs from both the dynamic and static scans of rats with an abscess in the right leg.

Figure 17.1:

A. Dynamic scan, 1 minute, normal.

A. Liver.
B. Lungs.

B. Dynamic scan, 1 minute, density boost.

A. Head.
B. Right hind leg (abscess).
C. Tail.

C. Dynamic scan, 5 minutes, normal.

A. Liver.
B. Lungs.

D. Dynamic scan, 5 minutes, density boost.

A. Head.
B. Right hind leg (abscess).
C. Tail.

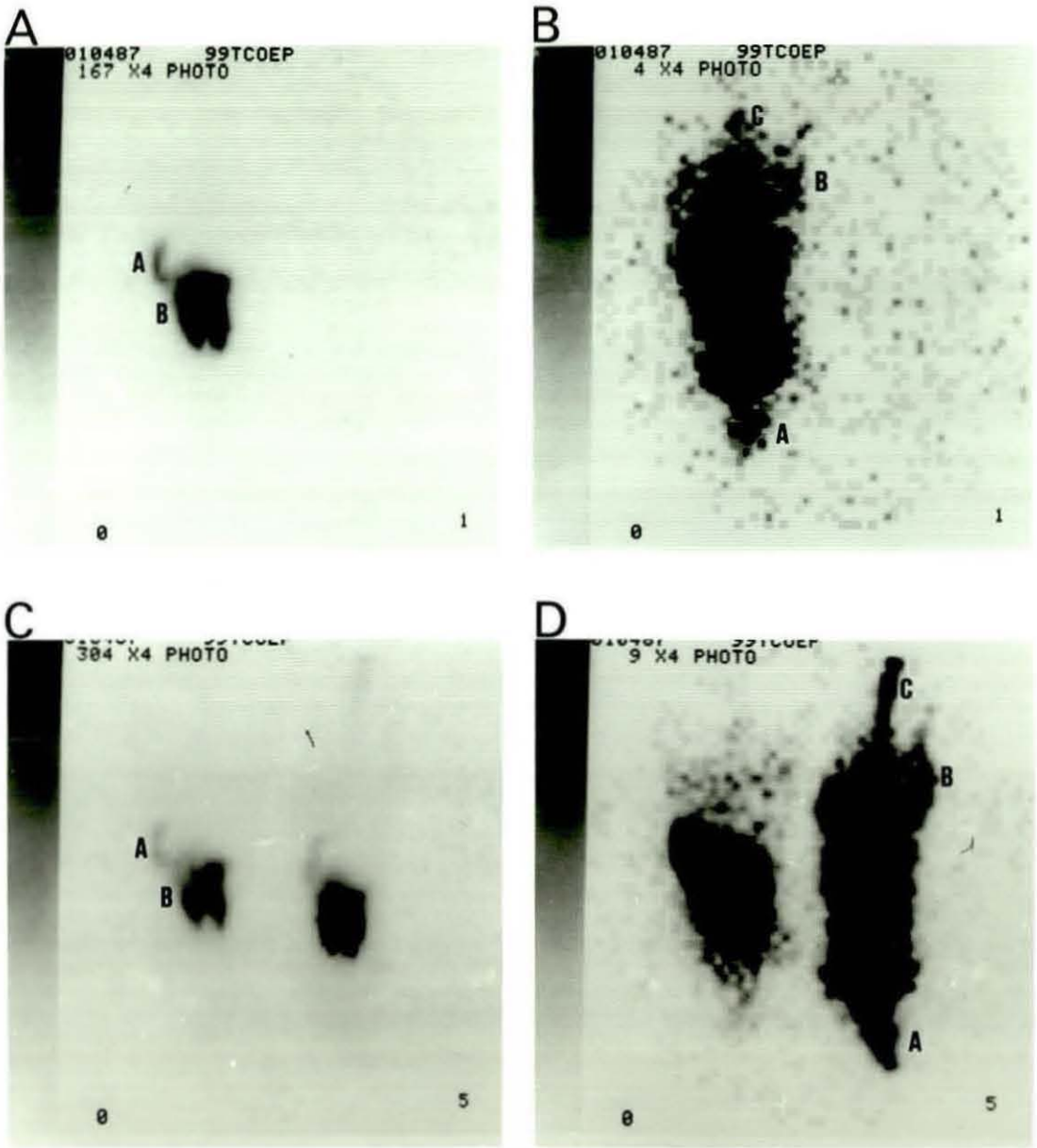
A
010487 99TCOEP
167 X4 PHOTO
A
B
0
1
B
010487 99TCOEP
4 X4 PHOTO
C
B
A
0
1
C
304 X4 PHOTO
A
B
0
5
D
9 X4 PHOTO
C
B
A
0
5

Figure 17.2:

A. Dynamic scan, 10 minutes, normal.

A. Liver.
B. Lungs.

B. Dynamic scan, 10 minutes, density boost.

A. Head.
B. Right hind leg (abscess).
C. Tail.

C. Dynamic scan, 17 minutes, normal.

A. Liver.
B. Lungs.

D. Dynamic scan, 17 minutes, density boost.

A. Head.
B. Right hind leg (abscess).
C. Tail.

A

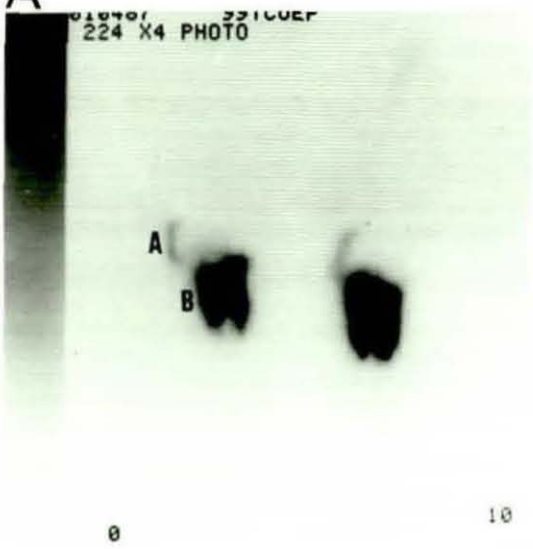
224 X4 PHOTO
A
B
0
10

B

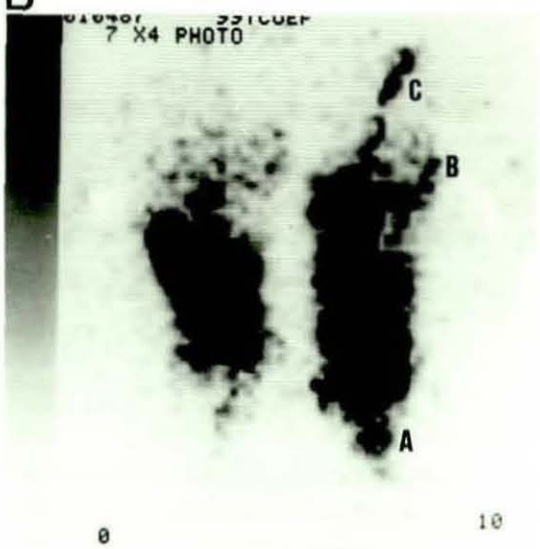
7 X4 PHOTO
C
B
A
0
10

C

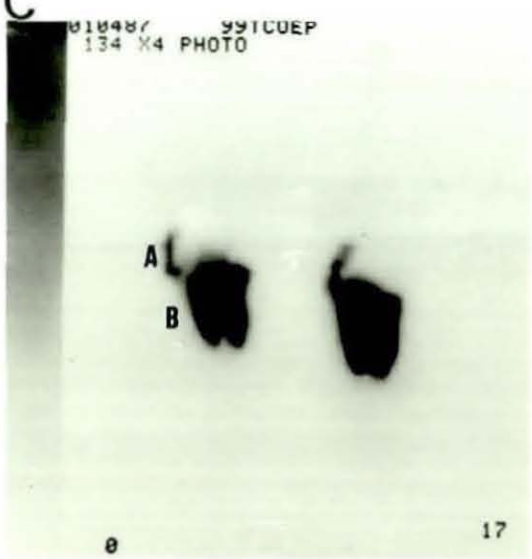
134 X4 PHOTO
A
B
0
17

D

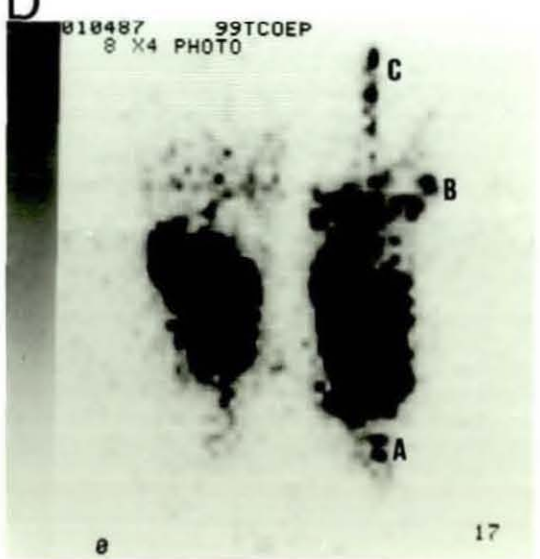
010487 99TCOEP
8 X4 PHOTO
C
B
A
0
17

Figure 17.3:

A. Dynamic scan, 29 minutes, normal.

A. Liver.

B. Lungs.

B. Dynamic scan, 29 minutes, density boost.

A. Head.

B. Right hind leg (abscess).

C. Tail.

A

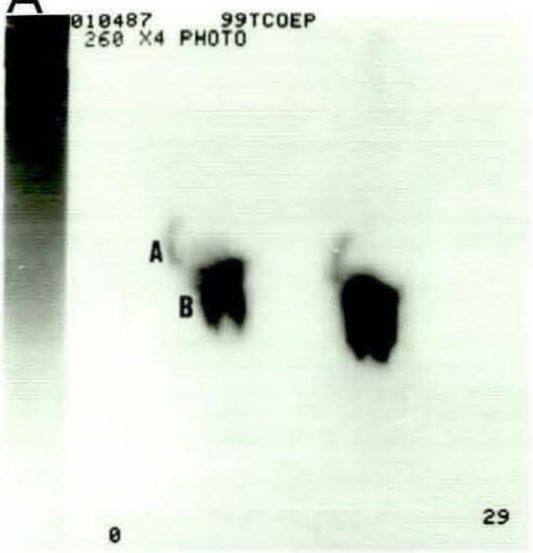
010487 99TCOEP
260 X4 PHOTO
A
B
0
29

B

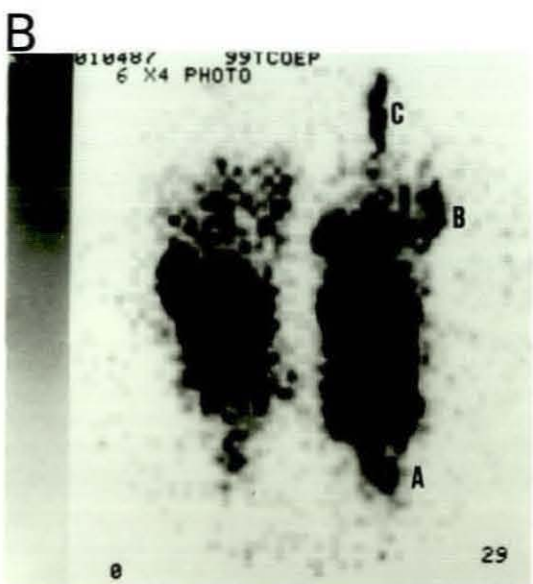
010487 99TCOEP
6 X4 PHOTO
C
B
A
0
29

Figure 17.4:

A. Static, 30 minutes, density boost.

A. Head.

B. Right hind leg (abscess).

C. Tail.

B. Static, 1 hour, density boost.

A. Head.

B. Right hind leg (abscess).

C. Tail.

A

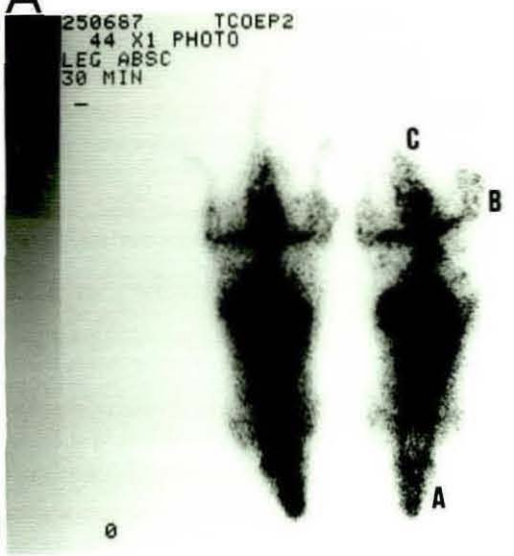
250687 TCOEP2
44 X1 PHOTO
LEG ABSC
30 MIN
C
B
A
0

B


250687 TCOEP2
27 X1 PHOTO
LEG ABSC
1 HOUR
C
B
A
0

3.2 α,β,γ,δ-Tetraphenylporphyrin Studies.

Substituting H_2-TPP for H_2-OEP, an analogous green complex can be prepared indicating that this is probably a general route for labelling porphyrins with 99-Tc. The electronic spectrum of the complex is reproduced in figure 18 showing two sharp absorptions at 596 and 556nm with a shoulder at 467nm. The Soret band occurs at 425nm in comparison with that of H_2-TPP which is found at 415nm (figure 19).

The visible spectrum of the complex compares with that of the free base porphyrin which is four banded (646, 591, 549 and 514nm) and the protonated porphyrin H_4-TPP^{2+} which is two banded (591 and 549nm). These variations follow the same trend as in the OEP studies.

Figures 20, 21 and 22 reproduce the electronic spectra from the redox reactions of the Tc-TPP complex. Figure 20 shows that on addition of pyridine the shoulder at 467nm begins to disappear and a new peak at 403nm emerges in the form of a shoulder on the main Soret band. The further addition of reducing agent causes a total loss of the shoulder at 467nm (figure 21) which can be concluded to be caused by pyridine since it is present in figure 22 which is a control reaction of the Tc-TPP complex with sodium dithionite (reducing agent). However, interestingly the peak around 400nm is far more pronounced rather than being in the form of a shoulder as compared to figures 20 and 21.

Figure 18

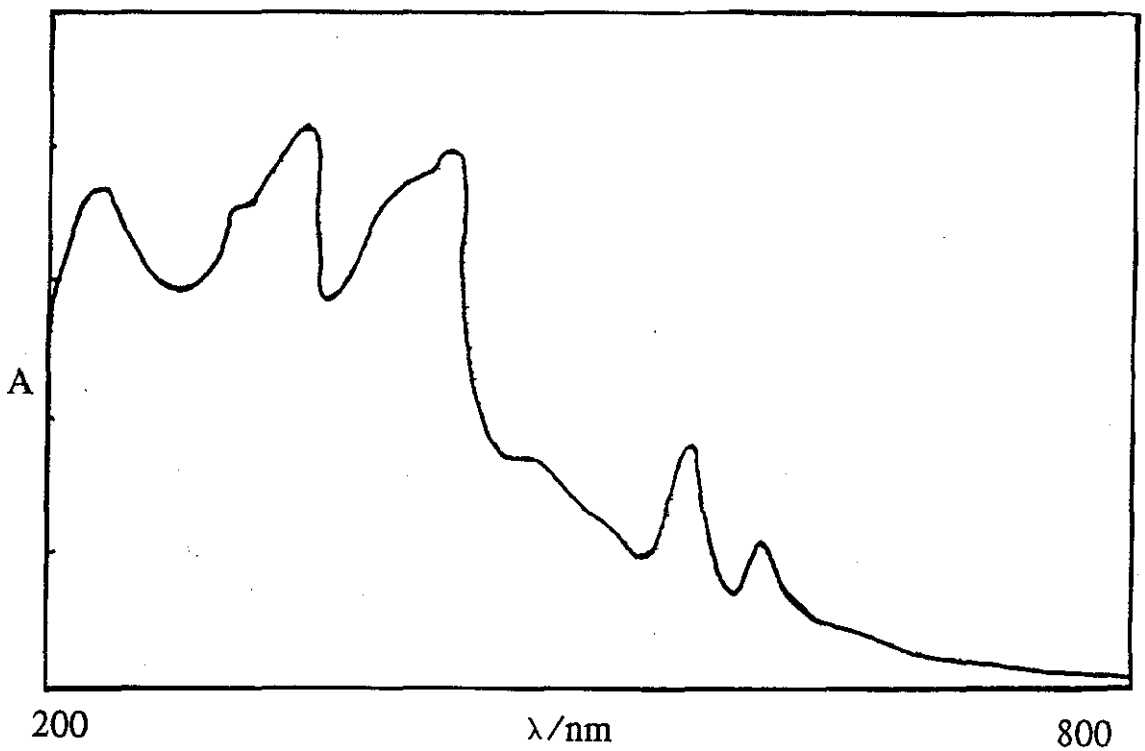

Absorbance (A) is in arbitrary units.

Figure 18 shows the electronic spectrum of the Tc–TPP complex. Extinction coefficients are unknown although the ratio of peak heights does not vary with concentration.

Figure 19.

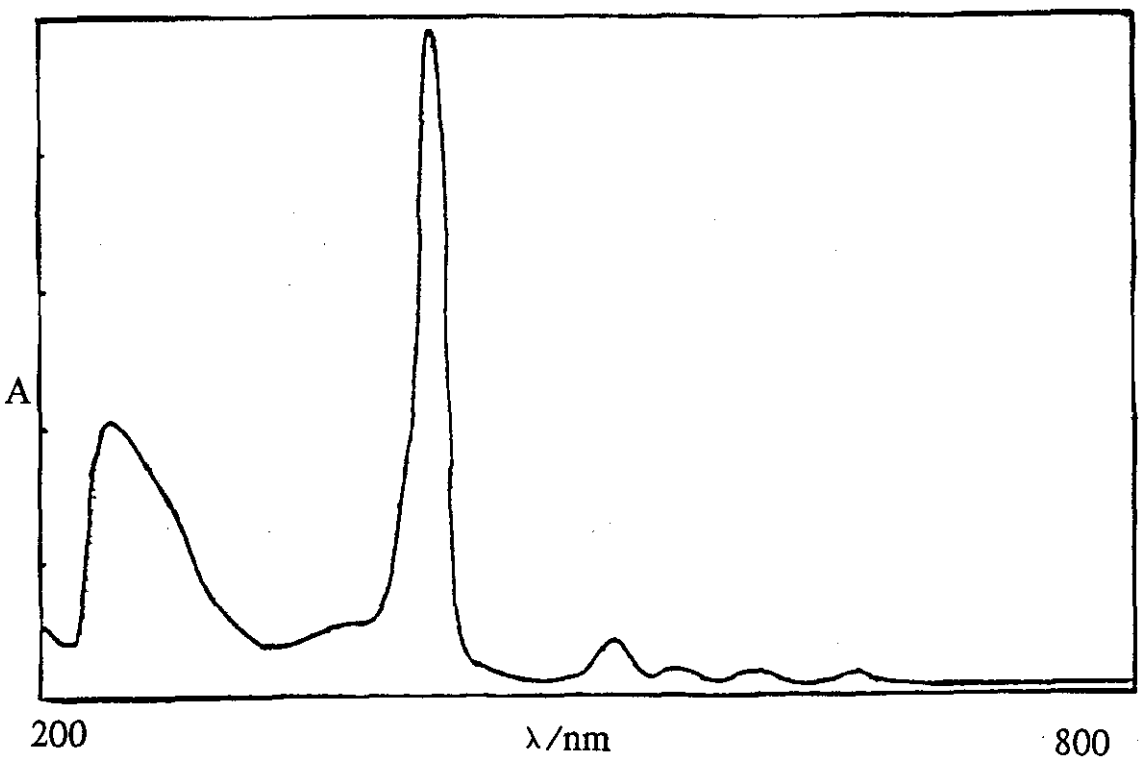

Absorbance (A) is in arbitrary units.

Figure 19 shows the electronic spectrum of H_2–TPP indicating the intense absorption of the Soret (B) band at 415nm.

Figure 20.

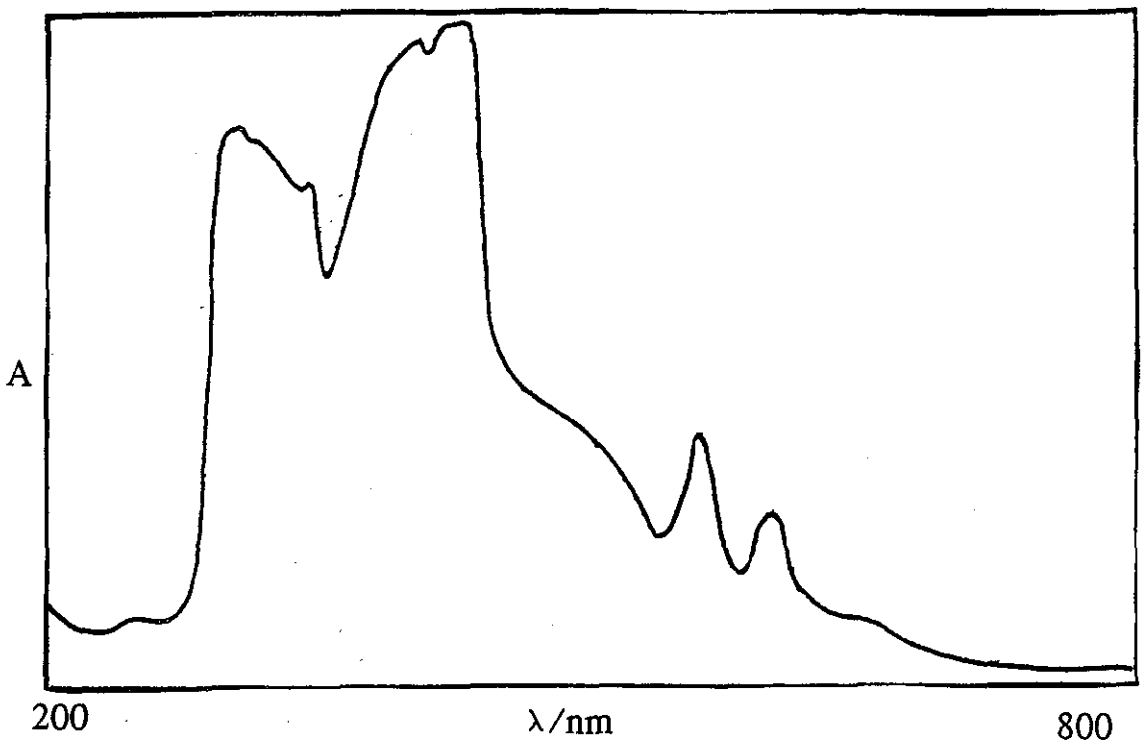

Absorbance (A) is in arbitrary units.

Figure 20 shows the effect of the addition of pyridine on the electronic spectrum of the Tc-TPP complex. Peak height ratios remain constant with dilution.

Figure 21.

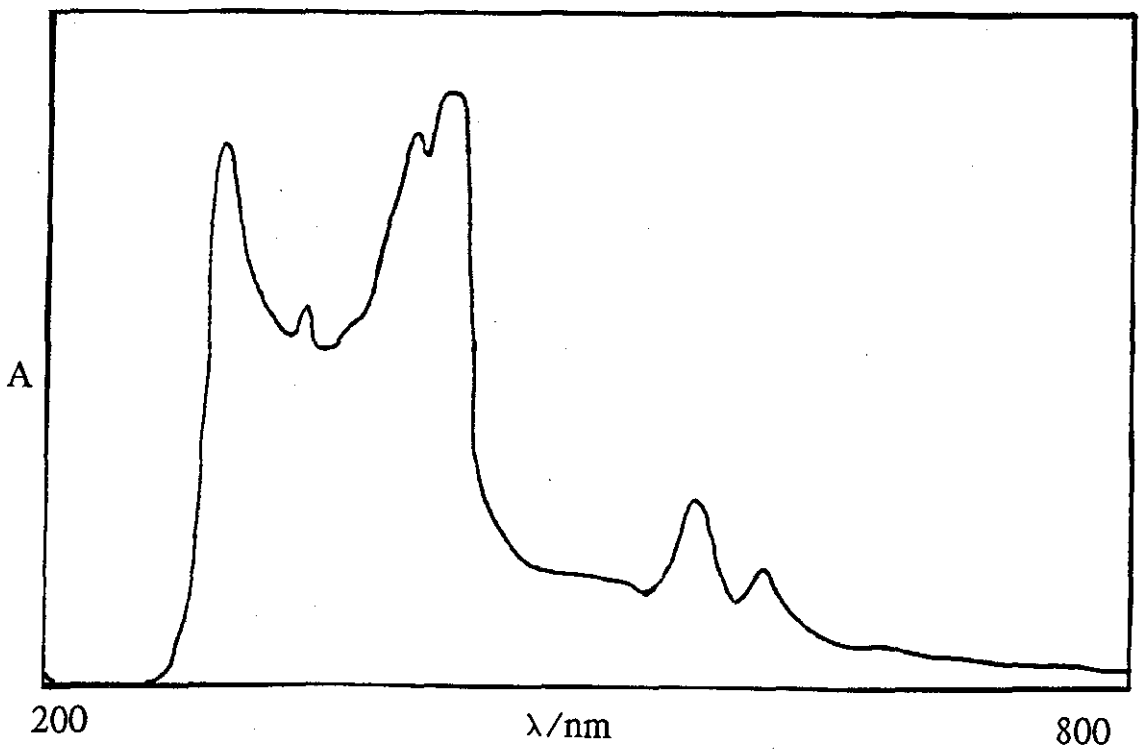

Absorbance (A) is in arbitrary units.

Figure 21 shows the effect on the electronic spectrum of the Tc–TPP complex caused by the addition of pyridine followed by sodium dithionite reduction. Peak height ratios do not vary with dilution.

Figure 22.

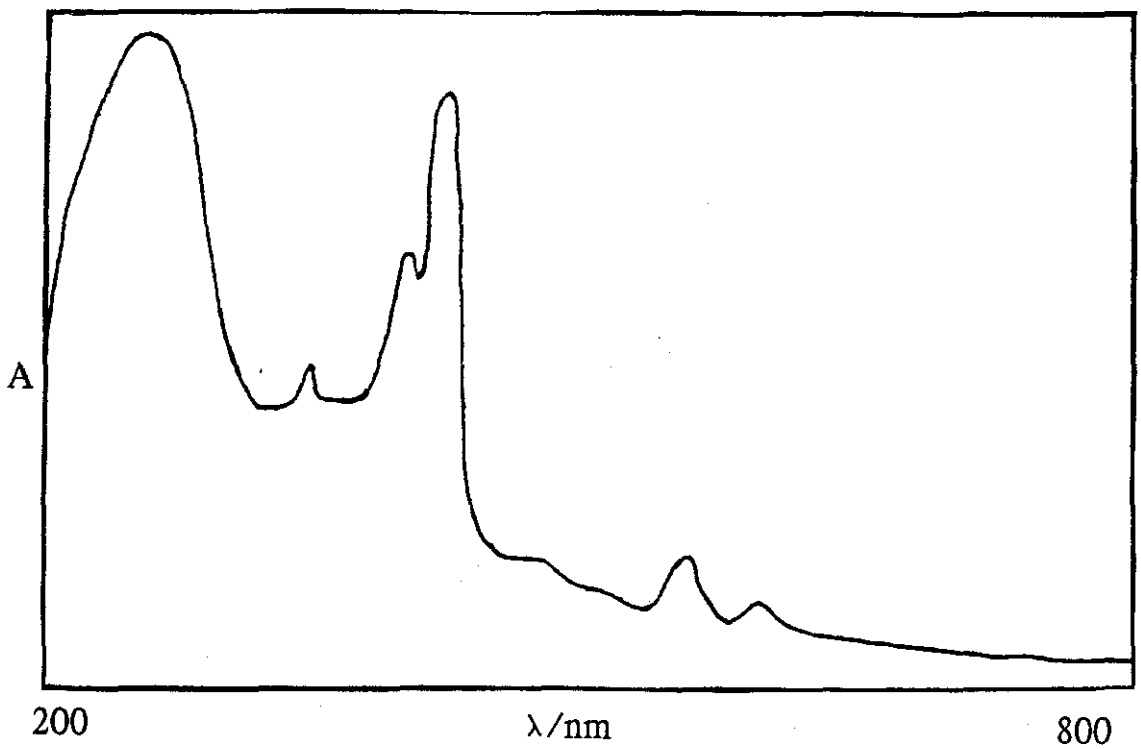

Absorbance (A) is in arbitrary units.

Figure 22 shows the effect on the electronic spectrum of the Tc–TPP complex caused by sodium dithionite reduction. Peak height ratios do not vary with dilution.

Vibrational spectra of porphyrins and metalloporphyrins are difficult to obtain due to the high extinction coefficients of the compounds resulting in difficulties in the preparation of KBr discs, however one was obtained even if it only highlighted the fingerprint region. This showed three extra absorptions as compared to H_2–TPP at 979, 900 and 842cm^{-1} respectively, the former possibly representing a Tc=O stretching frequency, however, definite interpretation is impossible.

The green complex appeared to be neutral by electrophoresis under similar conditions for the Tc–OEP complex. Unfortunately insufficient solid was obtained to allow the measurements of the FAB+ mass spectrum and so further characterisation was not possible, except to protract that it is probably exactly analogous to the [TcO(OEP)OAc] complex as it seems to follow the trends similarly and is also the characteristic green colour. Biological evaluation has not yet been performed on this complex.

3.3 Tetraphenylporphyrindisulphonate Studies.

As in the previous two cases a characteristically green complex is formed in the same manner giving further evidence of a novel general route achieving Tc–99 insertion into porphyrins.

Figures 23 and 24 reproduce electronic spectra of the free base porphyrin and the complex respectively. As can be seen there are drastic differences between the two spectra. Figure 23 is typical of a free base porphyrin spectrum with absorptions at 644, 588, 546, 512nm, the Soret band appearing at 413nm. However, the Tc–$TPPS_2$ spectrum has major differences with an absorption at 597nm followed by a Soret band split into two absorptions (as is the case for OEP) occurring at 421 and 394nm. Another feature is the emergence of another absorption at 327nm (N band).

The spectrum of the protonated porphyrin, H_4–$TPPS_2^{2+}$ has absorptions at 594, 554 and 422nm (Soret) typical of these species. The electronic spectra of the redox reactions of the Tc–$TPPS_2$ complex are reproduced in figures 25, 26 and 27.

Figure 25 shows some drastic changes that occur to the electronic spectrum on addition of pyridine to the complex including the emergence of a new peak at 302nm.

Also in the Soret region the peak at 391nm has a greater absorbance than the one at 426nm – a reversal of that found in the complex, however, this changes back again on addition of sodium dithionite as shown in figures 26 and 27. However the addition of reducing agent to the pyridine solution causes the band at 300nm to drastically increase in absorbance compared to the other absorption peaks, whereas figure 27 shows that addition of reducing agent to the Tc–$TPPS_2$ complex on its own shows peaks of absorption at 555nm and 346nm that were previously absent.

The vibrational spectrum of the complex shows only two major additional vibrations to that of the free base porphyrin. These occur at 1615cm^{-1} and 980cm^{-1} respectively. The absorption at 1615cm^{-1} is well within the range found for metal–acetate stretching as previously stated [34], and the other absorption at 980cm^{-1} occurs in the region of Tc=O stretching frequencies although definite assignment is not possible.

An FAB+ mass spectrum was requested from Northwick Park Hospital, but never received.

Figure 23.

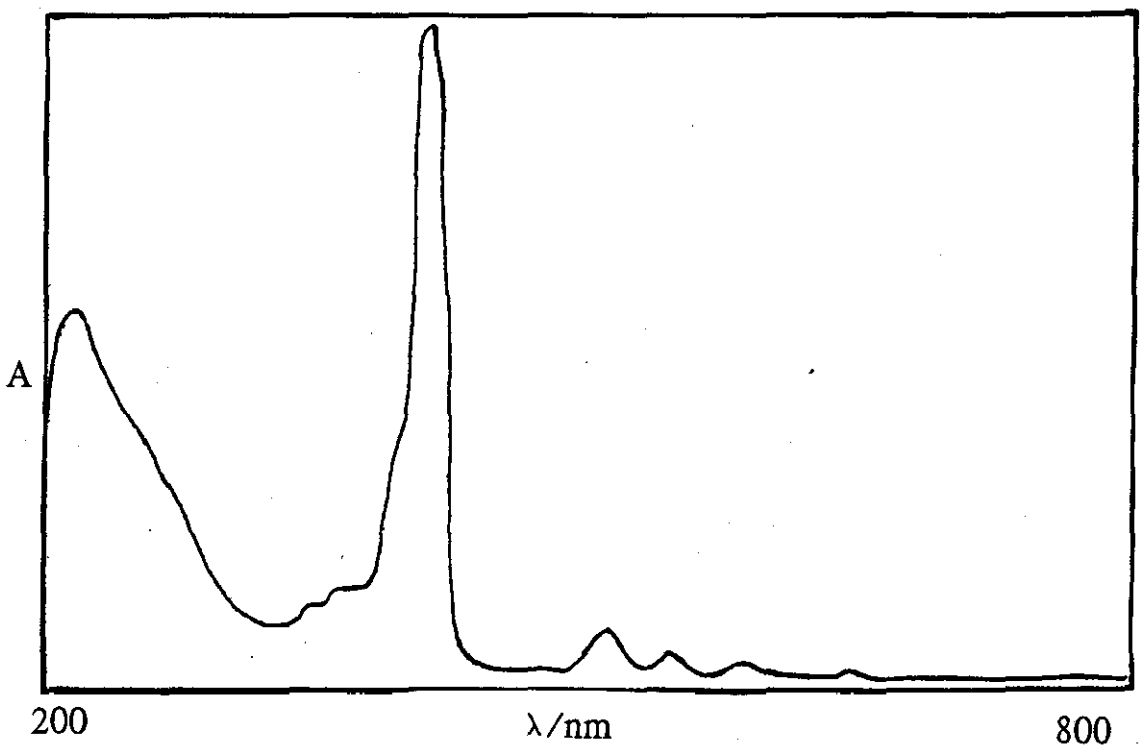

Absorbance (A) is in arbitrary units.

Figure 23 shows the electronic spectrum of H_2–$TPPS_2$.

Figure 24.

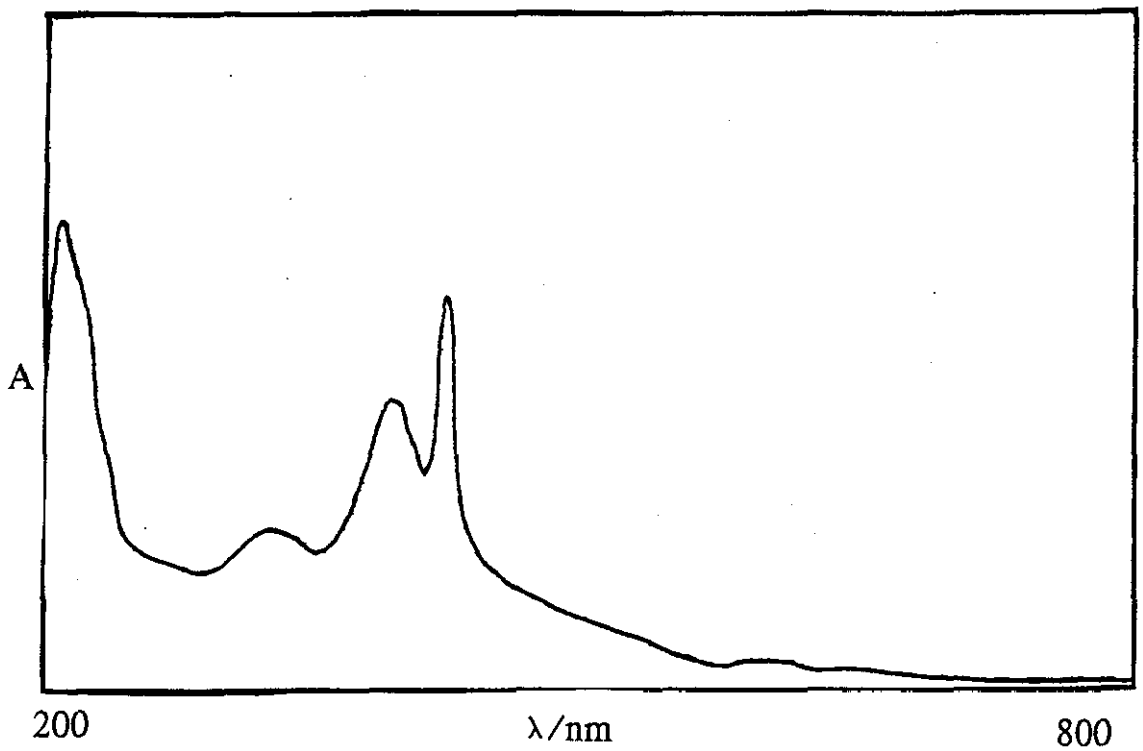

Absorbance (A) is in arbitrary units.

Figure 24 shows the electronic spectrum of the Tc–$TPPS_2$ complex, displaying a definite split in the Soret band. Extinction coefficients are unknown, however peak height ratios remain constant with varying concentrations.

Figure 25.

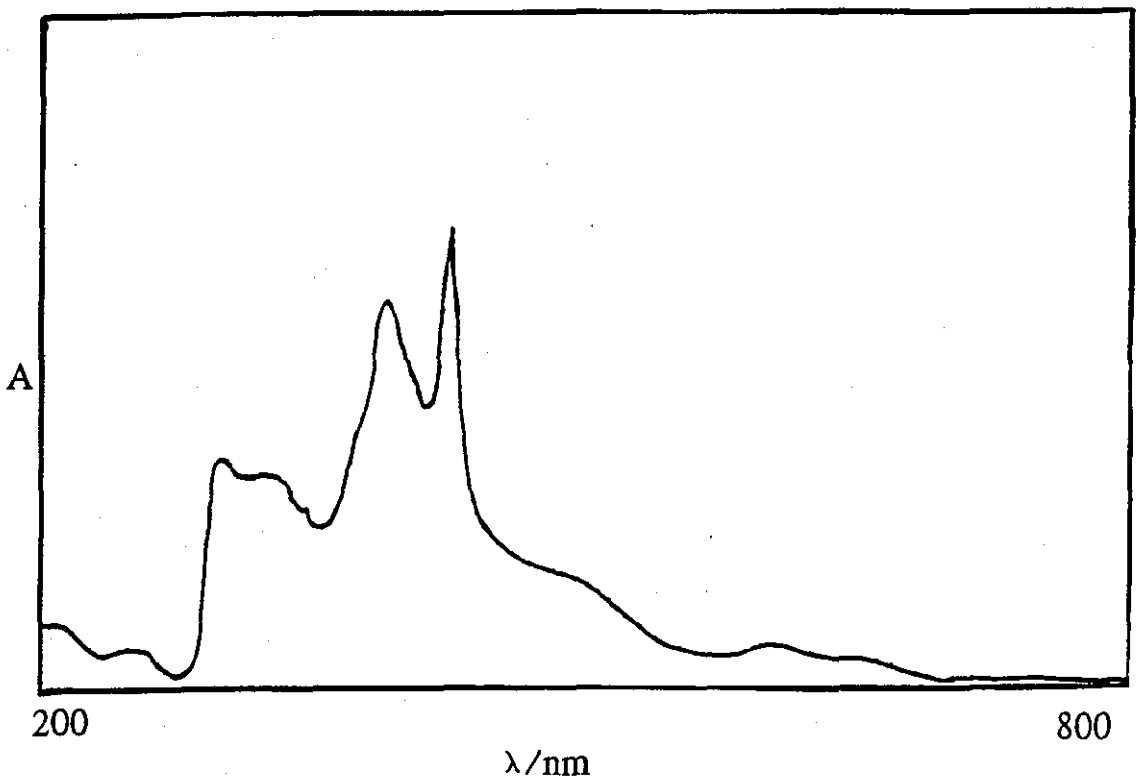

Absorbance (A) is in arbitrary units.

Figure 25 shows the effect on the electronic spectrum of the Tc–$TPPS_2$ complex caused by the addition of pyridine. Peak height ratios remain constant with dilution.

Figure 26.

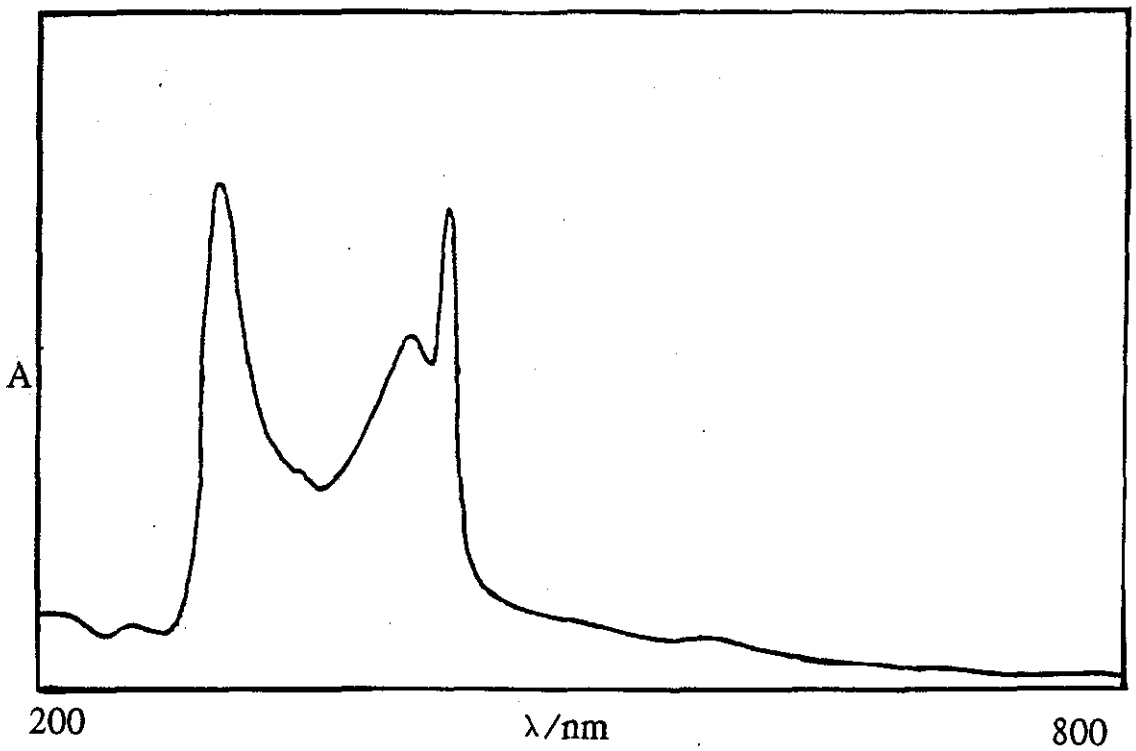

Absorbance (A) is in arbitrary units.

Figure 26 shows the effect on the electronic spectrum of the Tc–$TPPS_2$ complex caused by the addition of pyridine followed by sodium dithionite reduction. Peak height ratios remain constant with dilution.

Figure 27.

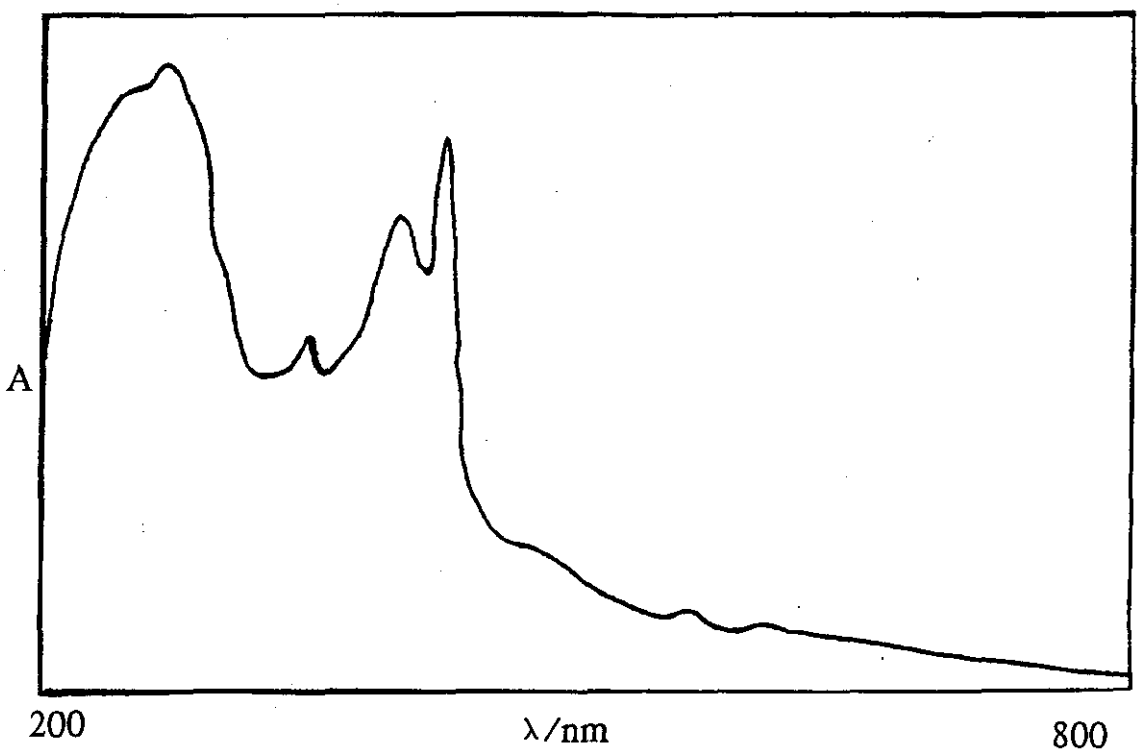

Absorbance (A) is in arbitrary units.

Figure 27 shows the effect on the electronic spectrum of the Tc–$TPPS_2$ complex caused by sodium dithionite reduction. Peak height ratios remain constant with dilution.

The complex is water soluble and appears anionic by electrophoresis, however this could be due to the highly acidic protons on the sulphonic acid groups.

The biological studies were carried out in the same manner as for the Tc–OEP complex although the water solubility made the preparation far better for injecting, avoiding the need for any solubiliser. The biodistribution results are shown in table 3.

Table 3– Biodistribution of Tc–$TPPS_2$ complex in abscessed rats.
(Expressed as an average of four rats.)

	% injected dose					
	15min.	62min.	3hrs.	5hrs.	8hrs.	4hrs.
Blood	0.91	0.37	0.35	0.37	0.28	0.25
Liver	18.7	21.2	19.3	18.5	16.6	14.5
Spleen	1.4	2.2	1.85	1.7	1.5	1.3
Lungs	0.77	0.68	0.69	0.71	0.64	0.61
Kidneys	12.3	21.7	33.8	31.7	28.4	9.8
Rt. Leg (Abscess)	0.89	1.07	1.20	1.54	1.25	0.50
L. Leg	0.74	0.61	0.52	0.48	0.32	0.31
Carcass	64.3	42.4	34.6	28.9	27.2	12.85

The values show the majority of the activity to be located in the liver and kidneys, however it is clear that the abscessed leg has an appreciably greater amount of activity associated with it compared to the normal leg. The ratios of activity in the abscessed leg : normal leg 2.3 hours after injection are shown in table 4.

Table 4.

	ratio abscessed : normal
rat 1	3.97
rat 2	2.76
mean	3.365

This is appreciably greater than obtained with the Tc–OEP complex, probably due to better solubility characteristics

Figure 28 shows a series of photographs obtained from a static scan taken on two rats injected with the preparation. One rat has an abscess in the right leg and the other has an internal abscess and also one in the right leg.

Figure 28.1:

A. Static, 30 minutes, normal, internal abscess.

A. Active marker placed on collimator at level of kidneys.

B. Kidneys.

C. Abscess.

B. Static, 1 hour, zoom, internal abscess.

A. Kidneys

B. Abscess.

A


24 X1 PHOTO
INT. ABSC./30 MIN
A
B
C
0

B


55 X1 PHOTO
INT ABSC;
1 HOUR
ZOOM
A
B
0

Figure 28.2:

A. Static, normal, internal and leg abscess.

A. Head.
B. Right hind leg (abscess).

B. Static, 1 hour, density boost.

A. Head.
B. Right hind leg (abscess).
C. Tail.

C. Static, 1.4 hours, density boost.

A. Head.
B. Left hind leg (normal).
C. Right hind leg (abscess).
D. Tail.

D. Static, 1.8 hours, density boost.

A. Head.
B. Right hind leg (abscess).
C. Tail.

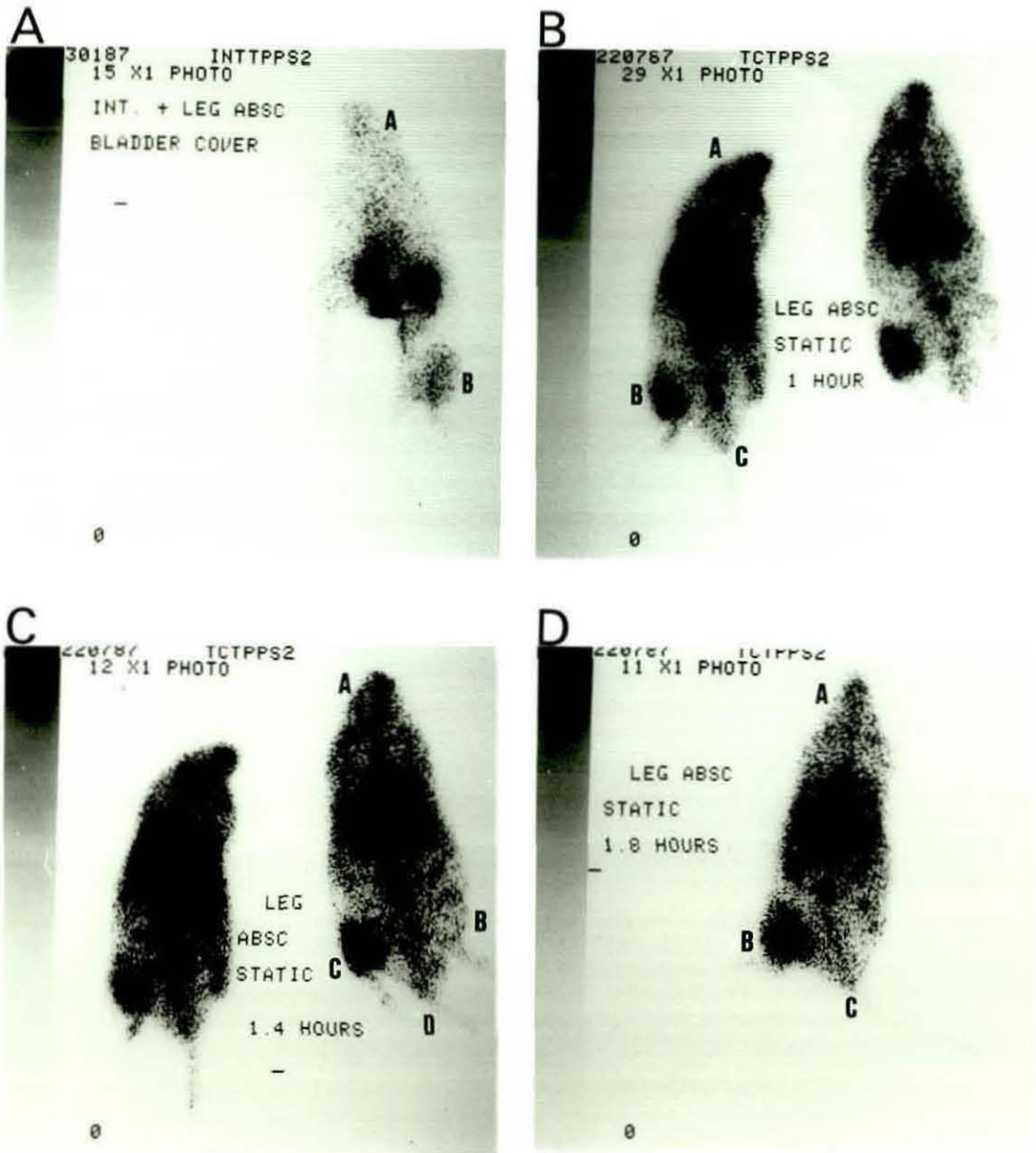
A
30187 INTTPPS2
15 X1 PHOTO
INT. + LEG ABSC
BLADDER COVER
A
B
0
B
220767 TCTPPS2
29 X1 PHOTO
A
LEG ABSC
STATIC
1 HOUR
B
C
0
C
TCTPPS2
12 X1 PHOTO
A
B
LEG
ABSC
STATIC
C
1.4 HOURS
D
0
D
11 X1 PHOTO
A
LEG ABSC
STATIC
1.8 HOURS
B
C
0

3.4 Phthalocyanine Studies.

Phthalocyanine (Pc) is insoluble in glacial acetic acid, even on prolonged heating, and so in this case the synthesis reverted back to using phenol as the solvent and hence the phenoxide rather than the acetate would be prepared. Figure 29 shows the electronic spectrum of free base phthalocyanine with absorptions at 691, 656, 595, 415 and 240nm. By comparison the Tc–Pc complex shows absorptions at 669, 605 and 412nm in the visible region (figure 30) and also at 258nm in the UV.

The control reaction (equivalent to the formation of the protonated species in the previous reactions) of simply phthalocyanine and phenol yields a product with absorptions at 688, 671, 654 and 242nm as shown in figure 31. The redox reactions of the Tc–Pc complex were carried out in the same manner as for the other complexes, however no real changes occurred in any of the spectra. This suggests that perhaps ligand exchange reactions are not so straight forward with the phenoxide as compared to the acetate.

Mass spectrum studies have not been performed on this complex and preliminary animal studies suggest that the activity is predominantly confined to the liver.

Figure 29.

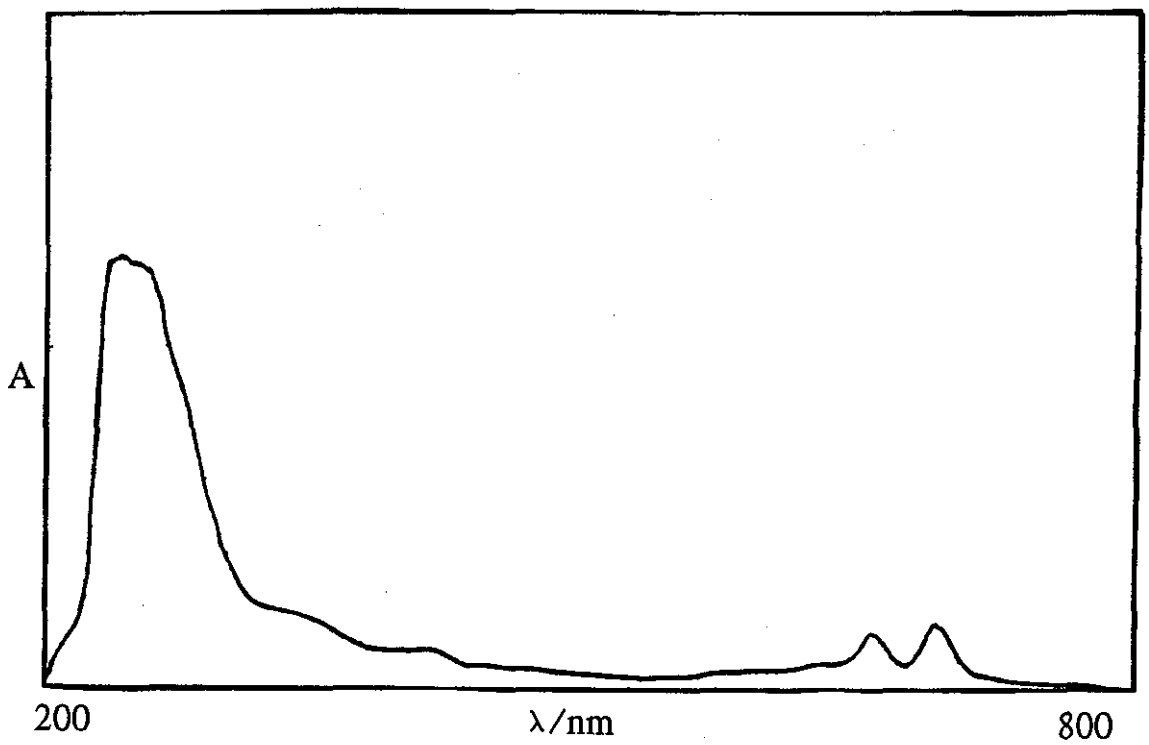

Absorbance (A) is in arbitrary units.

Figure 29 shows the electronic spectrum of phthalocyanine.

Figure 30.

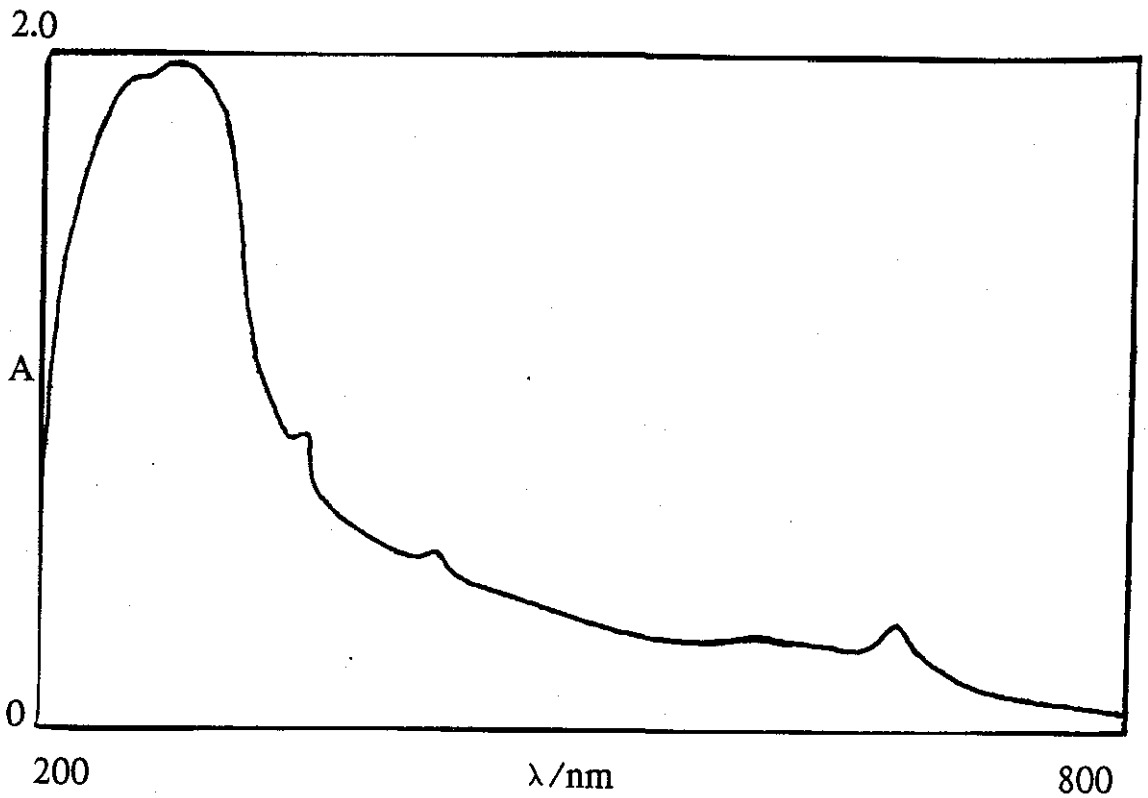

Figure 30 shows the electronic spectrum of the Tc–Pc complex.

λ_{max}/nm	Σ /mol^{-1}dm^{3}cm^{-1}
669	1.28x10^3
605	1.32x10^3
412	2.21x10^3
258	8.25x10^3

Figure 31.

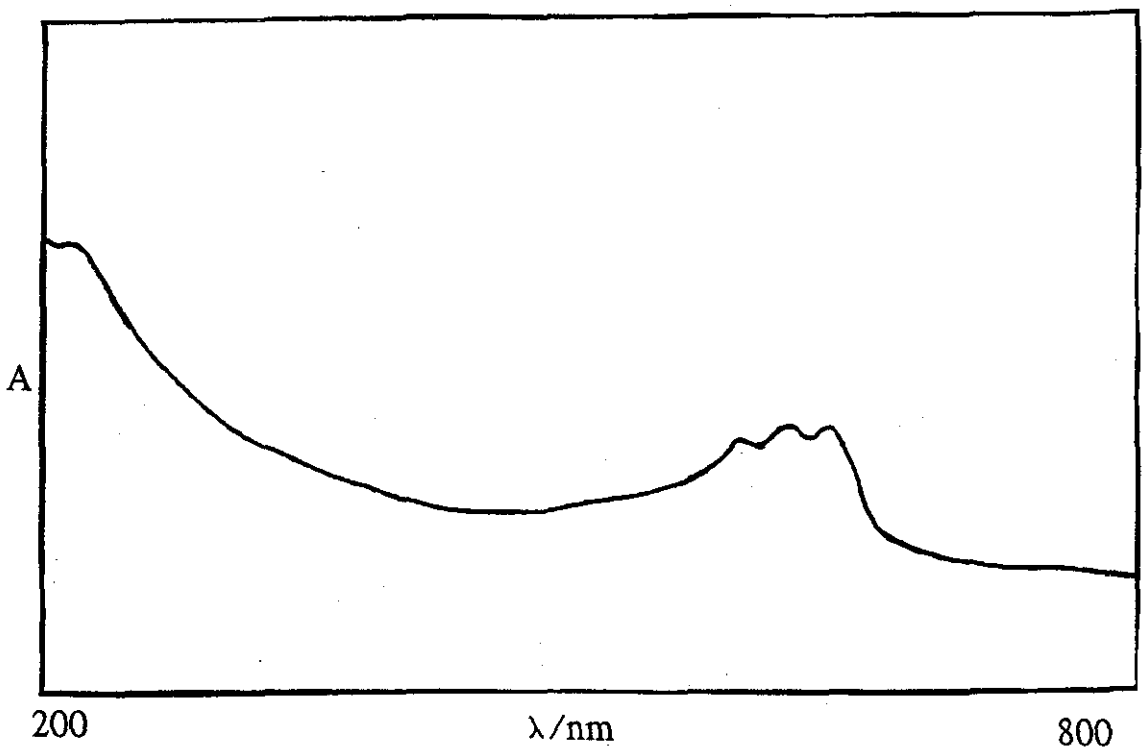

Absorbance (A) is in arbitrary units.

Figure 31 shows the visible spectrum of the product from the control reaction between phthalocyanine and phenol.

4. Conclusions and Future Work.

In conclusion it can be said that this project achieved its aim in synthesising novel technetium–porphyrin complexes of the general formula PorphTc(O)OAc, via a novel route starting with the metal oxide as opposed to the metal acetate, and also carried out preliminary biological evaluation tests on most of the complexes synthesised.

The most logical forward step from here would be to study the reduced species that have lost the technetium oxo core and try to develop a preparation suitable for injectable purposes. This would provide a potentially valuable alternative since most of the present technetium radiopharmaceuticals contain the Tc=O core.

Furthermore, it will also be of importance to study in greater detail the true biodistribution of these complexes *in vivo*. These studies should include the assessment of the degree of metabolism of such ligands so that an accurate idea of the significance of the observed signal can be concluded. This will allow a more detailed characterisation of the usefulness of Tc–labelled porphyrins in the imaging of specific clinical conditions.

REFERENCES.

[1] R. Colton, *The Chem. of Re and Tc,* Wiley–Interscience, **1966.**

[2] G. Subramanian, B.A. Rhodes, J.F. Cooper and V.J. Jodd (ed), *Radiopharmaceuticals*, J.N.M., N. York, **1975.**

[3] I. Ikeda, O. Inone and K. Kuvata, *Int. J. Nuc. Med and Biol,* **1977,** *4*, 56.

[4] M. Molter, *Chem. Ztg.*, **1979,** *103*, 41.

[5] G.D. Zanelli *et al, N. Med. Comm.*, **1986,** *7*, 17.

[6] L.J. Boucher, Coord. *Chem. Rev.*, **1972,** *7*, 289.

[7] A. Goldberg and C. Rimington. *Diseases of Porphyrin Metabolism*, Thomas, Springfield, Mass., **1962.**

[8] G.A. Kyriazis, H. Balin and R.L.Lipson, *Am. J. Obstet. Gynecol.*, **1973,** 376.

[9] A.D. Adler (ed), *The Chemical and Physical Behaviour of Porphyrin Compounds and Related Structures, Ann. N.Y. Acad Sci.*, **1973,** 206.

[10] D. Ostfeld and N.Tsutsui, *Acc. Chem. Res.*, **1974,** *7*, 52.

[11] J.E. Falk, *Porphyrins and Metalloporphyrins,* Elsevier, N.York, **1964.**

[12] M. Tsutsui *et al, J. Am. Chem. Soc.*, **1969**, *91*, 6262.

[13] C.P. Wong et al, J. Am. Chem. Soc., **1974**, 96, 7149.

[14] A.D. Adler *et al, J. Inorg. Nuc. Chem. Lett.*, **1970**, *32*, 2443.

[15] J.W. Buchler and K. Rohbock, *Inorg. Chem. Lett.*, **1972**, *8*, 1073.

[16] L.J. Boucher, *J. Am. Chem. Soc.*, **1968**, *90:24*, 6640

[17] M. Tsutsui, *J. Am. Chem. Soc.*, **1975**, *97:14* 3952.

[18] G.D. Dorough *et al, J. Am. Chem. Soc.*, **1951**, *73*, 4315.

[19] M. Gouterman, *J. Mol. Spectrosc.*, **1972**, *44*, 37.

[20] J.R. Platt, *Radiation Biology* (A. Hollaender ed.), Vol III, Ch. 2, McCuran-Hill, N. York, **1956**.

[21] M. Gouterman *et al, J. Mol Spectrosc.*, **1965**, *16*, 451.

[22] M. Gouterman *et al, J. Mol Spectrosc.*, **1971**, *38*, 16.

[23] A. Treibs, *Ann. Chem.*, **1969**, *728*, 115.

[24] M. Calvin, *Rev. Pure Appl. Chem.*, **1965**, *15*, 1.

[25] G.D. Zanelli *et al, Br. J. Radiol.*, **1981**, *54*, 403.

[26] N. Forster *et al, J. Nuc. Med.*, **1985**, *26*, 756.

[27] H. Fischer and R. Baumler, *Liebigs Ann. Chem.*, **1928**, *468*, 58.

[28] A.Antonini and M. Brunon, *Hemoglobin and Myoglobin in their reactions with ligands*, North-Holland, Amsterdam, **1971**.

[29] M. Gouterman, *J. Chem. Phys.* **1959**, *30*, 1139.

[30] F. Baumann *et al, Angew Chem.*, **1956**, *68*, 133.

[31] J. Rousseau *et al, Int. J. Appl. Rad. Isot.*, **1983**, *34(3)*, 571.

[32] J. Rousseau *et al, Int. J. Appl. Rad. Isot.*, **1985**, *36(9)*, 709.

[33] K. Yoshihava *et al, Radiochim. Acta.*, **1974**, *21*, 96.

[34] J.W. Buchler *et al, Ann. N. Y. Acad. Sci.*, **1973**, *206*, 116.

[35] A.G. Jones and A. Davison, *Inorg. Chem.*, **1983**, *22*, 2292.

[36] J.W. Buchler in D.H. Dolphin (ed), *The Porphyrins, Vol 2, Academic Press*, **1978**, Chap. 10, p389.

PART TWO

The Properties of Opioid Agonist and Antagonist Binding

CHAPTER1: GENERAL INTRODUCTION

1.1 Historical

Pain is a subjective experience that is interpreted as symptomatic evidence of actual or potential tissue damage. Nociception is the nervous process giving rise to the sensation of pain and therefore serves a useful function in that it signals the presence of an injurious stimulus. The sensation of pain is often dependent on the psychological state of the individual. However it is not always possible to cure the underlying cause of discomfort and as a result drugs that can alleviate the pain and associated anxiety are extremely useful.

Drugs used to relieve pain are known as "analgesics". This term comes from the Greek word meaning "painlessness". The main group of compounds that are used clinically to relieve severe pain are termed "opioid analgesics". The term opioid is derived from the word opium, describing the unripe exudate from the poppy *Papaver Somniferum*. The effects of opium were known to the ancient Babylonians around 4000 BC, being used to pacify children and as a sleeping draught. Opium first appeared in a medical text in China (1000 AD) as a treatment for diarrhoea.

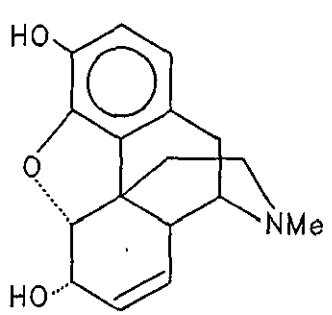

Figure 1.1: Morphine

In 1803, the chief alkaloid component was isolated from opium by the German pharmacist Serturner who called it "morphia" (after Morpheus, the Greek god of dreams). The name morphine is now used in accordance with alkaloid nomenclature (figure 1.1). Although it is the most exploited analgesic compound, it also has a range of other pharmacological actions (table 1.1).

Table 1.1: Pharmacological actions of morphine

Central nervous system
Analgesia
Euphoria/dysphoria
Sedation (although excitation in some species such as cat)
Antitussive
Respiratory depression
Hypotension
Miosis (pin-point pupils)
Nausea and vomiting
Tolerance and dependence

Peripheral effects
Constipation
Bronchial constriction
Dilatation of cutaneous blood vessels
Pruritis

Due to these various effects, but mainly those of euphoria and dependence which give rise to abuse potential, a wide range of analogues have been synthesised in an attempt to produce an analgesic devoid of unwanted properties. However, although many novel and active compounds have

been prepared and evaluated morphine is still largely the drug of choice for severe pain.

1.2 The Opioid Receptor

It is necessary to understand the interaction of the drug in a physiological system in order to avoid wasted effort in the search for novel compounds. Largely the effect of a drug leading to a biological response can be explained by an interaction between the drug molecules and a macromolecular complex known as a receptor. Various possibilities of interaction exist, for example the drug may activate the receptor and thus trigger a response. A compound with such effect is known as an agonist. Conversely an antagonist will block the effect of an agonist i.e. it has "affinity" for the receptor but no "efficacy" to stimulate a response . Some compounds fall between these two categories and are known as partial agonists or mixed agonist–antagonists. Such compounds have affinity for the receptor but can never achieve a maximal response compared to a pure agonist.

Early manipulations of the morphine molecule resulted in antagonists such as nalorphine (1) shown in figure 1.2. This compound antagonises the effects of morphine (3,4) however nalorphine also produces analgesia (5). This observation led Martin (6) to propose that morphine and nalorphine act at different receptors. Other ideas of multiple receptors in agreement with this were those of Portoghese (7) based on stereochemical requirements of methadone–like compounds. This expanded the concept initially described by Beckett and Casy (8), which considered a single receptor. The development of naloxone (2, figure 1.3) as a pure antagonist led to the definition of opioid receptor involvement in an observed response being sensitive to naloxone.

Using the chronic spinal dog preparation Martin and colleagues (9–12) observed the effects of a number of morphine related compounds. Differences in behaviour, sensitivity to antagonism by naloxone and the related antagonist naltrexone (figure 1.4), and cross tolerance led them to conclude the presence of three different receptors in this preparation each identified with a prototypic agonist. Morphine effects were said to be mediated by μ – receptors, ketocyclazocine (figure 1.5) by κ–receptors and n–allylnormetazocine (figure 1.6) by σ –receptors.

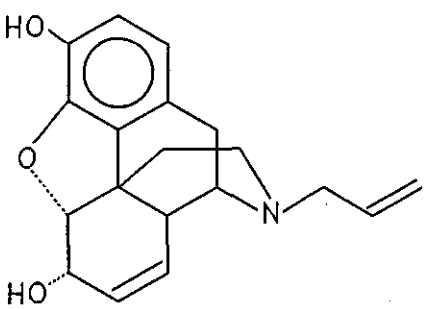

Figure 1.2: Nalorphine

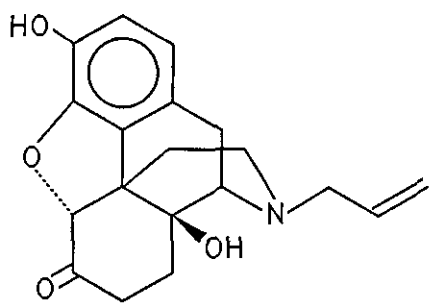

Figure 1.3: Naloxone

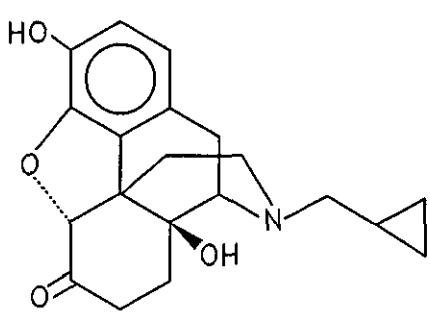

Figure 1.4: Naltrexone

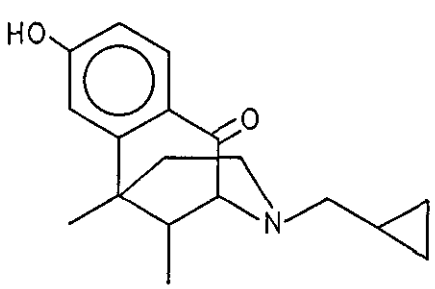

Figure 1.5: Ketocyclazocine

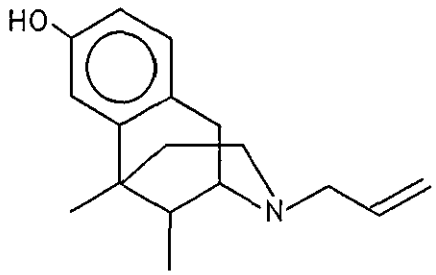

Figure 1.6: N-allylnormetazocine [SKF10,047]

In vitro bioassays developed by the Kosterlitz group to examine opioid drugs such as the guinea-pig ileum myenteric plexus longitudinal muscle and the mouse vas deferens endorsed the existence of opioid μ- and κ-receptors. Electrical stimulation of these tissues elicit contractions which can be reduced in a dose-dependent manner by opioid agonists. The investigators found that ketocyclazocine along with other benzomorphans had only one quarter of the agonist potency in the mouse vas deferens as in the guinea-pig ileum compared to normorphine (13).

Complementary to these bioassays was the development of radioligand binding studies, which also added further evidence of a heterogeneous population of opioid receptors. Binding assays, unlike pharmacological bioassays which measure a response are concerned with the investigation of the recognition sites for a particular compound. These recognition sites are normally located on a receptor and their interaction with an opioid ultimately leads to the biological response. Goldstein (14) demonstrated the stereospecificty of binding by comparing levorphanol (figure 1.7) with its (+) isomer dextrorphan. However this only represented 2% of the total binding of the tritiated ligand to mouse brain homogenates. The later availability of opioids labelled with greater specific activity, initially [^{3}H]naloxone and [^{3}H]etorphine, has allowed stereospecific binding of >90%

and thus more detailed studies (15–19).

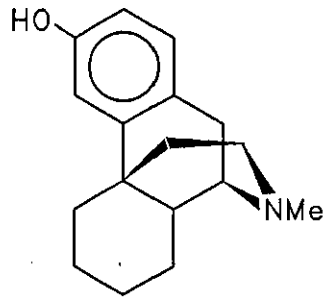

Figure 1.7: Levorphanol

Binding of opioids to specific receptor sites is complex and influenced by a number of factors. Specific binding is reduced by proteolytic enzymes and alkylating agents such as N–ethylmaleimide. This suggests that the recognition site occurs in a protein environment with sulphydryl groups nearby (15). Further studies suggested the presence of two thiol groups, one close to the binding site on the receptor and one more remote that appears to control affinity (84, 85). Opioid binding is also affected by temperature and pH (16), and monovalent cations in particular sodium (15,16,20). In general agonist affinity is reduced in the presence of NaCl whereas the affinity of antagonists is unchanged or even increased (20,21). This led to the separation of so–called "agonist" and "antagonist" conformations of the receptor.

Subcellular fractionation of brain tissue showed opioid binding sites to mainly occur in the synaptosomal fraction (19,22). This suggests a location on nerve terminals implying a role in synaptic function.

1.3 Endogenous Opioid Peptides

It became apparent to investigators that if opioid receptors occur within the body then endogenous modulators must exist. Martin (6) suggested that 'morphine-like compounds might mimic an ongoing biochemical process'.

In 1975 Hughes and Kosterlitz isolated from porcine brain substances possessing opioid-like activity which they termed enkephalins (23). These were shown to be two pentapeptides namely [Leu^5]enkephalin and [Met^5]enkephalin, the variation occuring at the C-terminus. Figure 1.8 shows the enkephalins. Subsequently various extended derivatives of these peptides have since been discovered.

The peptide β-lipotropin was shown to contain the [Met^5]enkephalin sequence as amino acid residues 61-65 (24). Digestion of the peptide by trypsin caused release of a so-called C-fragment, residues 61-91 (25). This residue was found to exist in porcine pituitary (26) and in isolated tissue bioassay had opioid activity thirty times that of [Met^5]enkephalin (27). The parent peptide β-lipotropin had no such activity and the C-fragment was renamed β-endorphin (28).

A third group of endogenous opioid peptides was isolated by Goldstein (29). These were shown to be extensions of [Leu^5]enkephalin. Initially a thirteen amino acid peptide was discovered to be highly potent in opioid bioassay systems and was named dynorphin A(1-13). Subsequently other dynorphin fragments have been recognised (see Table 1.2).

As can be seen from Table 1.2, the three groups of endogenous peptides derive from different precursors. The products are released by cleavage at basic amino acid residues, thus proenkephalin (A) gives rise to the enkephalins (30), β-endorphin is derived from proopiomelanocortin (31)

and the dynorphins result from prodynorphin (30).

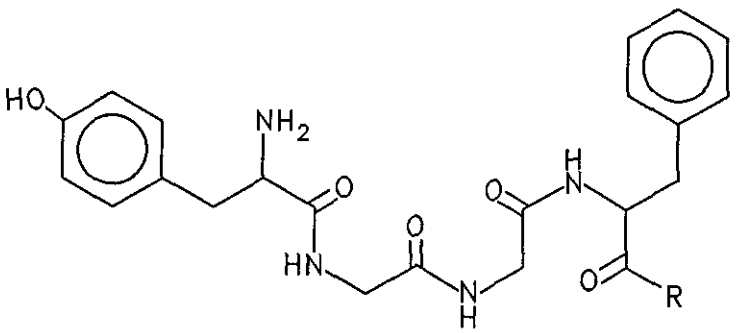

Tyr–Gly–Gly–Phe–R

when R=

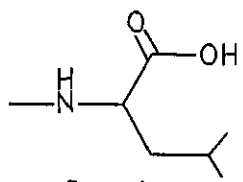

Leucine

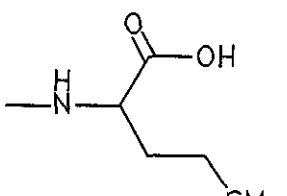

Methionine

Figure 1.8: **THE ENKEPHALINS**

Table 1.2: The Major Endogenous Opioid Peptides

Opioid Peptide	Precursor	Reference
[Met^5] enkephalin	proenkephalin A	30
[Leu^5] enkephalin	proenkephalin A	30
β-endorphin	proopiomelanocortin A	31
Dynorphin A (1-17)	prodynorphin	29, 30
Dynorphin A (1-13)	prodynorphin	29
Dynorphin A (1-9)	prodynorphin	

β-endorphin is: Tyr-Gly-Gly-Phe-Met-Thr-Ser-Glu-Lys-Ser-Gln-Thr-Pro-Leu-Val-Thr-Leu-Phe-Lys-Asn-Ala-Ile-Ile-Lys-Asn-Ala-His-Lys-Lys-Gly-Gln

Dynorphin A (1-17) is: Tyr-Gly-Gly-Phe-Leu-Arg-Arg-Ile-Arg-Pro-Lys-Leu-Lys-Trp-Asp-Asn-Gln

However, the use and investigation of natural peptides in both *in vitro* and *in vivo* systems is hampered by the problems of metabolism and degradation (32). These difficulties have in some way been overcome in two different manners. In the enkephalins, the substitution of Gly^2 with D-Ala (33) and Leu^5 or Met^5 by the corresponding D-isomer (34) has resulted in increased agonist potency without affecting receptor selectivity. As an alternative inclusion of specific enzyme inhibitors to reduce proteolysis at the N-terminus, Gly^3-Phe^4 bond and C-terminus has also been successful (35).

The actions of the enkephalins in the guinea-pig ileum and mouse vas deferens could not be accounted for in terms of opioid μ-, κ- and σ-receptors as defined by Martin. [Met^5]enkephalin was twenty times more potent than normorphine in the mouse vas deferens whilst the two compounds were equipotent in the guinea-pig ileum (24). In addition to this in the mouse vas deferens the enkephalins required ten times more naloxone to antagonise their effects than did morphine. However in the guinea-pig ileum the same amount of naloxone would antagonise both morphine and the enkephalins (36). From these observations Kosterlitz proposed two types of receptor for opioid peptides. These were the μ-receptor at which morphine acts preferentially and which predominates in the guinea-pig ileum and the δ-(enkephalin preferring) receptor, predominating in the mouse vas deferens. However the κ-receptor, for which the benzomorphans show selectivity, is also found in the guinea-pig ileum (36, 37). Subsequently the mouse vas deferens has been shown to possess μ-, δ- and κ-receptors (38). Today these are the three recognised opioid receptors, with the σ-site of Martin considered non-opioid, since naloxone reversibility, an essential feature of opioid activity is not observed (81). This classification was confirmed by binding studies in particular with the availability of selective ligands as discussed below.

1.4 Improved Selectivity of Drugs

Structural modification of the enkephalin molecule has been employed to improve selectivity at both μ- and δ-receptors. For example Tyr-D-Ala-Gly-MePhe-Gly-ol (DAGOL) is a selective μ-agonist (39,40). The bis-penicillamine derivative [D-Pen^2, D-Pen^5]enkephalin (41, figure 1.9) is highly δ-selective. Not only do these compounds show increased selectivity but they are also more stable with greater resistance to proteolysis.

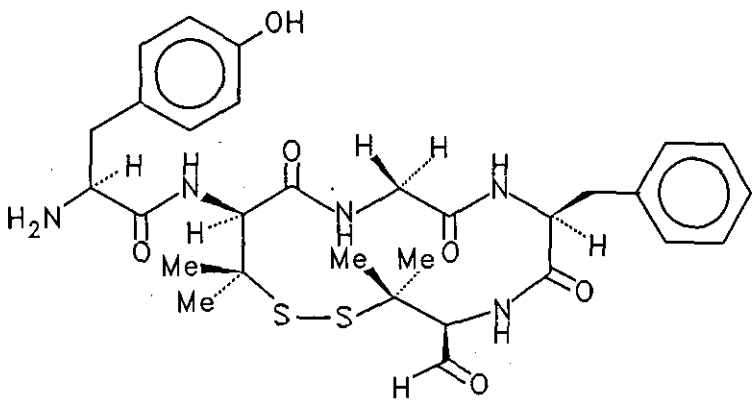

Figure1.9: [D-Pen^2,D-Pen^5]enkephalin

The early κ-agonists which included compounds such as ethylketocyclazocine and bremazocine (figure 1.10) displayed degrees of cross-reactivity with μ- and δ-sites (42-47). However by using appropriate concentrations of selective agonists to suppress binding at μ- and δ-sites, a more accurate study of the κ-site was possible and confirmed the presence of this receptor type in rat and guinea-pig brain (44-46). This was not ideal and now more selective κ-agonists are available , for example U-50488H and U-69593 both made by the Upjohn company (48-50). These two compounds are benzeneacetamide derivatives and differ structurally from the peptide and opiate alkaloid nucleus (see figures 1.11

and 1.12). Suggestions that these compounds may recognise a subtype of the κ-opioid receptor are discussed in the following section.

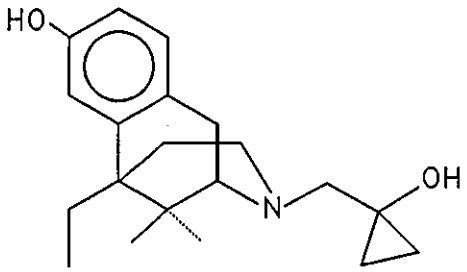

Figure 1.10: Bremazocine

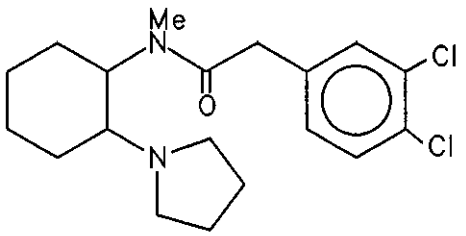

Figure 1.11: U-50488H

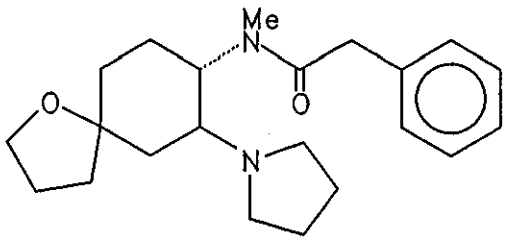

Figure 1.12: U-69593

Similarly with antagonists most of the early compounds were unselective such as naloxone (2), or showed a small degree of selectivity such as MR2266 (44). However in more recent years a number of highly selective antagonists for all three opioid receptors have become available, such as ICI 174864 (55). These are discussed in more detail later.

1.5 Receptor Subtypes

Perhaps the most controversial aspect of recent opioid research has been the subject of opioid receptor subtypes. Thus various investigators have claimed the presence of subtypes for both μ– and κ–opioid receptors.

1.5.1 μ–Subtypes

In 1975 Pasternak and coworkers (61) reported high and low affinity binding components using [^{3}H] dihydromorphine and [^{3}H] naloxone in rat brain preparations both by competition and saturation assays. Subsequent analysis using the stable peptide [^{3}H]D–Ala^2, D–Leu^5]enkephalin and [^{3}H]dihydromorphine in competition assays with a variety of unlabelled ligands led them to name the high affinity component μ_1 which was claimed to be a common site for both opiates such as morphine and peptides such as [D–Ala^2, D– Leu^5]enkephalin (62). The low affinity component was composed of a μ_2–(morphine) site and a δ–(enkephalin) site. Further evidence for this μ_1/μ_2 subdivision was revealed by the use of two irreversibly acting antagonists. These compounds, namely naloxazone (figure 1.13) and naloxonazine (figure 1.14) are based on the structure of naltrexone and were claimed to irreversibly eliminate the the high affinity (μ_1) component (63–65). Because these compounds had the same effect on the binding of a series of μ–, δ–and κ–agonists and some antagonists (65,66) the investigators suggested that the high and low affinity states did not correspond to agonist/antagonist conformations controlled by NaCl.

Naloxazone and naloxonazine have also been used to evaluate the *in vivo* pharmacological significance of μ_1–sites in both rats and mice. Pasternak and coworkers (67) proposed that μ_1–sites were responsible for supraspinal analgesia, since pretreatment with either naloxazone or naloxonazine caused an 11–fold shift in the ED_{50} of morphine as measured by tail flick and

writhing (68). However, μ_1 blockade did not alter the respiratory depression caused by morphine (68,69) or signs associated with dependence (70).

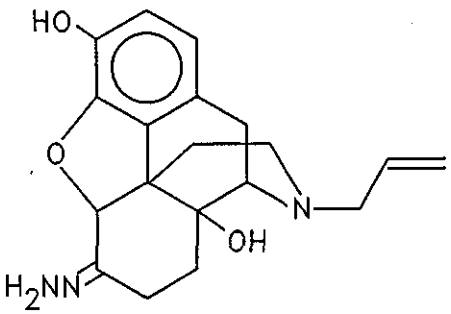

Figure 1.13: Naloxazone

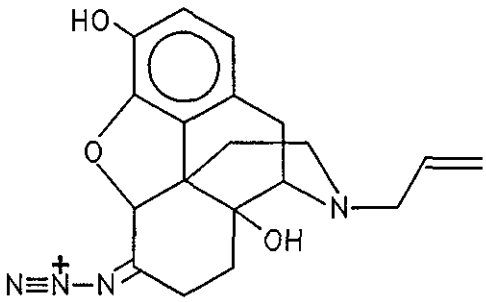

Figure 1.14: Naloxonazine

1.5.2 κ–Subtypes

In recent years much interest has been focussed upon the κ–opioid receptor. This is due to the fact that agonists acting at this site display much less respiratory depression and euphoria. However, they do exhibit other side-effects such as psychomimetic actions (71) and sedation (17).

The first reported suggestion that the κ–receptor population was not homogeneous and may comprise subtypes appeared in 1982 (72). The binding of [^{3}H]ethyl ketocyclazocine to guinea-pig spinal cord, a tissue the authors believed contained no μ– or δ– receptors as no binding was observed with labelled dihydromorphine or [D–Ala^2, D– Leu^5]enkephalin, was shown to be heterogeneous. The binding was separated into two components by [D–Ala^2, D–Leu^5]enkephalin (DADLE). These two components were named κ_1 (DADLE sensitive) and κ_2 (DADLE insensitive). However these results

could be accounted for by the unselectivity of the radioligand and also the presence of μ– and δ–sites (165). More recent studies have shown that suppression of these sites still left a non–homogeneous population (156).

The introduction of synthetic κ–selective agonists such as U–50488H and U–69593 (48,50) appeared to complicate matters further. These compounds and also the endogenous dynorphins have been shown (73,74,48) to recognise a subpopulation of κ–sites recognised by compounds such as EKC as traditionally defined by Martin (17). Because of this they appear to displace the κ–component defined by unselective labelled ligands such as bremazocine and diprenorphine in a biphasic manner (75–77). Morris and Herz (78) presented an autoradiographic study of [^{3}H]diprenorphine (an unselective antagonist) in rat brain which demonstrated naloxone sensitive binding sites that could not be accounted for in terms of μ–, δ– or κ– (U–50488H sensitive) sites, and may well therefore be subtypes of the κ–opioid site.

Functional studies have also been employed to try and distinguish κ–receptor subtypes. Studies (80) suggest that in the mouse vas deferens chronic administration of κ–opioids causes tolerance. A range of κ–agonists exhibited different degrees of cross–tolerance, suggesting heterogeneity. For example, vasa from mice tolerant to ethylketocyclazocine (EKC) showed only partial cross–tolerance towards Mr2034. Another functional assay implying κ–heterogeneity concerns neuroendocrine function. Iyengar and colleagues (160) showed that the actions of four κ–agonists, Mr2034, U–50488H, EKC and tifluadom, in raising plasma corticosterone levels and lowering plasma TSH levels were reversed by naloxone, but only the effects of tifluadom and EKC were reversed by WIN 44,441–3 (a non– selective antagonist). However, many of these agonists are not particularly selective (107), and so it is difficult to conclude whether subtypes of the κ–opioid receptor do actually exist.

One major problem appears to be in the actual definition of the kappa receptor itself, and unequivocable conclusions cannot be made until such a definition can be agreed and furthermore a convincing physiological assay is designed. This situation may well be aided by Portoghese's recent κ-selective antagonist norbinaltorphimine (57). Molecular biology techniques which will distinguish chemical differences between proteins will provide a definitive answer.

1.6 G Proteins and Opioid Receptors

Presently most binding assays are performed in low ionic strength buffers such as Tris.HCl. However this is far from physiological conditions due to a lack of many ions and nucleotides, which control the functioning of receptor and effector proteins in the membrane. Consequently such binding assays show little correlation with *in vitro* and *in vivo* pharmacological observations (58).

The observation that sodium ions decrease agonist binding without affecting antagonist binding was one of the first discoveries in opioid binding experiments (20, 82). Similarly, the finding that guanine nucleotides (i.e. GTP and analogues) regulate the binding of opioids was the key that associated opioid receptors with G-protein (receptor-controlled guanine nucleotide-binding regulatory protein) function. Early studies (83–85) showed that guanine nucleotides decreased opioid agonist binding in both brain membranes and also in neuroblastoma x glioma NG108-15 cells (86). In these preparations the effects were shown to be specific for guanine nucleotides, since adenine and other nucleotides were ineffective. Childers and Snyder (84,85) showed that guanine nucleotides effectively discriminated between agonist and antagonist binding when assays were conducted in the presence of sodium ions. The same investigators (85) demonstrated that guanine nucleotides increase both association and dissociation rates of opioid

binding. Dissociation rates are increased more than association rates and the net result of GTP (or analogues of GTP) addition is a decrease in steady-state binding.

There are many parallels between the actions of sodium ions and those of guanine nucleotides including:

i) Both sodium ions and GTP affect agonist but not antagonist binding, although the maximum agonist-antagonist differentiation of GTP effects are seen only in the presence of sodium ions (85).

ii) Both affect kinetics of agonist binding by increasing dissociation rates (85).

iii) Effects as analysed by Scatchard plots (see chapter 3) of the data are confusing with reports of both a decrease in agonist affinity and receptor number (Bmax) (87, 82). These contradictions may be explained by reference to other receptor systems. For example, with muscarinic cholinergic receptors, GTP eliminates agonist binding sites because the affinity of agonist binding has decreased to a point where it is not detectable in binding assays (88). The net result is a decrease in Bmax although the mechanism involves a decrease in affinity.

iv) The effects of both are specific (83-86).

v) Reactions involving sulphydryl blocking agents such as N-ethylmaleimide affect both sodium and guanine nucleotide regulation of opioid binding (89). However, reagent effects are opposite, decreasing regulation of binding by guanine nucleotides while increasing regulation of binding by sodium.

vi) Sodium and guanine nucleotide effects are additive, at least for μ- and δ-sites (85), although uncertainty surrounds κ-sites (90).

These results suggest that sodium and guanine nucleotides may act at separate, though related sites, to regulate opioid agonist binding. The net effect of the addition of sodium ions and/or guanine nucleotides appears to shift the binding site into a low agonist affinity state. The mechanisms involved are not entirely understood, however many ideas are emerging with increased knowledge of receptor-effector systems.

Receptor-controlled guanine nucleotide-binding regulatory proteins (G proteins) that function as intermediaries in transmembrane signalling pathways consist of three major protein groups : receptor, G protein and effectors (91). The involvement of a G protein in signal transduction was first suggested by the requirement of GTP for hormonal activation of adenylyl cyclase (92). Since then many neurotransmitters including opiates (93) have been shown to mediate inhibition of adenylyl cyclase by a GTP-dependent process. These receptors are sensitive to sodium ions and the negative heterotropic effects of guanine nucleotides on agonist binding are observed with the same membranes showing the GTP dependency of agonist inhibition of adenylyl cyclase (94). These findings suggest that receptor-G protein complexes are involved in the inhibitory process. The G protein involved in this inhibition of adenylyl cyclase has been termed Gi. This protein was isolated and identified following a study of the mechanism of action of pertussis toxin elaborated by Bordetella pertussis (95, 96). The effects of the toxin on the enzyme adenylyl cyclase appeared to result from ADP-ribosylation of a 41-kd membrane protein. Purification of the substrate for pertussis toxin revealed a guanine nucleotide-binding protein. Other G proteins are also known, Gs stimulates adenylyl cyclase and therefore has the opposite effect to Gi. Another G protein exists whose

exact function is unknown and is termed Go (99).

Based on studies of β –adrenergic receptors, DeLean and coworkers proposed a ternary complex model (98) to explain agonist specific binding properties. The model involves the interaction of the agonist (A), the receptor (R) and an additional component assigned X. This component X was postulated to represent a G protein (nucleotide binding site). The model is reproduced in figure 1.15.

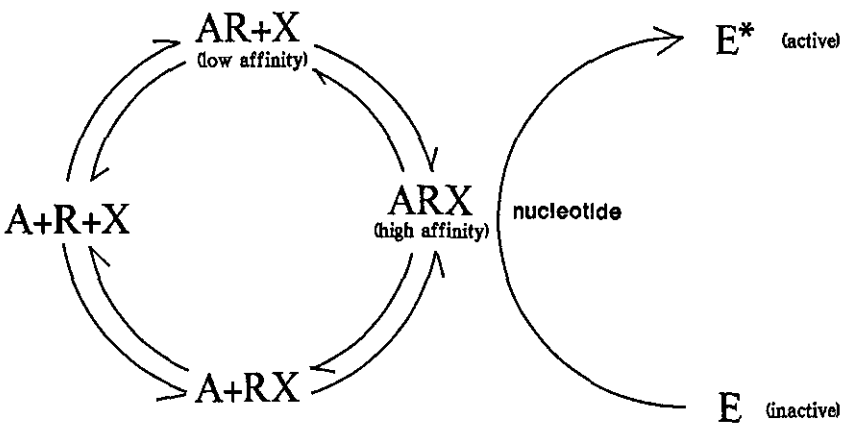

Figure 1.15

More recently Gilman has proposed a cyclic scheme explaining interactions of receptor, G protein, nucleotide and effector (99). This scheme is reproduced in figure 1.16, and is also based on the β –adrenergic receptor. However, it has become accepted as a general model of receptor–G protein interaction applicable to opioid systems (59, 100).

The interaction between R and G is antagonised by guanine nucleotide, either GTP or GDP. The AR complex stimulates dissociation of G.GDP which precedes binding of GTP. AR also stimulates nucleotide binding even when most of the bound GDP has been induced to dissociate by interaction of G.GDP with AR. The accumulation of significant levels of Gα.GTP via AR–stimulated nucleotide exchange leads to the stimulation of steady–state

GTPase activityof the G protein. This, in turn activates the effector system. Reconstitution of R and G results in the establishment of guanine nucleotide–sensitive agonist binding to the receptor.

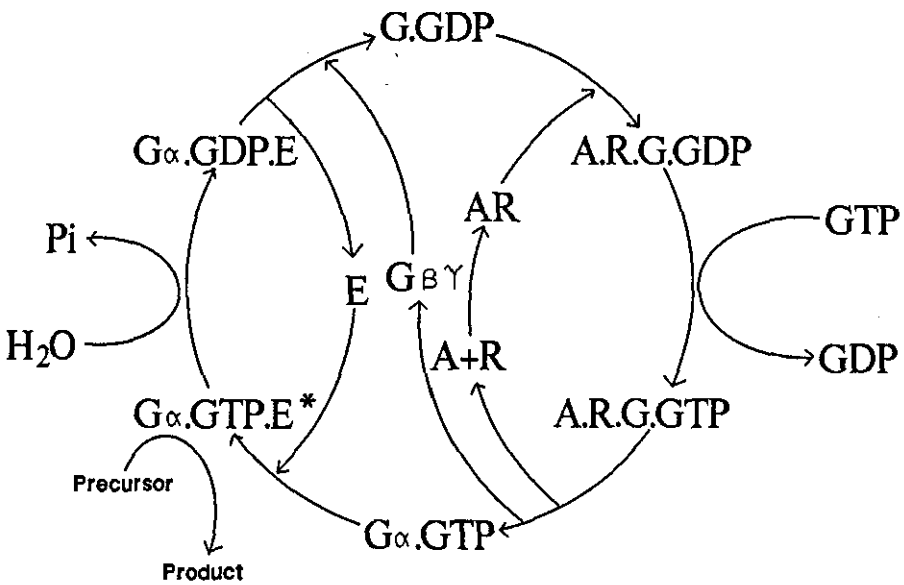

Figure 1.16

1.7: Aims

Most binding assays are performed in low ionic strength buffers. The purpose of the present project was to characterise opioid binding under conditions in which Na^+ ions and guanine nucleotides are present. Since this results in loss of agonist affinity (58) it is likely to be necessary to use [^{3}H]antagonists to accurately define opioid sites under these conditions. Thus the profiles a series of selective opioid antagonists were to be studied. Suitable examples of these ligands would then be used to further knowledge of opioid binding sites and also opioid–sensitive isolated tissue bioassay preparations, and therefore provide data more meaningful for comparison of *in vitro* with *in vivo* studies.

CHAPTER 2: MATERIALS AND METHODS

2.1: Animals

Male animals were used throughout the study.

Wistar rats (250–300g) were supplied by the Animal Unit, University of Nottingham.

Dunkin–Hartley guinea–pigs (300–400g) were obtained from David Hall, Newchurch, Burton–upon–Trent.

Animals were fed on standard laboratory diet (Pilsbury) and kept in cages of 3–6 animals under ambient temperature (20°C), in a dark–light cycle of 12 hours. Guinea–pig diet was supplemented with vitamin C added to the drinking water.

2.2: Chemicals

2.2a: General

Ecoscint A scintillation fluid, National Diagnostics, Somerville, New Jersey, U.S.A.

Trizma Base (Tris(hydroxymethyl)aminomethane), Sigma, Poole, U.K.

5'–guanylylimidodiphosphate sodium salt (GppNHp) was purchased from Sigma, Poole, U.K. and stored dessicated at –20°C prior to use.

Unless otherwise stated all other chemicals used were of analytical grade.

2.2b: Drugs and Peptides

The following were purchased as shown:

D-Phe,Cys,Tyr,D-Trp,Orn,Thr,Pen,Thr-NH_2 (CTOP), Peninsula Laboratories, Wigan, U.K.

Dynorphin 1-13, [D-Pen^2, D-Pen^5]enkephalin and ICI 174864 (N,N-diallyl-Tyr-Aib-Aib-Phe-Leu-OH) arginine salt (where Aib = α-aminoisobutyric acid), Cambridge Research Biochemicals, Cambridge, U.K.

Naloxone hydrochloride and [D-Ala^2,MePhe^4,Gly-ol^5]enkephalin , Sigma, Poole, U.K.

The following compounds were kindly donated as follows:

Cyprodime hydrobromide [(-)-*N*-(Cyclopropylmethyl)-4,14- dimethoxy--morphinan-6-one] and RX8008M (16-methyl-cyprenorphine): C.F.C. Smith, Reckitt and Colman, Hull, U.K.

(+)SKF10,047 (N-allylnormetazocine): National Institute on Drug Abuse, U.S.A.

U-50488H base (*trans*-3,4-dichloro-N-methyl-N-[2-(1-pyrrolidinyl)-cyclohexyl]-benzeneacetamide) and U-69593 base ((5α,7α,8β)-(+)-N--methyl-N-(7-(1-pyrrolidinyl)-1-oxaspiro[4,5]dec-8-yl)benzene-acetamide: The Upjohn Company, Kalamazoo, U.S.A.

Xorphanol mesylate: H. Parrs, New York, U.S.A.

Norbinaltorphimine hydrochloride and naltrindole hydrochloride: Glaxo Group Research, Ware, U.K.

Ethylketocyclazocine: Sterling–Winthrop, U.S.A.

Morphine sulphate: McFarlane–Smith, U.K.

Fentanyl citrate: Janssen Pharmaceuticals, Sweden.

ICI204448 ((*R*,*S*)–N–[2–(N–methyl–3,4–dichlorophenyl–acetamido)–2–(3–carboxyphenyl)–ethyl]–pyrrolidine hydrochloride):
ICI Pharmaceuticals, Alderley Park, U.K.

All compounds were stored dessicated as the dry powder or as 1mM or 10mM stock solutions in distilled water or, for dynorphin 1–13, ICI204448, M8008 and xorphanol mesylate in dimethylsulphoxide, at –20°C. Compounds were diluted with distilled water as required before use.

2.2c: Tritiated ligands

The following radioligands were obtained from Amersham International plc, U.K. :

[N–allyl–2,3–^{3}H]naloxone (55 Ci/mmol), [Phenyl–3,4–^{3}H]U–69593 (60 Ci/mmol) and [15,16–n–^{3}H]diprenorphine (48–49 Ci/mmol), as ethanol solutions and stored at –20°C.

[Tyrosyl–3,5–^{3}H][D–Ala^{2},D–Leu^{5}]enkephalin (39.5 Ci.mmol) and [Tyrosyl–3,5–^{3}H][D–Pen^{2},D–Pen^{5}]enkephalin (27 Ci/mmol) in 0.05M acetic acid, were stored at +4°C.

2.3: Ligand Binding Assay Methods

2.3.1: Buffers

Ligand binding assays were performed in Tris.HCl buffer (50mM, pH 7.4) in the absence or presence of 100mM NaCl and 50μM GppNHp as indicated.

2.3.2: Preparation of homogenates

Rats or guinea-pigs were sacrificed by cervical dislocation and promptly decapitated. The brain minus cerebellum of rat and guinea-pig and cerebellum of guinea-pig were removed. The tissues were either used immediately or stored over liquid nitrogen at -150°C to -180°C for up to one month.

Central nervous system tissue was homogenised in 10x w/v Tris.HCl buffer (50mM, pH 7.4) using a Kinematica Polytron homogeniser on setting 7 employing two x ten second bursts. After centrifugation (LKB Hitachi Ultrospin, 48,000g for 20 minutes), the supernatant was discarded and the resultant pellets were resuspended in approximately 20x w/v Tris.HCl buffer (50mM, pH 7.4) and incubated at 37°C for 30 minutes in order to facilitate degradation and dissociation of endogenous opioid peptides. Following this the homogenate was recentrifuged at 48,000g for 20 minutes. The pellets were then finally resuspended in 80x w/v of Tris.HCl buffer (50mM, pH 7.4). The resulting homogenates were used immediately. In assays employing Na^+ ions the above procedure was carried out with the exception that the Tris.HCl contained 100mM NaCl.

2.3.3: Binding Assays

Competition Assays

To the final homogenate, containing approximately 0.8 mg/ml protein, the primary labelled ligand, unlabelled competing ligand, water or 10μM naloxone (to define non-specific binding) were added in 20 μl aliquots to a final assay volume of 1ml. In cases where suppression of binding to μ-, δ- or κ-sites was required unlabelled ligands were added as appropriate (outlined in pertinent chapters). 50μM GppNHp was added as required.

The assay tubes were incubated at 25°C for 40 minutes. The assay was terminated by the addition of 4ml ice-cold Tris.HCl buffer (50mM, pH 7.4) containing 100mM NaCl where necessary followed by rapid filtration through Whatman GF/B glass filters either using a Millipore 1225 sampling manifold or a Brandel M48R cell harvester. The filters were rinsed three times with 4ml ice-cold Tris.HCl buffer (50mM, pH 7.4), or where appropriate, ice-cold Tris.HCl buffer containing 100mM NaCl. The filter discs with retained membranes and radioactive residue were transferred to vial inserts and after the addition of Ecoscint A, were counted on a Philips PW4700 liquid scintillation counter. Counting efficiency was approximately 40%. The determination of IC_{50} values and Hill slopes is outlined in chapter three.

Saturation Assays

The assay mixture was as above but varying concentrations of primary labelled ligand were used over the concentration range of 0.04-10nM. Naloxone (10μM) was used to define non-specific binding. The suppression of binding to certain opioid sites is discussed in appropriate chapters. Data analysis was performed by Scatchard transformation and the program LIGAND as discussed in chapter three.

Protein Determination

Protein content was estimated according to the method of Lowry (102), using the modification of Schacterle and Pollack (103).

2.4: Isolated Tissue Bioassay

2.4.1: Buffer

Isolated tissue bioassays were performed in Krebs buffer comprising (g/l) in distilled water:

NaCl	6.92
KCl	0.35
KH_2PO_4	0.16
$CaCl_2.2H_2O$	0.375
$NaHCO_3$	2.1
$MgSO_4.7H_2O$	0.29
D–glucose	2.0

2.4.2: Tissue

The system used was the guinea–pig ileum myenteric plexus longitudinal muscle preparation (GPMPLM). Strips of myenteric plexus logitudinal muscle were isolated according to the method of Paton and Zar (101). Tissues were mounted in 3ml organ baths containing Krebs solution at 37°C aerated with 95% O_2/5% CO_2.

2.4.3: Bioassay

Contractions of the longitudinal muscle were elicited by stimulation through platinum ring electrodes mounted above and below the tissues. Pulses with a width of 0.4msec and a frequency of 0.2Hz were delivered at supramaximal voltage, determined daily for each tissue. Contractions were measured isotonically using Harvard Bioscience transducers under a tension of 0.8g, and recorded on a Washington 480 chart recorder.

After allowing the tissue 60 minutes equilibration, cumulative dose–response curves were constructed for the inhibition of twitch induced by opioid agonists. After each agonist the bath fluid was changed by overflow until the twitch height returned to control values. To determine the antagonist equilibrium dissociation constant (Ke) for naloxone, the antagonist was added to the bath for 30 minutes, then without washout, dose–response curves to the agonists were reassayed. The Ke value was determined by Schild analysis as discussed in chapter three.

CHAPTER 3: DATA ANALYSIS

3.1: Binding Assays

Determination of radioligand binding constants

The principle of the law of mass action provides the basis for the following binding equations. A simple bimolecular interaction is assumed between a drug (D) and its binding site (R) yielding the complex DR.

At conditions of equilibrium;

$$D + R \underset{k_2}{\overset{k_1}{=}} DR \qquad \text{equation 1.}$$

A measure of the affinity of a ligand for its binding site is known as the equilibrium dissociation constant, K_D, where;

$$K_D = \frac{k_2}{k_1} = \frac{[D]\,[R]}{[DR]} \qquad \text{equation 2.}$$

Saturation binding studies

Saturation experiments can be used to determine the K_D for a radiolabelled ligand. The total concentration of radioligand [Dt] is increased and [DR] is determined at equilibrium as a function of [D] since the total binding site population [Rt] remains constant.

Because [Rt] = [R] + [DR], therefore [R] = [Rt–DR] and so;

$$K_D = \frac{[Rt - DR]\,[D]}{[DR]} \qquad \text{equation 3.}$$

which can be rearranged to

$$[DR] = \frac{[Rt]\,[D]}{K_D + [D]} \qquad \text{equation 4.}$$

when $K_D = [D]$ then

$$[DR] = \frac{[Rt]}{2} \qquad \text{equation 5.}$$

such that the K_D is equivalent to the concentration of radioligand occupying 50% of the total binding sites. Equation 4 is equivalent to the Langmuir adsorption isotherm in that it describes a rectangular hyperbola given by

$$[D] = \frac{r}{1 - r}\,(K_D) \quad \text{when} \quad r = \frac{[DR]}{[Rt]}$$

In this case r represents the proportion of the total potential sites occupied by the ligand.

Scatchard analysis

Scatchard (104) manipulated equation 4 to give a straight line graph:

$$\frac{[DR]}{[D]} = \frac{[Rt]}{K_D} - \frac{[DR]}{K_D} \qquad \text{equation 6}$$

where; [DR] = B (Specifically bound radioligand)

[D] = F (Free radioligand)

[Rt] = Bmax (Total number of binding sites)

so that,

$$\frac{F}{B} = \frac{B_{max}}{K_D} - \frac{B}{K_D} \qquad \text{equation 7}$$

whereupon a plot of B/F versus B yields a slope of $-1/K_D$ and an intercept on the abscissa of Bmax.

B (specifically bound radioligand) represents

total counts bound – non–specific binding

F (unbound radioligand) represents

total counts added – counts specifically bound

The data can be assessed in terms of concentration by dividing the sample dpm by that obtained from the specific activty of the radioligand. Scatchard analysis gives a rapid estimation of binding parameters although it has a number of inherent drawbacks.

The bound term is present in both axes and as a result any error will be manifested in two dimensions, causing an increase in the scattering of points. Another problem arises on transformation of the data from the hyperbolic saturation curve to the linear Scatchard plot because the points change from being evenly spaced to compressed. This occurs particularly at high concentrations of free ligand, resulting in the possibility of a false estimation of Bmax. False heterogeneity may also be implied when a methodological artefact produces a non–linear plot and conversely true heterogeneity may not be observed due to scattering of data points or if the radioligand has

a similar affinity at each site. Finally non-weighted linear regression of the Scatchard plot is statistically invalid and should be avoided due to non-uniform errors present in both coordinates of the Scatchard plot. As a result computer programs have been developed to overcome these problems.

The main computer aided system currently employed involves non-linear curve-fitting algorithms of the saturation binding isotherm. This is known as LIGAND (105), and allows highly accurate estimations of Bmax and K_D. This method of analysis has many advantages over conventional Scatchard plots in that:

i) It allows simultaneous analysis of several displacement curves obtained for different unlabelled ligands, within an experiment. By combining the information a more precise and accurate estimate of common parameters is obtained.

ii) It provides direct and explicit statistical testing for alternative models or hypotheses.

iii) Weighting is provided to compensate for the non-uniformity of variance of the dependent variable such as the bound ligand concentration.

iv) It utilises total ligand concentration as the independent variable and total binding rather than specific binding may be examined. This eliminates errors caused by subtraction of non-specific binding.

v) It provides a variety of statistical methods for evaluating the "goodness of fit" for a given model.

However, despite the above comments it is the quality of the original data which determines the accuracy and precision of any form of analysis, either

manual or computer-aided.

Competition Binding Analysis

Competitive inhibition assays can be employed to determine the affinity of an unlabelled competing ligand for the binding site. In this method several different concentrations of unlabelled competing ligand are employed to displace the labelled ligand. It is usual to determine the IC_{50} of the unlabelled competing ligand which is the concentration which results in 50% inhibition of the binding of the radioligand.

In such an experiment both [Rt] and [D] are constant while the concentration of the unlabelled competing ligand [I] is variable, such that at equilibrium [DR] is a function of [I] viz.

$$[DR] = \frac{[D]\,[Rt]}{K_D\,(1 + [I]/Ki) + [D]} \qquad \text{equation 8.}$$

where [I] = concentration of free unlabelled ligand

Ki = equilibrium dissociation constant for the interaction of the unlabelled ligand with the binding site.

The function Ki is defined as:

$$Ki = \frac{[R]\,[I]}{[RI]} \qquad \text{equation 9.}$$

The IC_{50} can be used to calculate the equilibrium dissociation constant (Ki) for the competing ligand via the Cheng and Prusoff equation (108):

$$Ki = \frac{IC_{50} \cdot K_D}{K_D + [D]} \qquad \text{equation 10.}$$

It is often difficult to determine the free competing ligand concentration and as a result it is assumed that the free concentration is equal to the total concentration. However this depends on the amount bound being low (usually <10%) with respect to the equilibrium dissociation constant. This means that if the total binding sites present are equal to or greater than the equilibrium dissociation constant then the Ki value obtained from equation 10 will be too high (105).

Hill Plot

The transformation of Hill (106) allows linearlisation of a competition displacement curve. Rearranging equation 4 gives;

$$\frac{[DR]}{[Rt]} = \frac{[D]}{K_D + [D]} \qquad \text{equation 11.}$$

where [DR]/[Rt] is the proportion of binding sites occupied by the radioligand and can be renamed r. If this term is substituted into equation 8, rearrangement gives

$$[D] = \frac{r}{1 - r} \quad (K_D) \qquad \text{equation 12.}$$

This describes the interaction of one molecule of radioligand with a single binding site, therefore in general terms

$$[D]^n = \frac{r}{1 - r} \quad (k) \qquad \text{equation 13.}$$

where n represents the number of radioligand molecules interacting with a single binding site and k is a constant.

A plot of log (r/1–r) versus log[D] yields a straight line, the slope corresponding to the Hill coefficient. The IC_{50} is the concentration at which log (r/1–r) = 0. A slope of unity indicates that the competing ligand is displacing the radioligand from a single class of binding sites, or from a heterogeneous population of sites for which the competing ligand has the same affinity. A shallow slope yielding a Hill coefficient less than one suggests the competing ligand is binding to multiple binding sites with different affinities. However it could also represent interconverting forms of a single class of binding site (107). A steep slope with a Hill coefficient greater than one implies cooperativity of ligand binding.

3.2: Isolated Tissue Bioassay

Agonist Dose–Response Curves

An opioid agonist will reduce the electrically induced twitch of the guinea–

pig ileum myenteric plexus longitudinal muscle tissue in a dose-dependent manner. The amount of inhibition is calculated as follows:

$$\% \text{ inhibition} = 100 - \frac{(\text{deflection} \times 100)}{\text{original deflection}} \qquad \text{equation 14.}$$

A plot of % inhibition versus log (agonist concentration) yields a dose-response curve from which an IC_{50} value can be obtained.

Interaction Between An Agonist And A Competitive Antagonist

A competitive antagonist may be regarded as a drug that interacts reversibly with a set of receptors to form a complex, but the antagonist-receptor complex does not elicit a response . The antagonist-receptor interaction is characterised by a dissociation constant (K_A), and as with an agonist, the equation for the dissociation constant of the antagonist from the complex follows from the law of mass action:

$$K_A = \frac{[A][R]}{[AR]} \qquad \text{equation 15.}$$

where [A] and [AR] represent the concentrations of antagonist and antagonist-receptor complex respectively.

When both an agonist and antagonist for a receptor are present, the concentration of free receptors is given by:

$$[R] = [Rt] - [DR] - [AR]$$

dividing through by [DR]:

$$\frac{[R]}{[DR]} = \frac{[Rt]}{[DR]} - 1 - \frac{[AR]}{[DR]}$$

however, $[R]/[DR] = K_D/[D]$ and $[AR] = [A][R]/K_A$. Substituting these into the above and rearranging gives:

$$\frac{[Rt]}{[DR]} = \frac{K_D K_A + K_D[A] + K_A[D]}{K_A[D]} \qquad \text{equation 16.}$$

The reciprocal of this equation gives the fraction of receptors occupied by the agonist in terms of concentrations and dissociation constants of the agonist and antagonist.

In the presence of a competitive antagonist, the agonist dose–response curve is shifted to the right. The curves have the same form, the maximal response remains the same and the linear portions of the curve are parallel. The essential feature of competitive antagonism is that the effect of the antagonist can be overcome by increasing the agonist concentration.

The degree of shift to the right of the agonist dose–response curve is proportional to the antagonist concentration, and the affinity of the antagonist for the receptors is inversely proportional to the antagonist–receptor dissociation constant K_A. The value of K_A can be determined from the

concentrations of agonist producing equal responses in the absence ([D]o) and presence ($[D]_A$) of antagonist. Since the responses are equal, the receptor occupancy by the agonist is assumed to be the same. Therefore from equations 11 and 16:

$$\frac{[D]_o}{[D]_o + K_D} = \frac{K_A[D]_A}{K_D K_A + K_D[A] + K_A[D]}$$

By taking reciprocals and dividing by the denominators then:

$$1 + K_D / [D]_o = 1 + [A] K_D / [D]_A K_A + K_D / [D]_A$$

which reduces to :

$$\frac{[D]_A - 1}{[D]_o} = \frac{[A]}{K_A}$$ equation 17.

When the concentration of antagonist ($[A]_2$) is such that $[D]_A = 2[D]o$ then:

$$[A]_2 = K_A$$

The value of the antagonist dissociation constant is given by the concentration of the antagonist with which the ratio of concentrations of agonist producing equal responses in its presence ($[D]_A$) and absence ([D]o) equals 2.

The negative logarithm of the molar concentration of antagonist with which the ratio of equi-effective concentrations of agonist in the presence and absence of antagonist is two has been designated by Schild (109) as the pA_2 value, thus:

$$pA_2 = -\log [A]_2$$

This procedure involves no assumption about the relationship of the response to the proportion of receptors occupied, since the responses are equal and it is indepedent of the agonist used, provided that only the antagonist competes with the agonist for the receptor.

Schild Plot

Equation 17 may be rewritten as:

$$K_A = \frac{[A]}{x - 1}$$

where x = dose ratio, representing

$$\frac{IC_{50} \text{ in presence of A}}{IC_{50} \text{ in absence of A}}$$

and [A] is the antagonist concentration.

By using various antagonist concentrations it is possible to construct a plot of log (x – 1) versus log [A]x. This gives a straight line, the intercept on the abscissa corresponding to the pA_2. This can be readily converted to the dissociation constant as outlined above.

The value represented as K_A in the preceding scheme is generally referred to as Ke, the equilibrium dissociation constant.

Single Dose Ke Determination

The most accurate way to estimate the Ke (or pA_2) of an antagonist is by way of full Schild analysis, as above. However a quicker method, also devised by Schild, gives an approximate value. Instead of using a series of antagonist concentrations, just a single dose is chosen. The Ke value is calculated according to equation 17. Despite the lower accuracy compared to creating a Schild plot, it is often favoured due to time and experimental considerations.

3.3: Statistical Analysis

Unless otherwise stated in the text all results are represented as the statistical mean ± the standard error of the mean (sem). All experiments were designed to conform as far as possible to randomised criteria. Animals used were chosen randomly from a large population. The Student's t–test (unpaired) was used to determine whether slopes from both Hill and Schild plots significantly differed from unity.

CHAPTER 4: BINDING PROFILES OF SOME NEWER SELECTIVE OPIOIDS/OPIATES

Introduction

Selective opioid antagonists are necessary for the unambiguous determination of the receptor selectivity of opioid agonists. Although antagonists such as naloxone (2) have been used extensively as research tools, the proposed existence of multiple opioid receptor types (μ–, δ– and κ–) has meant a need for highly selective antagonists.

Antagonists were developed showing a certain degree of selectivity such as MR2266 (44) and Win 44,441–3 (162). However, one of the first truly selective opioid antagonists was ICI 174864 (N,N–diallyl–Tyr–Aib– Aib–Phe–Leu–OH) (55), a peptide based on [Leu^5]enkephalin which shows selectivity for the δ–opioid receptor. However, in binding assays the inclusion of Na^+ ions in the buffer is necessary to obtain an affinity of ICI 174864 at the δ–site over both μ– and κ–sites in line with its Ke of 30nM determined in *in vitro* bioassay systems such as the mouse vas deferens (21). In the absence of Na^+ ions an affinity of 200nM is obtained although selectivity is retained.

In recent years a number of further antagonists claimed to be selective for a single type of opioid receptor have emerged. It is necessary therefore to characterise the binding profiles of these newer selective antagonists in order that they may be employed to further investigate the properties of opioid receptors, and particularly to see if they might help solve the problems of receptor subtypes. The compounds chosen to study include:

Norbinaltorphimine (NorBNI), a synthetic bidentate antagonist, with reported

selectivity for the κ-opioid receptor of >50-fold, both in binding and isolated tissue bioassays (57, 51, figure 4.0a).
Naltrindole, a synthetic indolomorphinan antagonist, reportedly >100- fold selective for the δ-opioid receptor, as determined by *in vitro* bioassays (56, figure 4.0b).
M8008 (16-methylcyprenorphine), an oripavine antagonist shown to possess selectivity for the δ-opioid receptor (2.4-fold over μ- and 80-fold over κ-) in *in vitro* bioassays (97, figure 4.0c).
Cyprodime, a synthetic methoxymorphinan antagonist, over 30-fold selective for the μ-opioid receptor in isolated tissue bioassays and also in preliminary binding assays (54, figure 4.0d).
D-Phe,Cys,Tyr,D-Trp,Orn,Thr,Pen,Thr-NH_2 (CTOP), a synthetic peptide analogue of somatostatin, with >1000-fold selectivity for the μ-opioid receptor (52,53).

Materials and Methods

Homogenates of central nervous system tissue were prepared and binding assays carried out as described in chapter two. Assays were performed in Tris.HCl buffer in the absence and presence of 100mM NaCl and 50μM GppNHp . κ-Sites were studied in guinea-pig cerebellum homogenates, δ-sites in NG108-15 cells and rat brain homogenates and μ-sites in rat brain homogenates.

Radiolabelled ligands used to label opioid binding sites were [^{3}H]diprenorphine, [^{3}H]naloxone, [^{3}H]DADLE and [^{3}H]DPDPE. Details of suppressing conditions are described in relevant result sections. Non-specific binding was defined throughout with 10μM naloxone.

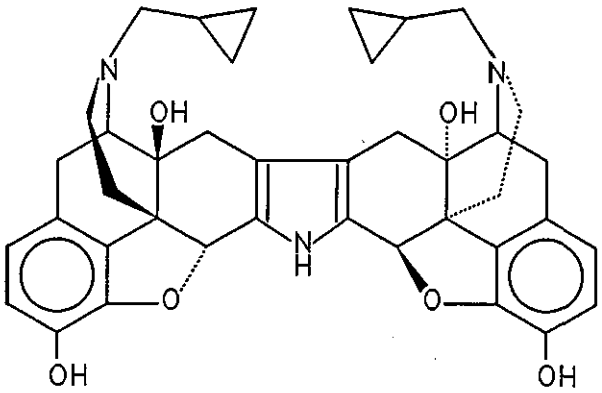

Figure 4.0a: Norbinaltorphimine (NorBNI)

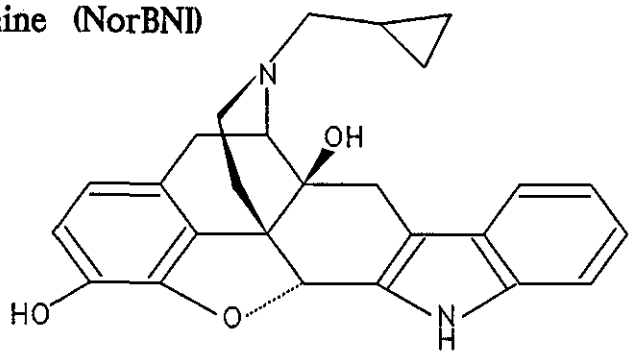

Figure 4.0b: Naltrindole

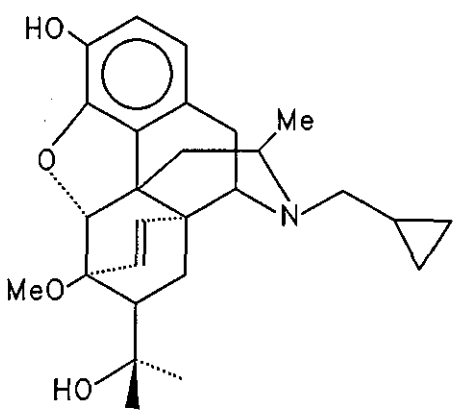

Figure 4.0c: M8008 (16-methylcyprenorphine)

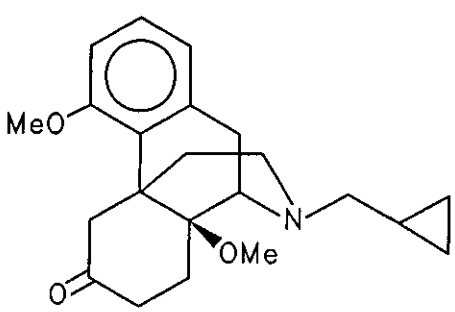

Figure 4.0d: Cyprodime

Results

a) μ-Receptor studies

The affinity of NorBNI at μ- sites was studied both in Tris.HCl buffer and with the addition of 100mM NaCl and 50μM GppNHp. μ-Sites were studied under both conditions using [^{3}H]naloxone which at a low concentration and in rat brain which contains a low level of κ-receptors (45) will mainly label μ-sites (58), due to its slight μ-selectivity (107).

Figure 4.1 shows NorBNI to displace [^{3}H]naloxone with low affinity from μ- sites in both the presence and in the absence of NaCl and GppNHp, affording IC_{50} values >50nM (see table 4.1).

The displacement of [^{3}H]naloxone from rat brain homogenates by naltrindole (figure 4.2) afforded an IC_{50} in Tris.HCl of 17.2±4.4nM and 13.1±1.5nM in the presence of 100mM NaCl and 50μM GppNHp. Hill coefficients were not significantly different from unity (table 4.1).

Cyprodime displaced specifically bound [^{3}H]naloxone to μ-sites in rat brain as shown in figure 4.3, affording an IC_{50} in Tris.HCl of 17.3±3.2nM and a Hill coefficient of 0.95±0.04. In the presence of NaCl and GppNHp the affinity was unchanged with an IC_{50} of 28.2±7.3nM and Hill coefficient of 0.94±0.02 (table 4.1). Another μ-selective ligand, CTOP displaced [^{3}H]naloxone with high affinity (figure 4.4). In Tris.HCl, CTOP afforded an IC_{50} of 3.09±0.20nM which shifted to a lower affinity (IC_{50} of 18.7±5.5nM) in the presence of NaCl and GppNHp . In both cases Hill coefficients were close to unity (1.2±0.1 and 1.03±0.02 respectively). The tailing-off in the binding of CTOP to μ-sites is similar to that observed in the displacement of labelled naloxone by itself (not shown).

As shown in figure 4.5 M8008 readily displaces [^{3}H]naloxone from rat brain homogenates affording an IC_{50} of 6.08±1.6nM and Hill coefficient of 0.93±0.06 in Tris.HCl. However in the presence of 100mM NaCl and 50μM GppNHp the concentration inhibition curve for M8008 shifts approximately 6-fold to higher affinity (IC_{50} 0.91±0.2nM).

Table 4.1: Displacement of 0.2nM [^{3}H] naloxone from rat brain homogenates by opioid antagonists

	Tris.HCl		+NaCl/GppNHp*	
	IC_{50}(nM)	Hill Coefficient	IC_{50}(nM)	Hill Coefficient
NorBNI	72.9±5.2	0.68±0.04$	50.2±12.5	0.77±0.1
Naltrindole	17.2±4.4	0.82±0.02$	13.1±1.5	0.82±0.04
Cyprodime	17.3±3.2	0.95±0.04	28.2±7.3	0.90±0.02
CTOP	3.09±0.2	1.20±0.1	18.7±5.5	1.03±0.02
M8008	6.08±1.6	0.93±0.06	0.91±0.2	0.86±0.06

Values represent mean±sem from at least three separate determinations.

*Tris.HCl 50mM, NaCl 100mM, GppNHp 50μM.

$Indicates Hill coefficient significantly less than unity ($P < 0.01$) as determined by Student's t-test

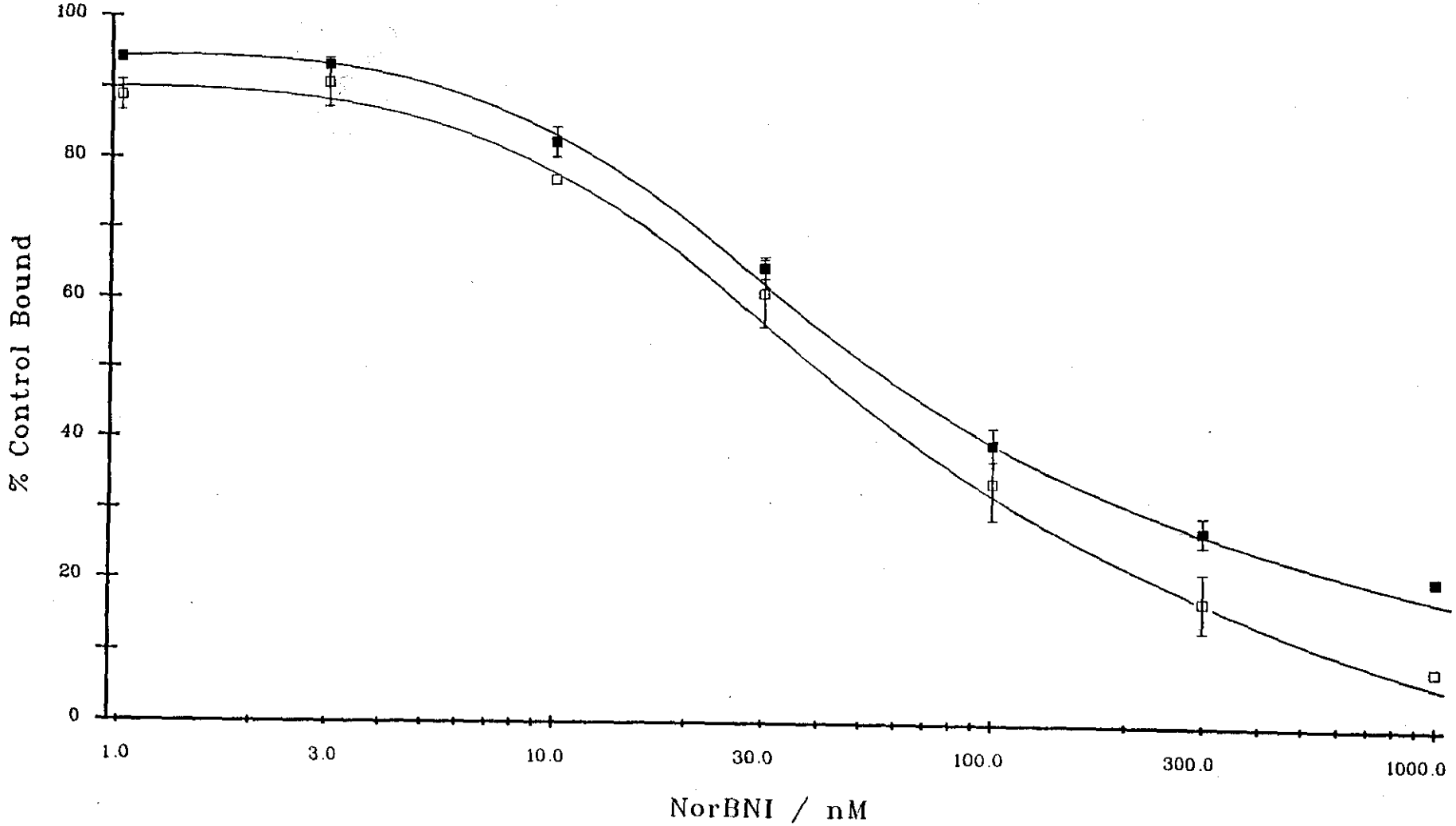

Figure **4.1** : Displacement of [^{3}H]naloxone (0.21 ± 0.02nM) from rat brain homogenates in Tris.HCl (50mM, pH 7.4) in the absence (closed symbols) and presence (open symbols) of 100mM NaCl and 50μM GppNHp by NorBNI.

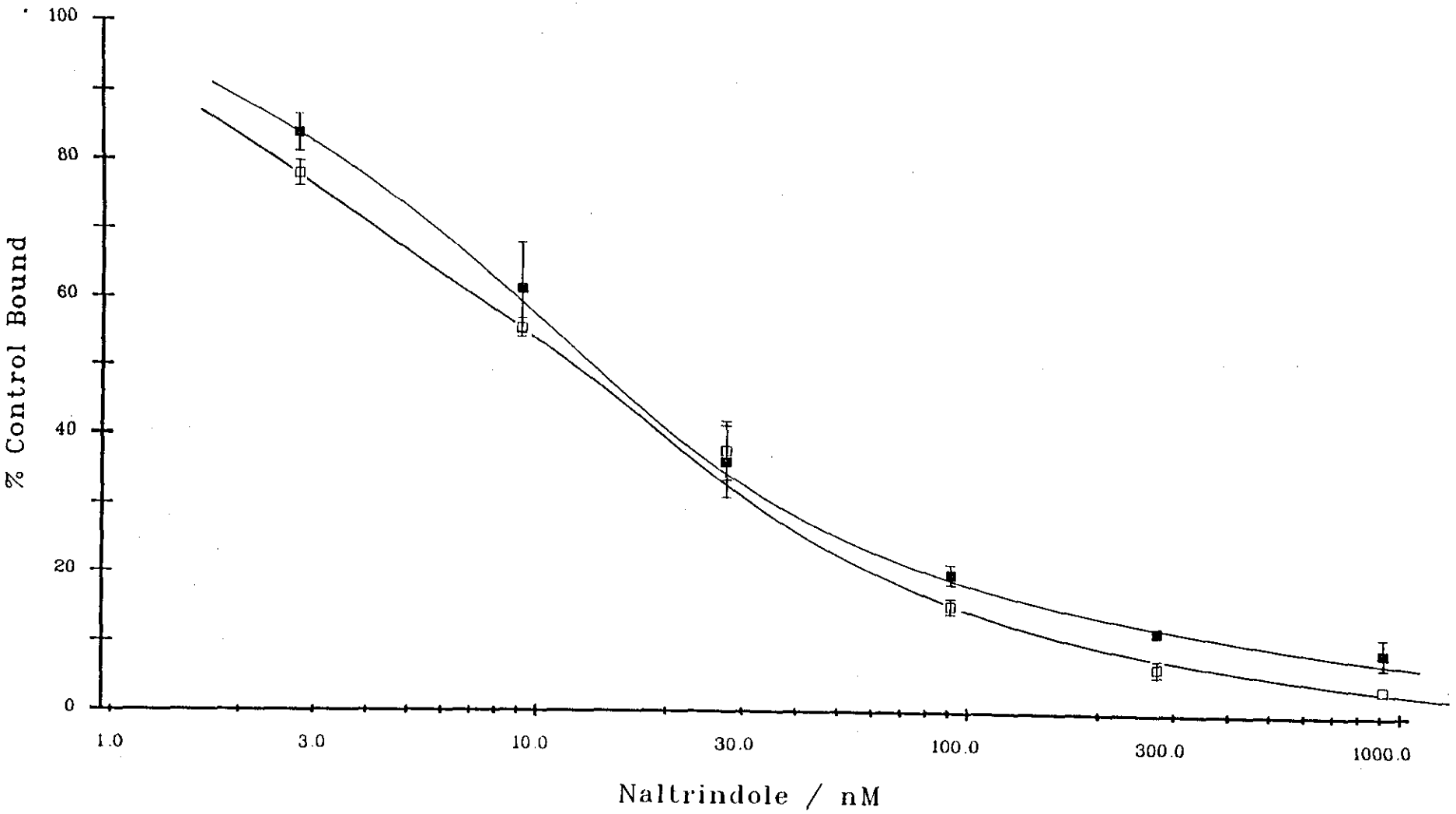

Figure **4.2** : Displacement of [^{3}H]naloxone (0.21 ± 0.03nM) from rat brain homogenates in Tris.HCl (50mM, pH 7.4) in the absence (closed symbols) and presence (open symbols) of 100mM NaCl and 50μM GppNHp by naltrindole.

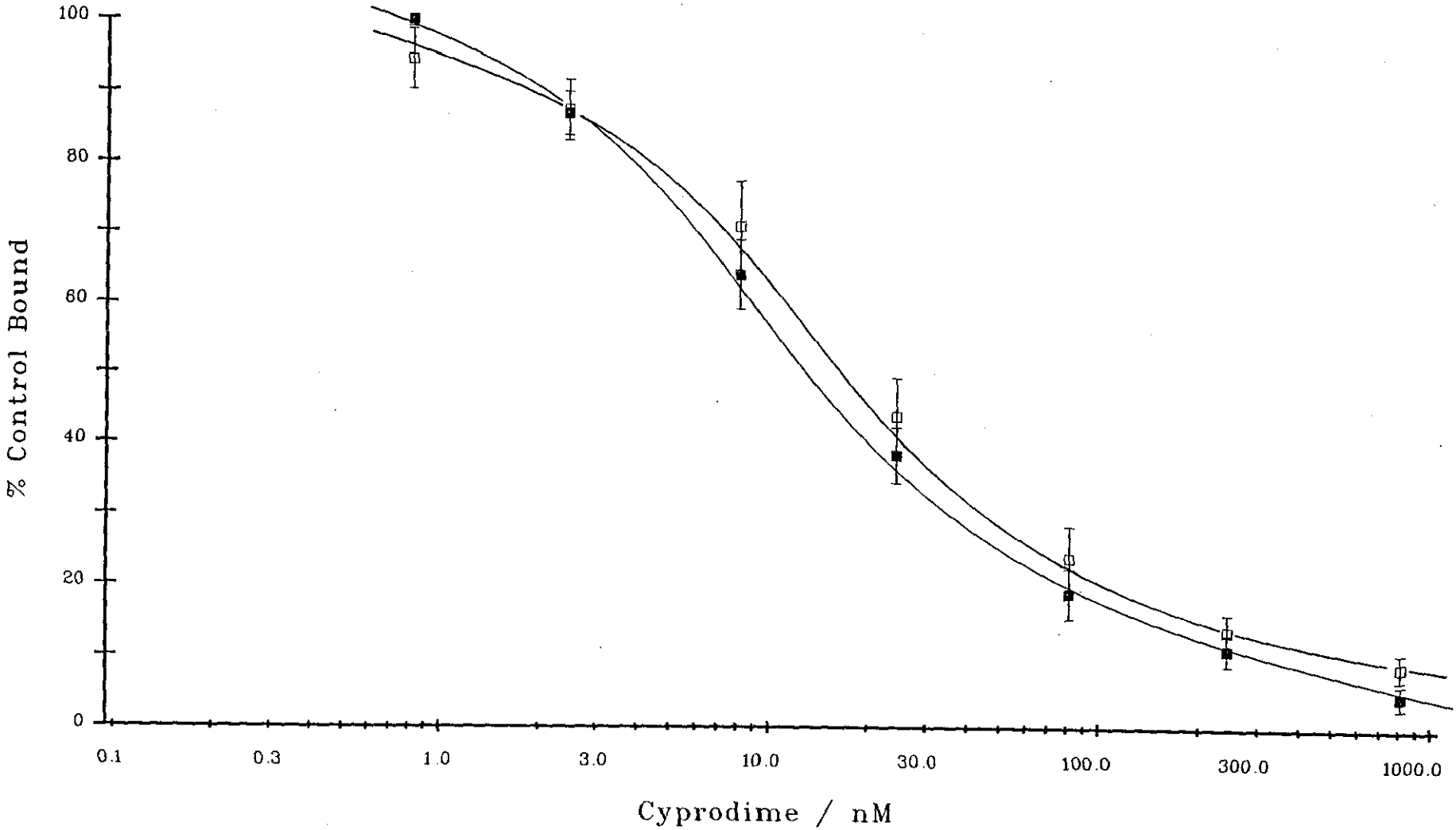

Figure **4.3** : Displacement of [^{3}H]naloxone (0.28 ± 0.04nM) from rat brain homogenates in Tris.HCl (50mM, pH 7.4) in the absence (closed symbols) and presence (open symbols) of 100mM NaCl and 50μM GppNHp by cyprodime.

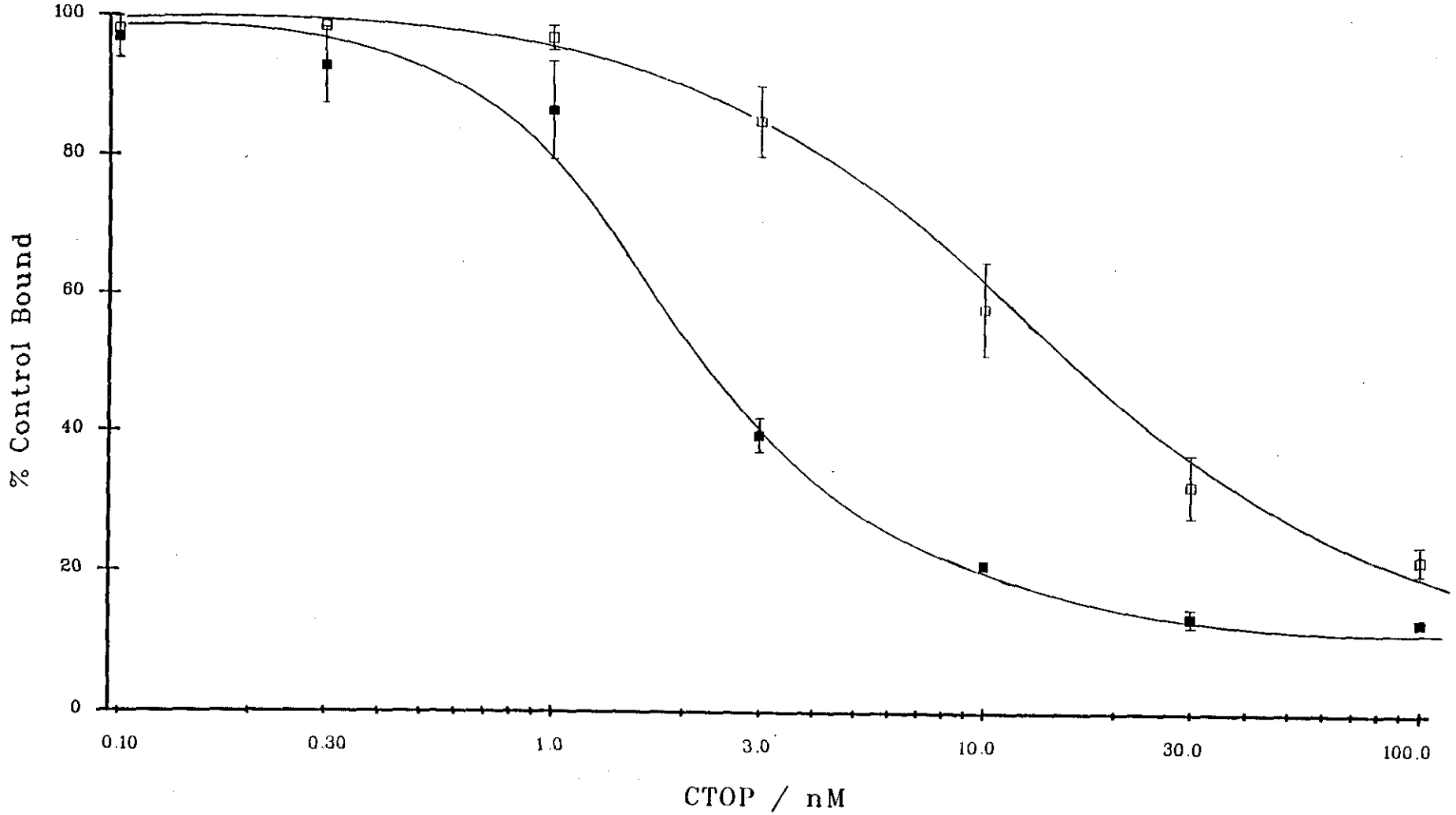

Figure 4.4 : Displacement of [^{3}H]naloxone (0.25 ± 0.02nM) from rat brain homogenates in Tris.HCl (50mM, pH 7.4) in the absence (closed symbols) and presence (open symbols) of 100mM NaCl and 50μM GppNHp by CTOP.

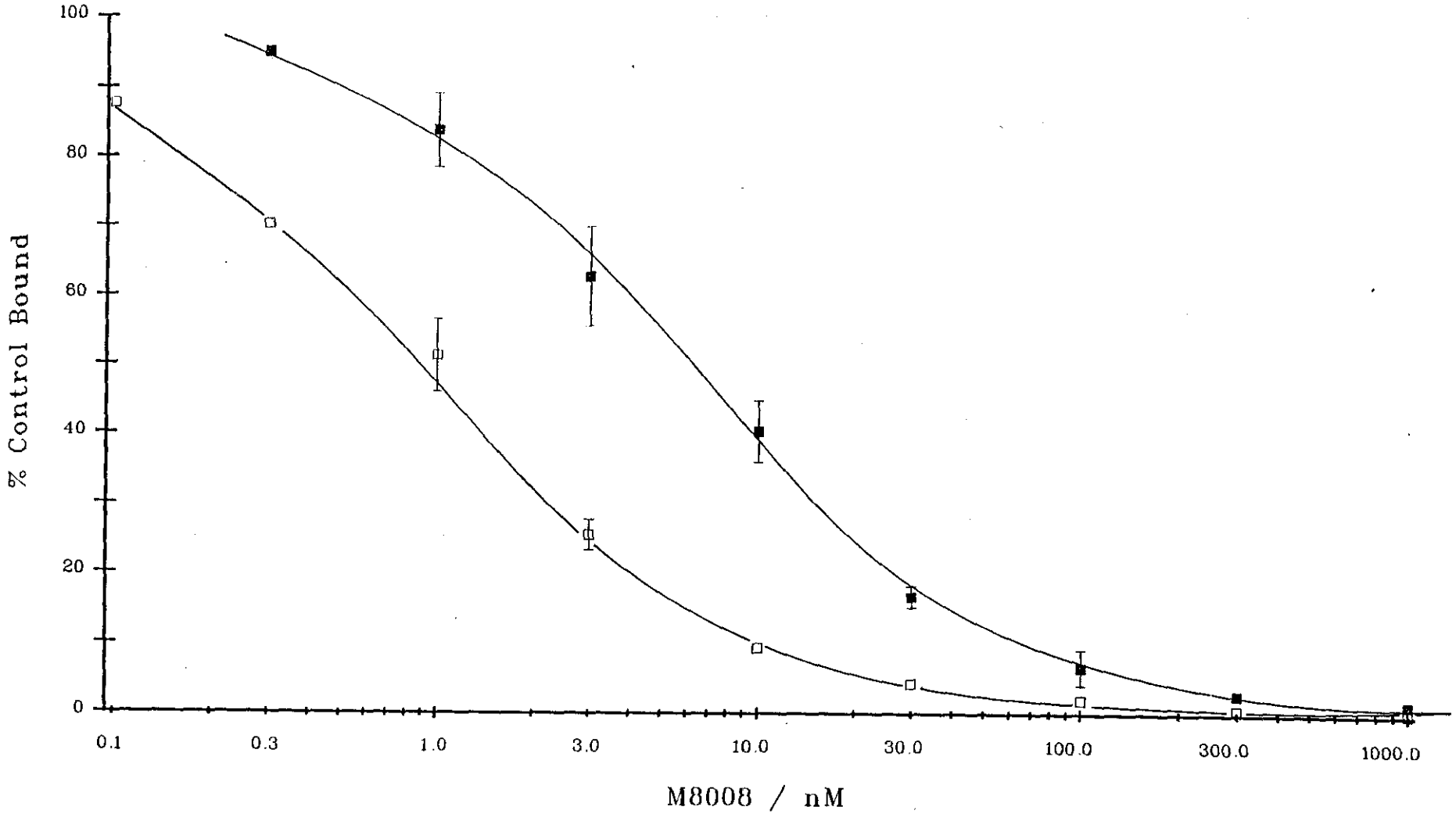

Figure **4.5** : Displacement of [^{3}H]naloxone (0.86 ± 0.1nM) from rat brain homogenates in Tris.HCl (50mM, pH 7.4) in the absence (closed symbols) and presence (open symbols) of 100mM NaCl and 50μM GppNHp by M8008.

b) κ–Receptor studies

NorBNI displaced [^{3}H]diprenorphine (0.2nM) specifically bound in homogenates of guinea–pig cerebellum in Tris.HCl buffer with high affinity. However, as seen in figure 4.6 the displacement curve has a biphasic profile. Approximately 65% of the binding represented high affinity sites for NorBNI affording an IC_{50} of 0.50±0.05nM (n = 3), and are thus presumed to be κ–sites. This is supported by studies with the κ–selective agonist U–69593 which displaced a similar amount of specifically bound radioligand with an IC_{50} of 16.2±4.8nM. In the presence of 100mM NaCl and 50μM GppNHp the profile for NorBNI remained the same but shifted to the left, and then only for the presumed κ–component. In contrast the displacement curve for the agonist U–69593 shifted some ten times to the right (figure 4.6).

Although the opiate receptor population in guinea–pig cerebellum is largely of the κ–type (110), this tissue does contain approximately 20% of other sites as confirmed above. Thus, in order to study the binding of NorBNI to a more homogeneous population of κ–binding sites the displacement experiments were repeated in the presence of the alkaloid M8008 (figure 4.0c). This compound is an opiate antagonist, which has a 30–fold selectivity for μ– and an 80–fold selectivity for δ– over κ–receptors measured in the mouse vas deferens (97). This implies an ability to selectively suppress the non–κ component of the guinea–pig cerebellum. Although M8008 had not been studied in binding assays, its selectivity for μ–and δ–over κ–sites was confirmed (this study). Assuming published affinities at the three receptor types for diprenorphine (107) of μ–0.84nM, δ–1.42nM and κ– 2.24nM, and M8008 (97) of μ– 1.77nM, δ– 0.73nM and κ– 59.6nM, and employing the occupancy equation 8 (chapter three) a 20nM concentration of the latter antagonist will have the effect of increasing the κ–component of opioid binding in the guinea–pig cerebellum to approximately 94% of the total opioid sites. Figure 4.7 shows a theoretical plot of the displacement of

[^{3}H]diprenorphine by M8008 from guinea-pig cerebellum homogenate which demonstrates this, and the actual displacement as represented in figure 4.11 confirms that M8008 recognises a non κ-component in this tissue.

The ability of NorBNI to displace [^{3}H]diprenorphine (0.26±0.04nM) from such defined κ-sites is shown in figure 4.8. An approximate 10-fold shift to higher affinity in the presence of Na^+ ions and GppNHp is again observed, however shallow Hill slopes were still obtained (table 4.2).

The δ-antagonist naltrindole displaced specifically bound [^{3}H]diprenorphine in the presence of 20nM M8008 from guinea-pig cerebellum homogenates with low affinity (figure 4.9). In Tris.HCl an IC_{50} of 63.5±20.7nM was observed compared to 24.0±5.3nM in the presence of 100mM NaCl and 50μM GppNHp.

The two μ-selective ligands cyprodime and CTOP also showed low affinity for κ-sites when displacing [^{3}H]diprenorphine from guinea-pig cerebellum homogenates. Figure 4.10 depicts the binding of cyprodime at κ-sites, giving an IC_{50} of >500nM. Hill slopes were consistent with binding to a single class of sites (table 4.2). CTOP exhibited even lower affinity at such defined κ-sites affording only 25% displacement of [^{3}H]diprenorphine from guinea-pig cerebellum homogenates at a level of 1μM. This occurred both in the absence and presence of 100mM NaCl and 50μM GppNHp. Table 4.2 summarises the data obtained for CTOP and cyprodime.

M8008 has a low affinity for κ-sites in guinea-pig cerebellum labelled with [^{3}H]diprenorphine. In Tris.HCl M8008 yields an IC_{50} of 209.4±9.9nM compared with 105.4±23.4nM in the presence of 100mM NaCl and 50μM GppNHp (figure 4.11). Shallow Hill slopes were obtained, confirming the presence of the non-κ component in this assay (table 4.2).

Table 4.2: Displacement of [^{3}H]diprenorphine (0.3nM) from guinea- pig cerebellum homogenates by opioid antagonists.

	Tris.HCl		+NaCl/GppNHp*	
	IC_{50}(nM)	Hill Coefficient	IC_{50}(nM)	Hill Coefficient
M8008	209.4± 9.9	0.84±0.03	105.4± 23.4	0.60±0.07
NorBNI^{x}	2.5±0.7	0.71±0.2	0.23±0.05	0.55±0.05$^{\$}$
Naltrindole^{x}	63.5± 20.7	0.78±0.06	24.0± 5.3	0.77±0.08
Cyprodime	521± 22.5	0.62±0.08	820.6± 292	0.98±0.2
CTOP	›1000		›1000	

Values represent mean ±sem from at least three separate determinations.

*Tris.HCl 50mM, NaCl 100mM, GppNHp 50μM.

$^{\$}$ Indicates Hill coefficient significantly less than unity ($P<0.01$) as determined by Student's t-test.

^{x} In the presence of 20nM M8008.

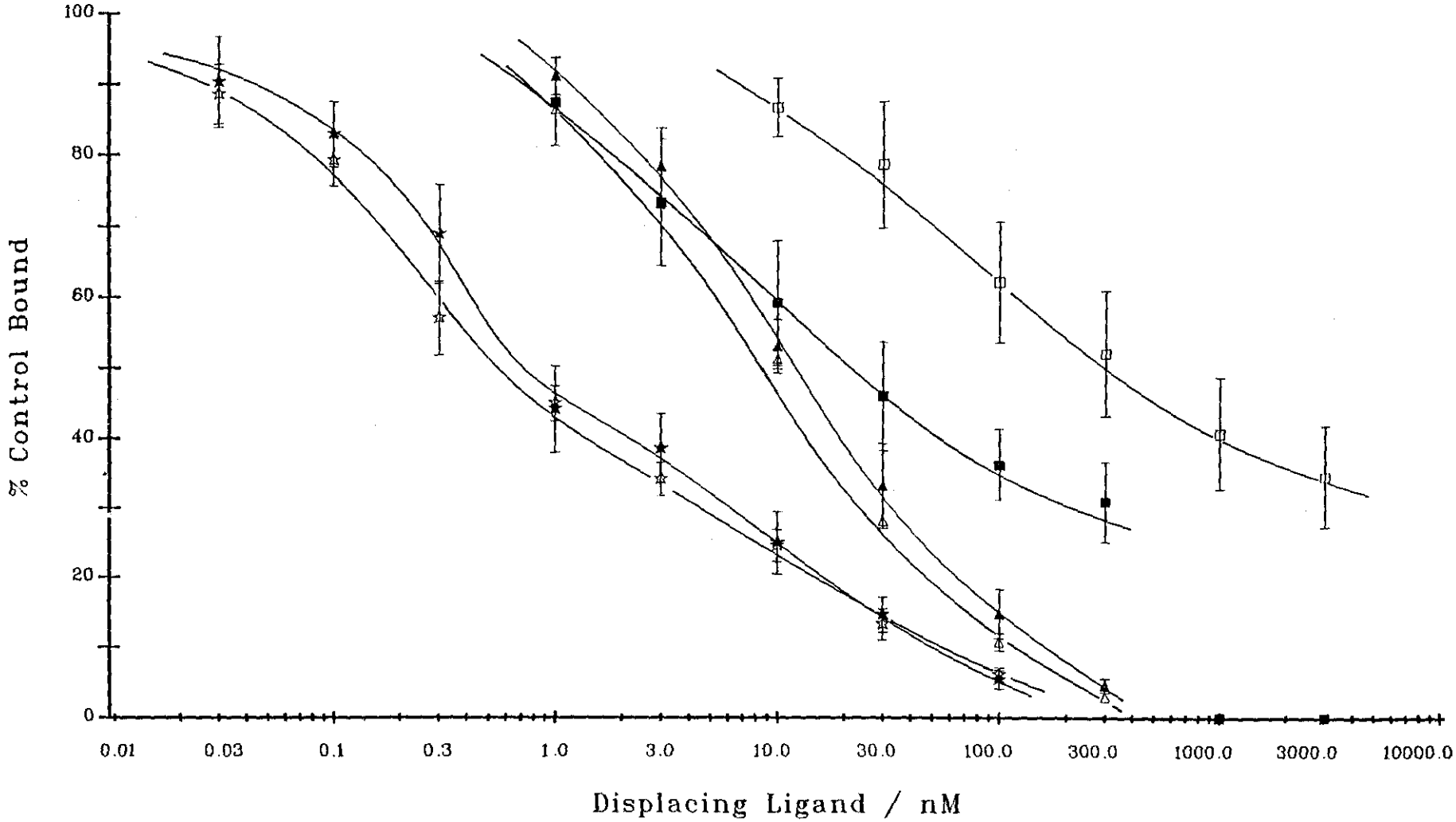

Figure **4.6** : Displacement of [^{3}H]diprenorphine (0.2nM) from guinea-pig cerebellum homogenates in Tris.HCl (50mM, pH 7.4) in the absence (closed symbols) and presence (open symbols) of 100 mM NaCl and 50μM GppNHp by NorBNI (stars), naloxone (triangles) and U69593 (squares).

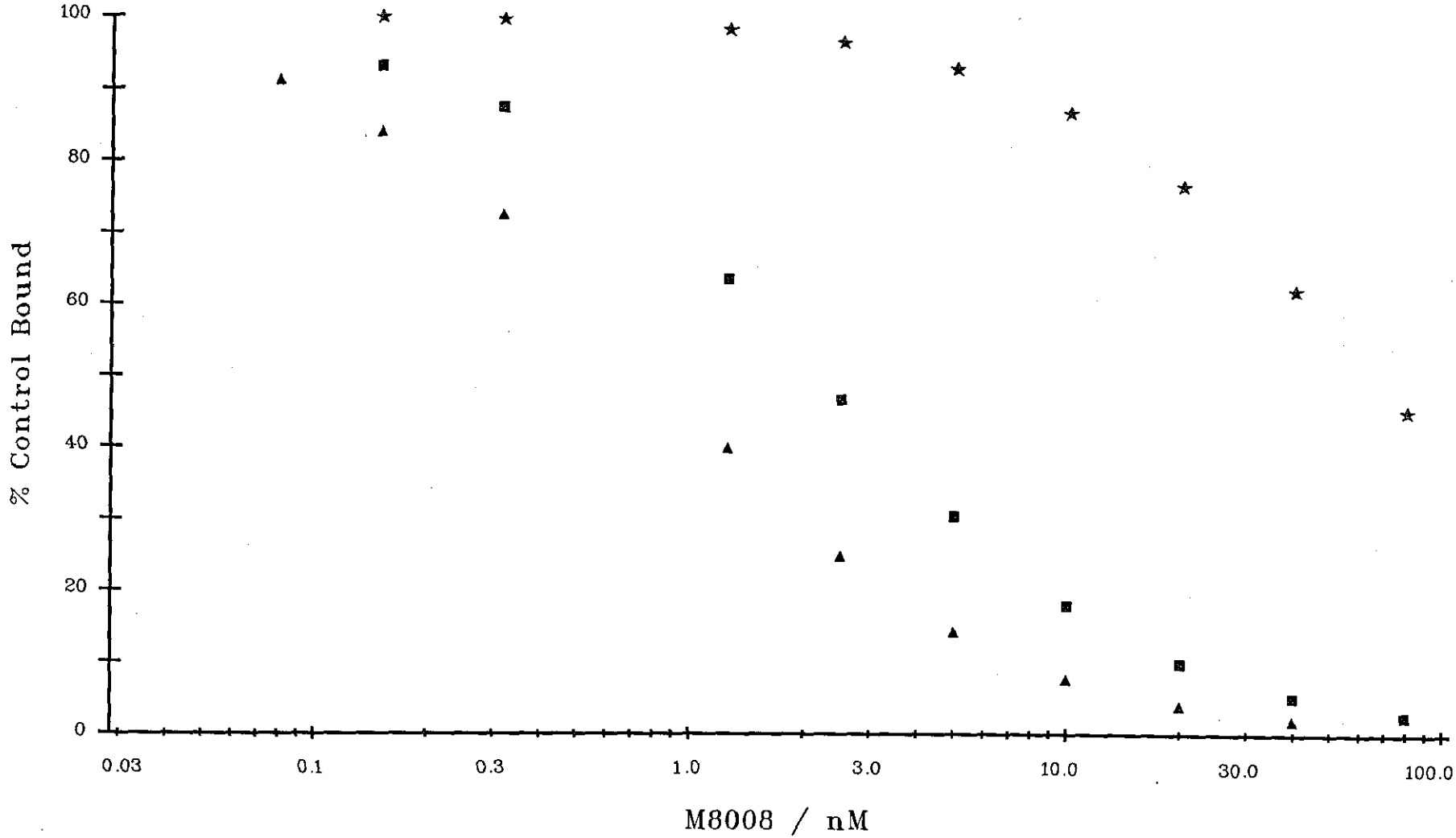

Figure 4.7: Theoretical plot representing displacement of [^{3}H]diprenorphine (0.2nM) from guinea-pig cerebellum homogenates by M8008 at μ-sites (square symbols), δ-sites (triangular symbols) and κ-sites (star symbols).

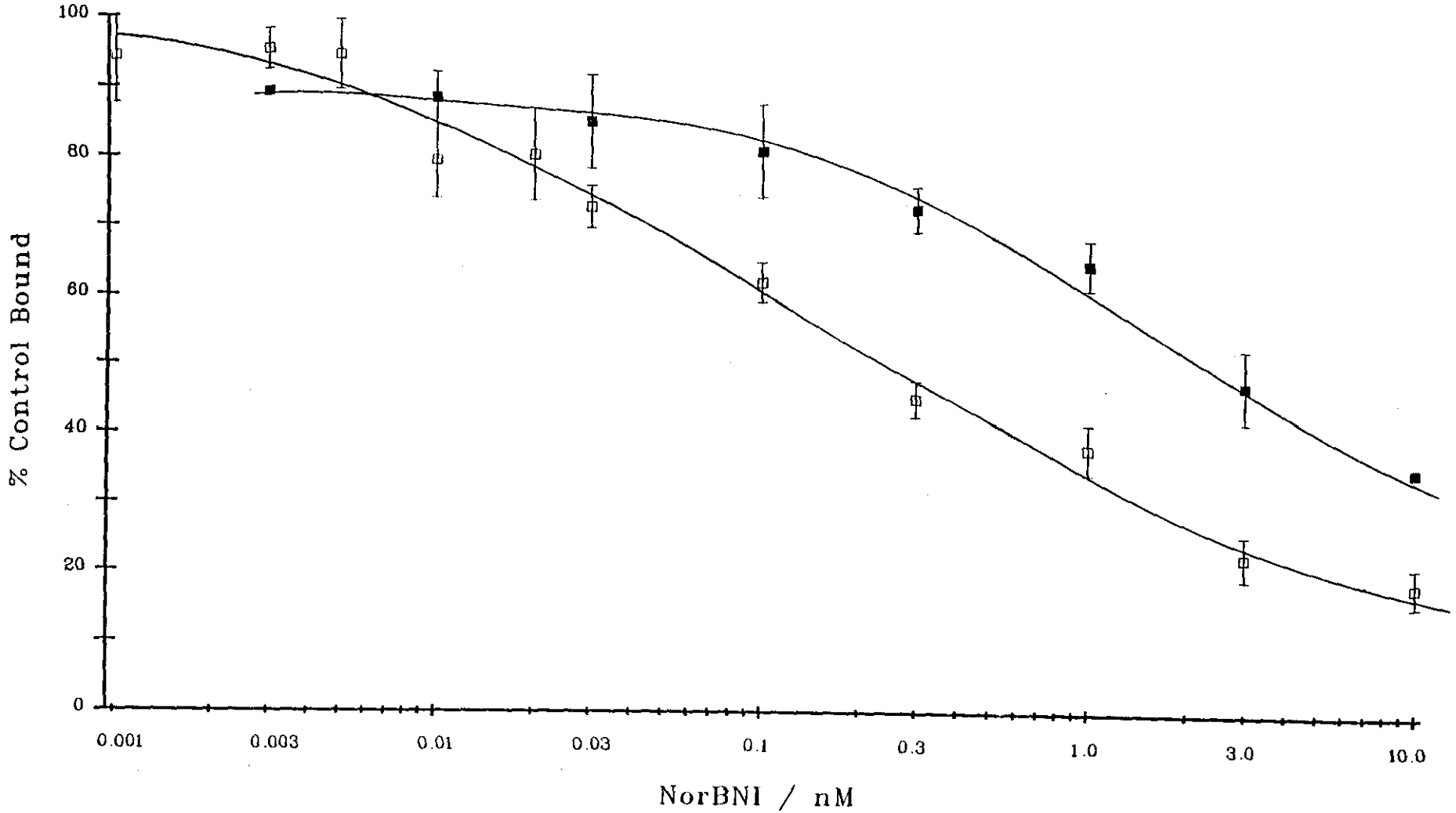

Figure **4.8** : Displacement of [^{3}H]diprenorphine (0.26 ± 0.03nM) in the presence of 20nM M8008 from guinea-pig cerebellum homogenates in Tris.HCl (50mM, pH 7.4) in the absence (closed symbols) and presence (open symbols) of 100mM NaCl and 50μM GppNHp by NorBNI.

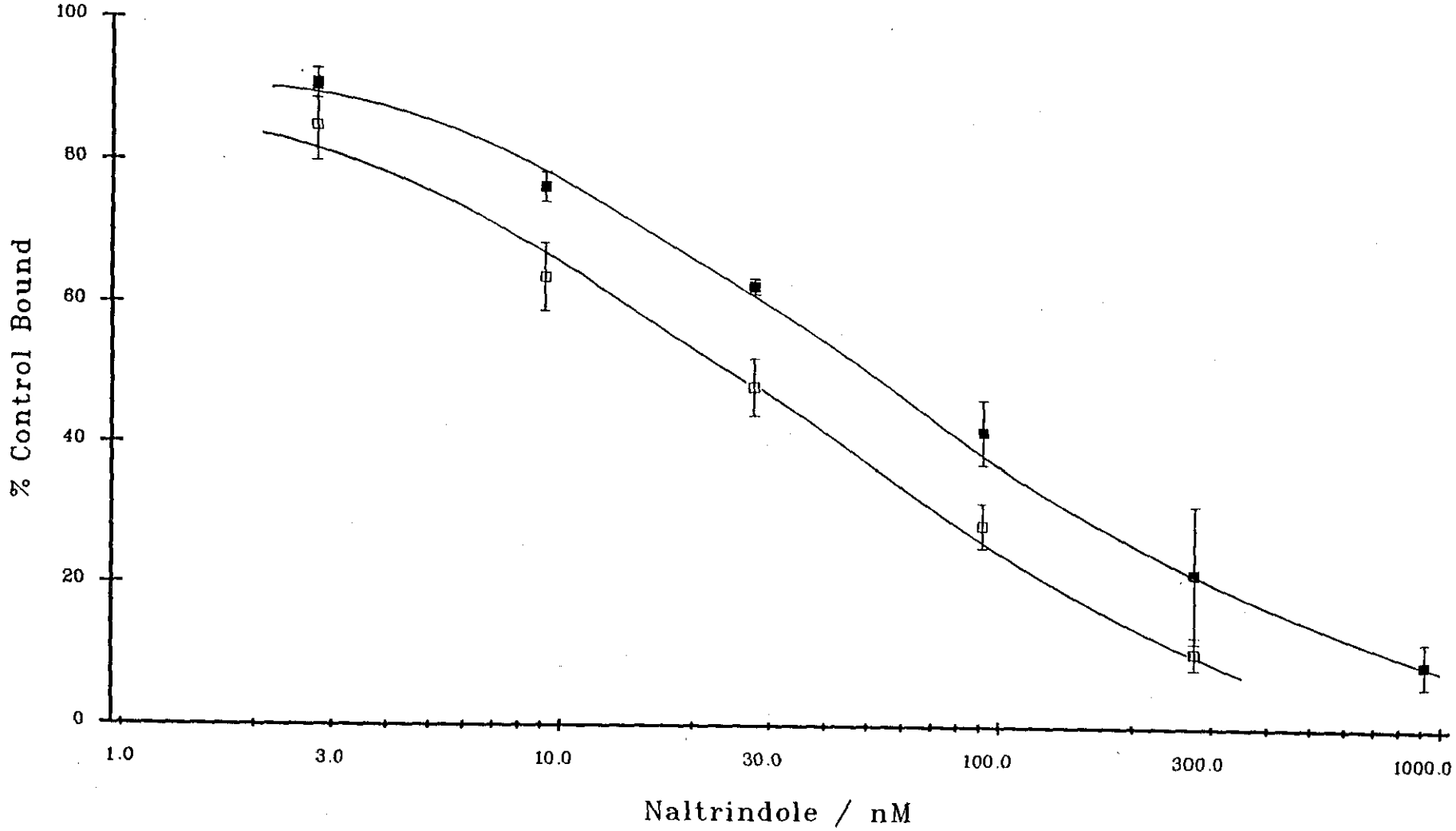

Figure 4.9 : Displacement of [^{3}H]diprenorphine (0.2 ± 0.01nM) in the presence of 20nM M8008 from guinea-pig cerebellum homogenates in Tris.HCl (50mM, pH 7.4) in the absence (closed symbols) and presence (open symbols) of 100mM NaCl and 50μM GppNHp by naltrindole.

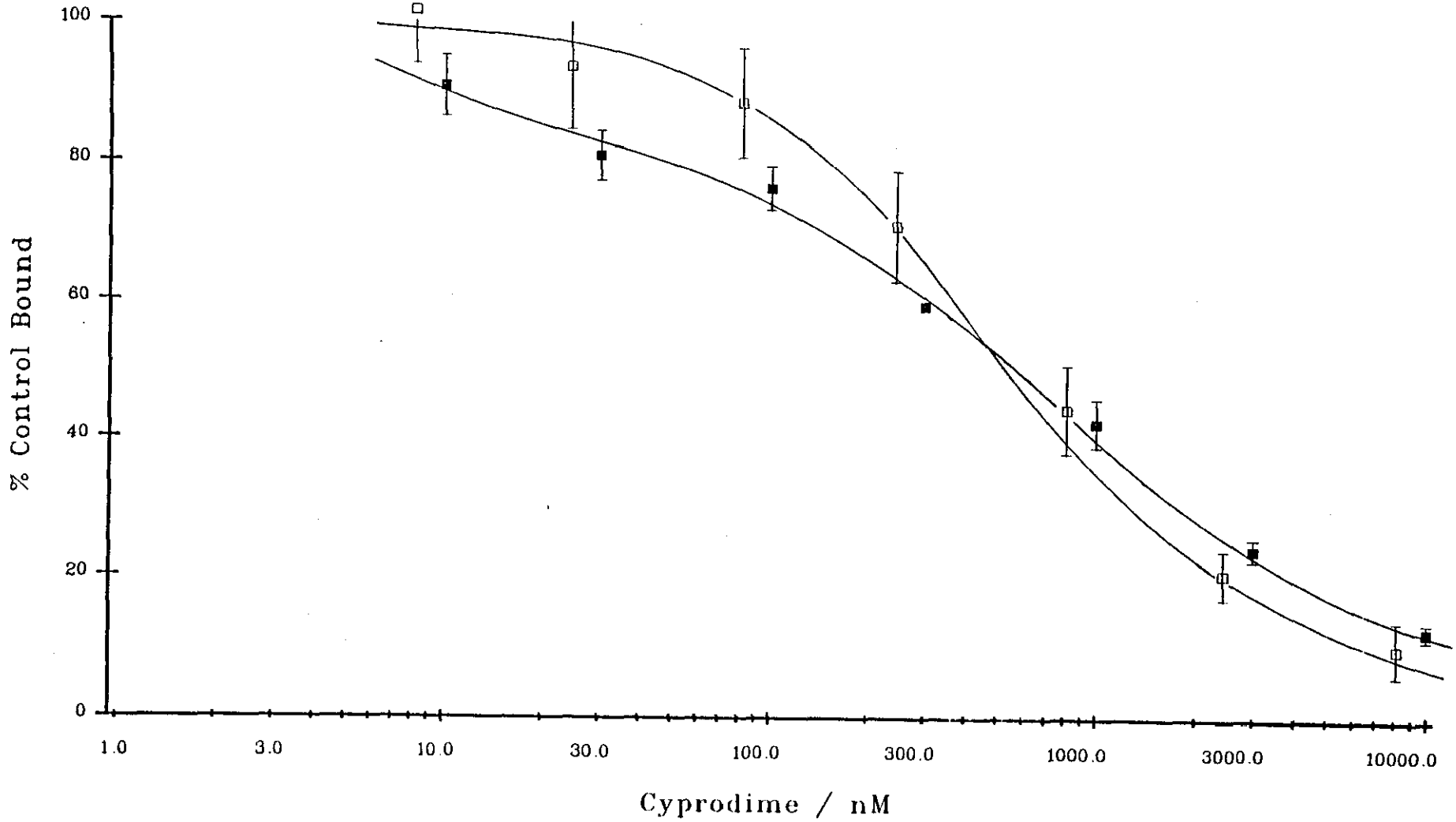

Figure **4.10** : Displacement of [^{3}H]diprenorphine (0.23 ± 0.01nM) from guinea-pig cerebellum homogenates in Tris.HCl (50mM, pH 7.4) in the absence (closed symbols) and presence (open symbols) of 100mM NaCl and 50μM GppNHp by cyprodime.

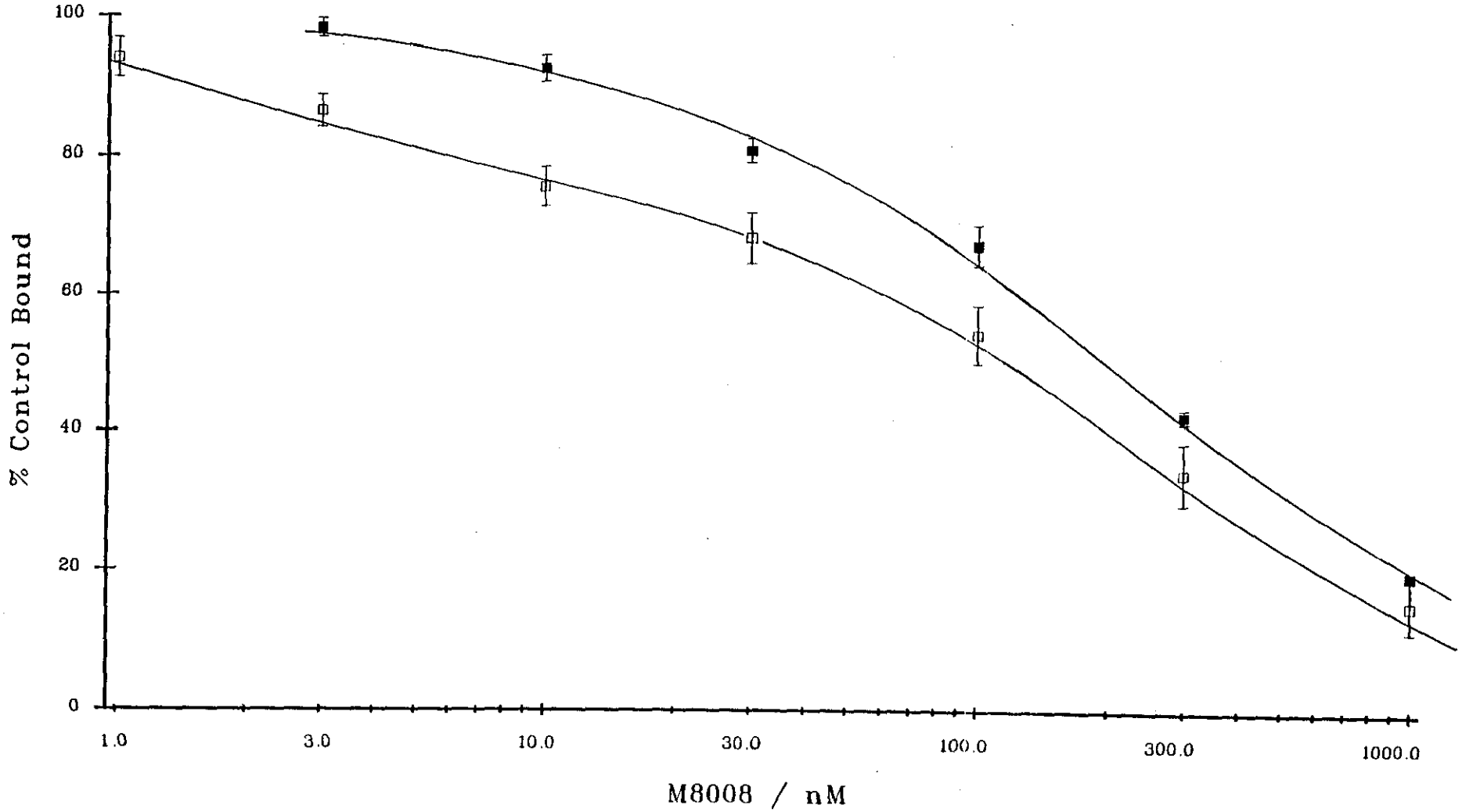

Figure **4.11** : Displacement of [^{3}H]diprenorphine (0.4 ± 0.08nM) from guinea-pig cerebellum homogenates in Tris.HCl (50mM, pH 7.4) in the absence (closed symbols) and presence (open symbols) of 100mM NaCl and 50μM GppNHp by M8008.

c) δ–Receptor studies

In Tris.HCl δ–sites in rat brain were labelled with either [^{3}H]DPDPE or [^{3}H]DADLE in the presence of 50nM DAGOL to suppress binding to μ–sites. In the presence of NaCl and GppNHp these agonist radioligands will not bind efficiently due to low agonist affinity under these conditions. Thus δ–binding under conditions promoting low agonist affinity states was studied by employing [^{3}H]diprenorphine to label δ–sites in NG108–15 cell homogenates which contain exclusively δ–receptors (111). Such studies were performed for NorBNI. However loss of this cell line meant that other means had to be found to assess δ– binding under so called "agonist" and "antagonist" conditions. Thus it was decided to use rat brain homogenates which contain a large number of δ–sites (45). Binding sites were labelled with [^{3}H]diprenorphine, employing NorBNI to suppress κ–binding and cyprodime (CTOP was not available at the time) to suppress μ–binding. The results in this chapter show cyprodime to have a good μ/κ selectivity (›30–fold). In isolated tissue bioassay (54) cyprodime is claimed to be ›100–fold selective for μ– over δ–receptors. The conditions employed, namely 20nM NorBNI and 1.26μM cyprodime create, using the receptor occupancy equation 8 on a spreadsheet format (152), a homogenate which comprises 88% δ–sites, although approximately 50% of the original number of δ–sites are occluded. The suppressing ligands create a similar final homogenate using any of the affinity values determined by different means as shown in table 4.3.

NorBNI has low affinity for δ–sites affording IC_{50} values ›60nM both in the presence and absence of NaCl and GppNHp (figure 4.12), and no shift is observed with the varying buffer conditions.

Naltrindole displaces labelled [^{3}H]diprenorphine from rat brain homogenates in the presence of 20nM NorBNI and 1.26μM cyprodime with high affinity

affording an IC_{50} of 0.26±0.2nM (figure 4.13). In the presence of 100mM NaCl and 50μM GppNHp the affinity of naltrindole increases markedly (IC_{50} 1.42±0.6pM). Under the experimental conditions used the δ-component represented approximately 65% of specific [^{3}H]diprenorphine binding. Hill coefficients for this δ-component were close to unity (0.96±0.2 and 0.91±0.08 respectively).

Table 4.3: Determination of suppressing conditions to enable δ-binding assays to be performed in rat brain homogenates.

	μ	δ	κ	(Ref)
% no. sites in rat brain	46	42	12	(45)
affinity [^{3}H]diprenorphine (nM)	0.84	1.42	2.24	(107)
Cyprodime affinities (nM):				
Tris.HCl	17.3	626	521	(chapter4)
+NaCl/GppNHp	28.2	1020$^+$	820	(chapter4)
isolated tissue	55.4	6108	1551	(54)
NorBNI affinities (nM):				
Tris.HCl	72.9	62.1	2.5	(chapter4)
+NaCl/GppNHp	50.2	63.8	0.23	(chapter4)
isolated tissue	33	20	0.4	(56)

$^+$This value is an estimate based on the shift at μ- and κ-sites.
As concentration of [^{3}H]diprenorphine used is below its K_D then the IC_{50} values approximate to the Ki.

In Tris.HCl cyprodime displaced [^{3}H]DPDPE from rat brain homogenates with low affinity (figure 4.14), giving an IC_{50} of 625.6±265nM, confirming its usefulness as a suppressing ligand being ›30–fold selective for μ– over δ–sites. The Hill slope was not significantly different from unity (table 4.3). The μ– selective peptide CTOP displaced [^{3}H]DADLE in the presence of 50nM DAGOL to suppress binding to μ–sites from rat brain homogenates in Tris.HCl with very low affinity. Indeed, only approximately 30% displacement was achieved at a concentration of 1μM.

The oripavine M8008 displaced [^{3}H]DPDPE (3.5±0.3nM) from rat brain homogenates in Tris.HCl with high affinity (figure 4.15) affording an IC_{50} of 4.3±0.54nM and a Hill coefficient of 0.93±0.07, consistent with binding to a single population of sites. Again [^{3}H]diprenorphine in rat brain in the presence of 1.26μM cyprodime and 20nM NorBNI was employed to label δ–sites (see earlier). In Tris.HCl M8008 displaced specifically bound [^{3}H]diprenorphine to such defined δ–sites with an IC_{50} of 16.7±1.9nM. Figure 4.16 shows that the addition of 100mM NaCl and 50μM GppNHp had no effect on the displacement profile (IC_{50} 21.8±6.2nM). In both cases shallow Hill slopes were obtained, presumably representing binding to unsuppressed μ– and κ–sites. Table 4.4 summarises the data obtained for ligand binding assays at δ–sites.

For comparitive purposes naloxone has been determined in this laboratory with affinities (Ki/nM) of 0.7±0.4 at μ–sites, 19.8±4.3 at δ–sites and 10.1±1.8 at κ–sites (150). These were determined in Tris.HCl and did not change with the addition of 100mM NaCl and 50μM GppNHp.

Table 4.4: Displacement from δ-sites labelled in rat brain homogenates by opioid antagonists

	Tris.HCl		+NaCl/GppNHp*	
	IC_{50}(nM)	Hill Coefficient	IC_{50}(nM)	Hill Coefficient
NorBNI	62.1±20.4[a]	0.93±0.07	63.8±1.3[b]	0.97±0.01
Naltrindole	0.26±0.2[c]	0.96±0.2	0.0014±0.0006[c]	0.91±0.08
Cyprodime	625.6±265[d]	0.72±0.1	nt	
CTOP	›1000[a]		nt	
M8008	4.31±0.5[d] 16.7±1.9[c]	0.93±0.07 0.62±0.01[$]	21.8±6.2[c]	0.62±0.06[$]

Values represent mean±sem from at least three separate determinations.

*Tris.HCl 50mM, NaCl 100mM, GppNHp 50μM.

[$]Indicates Hill coefficient significantly less than unity ($P < 0.01$) as determined by Student's t-test

Definition of binding sites as follows:

a: [^{3}H]DADLE (0.90±0.10nM) in the presence of 50μM DAGOL.

b: [^{3}H]diprenorphine (0.30±0.02nM) in NG108-15 cell homogenates.

c: [^{3}H]diprenorphine (0.65±0.04nM) in the presence of 1.26μM cyprodime and 20nM NorBNI.

d: [^{3}H]DPDPE (3.5±0.3nM).

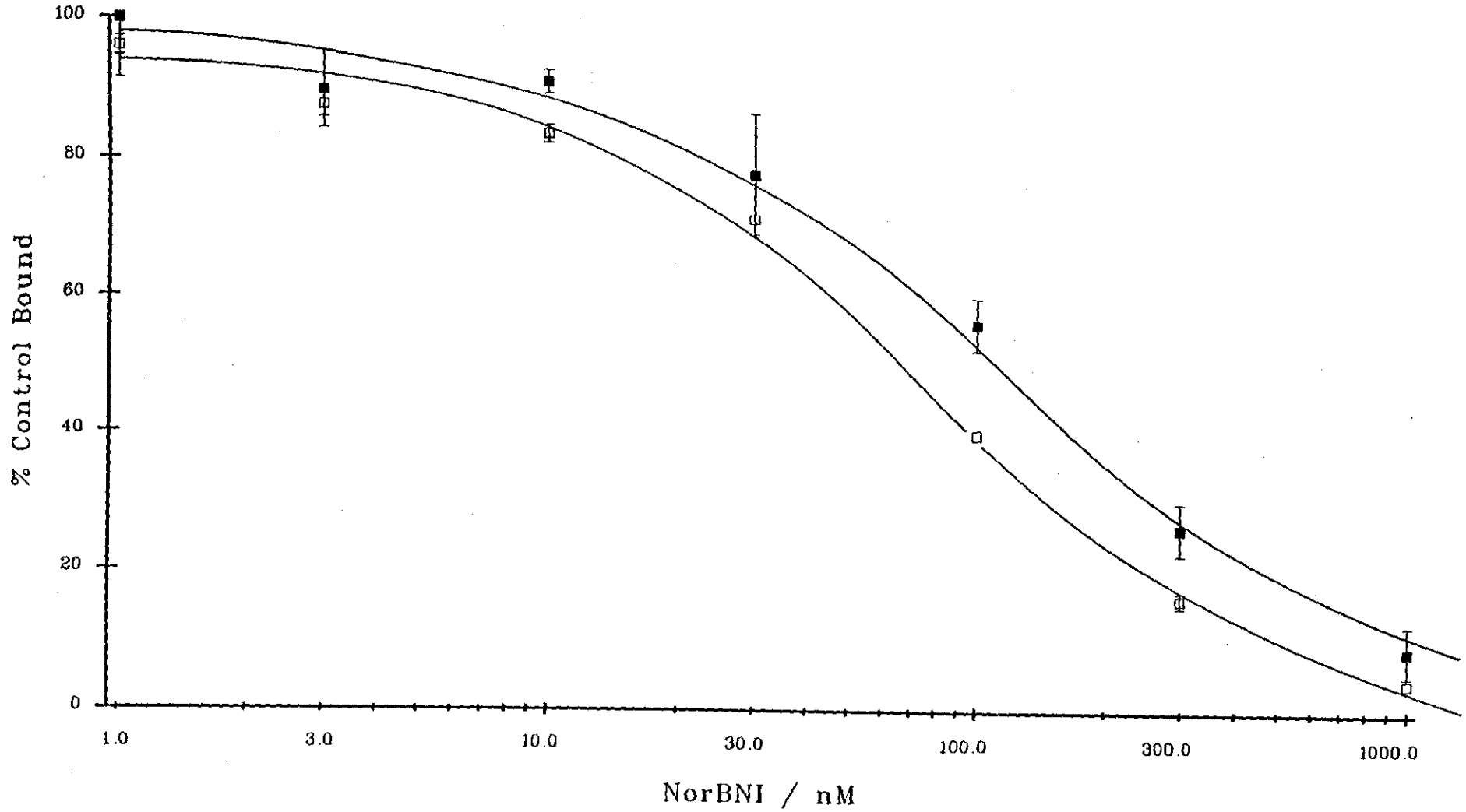

Figure **4.12** : Displacement of [^{3}H]DADLE (0.9 ± 0.1nM) in the presence of 50nM DAGOL from rat brain in Tris.HCl (50mM, pH 7.4) by NorBNI (closed symbols), and [^{3}H]diprenorphine (0.3 ± 0.04nM) from NG108-15 cell homogenates in the presence of 100mM NaCl and 50μM GppNHp (open symbols).

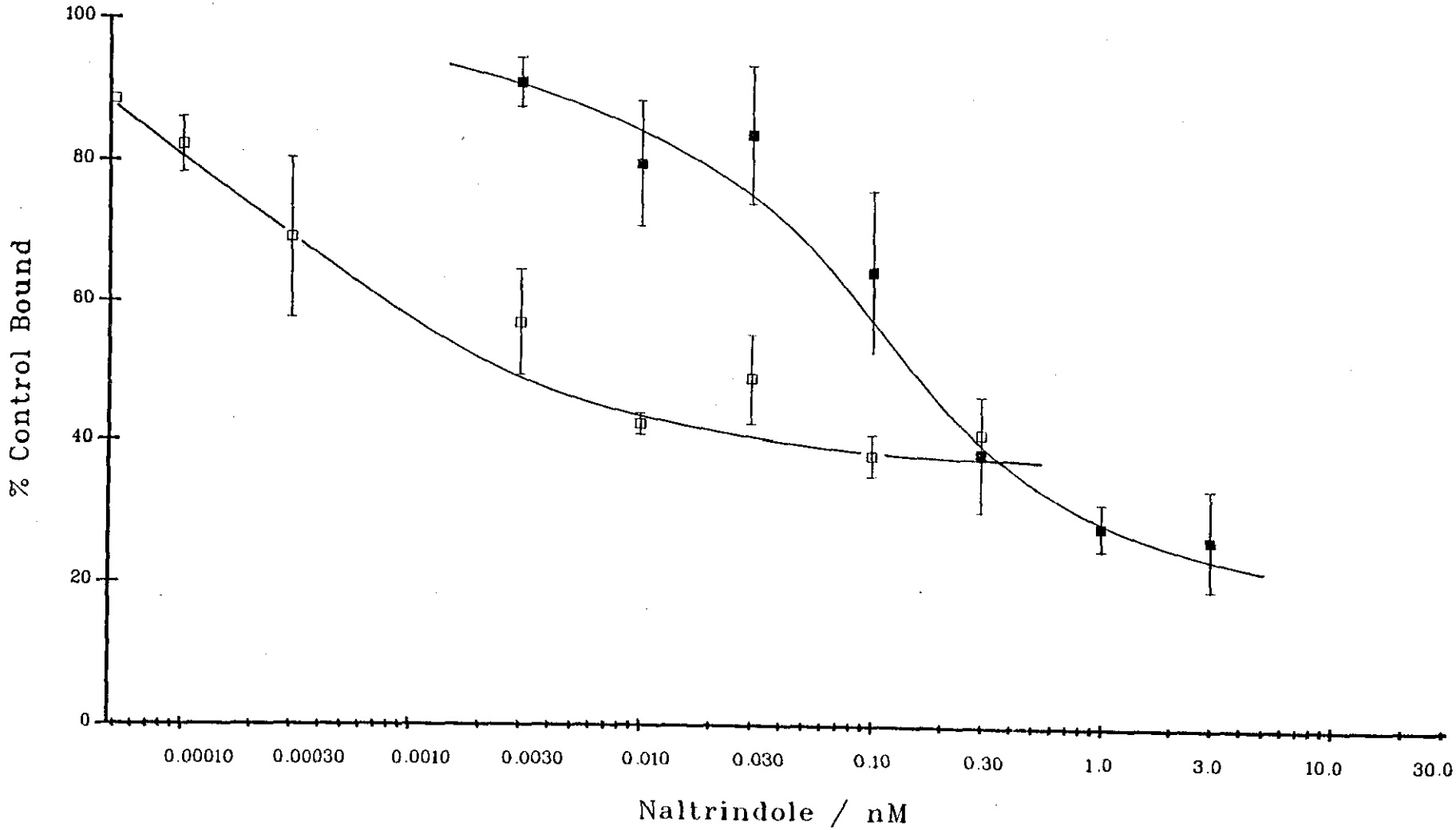

Figure **4.13** : Displacement of [^{3}H]diprenorphine (0.64 ± 0.03nM) in the presence of 1.26μM cyprodime and 20nM NorBNI from rat brain homogenates in Tris.HCl (50mM, pH 7.4) in the absence (closed symbols) and presence (open symbols) of 100mM NaCl and 50 μM GppNHp by naltrindole.

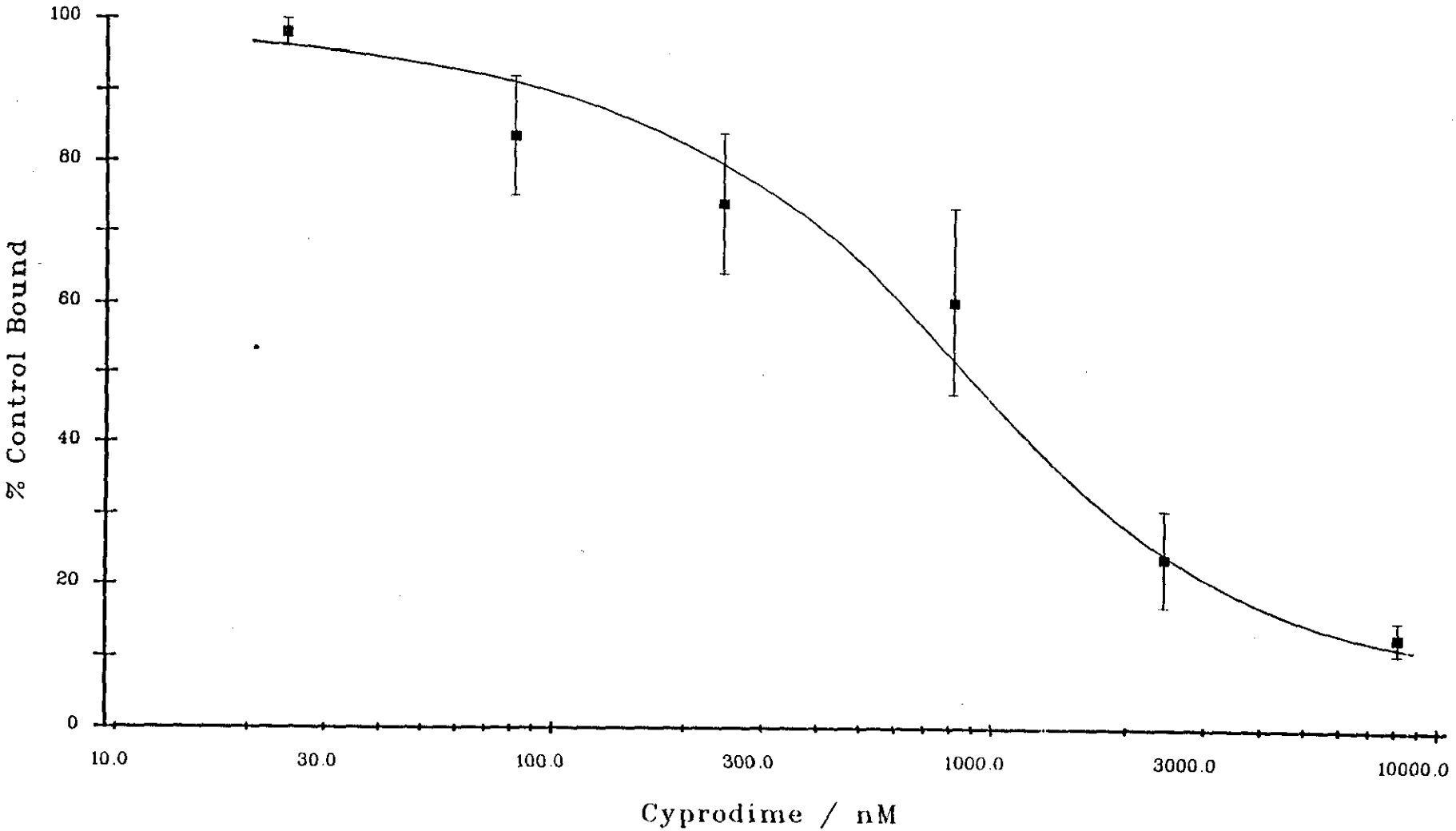

Figure **4.14** : Displacement of [^{3}H]DPDPE (3.78 ± 0.4nM) from rat brain homogenates in Tris.HCl (50mM, pH 7.4) by cyprodime.

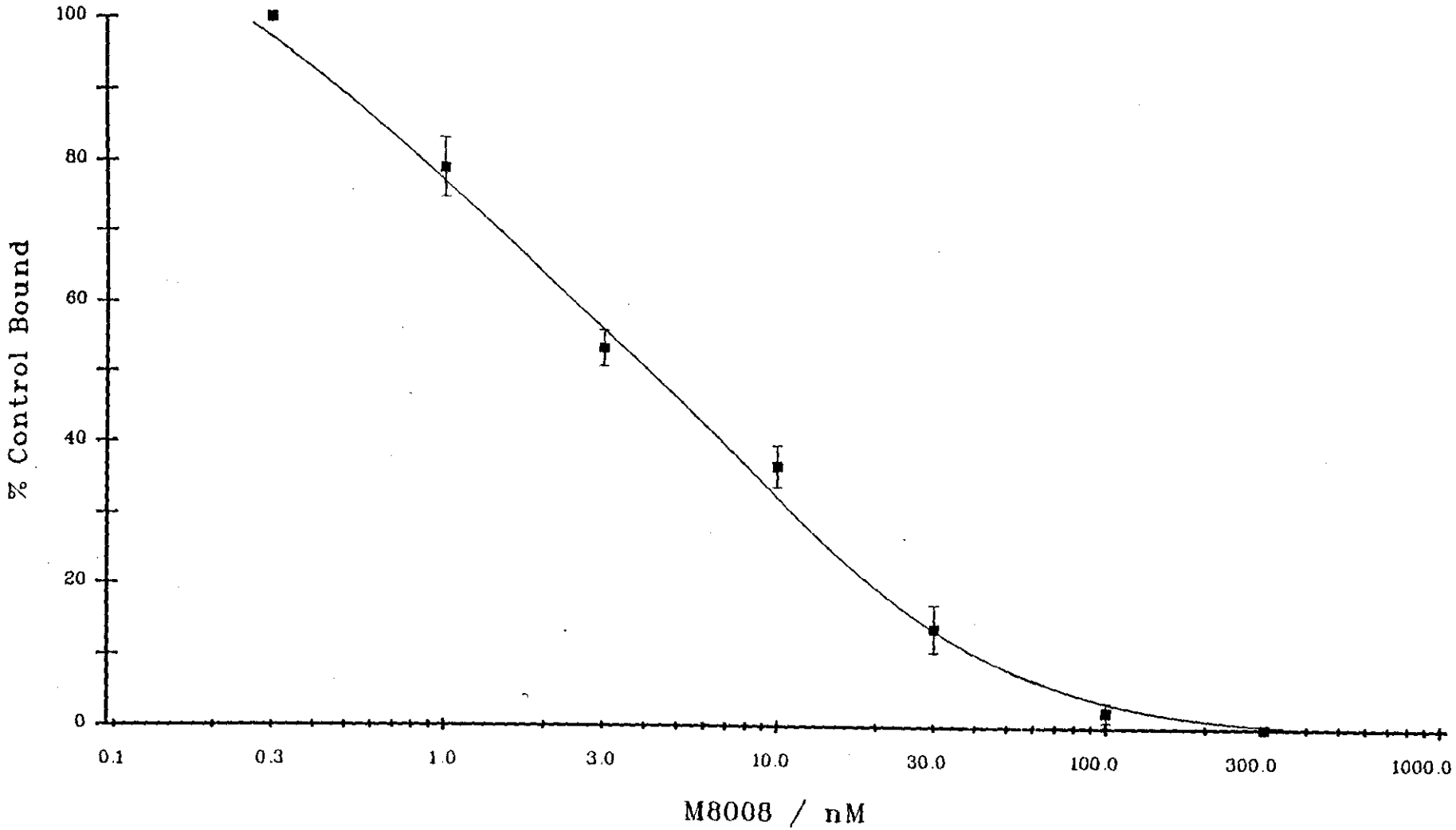

Figure **4.15** : Displacement of [^{3}H]DPDPE (3.5 ± 0.3nM) from rat brain homogenates in Tris.HCl (50mM, pH 7.4) by M8008.

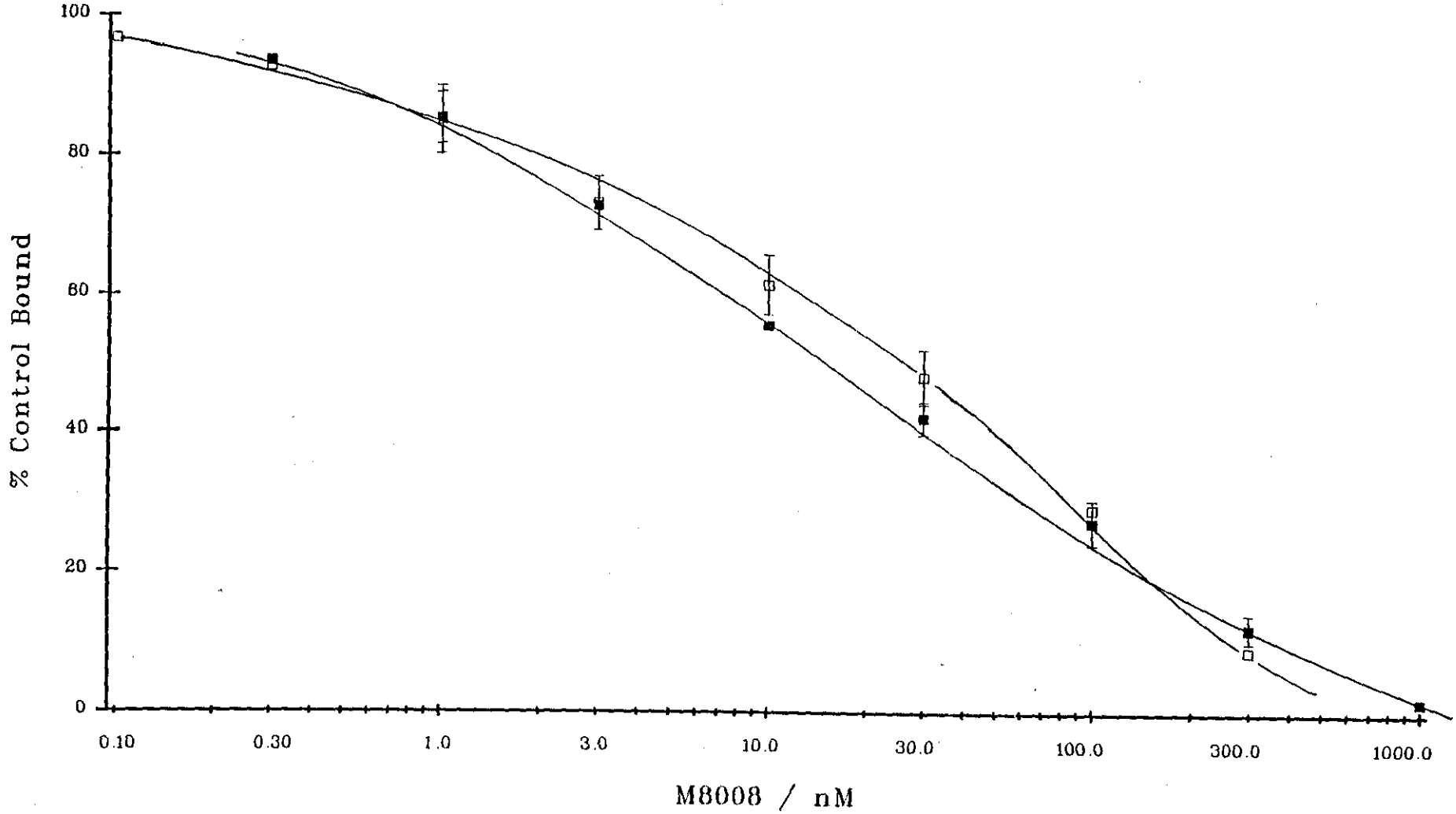

Figure **4.16** : Displacement of [^{3}H]diprenorphine (0.99 ± 0.01nM) in the presence of 1.26μM cyprodime and 20nM NorBNI from rat brain homogenates in Tris.HCl (50mM, pH 7.4) in the absence (closed symbols) and presence (open symbols) of 100mM NaCl and 50μM GppNHp by M8008.

Discussion

This study has examined the ability of a series of opioid antagonists to compete at μ–, δ– and κ–sites in order to determine whether the reported selectivity in isolated tissue assays extends to ligand binding assays and whether the reported variation of ICI 174864 with altered conditions, that is the presence of NaCl and GppNHp is a common phenomenon.

The results show the δ–antagonist naltrindole to be by far the most selective compound studied. In binding assays in Tris.HCl naltrindole is 66–fold more selective for δ– over μ–sites and 250–fold more selective for δ– over κ–sites. In the presence of NaCl and GppNHp these figures increase to 9330–fold and 17000–fold respectively.

Two μ–opioid receptor antagonists cyprodime and CTOP were studied. Cyprodime is approximately 30–fold selective for μ– over κ– and δ– sites whilst the findings confirm the highly μ–selective nature of CTOP, more so than cyprodime. Indeed at both κ– and δ–sites 1μM CTOP could only displace approximately 25% of the specific binding of radioligands.

On the other hand the oripavine antagonist M8008 proved to be the least selective of the antagonist compounds tested being almost equieffective at μ– and δ–sites. This is shown up in the shallow profiles obtained in the displacement of [^{3}H]diprenorphine from rat brain in the presence of μ– and κ– suppression. Any under–suppression of the μ–component in this experiment would result in a flattening of the displacement curve, due to lack of selectivity.

The opioid antagonist NorBNI is confirmed to be κ–selective, with selectivity ratios (>200–fold) similar to those previously reported (51).

These antagonists, in particular naltrindole, NorBNI and CTOP, being so selective should be useful in defining opioid sites. The guinea-pig cerebellum is known to contain approximately 80%κ-sites, but the remainder is thought to be a mixture of μ- and δ-sites (110). Using the above antagonists there is evidence for the non-κ component of the guinea-pig cerebellum being a population of μ-sites. This is shown by the displacement of [^{3}H]diprenorphine from guinea-pig cerebellum by cyprodime. A high affinity site (presumably μ-) is observed followed by a much larger and lower affinity site representing the κ-component. The shallow profile of NorBNI at κ-sites is evident even in the presence of 20nM M8008 which provides a population of 94% κ-sites. This may suggest the presence of different components to the κ-binding profile since antagonists are not believed to differentiate different affinity states (58). However the marked shift observed for NorBNI at the κ-site may relate to it having higher affinity for a different state of the receptor. At δ-sites however, naltrindole affords Hill slopes of unity even though this compound exhibits marked potency shifts under different conditions.

It is important to realise that binding assays are generally performed in low ionic strentgh buffers (for example 117). However, such buffers are grossly unphysiological, in particular lacking Na^+ and guanine nucleotides both of which are known to reduce agonist affinity (58). In the presence of NaCl and GppNHp the antagonists naltrindole and NorBNI shift markedly to higher affinity at the sites for which they are selective, namely δ- and κ- respectively but not at the other sites. This property has been reported previously for the peptide δ-antagonist ICI 174864 (21). The oripavine M8008 shifts to higher affinity at μ-sites , although not to the same extent as naltrindole and NorBNI and apparently does not show this affinity change at δ-sites. In the case of cyprodime no apparent shift in affinity is observed. However this is in disagreement with a reported 20-fold shift to higher affinity at μ-sites in the presence of NaCl and GppNHp (54). In agreement

with data obtained using [^{3}H]CTOP (52), the affinity at μ-sites decreased 6-fold in the presence of NaCl and GppNHp. This implies the possibility that CTOP may have some intrinsic activity, since a shift to lower affinity in these conditions would be in line with agonist properties (20, 58). However according to Paterson (164) CTOP acts as an antagonist in isolated bioassay tissue systems.

The effects of ions and nucleotides on agonist binding is well documented for opioids (20, 58, 82) and a range of other systems such as dopaminergic (120), β-adrenergic (121) and α-noradrenergic (122). However, the property of antagonists shifting to higher affinity in the presence of NaCl and GppNHp appears to be unique to opioids. The closest analogy seems to be the inverse agonists of benzodiazepine receptors (123).These effects shown by particular opioid antagonists may be due to molecular properties of the compounds, however since they appear to be site-specific the receptor must also be taken into account. Costa and Herz have recently reported the inhibition of GTPase by the δ-antagonist ICI 174864 (153), opposing the effects of agonists which stimulate GTPase. They suggest that this action requires a functional G protein able to interact with the receptor and that it depends on the receptor occupancy by the antagonist. In addition, the degree of activity of the antagonist for GTPase is correlated with an ability of the antagonist to discriminate between the free and the G protein-bound form of the receptor by having high and low affinities. This suggests the compound has some form of efficacy , opposing the effects of what are generally considered as "true" agonists. Therefore the question arises as to why certain opioid compounds behave in such a manner, i.e. respond to NaCl and GppNHp by a shift to higher affinity.

The property has been previously reported (21) with no attempt at explanation. At the time it was considered to be associated with the peptide structure of ICI 174864, since this antagonist was the first to show such

a property. However, an alternative explanation is that this compound was the first truly selective antagonist, and all such selective compounds may prove to show such a response. In this respect CTOP would not be expected to show a shift as although it is selective it appears to respond in binding assays as though it has some agonist properties.

From a study of the structures it is apparent that all the opioid receptor antagonists which show a shift to higher affinity contain unsaturation in the same region of the molecule. The double bond in the C17–C18 bridge of M8008 is in the same spatial area as the indole ring of naltrindole and the pyrrole ring of NorBNI as shown in figure 4.17. In the case of ICI 174864 the phenylalanine (residue 4) can adopt an equivalent position. The addition of NaCl and GppNHp could cause a conformational change of the protein leading to the unmasking of a hydrophobic area of the receptor in the vicinity of where this part of the molecules bind via π–electrons . This would result in the compounds such as naltrindole, NorBNI, M8008 and ICI 174864 being more tightly bound to the receptor for which they display selectivity in the presence of NaCl and GppNHp than in its absence and consequently exhibiting a higher affinity. The reason why this effect occurs only at the site for which the compounds are selective is probably one of fit.

However, if this were simply the reason for the observed shift in affinity one may expect compounds such as etorphine (an oripavine like M8008) to act in a similar manner. This is not the case, and etorphine acts as an agonist under such conditions by shifting to lower affinity (154). Although one should note that the compounds displaying a shift in affinity are all selective antagonists whereas etorphine is a high intrinsic activity agonist with little selectivity.

In general antagonist properties in opiate molecules are afforded from either

an N–allyl or N–cyclopropylmethyl substituent on the piperidine ring of the alkaloid nucleus.

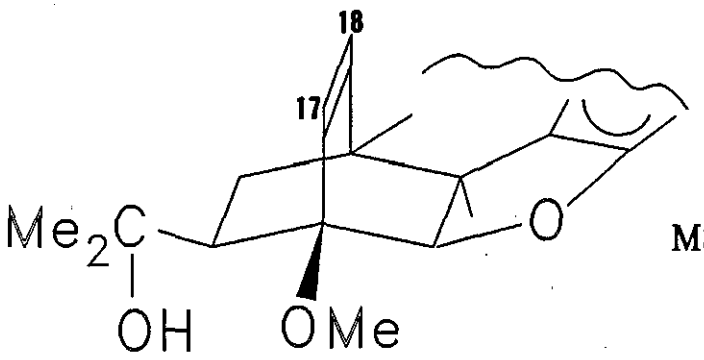

M8008

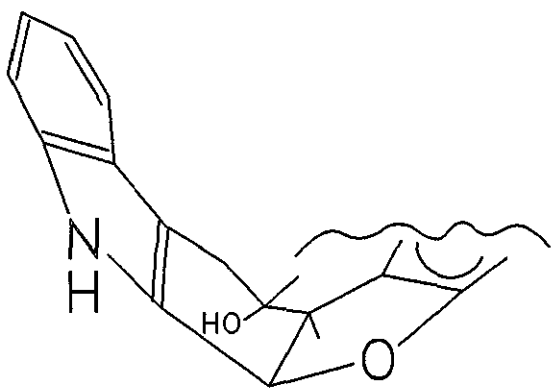

Naltrindole

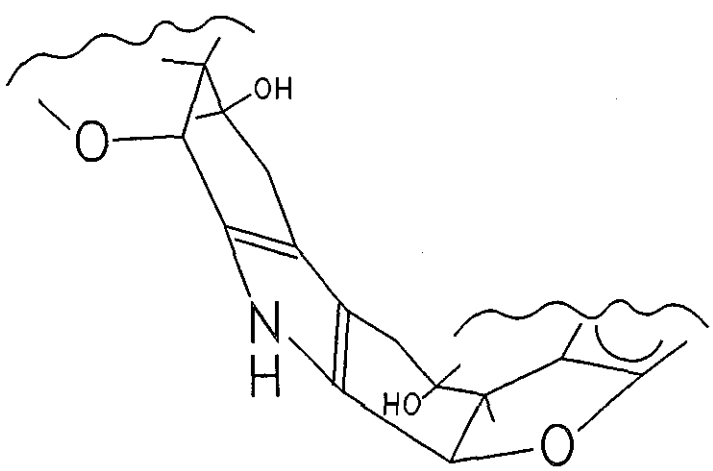

Norbinaltorphimine

Figure 4.17

This moiety could confer antagonist properties in two ways, either by binding to a specific location on the receptor or by forcing the lone pair of electrons on the ring nitrogen into such a position that it cannot bind to the receptor in a fashion necessary to activate a response. The latter possibility would be aided by antagonists containing a 14–OH group, which tend to be the purest antagonists such as naloxone. It is likely that the N–allyl or N–cyclopropylmethyl group is the reason for the general lack of effect of NaCl and GppNHp on antagonist binding relative to agonist binding. Thus, the presence of the C17–C18 double bond in etorphine could be overruled by the lack of a suitable N–substituent on the piperidine nitrogen.

Another observation which can be made is that these antagonists showing a shift to higher affinity are all conformationally rigid around C7. The addition of NaCl and GppNHp could conceivably open a "pocket" in the receptor into which the bulky substituents could easily fit and thus apparently increase the affinity of the compound. This argument could account for NorBNI, naltrindole and possibly also ICI 174864, depending on the configuration adopted by the peptide. However the case for M8008 is more complex. For M8008, rigidity in this part of the molecule could be achieved via intramolecular hydrogen–bonding between the C19–OH and the C6–OMe. The occurence of intramolecular C19–OH to C6–OMe hydrogen bonding has been demonstrated in the oripavines (124–127), although it is only thought to be of importance when large substituents are present on C19 (124), also the energy difference between the hydrogen–bonded and non hydrogen–bonded conformations of M8008 are very low (124). However diprenorphine, which does not show a shift in affinity (21) has a similar structure. This apparent anomaly may be due to the presence in diprenorphine of a saturated C17–C18 bridge, and also the lack of selectivity of this ligand (116). The extra protons would make it impossible for diprenorphine to achieve the same hydrogen–bonded structure due to steric overcrowding,

as represented in figure 4.18.

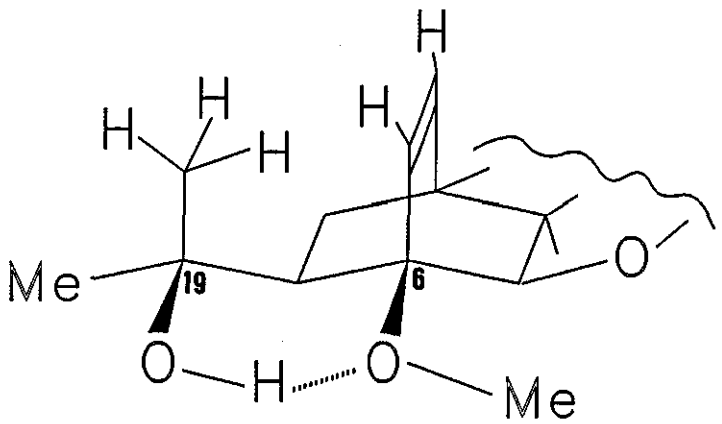

M8008

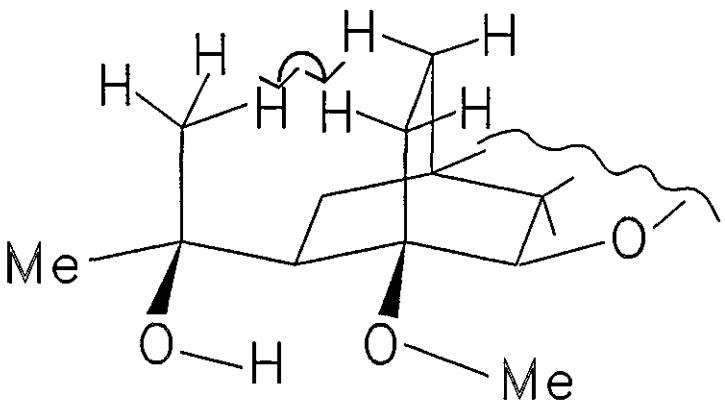

Diprenorphine

Figure 4.18

These factors taken together suggest that the conformational change necessary to confer rigidity is only one of a number of equienergetic configurations available to the molecule. This could explain the lesser shift in affinity of

M8008 compared to naltrindole, NorBNI and ICI 174864

In conclusion, this property of a shift to higher affinity in the presence of NaCl and GppNHp may be due to a variety of different parameters, probably including molecular interactions between the compound and the binding site for which it shows selectivity.These are not meant to be definitive reasons for the mechanism behind the shift but plausible explanations. However, the fact that these shifts occur cannot be ignored, especially as at least one compound in this group appears to have some efficacy in terms of GTPase activity (153).

These observed shifts demonstrate the importance of buffer composition in binding assays. If all assays were performed in physiologically relevant conditions these shifts would not be known since the compounds would only be examined in the context of their physiological environment. The possible consequences of such a shift are not immediately apparent since the physiologically relevant state is probably the low agonist affinity conformation (58). However, different affinity states may be present even though the major state will be of low agonist affinity (59). The higher affinity values obtained for the antagonists that display a shift are in line with their respective Ke values at the pertinent receptor, with the exception of naltrindole which shifts to an even higher affinity. These values are determined in bioassays under physiological conditions. The reason for the difference observed with naltrindole may be due to the presence of Mg^{++} in the bioassay system, but not in the binding assay. This ion is known to improve δ-binding (155). Thus much more information is needed to make conclusions regarding possible conformational changes induced in opiate receptor systems in response to agonists and antagonists.

CHAPTER 4: Appendix

The binding profile of the partial agonist xorphanol which is known to produce analgesia in man (113, 114) was also determined to complement preliminary studies previously carried out in this laboratory.

Initially the ability of the compound to displace the unselective antagonist [^{3}H]diprenorphine from guinea-pig brain homogenates was determined. Figure 4.19 shows that xorphanol displaces the radioligand from opioid binding sites affording an IC_{50} of 0.9±0.07nM in Tris.HCl and 3.6±0.6nM in Tris.HCl containing 100mM NaCl and 50μM GppNHp. In both buffer systems xorphanol displayed Hill coefficients close to unity (Table 4.5).

To determine whether xorphanol had any selectivity binding assays specific for μ-, δ- and κ-sites were performed. Figure 4.20 shows the ability of xorphanol to displace [^{3}H]naloxone from μ-sites in guinea-pig brain. In Tris.HCl an IC_{50} of 0.6±0.2nM is achieved whereas in the presence of Na^+ ions and GppNHp an approximate four fold shift to lower affinity occurs.

[^{3}H]DADLE in rat brain homogenates was employed to label δ-sites in the presence of 50nM DAGOL to suppress binding at μ-sites. Figure 4.21 shows xorphanol to bind to δ-sites with an IC_{50} of 1.4±0.5nM in Tris.HCl and a Hill slope of unity.

Xorphanol displaces [^{3}H]diprenorphine from guinea-pig cerebellar homogenates which can be regarded as an indication of affinity at κ-sites (figure 4.22). The shift to lower affinity in the presence of 100mM NaCl and 50μM GppNHp with an IC_{50} of 1.78±1.3nM compared to 0.47±0.1nM in Tris.HCl is not so evident at κ-sites compared to μ-sites (table 4.5).

Table 4.5: Binding Parameters of Xorphanol

Assay Conditions *	IC_{50} /nM	Hill Coefficient
total sites		
TRIS	0.89 ± 0.07	0.94 ± 0.38
TRIS–NaCl–GppNHp	3.6 ± 0.6	0.96 ± 0.15
μ–sites		
TRIS	0.62 ± 0.26	0.72 ± 0.16
TRIS–NaCl–GppNHp	2.6 ± 0.8	0.84 ± 0.1
δ–sites		
TRIS	1.4 ± 0.5	0.99 ± 0.08
κ–sites		
TRIS	0.47 ± 0.1	0.92 ± 0.04
TRIS–NaCl–GppNHp	1.78 ± 1.3	0.79 ± 0.07

Values represent mean ± sem from at least three separate determinations, No Hill coefficient was significantly less than unity as determined by Student's t–test.

* TRIS 50mM, NaCl 100mM, GppNHp 50μM.

Definition of binding sites is as follows:

Total sites: [^{3}H]diprenorphine (0.22±0.04nM) in guinea–pig brain homogenates.

μ–sites: [^{3}H]naloxone (0.28±0.04nM) in guinea–pig brain homogenates.

δ–sites: [^{3}H]DADLE (1.6±0.4nM) in rat brain homogenates in the presence of 50nM DAGOL.

κ–sites: [^{3}H]diprenorphine (0.33±0.03nM) in guinea–pig cerebellum homogenates.

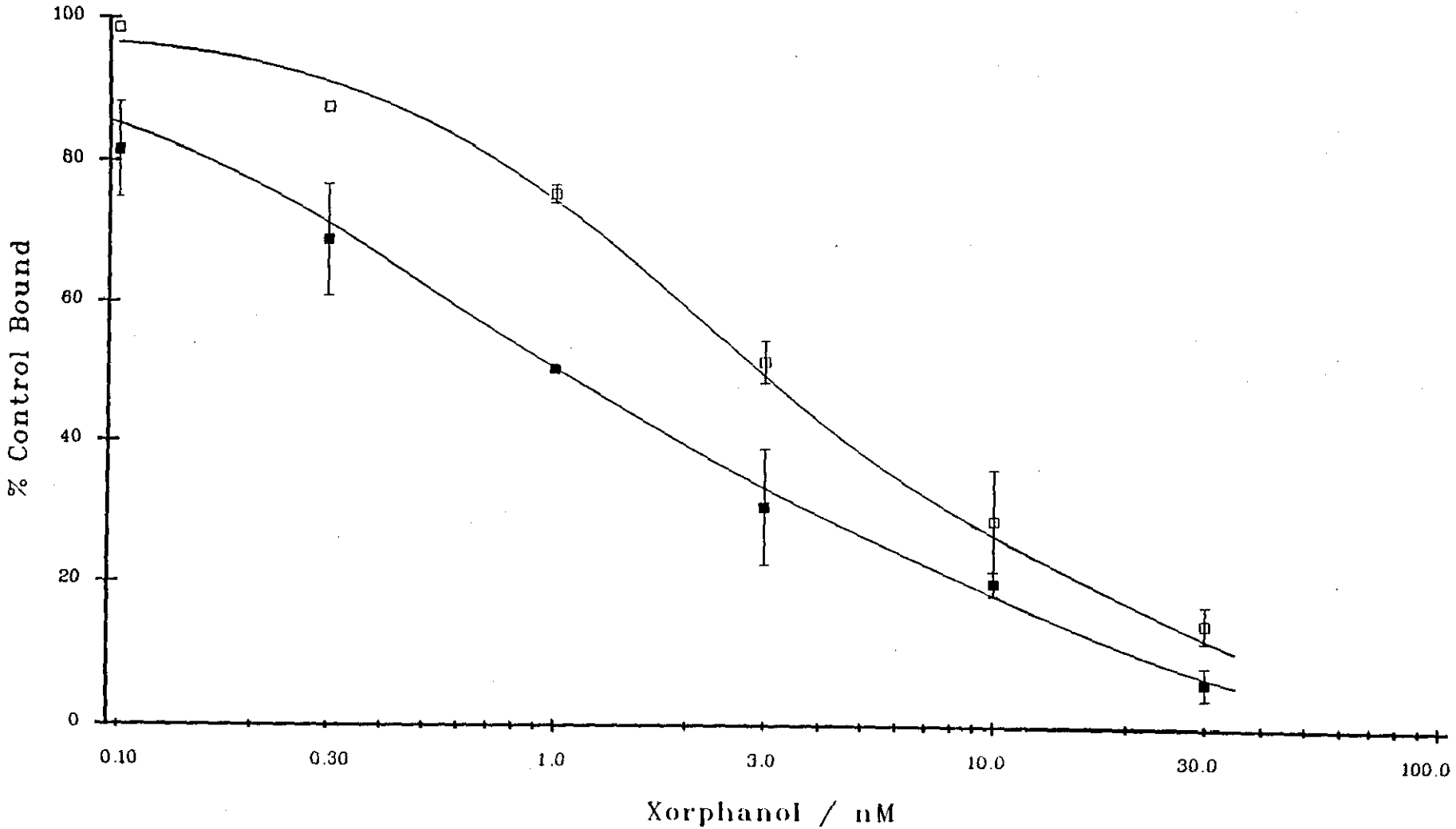

Figure **4.19** : Displacement of [^{3}H]diprenorphine (0.22 ± 0.04nM) from guinea-pig brain homogenates in Tris.HCl (50mM, pH 7.4) in the absence (closed symbols) and presence (open symbols) of 100mM NaCl and 50μM GppNHp by xorphanol.

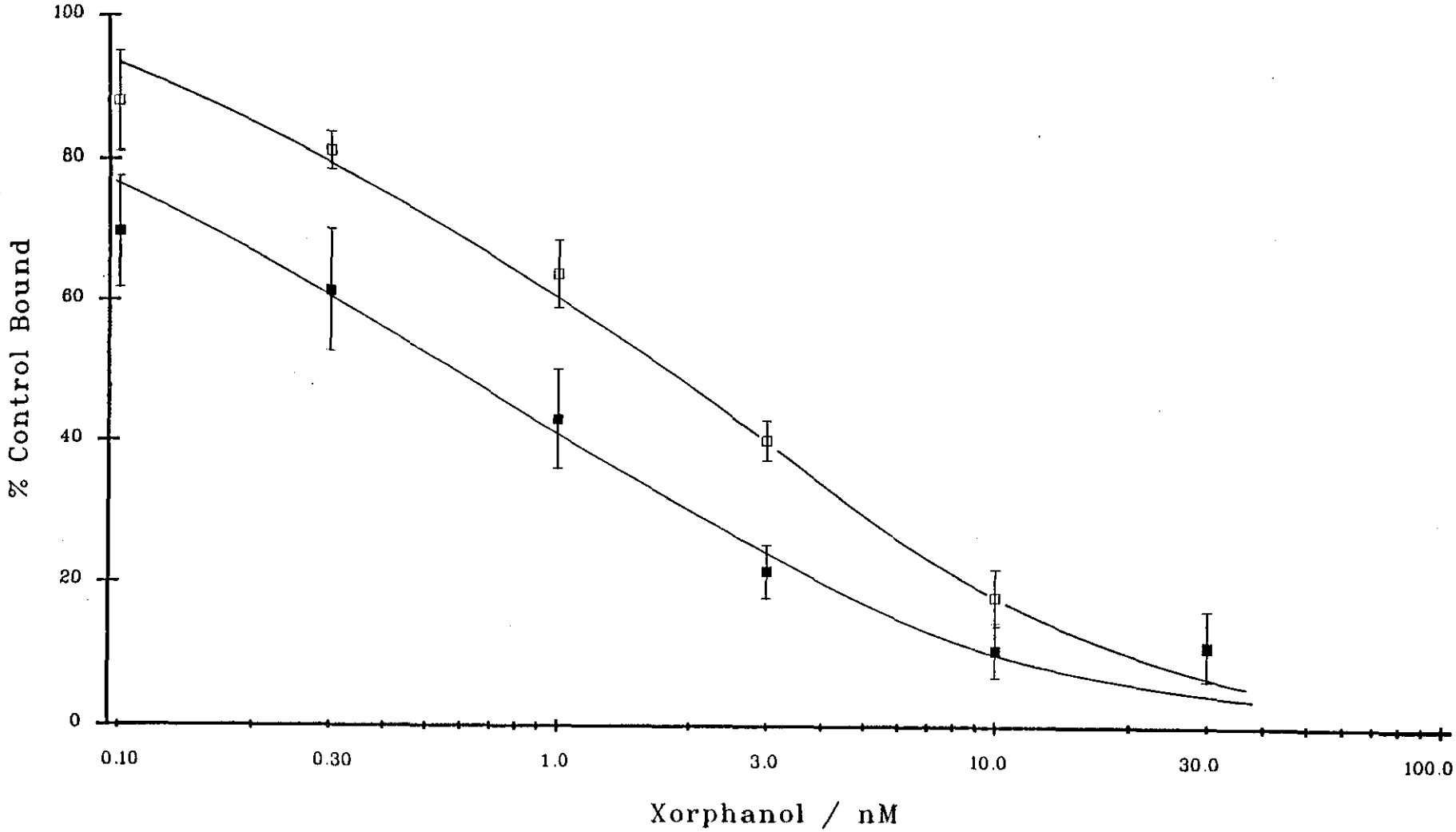

Figure **4.20** : Displacement of [^{3}H]naloxone (0.28 ± 0.04nM) from guinea-pig brain homogenates in Tris.HCl (50mM, *pH 7.4*) *in the absence (closed symbols) and* presence (open symbols) of 100mM NaCl and 50μM GppNHp by xorphanol.

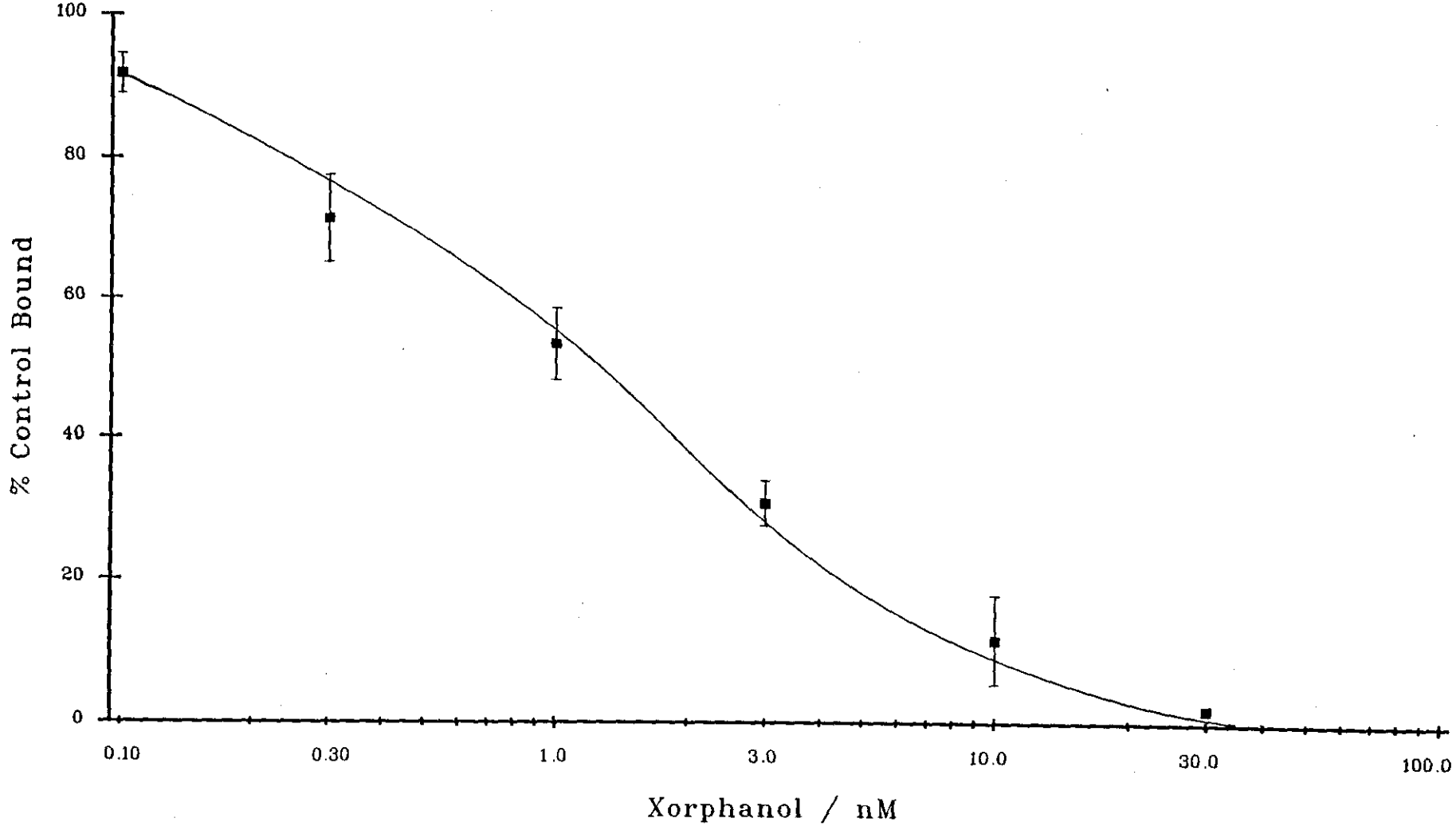

Figure **4.21** : Displacement of [^{3}H]DADLE (1.6 ± 0.4nM) in the presence of 50nM DAGOL from rat brain homogenates in Tris.HCl (50mM, pH 7.4) by xorphanol.

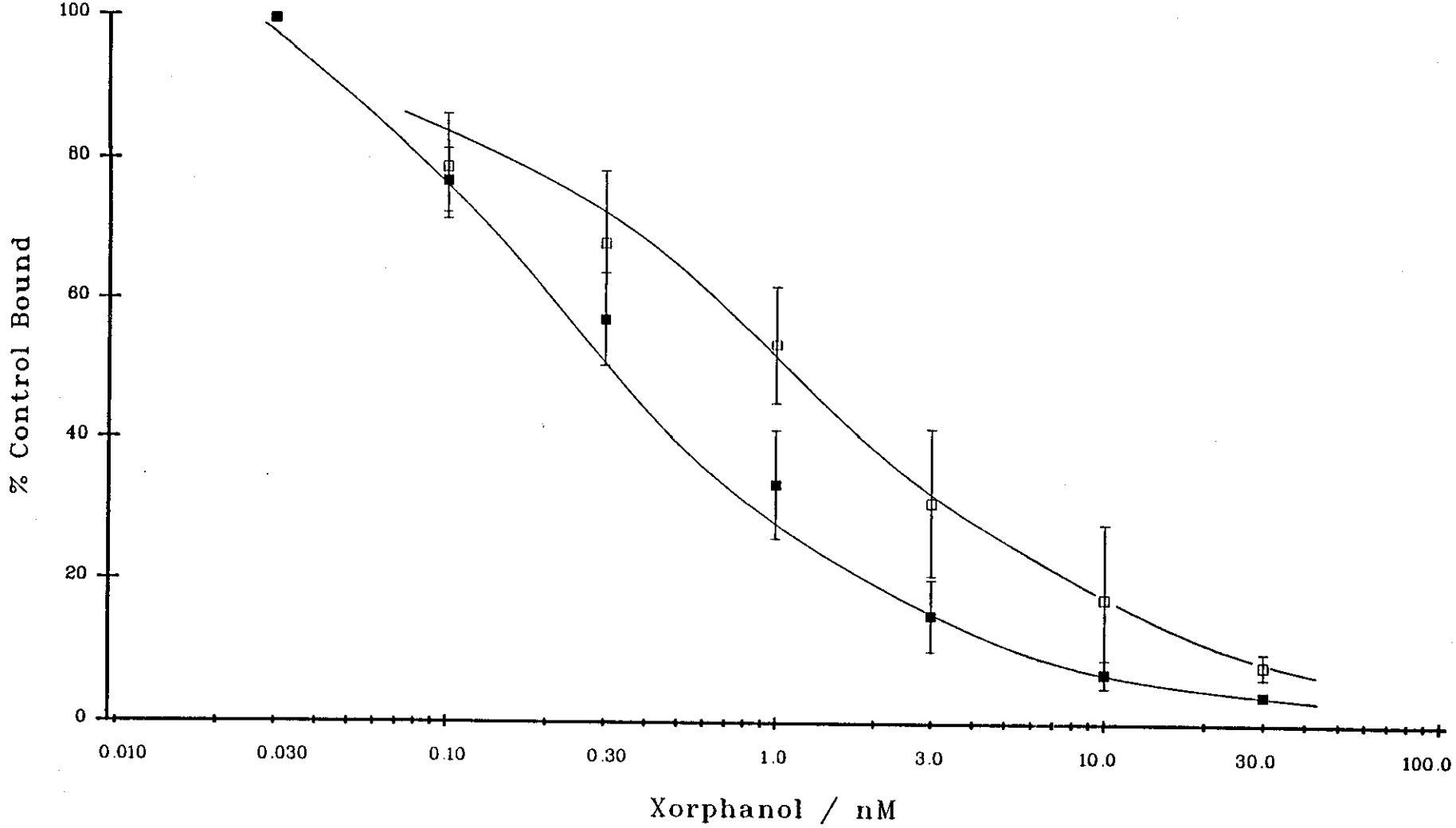

Figure **4.22** : Displacement of [^{3}H]diprenorphine (0.33 ± 0.03nM) from guinea-pig cerebellum homogenates in Tris.HCl (50mM, pH 7.4) in the absence (closed symbols) and presence (open symbols) of 100mM NaCl and 50μM GppNHp by xorphanol.

Discussion

The displacement of [^{3}H]diprenorphine by xorphanol from guinea-pig brain (-cerebellum) homogenates suggests that the compound is unselective for different opioid binding sites. This can be concluded from the value of unity for the Hill coefficient in a system containing all three recognised opioid binding sites in proportions 25% μ, 45% δ and 30% κ (49).

Xorphanol shifts approximately four-fold to lower potency in the presence of 100mM NaCl and 50μM GppNHp when displacing [^{3}H]diprenorphine from homogenates of guinea-pig cerebellum, a tissue enriched with κ-binding sites (110). Compounds with high efficacy shift markedly to lower affinity under these conditions (for example this study has shown the agonist U69593 to shift 10-fold to lower affinity). The small shift observed with xorphanol suggests that the compound is a weak agonist at κ-sites, in agreement with isolated tissue data from the guinea-pig myenteric plexus longitudinal muscle preparation (128) where xorphanol displayed actions charateristic of a partial agonist. Furthermore, xorphanol acts as an antagonist in the rabbit vas deferens preparation (128), a tissue known to contain opioid receptors only of the κ-type (129), but at which only high efficacy κ-ligands act as agonists.

A similar small shift to lower potency characteristic of a partial agonist is observed in the presence of NaCl and GppNHp when the binding of xorphanol to μ-sites labelled with [^{3}H]naloxone is determined. The observation corresponds to data obtained from rat vas deferens bioassays where antagonist actions of xorphanol are seen (128), although in this tissue only high efficacy μ-ligands act as agonists

In vivo models (130) have attributed the pharmacology of xorphanol to a predominant κ-component, and a smaller, though critical, mu-mediated

component. This correlates well with the binding data presented herein.

In binding assays xorphanol was least active at δ-sites when displacing [^{3}H]DADLE in the presence of 50nM DAGOL from rat brain homogenates. However xorphanol may well be an antagonist at δ-sites since it antagonises DADLE more potently than does ICI174864 in the hamster vas deferens (131), a tissue containing opioid receptors only of the δ-type (132).

In conclusion it can be said that in terms of binding xorphanol is equipotent at both μ- and κ-sites with lower affinity at δ-sites. Phase II clinical trials (113) reveal xorphanol to be a well-tolerated, orally active analgesic with a low dependence-liability and thus is potentially of clinical use.

CHAPTER 5: USE OF SELECTIVE ANTAGONISTS TO STUDY THE BINDING OF [^{3}H]DIPRENORPHINE TO RAT BRAIN HOMOGENATES

Introduction

Data from ligand binding assays has suggested diprenorphine should be considered as an unselective antagonist. Although it is generally considered as an antagonist diprenorphine does have some agonist properties at the κ-receptor in the guinea-pig ileum, a tissue with a high receptor reserve (112). Reported relative affinities of [^{3}H]diprenorphine as measured in binding assays at μ-, δ- and κ-opioid sites are 0.51, 0.3 and 0.19 respectively. These figures have led to diprenorphine being referred to as "the almost universal antagonist" (116). Indeed [^{3}H]diprenorphine labels all different affinity states of opioid receptors, both "agonist" and "antagonist" forms and has been used therefore to investigate binding under conditions where Krebs-type buffers rather than the traditional Tris buffers have been employed. Under the former conditions opioid agonists do not bind well due to a reduced affinity (58, 59).

One problem with [^{3}H]diprenorphine however is that it does appear to label many more sites than can be explained in terms of conventional opioid binding (78, 117). For example [^{3}H]diprenorphine labels twice the number of sites in rat spinal cord than are seen by another unselective ligand [^{3}H]bremazocine (156). All of these sites appear to be naloxone sensitive confirming their opioid nature. Also Morris and Herz find [^{3}H]diprenorphine binding in brain (78) even when μ-, δ- and κ- binding is suppressed.

In spite of the above findings however, *in vivo* radioligand binding assays in the mouse by Frost and colleagues suggest that [^{3}H]diprenorphine labels

mainly the μ-opioid binding site (118). This conclusion is based on the observations that naloxone and a μ-agonist, carfentanyl, displaced [^{3}H]diprenorphine both from the thalamus, which is reportedly enriched in μ-sites, and the striatum, which is enriched with δ-sites in a manner consistent with binding to a single site. However naloxone with a selectivity profile of affinities at μ-, δ- and κ-sites of approimately 2nM, 17nM and 27nM (107) is unlikely to distinguish different sites, particularly *in vivo* although carfentanyl displays affinities at 37°C of μ- 0.051nM, δ-4.7nM and κ-13nM and thus is a selective μ-ligand (163). The findings in bioassay that diprenorphine shows a 7-fold higher affinity for μ-receptors over δ- and κ-receptors (112) may however lend some support to the results of Frost and coworkers.

*

It was decided therefore to reinvestigate the binding of [^{3}H]diprenorphine to rat brain homogenates, a tissue reported to contain μ-, δ- and κ- receptors in the ratio 46, 42% and 12% respectively (45). The aim of this work was to tackle some of the inconsistencies which exist in the findings with this ligand. In order to establish the binding profile it was intended to make use of the antagonists characterised in chapter four.

Materials and Methods

Homogenates of rat brain minus cerebellum were prepared and binding assays carried out as described in chapter two. Assays were performed in Tris.HCl buffer containing 100mM NaCl and 50μM GppNHp.

[^{3}H]Diprenorphine was used to label opioid binding sites. Details of suppressing conditions are described in relevant results sections. Non-specific binding was defined using 10μM naloxone.

Results

[^{3}H]Diprenorphine bound to homogenates of rat brain in Tris.HCl containing 100mM NaCl and 50mM GppNHp. At a concentration of 0.5nM the specific binding comprised 87.5± 12.5% of the total bound ligand.

Under the conditions used however there was less than 10% of this specifically bound ligand displaced by NorBNI at concentrations (<10nM) consistent with its affinity for κ–receptors. At increased concentrations NorBNI displayed characteristics typical of displacement from a single population of binding sites, affording a Hill coefficient of 0.94±0.12, and an IC_{50} of 96.05±19.9nM (figure 5.1).

A similar lack of displacement with the δ–antagonist naltrindole was seen until a concentration much in excess of that expected to interact with δ–sites was reached. The obtained results at higher concentrations, namely an IC_{50} of 21.6±4.5nM and a Hill coefficient of 0.82±0.02 is again consistent with the idea that this ligand is recognising only a single class of sites (figure 5.2).

The selective σ –agonist (+)SKF 10,047 was unable to displace 50% of bound [^{3}H]diprenorphine even at a concentration of 3μM. The displacement curve (figure 5.6) suggests that a very small σ – component cannot be excluded. This contrasts with the work from Herz's laboratory (78) which suggests that [^{3}H]diprenorphine does not label σ –sites in rat brain, and the results of Tam (81) who finds no activity of diprenorphine at the σ –site defined with [^{3}H](±)EKC. The reasons for the discrepancy are not known but may relate to the very low level of σ –binding in these tissues.

The above results appear to confirm that at the level of [^{3}H]diprenorphine used this ligand is binding to a mostly single class of sites which are not

κ–, δ– or σ – as defined by displacements with the selective compounds. However the μ–antagonists cyprodime and CTOP (figure 5.3) did not show profiles consistent with binding to a single, presumably μ–, site. Both of these compounds afforded IC_{50} values approximately ten times greater than expected from the data presented in chapter four. This is as a consequence of heterogeneous binding as shown up in the shallow Hill coefficients (table 5.1).

Table 5.1 Displacement of [^{3}H] diprenorphine (0.3–0.8nM) from Rat Brain Homogenates.

Compound	IC_{50} /nM	Hill Coefficient
NorBNI	96.1 ± 19.9	0.94 ± 0.12
Naltrindole	21.6 ± 4.5	0.82 ± 0.02
Cyprodime	211 ± 34	0.70 ± 0.02 $
CTOP	363 ± 140	0.64 ± 0.05 $
DAGOL	1212 ± 218	0.47 ± 0.04 $
Morphine	671 ± 119	0.70 ± 0.01 $
Fentanyl	457 ± 31	0.60 ± 0.05 $
(+)SKF 10,047	› 3000	–

Values represent mean ± sem from at least three different determinations, performed in Tris.HCl (50mM, pH 7.4) in the presence of 100mM NaCl and 50μM GppNHp.
$ Indicates Hill coefficient significantly less than unity ($P<0.05$) as measured by Student's t-test.

The competition of [^{3}H]diprenorphine binding by the three μ–agonists morphine, DAGOL and fentanyl (figures 5.4 and 5.5) was similarly consistent with a heterogeneous binding of the radioligand. Although at high concentrations the ligands are able to displace the bound [^{3}H]diprenorphine very shallow displacement curves were obtained.

The results for the displacements are given in table 5.1. Because it is not known what sites are involved the data is presented as IC_{50} values with no attempt made to convert these to affinities.

To determine whether the apparently heterogeneous binding to μ-sites was due to a small percentage of labelled δ- and κ-sites the displacement curve for the agonist fentanyl was repeated in the presence of the κ-antagonist NorBNI and the δ-antagonist naltrindole at fifty times their affinity for the pertinent binding sites (10nM and 0.1nM respectively). In a further series of experiments the σ -agonist (+)SKF 10,047 was added to this "cocktail" at a concentration of 300nM. Neither of these conditions altered the displacement profile of fentanyl against [^{3}H]diprenorphine (figures 5.5 and 5.7).

This final assay was repeated with many more data points (figure 5.8) in order to analyse the data using the profram LIGAND (105) in terms of different models. Of five similar assays which were carried out all displacements had Hill coefficients lower than 0.5. Three out of the five gave data affording a significantly better fit for a two-site over a one-site model. The results of analysis by the non-linear curve fitting algorithm are given in table 5.2.

Table 5.2: LIGAND Analysis of Fentanyl displacement assay.

Compound	(app) Ki/nM	Bmax/fmol.mg^{-1}
site 1	38.5 ± 9	33.8 ± 6.4
site 2	1216 ± 442	10.3 ± 3.8

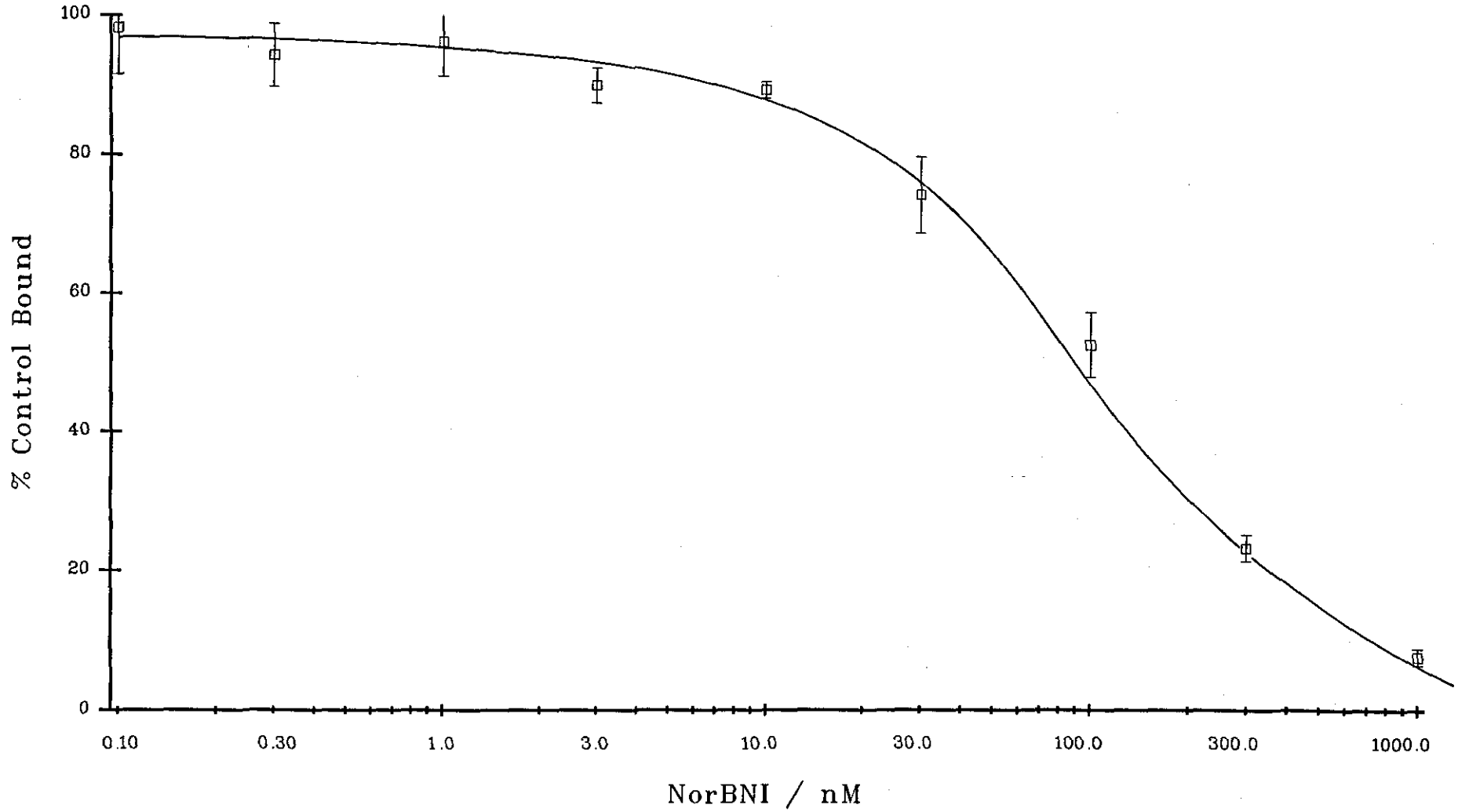

Figure 5.1: Displacement of [^{3}H]diprenorphine (0.86 ± 0.06nM) from rat brain homogenates in Tris.HCl (50mM, pH 7.4) containing 100mM NaCl and 50μM GppNHp by NorBNI.

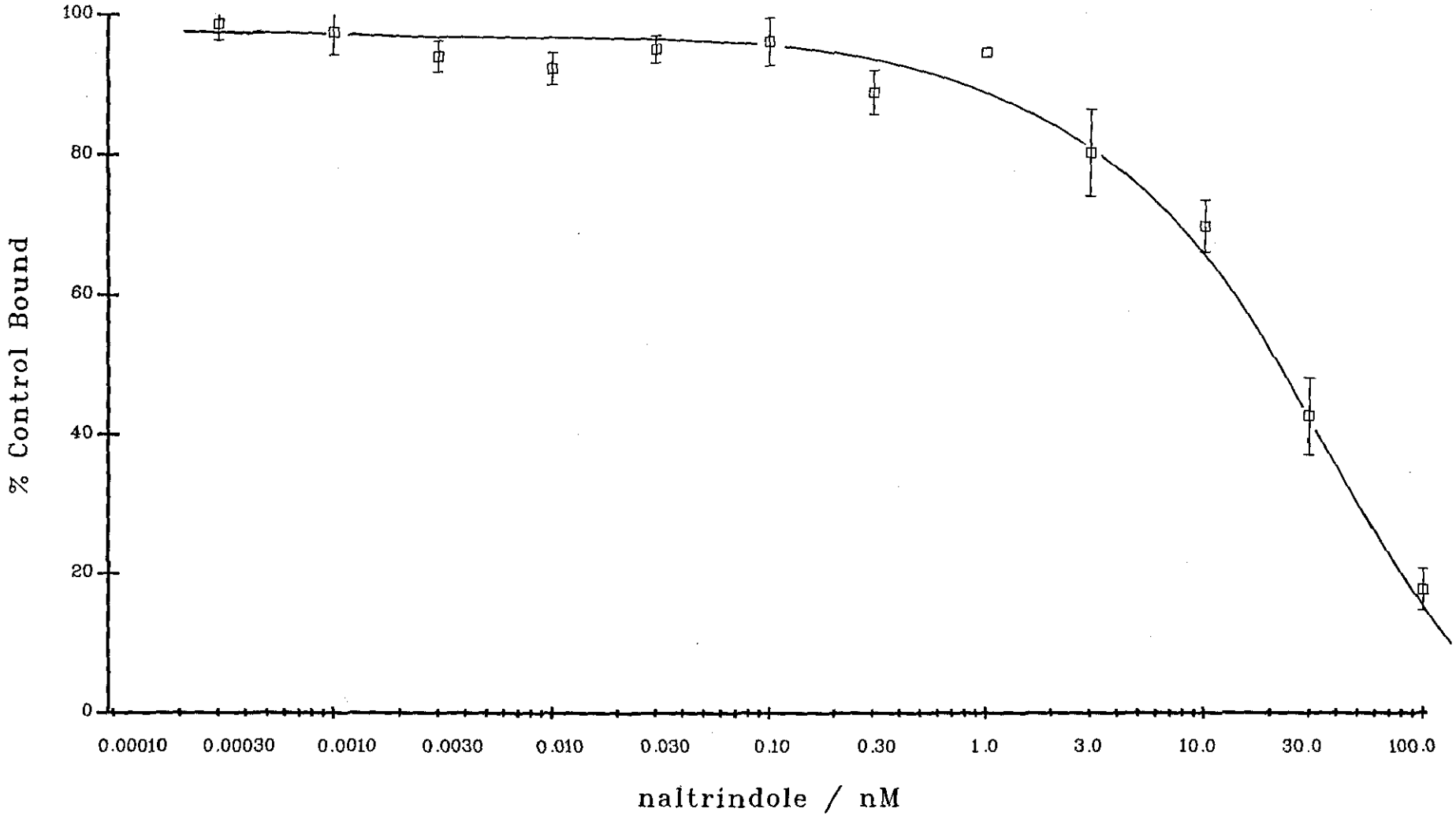

Figure 5.2: Displacement of [^{3}H]diprenorphine (0.34 ± 0.08nM) from rat brain homogenates in Tris.HCl (50mM, pH 7.4) containing 100mM NaCl and 50μM GppNHp by naltrindole.

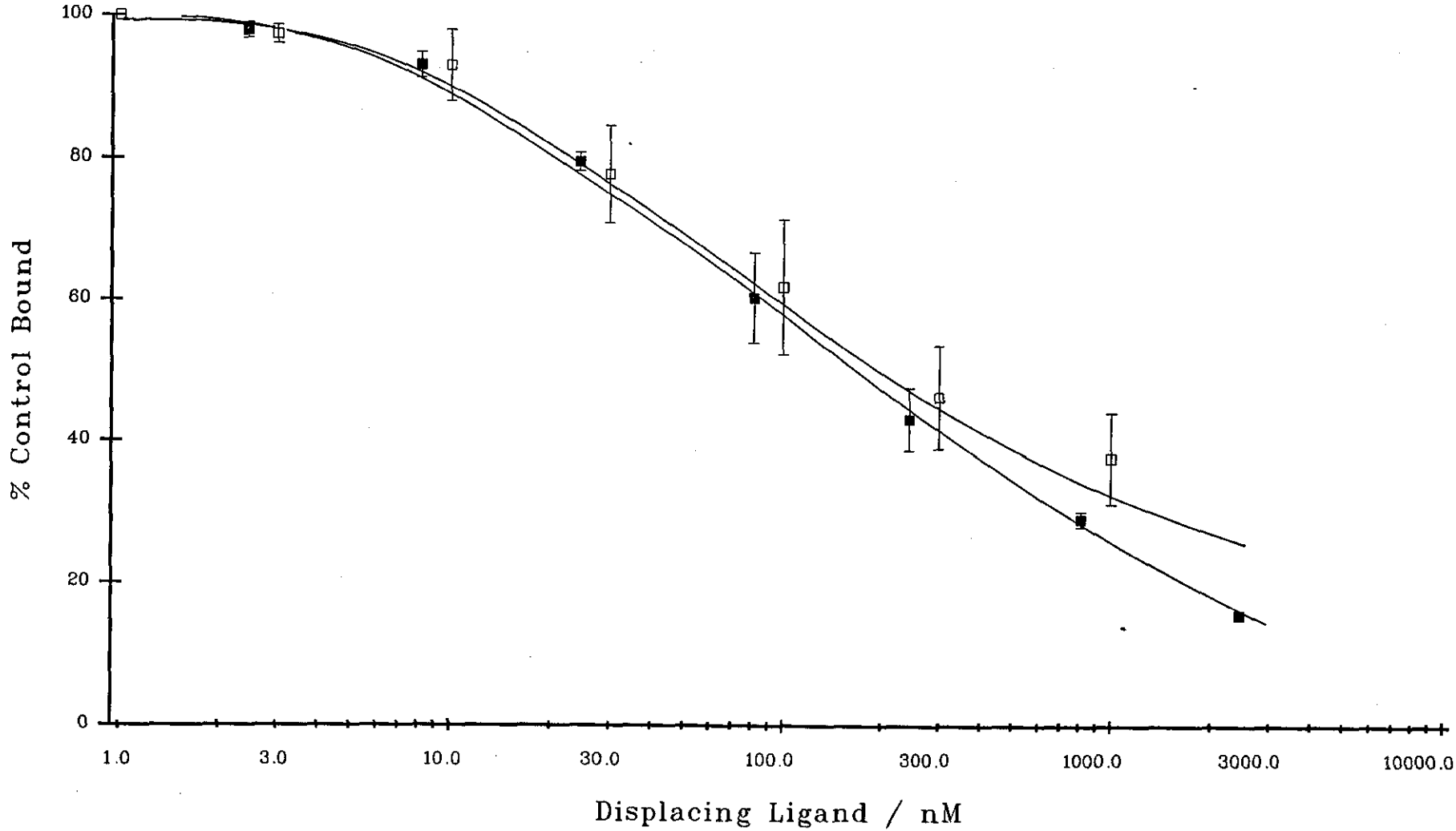

Figure 5.3: Displacement of [^{3}H]diprenorphine (0.68 ± 0.06nM) from rat brain homogenates in Tris.HCl (50mM, pH 7.4) containing 100mM NaCl and 50μM GppNHp by cyprodime (closed symbols) and CTOP (open symbols).

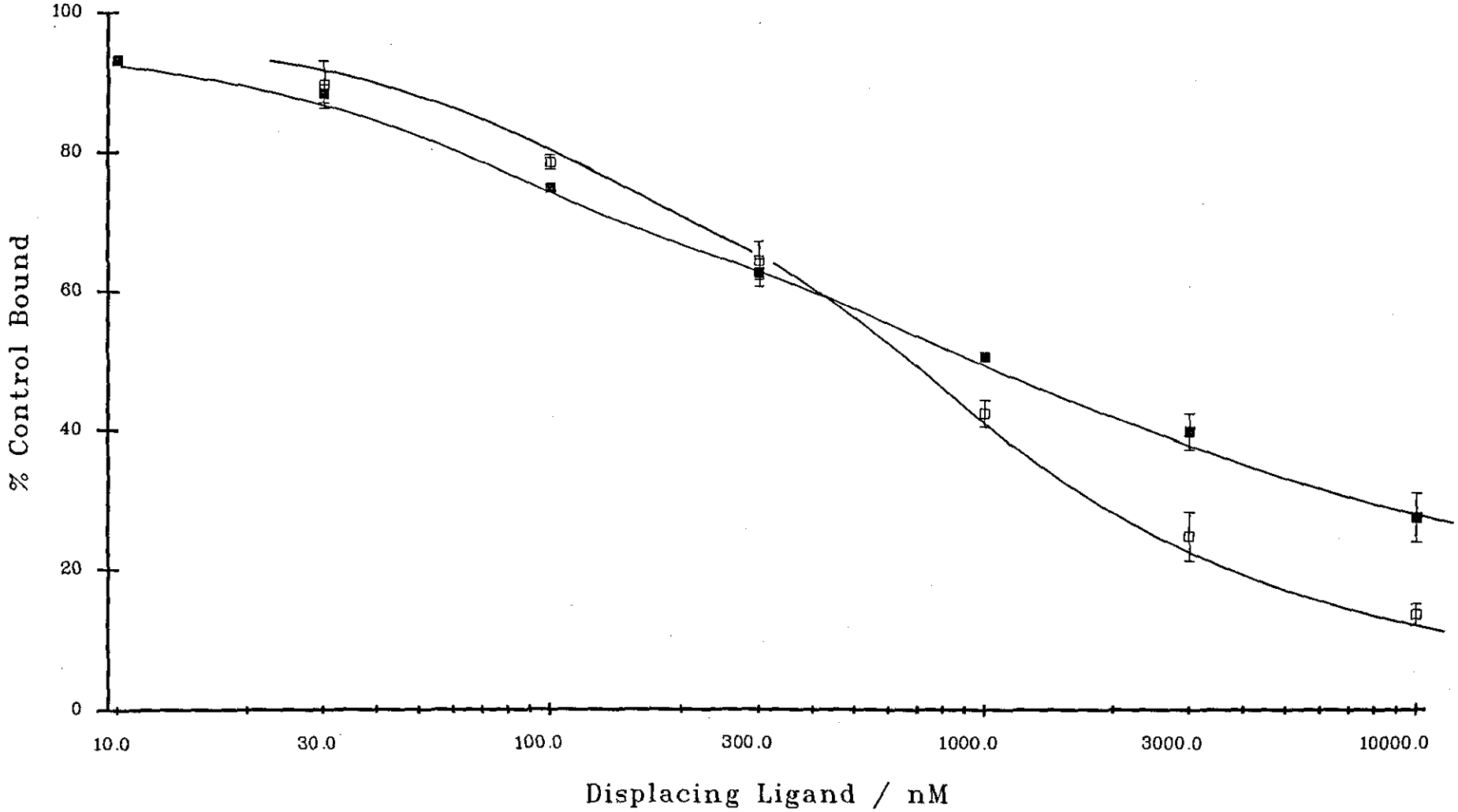

Figure 5.4: Displacement of [^{3}H]diprenorphine (0.41 ± 0.04nM) from rat brain homogenates in Tris.HCl (50mM, pH 7.4) containing 100mM NaCl and 50μM GppNHp by DAGOL (closed symbols) and morphine (open symbols).

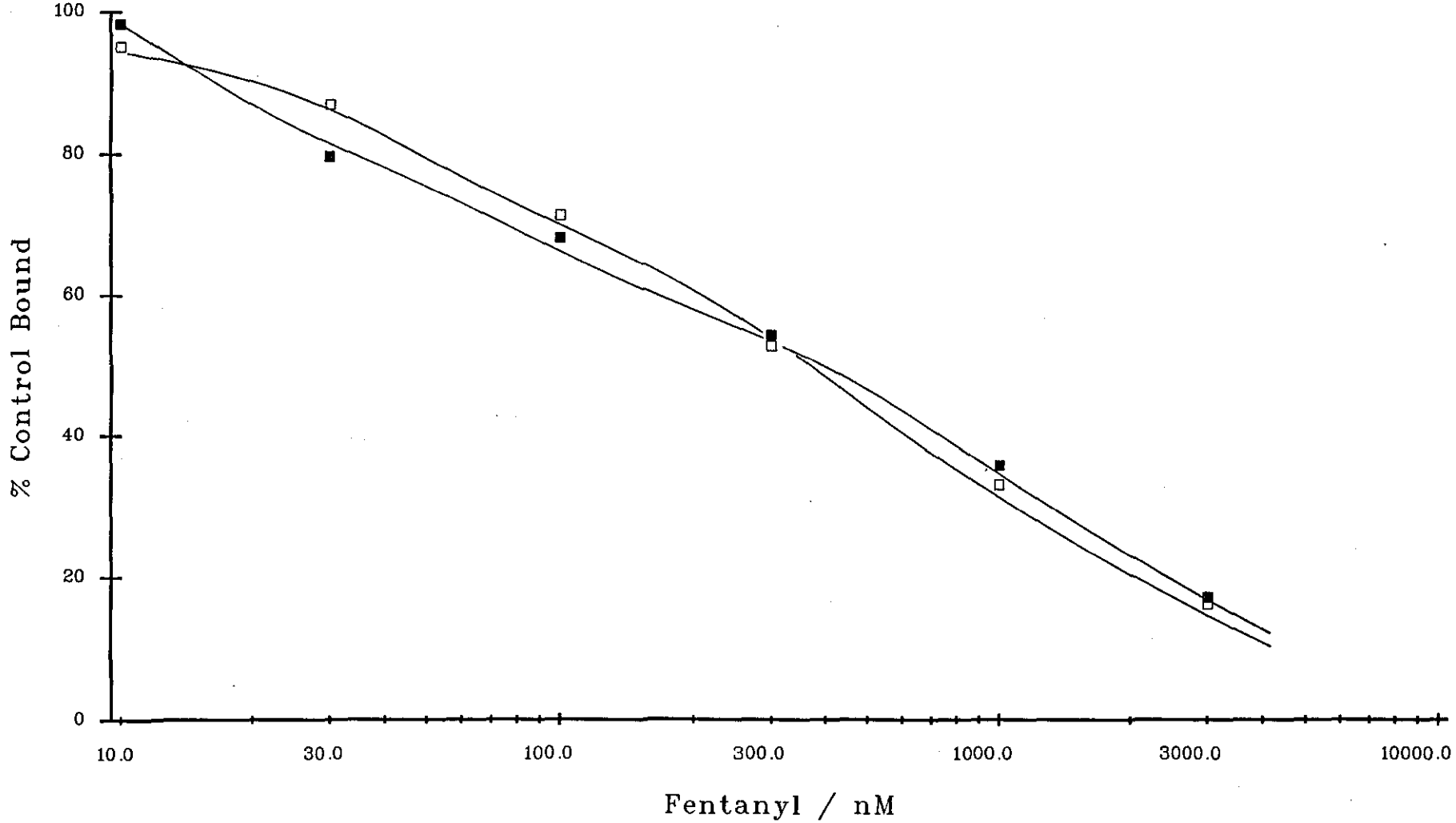

Figure 5.5: Displacement of [^{3}H]diprenorphine (0.3nM) from rat brain homogenates in Tris.HCl (50mM, pH 7.4) containing 100mM NaCl and 50μM GppNHp by fentanyl in the absence (closed symbols) and presence (open symbols) of 10nM NorBNI and 0.1nM naltrindole.

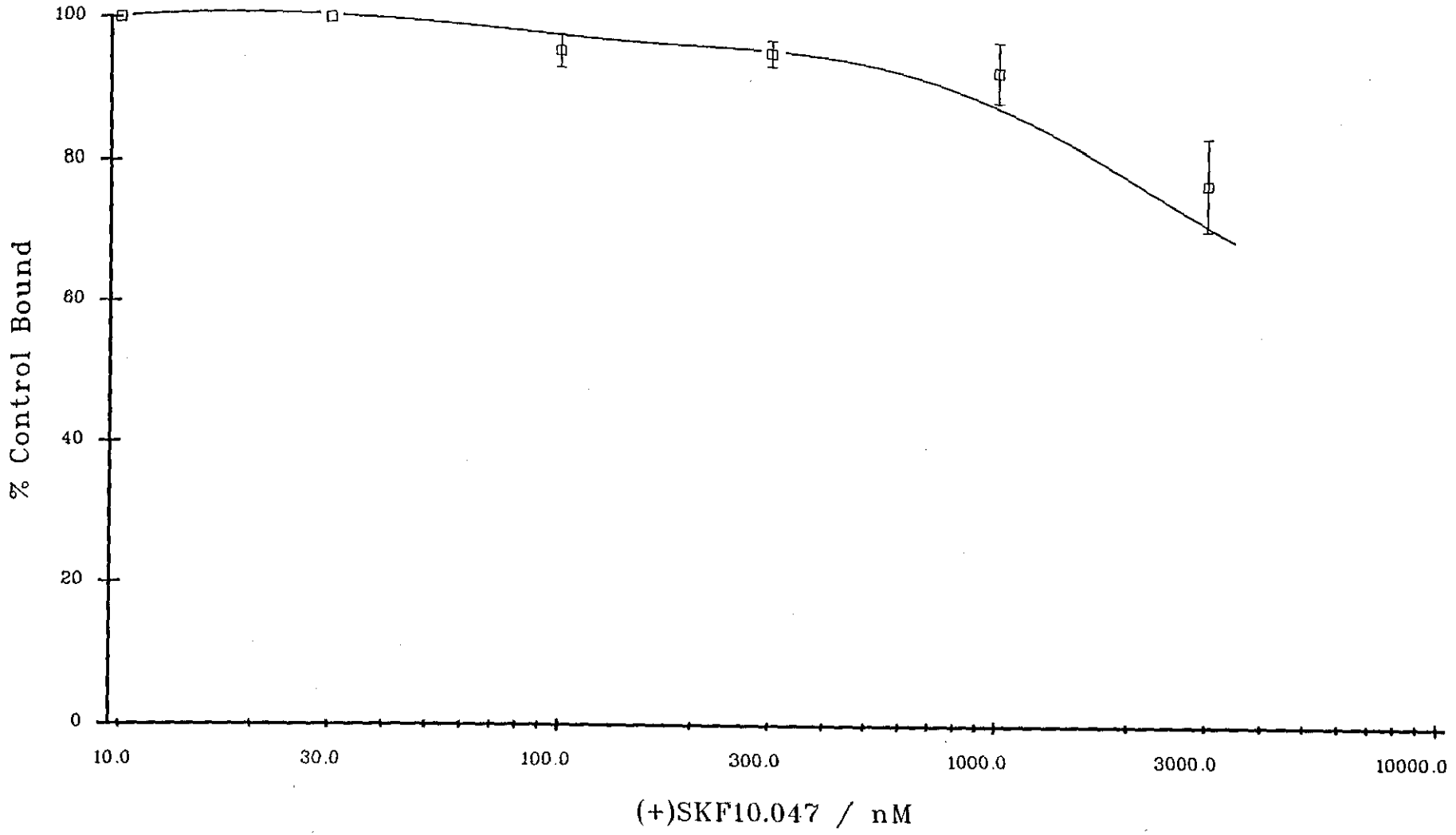

Figure 5.6: Displacement of [^{3}H]diprenorphine (0.71 ± 0.05nM) from rat brain homogenates in Tris.HCl (50mM, pH 7.4) containing 100mM NaCl and 50μM GppNHp by (+)SKF10,047.

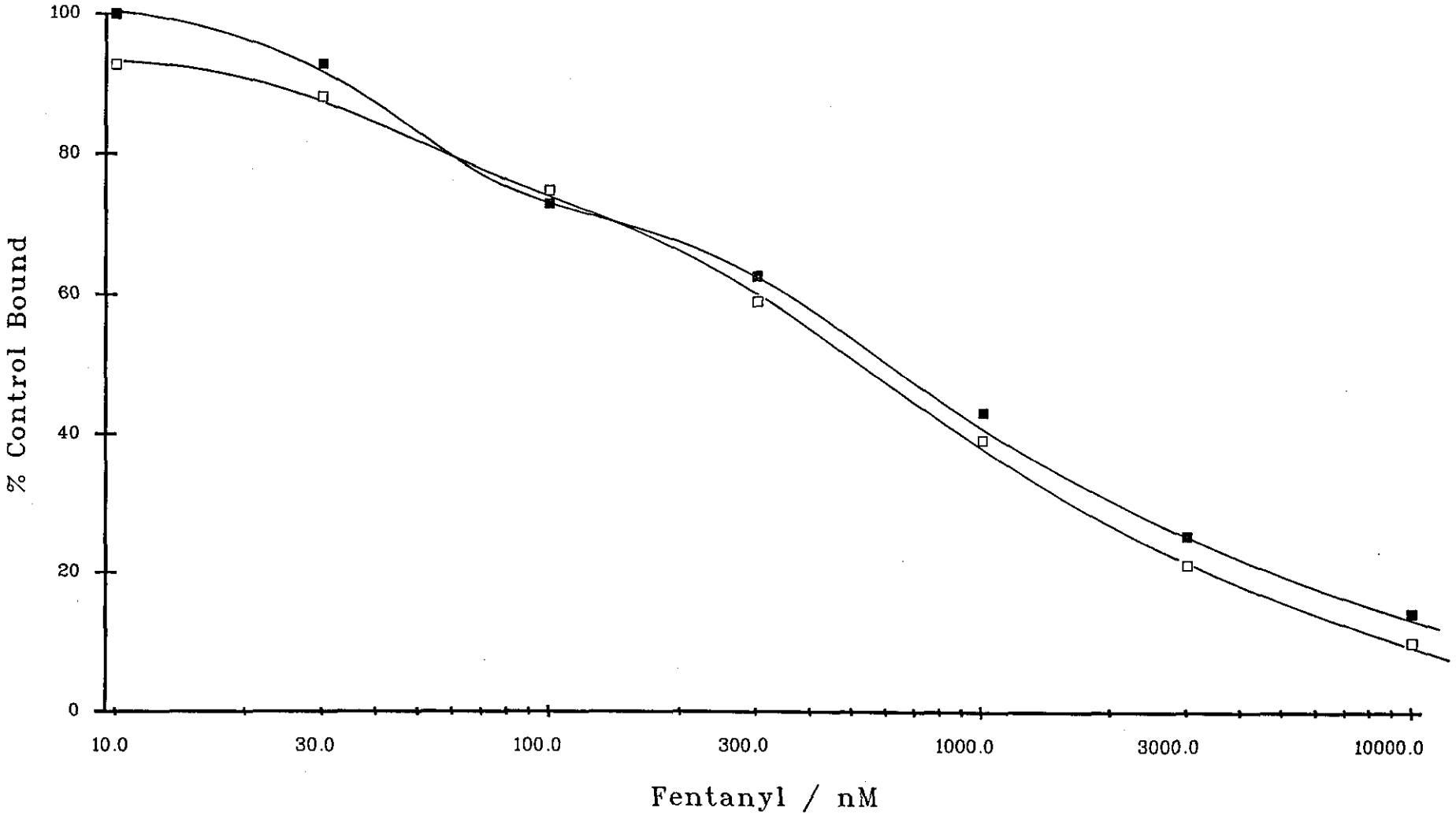

Figure 5.7: Displacement of [^{3}H]diprenorphine (0.61nM) from rat brain homogenates in Tris.HCl (50mM, pH 7.4) containing 100mM NaCl and 50μM GppNHp by fentanyl in the absence (closed symbols) and presence (open symbols) of 10nM NorBNI, 0.1nM naltrindole and 300nM (+)SKF10,047.

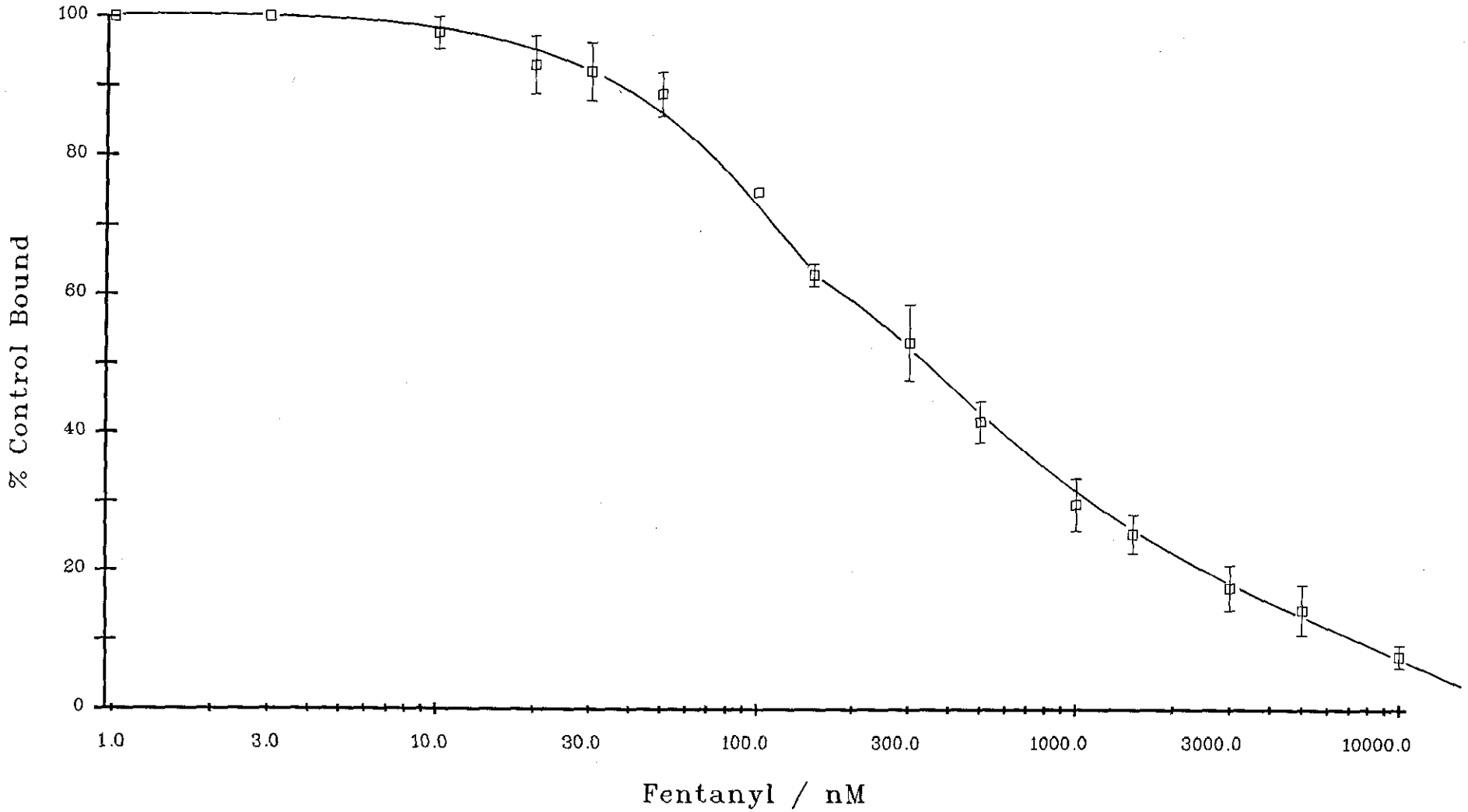

Figure 5.8: Displacement of [^{3}H]diprenorphine (0.58 ± 0.03nM) from rat brain homogenates in Tris.HCl (50mM, pH 7.4) containing 100mM NaCl and 50μM GppNHp by fentanyl in the presence of 10nM NorBNI, 0.1nM naltrindole and 300nM (+)SKF10,047.

To test out whether the presence of these two sites was due to a lack of suppression of δ- and κ-binding of [^{3}H]diprenorphine by the added ligands, analysis of the adequacy of suppression used in the eperiments was evaluated using the occupancy equation 8 outlined in chapter three and the data given in table 5.3.

Table 5.3: Data for calculation of theoretical occupancy curves.

	μ	δ	κ	(Ref)
% no. sites in rat brain	46	42	12	(45)
affinity [^{3}H]diprenorphine (nM)	0.84	1.42	2.24	(107)
affinity NorBNI (nM)	50.2	63.8	0.23	(chapter 4)
affinity naltrindole (nM)	13.1	0.0014	24.0	(chapter 4)

[^{3}H]Diprenorphine at 0.5nM labels a binding site population which consists of 36% δ-, 7% κ- and 57% μ-sites based on the above figures.

From equation 8 [DR] = [D] [Rt] / {K_D (1+ [I] / Ki) + [D]} the theoretical graphs (figures 5.9 and 5.10) showing sequential displacement of [^{3}H]diprenorphine (0.5nM) by firstly NorBNI followed by naltrindole can be generated. At the concentrations of suppressing ligands used the loss of site numbers is 12% for μ-, 98% for δ- and 95% for κ- resulting in a final population of 97% μ-, 2% δ- and 1% κ-sites. However, this could be an underestimate of the "purity" of the preparation since these calculations consider a population of sites which contains 36% δ- and 7% κ- opioid sites labelled at 0.5nM [^{3}H]diprenorphine. In this study <10% of non μ-sites appear to be labelled.

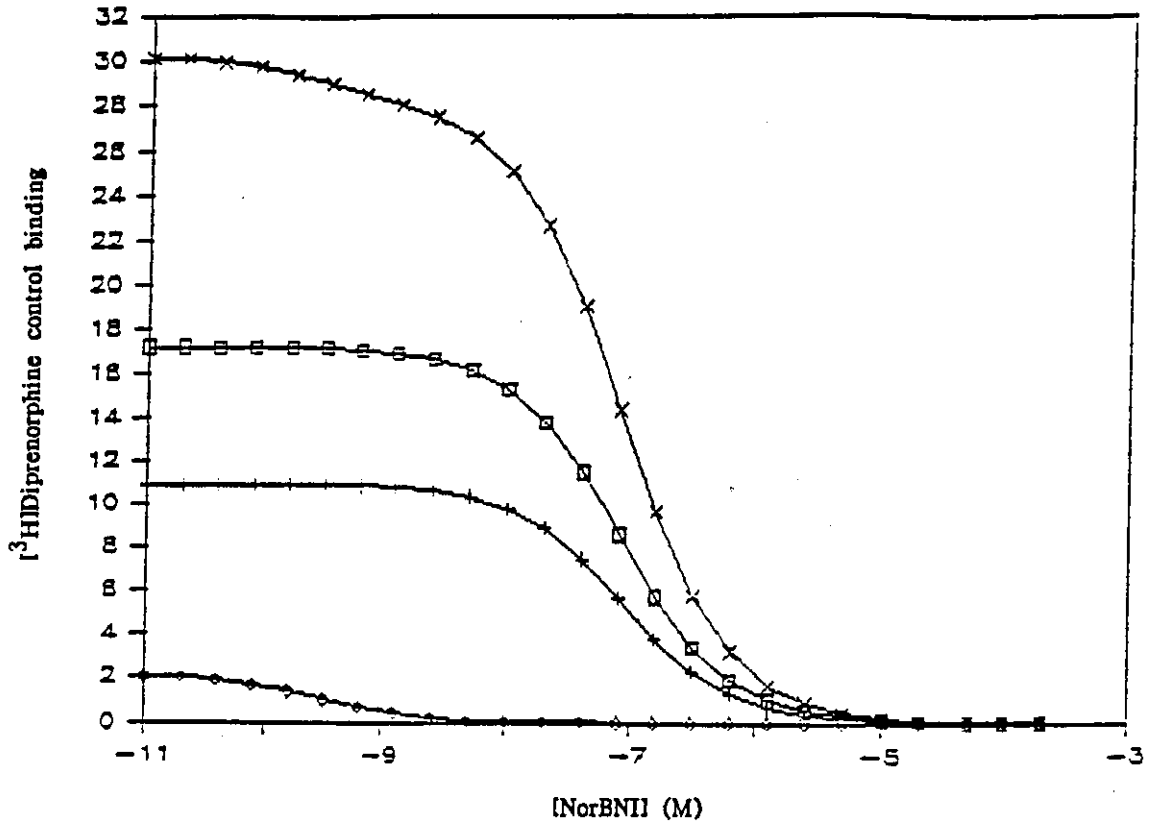

Figure 5.9: Theoretical plot representing displacement of [^{3}H]diprenorphine (0.5 nM) by NorBNI in rat brain homogenates from K− (o), δ− (+), μ− (□) sites, and total (X).

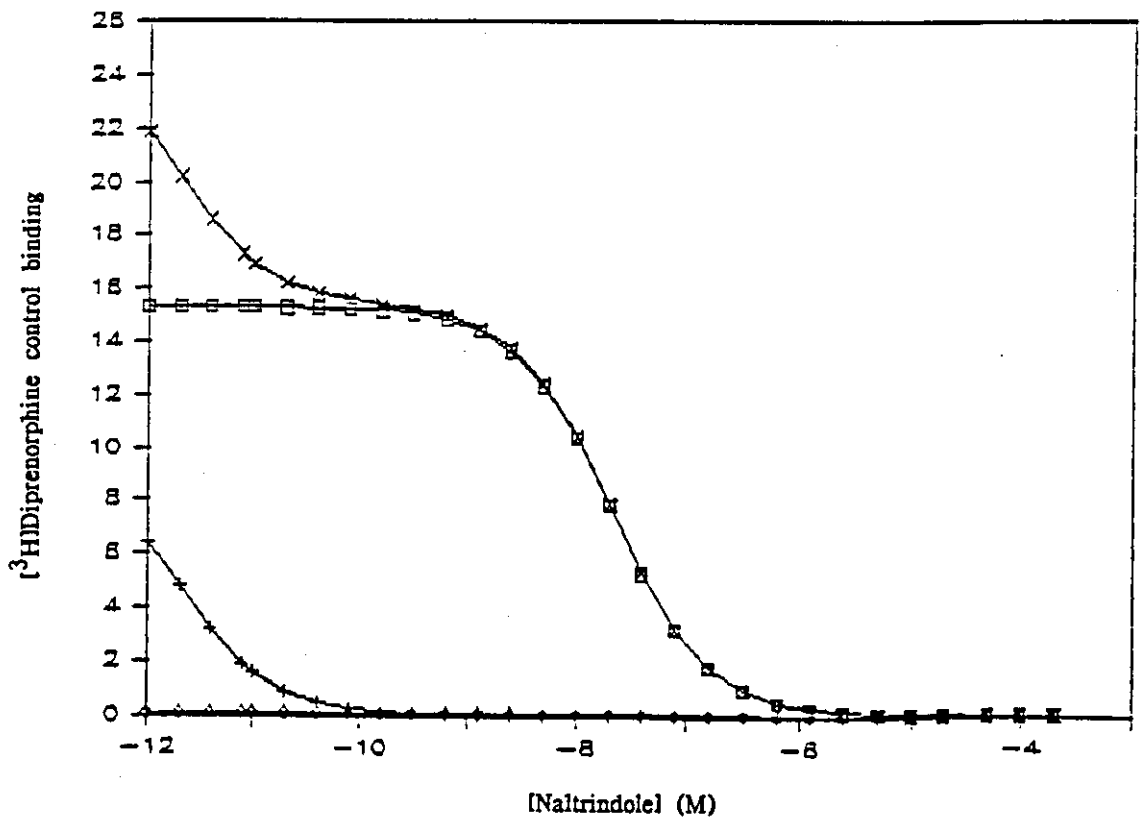

Figure 5.10: Theoretical plot representing displacement of [^{3}H]diprenorphine (0.5 nM) by Naltrindole in the presence of 20nM NorBNI in rat brain homogenates from K−(o), δ−(+), μ−(□) sites, and total (X).

Discussion

From the displacement curves obtained the results suggest that at the concentration used (0.5nM) in the presence of Na^+ ions and guanine nucleotide [^{3}H]diprenorphine is labelling a group of sites of which approximately 90% are not representative of δ–, κ– or σ –sites. The present studies may initially therefore be interpreted as confirmation of the data of Frost and colleagues (118), that [^{3}H]diprenorphine is largely labelling a μ–site following *in vivo* administration in the mouse. An earlier report also considers [^{3}H]diprenorphine to be μ– selective, though in this case μ– and κ–sites were not distinguished (134).

However since earlier in these present studies [^{3}H]diprenorphine has been used to label both κ– and δ–sites (chapter four) then obviously the results must be treated with a great deal of caution. It may be that in the rats used in this study, which contain a low number of κ–sites (45), the level of [^{3}H]diprenorphine employed is effectively labelling a largely μ–population based on its slightly higher affinity for this site (112). However by calculation the ratio of sites labelled in rat brain homogenates at a [^{3}H]diprenorphine concentration of 0.5nM would be expected to be 57% μ–, 36% δ– and 7% κ–sites. Therefore the published values for affinity of ligands and number of sites in rat brain do not quite approximate to the conditions used in the present experiments. This may relate to the presence of Na^+ ions and a guanine nucleotide analogue. In addition it has been previously reported that large variations can exist in receptor number, particularly for the δ–receptor, between species and or strains of animals (157). Consequently at higher concentrations of radioligand then it could be expected that all three opioid receptor sites are likely to be labelled (117). This would be in agreement with the findings of Jones and coworkers. In their work, following [^{11}C]diprenorphine distribution in the human brain by PET

scanning, then all opioid receptors in brain regions appear to be labelled (158).

If it is accepted that [^{3}H]diprenorphine in these experiments is labelling a largely μ-population then the apparent heterogeneity of binding, which exists even when binding to other sites is suppressed, must be explained. The obvious explanation that binding to δ-, κ- and σ-sites is still present and interfering with the binding does not seem to be valid following analysis of the conditions of occupancy. Curve fitting analysis of the data using the program LIGAND (105) suggests the presence of two sites, one of high affinity for μ-ligands and one of much lower affinity. These findings are in good agreement with the results of Werling and colleagues (59) who found K(app) values for DAGOL of 23nM and 1700nM in GTPγS-treated guinea-pig cortical membranes and 7315C cells. (GTPγS is, like GppNHp, a stable analogue of GTP).

The findings can be interpreted to suggest the presence of subtypes of the μ-receptor. Previously Pasternak and colleagues (62) have described μ_1- and μ_2-sites. The μ_1-site is a high affinity site that appears to be a common site for opioids, whilst the μ_2-site is a lower affinity site specific for μ-ligands. For this to be the case in the present experiments the antagonists used to suppress binding to non μ- sites would not have to recognise the common μ_1-site. This is unlikely but may be possible since it is reported that the antagonist naloxonazine alkylates specifically the high affinity μ_1-site (63-65), as discussed in the introduction.

A more plausible explanation of the heterogeneous binding may be the presence of different affinity states of the μ-opioid site. The μ- receptor is a G protein linked receptor and is therefore modulated by guanine nucleotides and Na^+ ions. In Tris buffers μ-ligands bind with high affinity

but in the presence of Na^+ ions and guanine nucleotides high affinity agonist binding is lost (58, 59). Antagonists are generally considered to bind equally well to both states of the receptor, although results in chapter four suggest that binding of certain of these compounds may be improved under these conditions. Therefore it is surprising that the antagonists cyprodime and CTOP show shallow displacement profiles, however from the data in chapter four there is a possibility that both compounds may display partial agonist properties and therefore be able to distinguish different affinity states. Carroll and coworkers (58) have compared binding in the low ionic strength buffer HEPES with that seen in Krebs buffers containing GppNHp where a low affinity of binding results. Importantly binding under the latter conditions correlates very well with affinities of μ-ligands determined in isolated tissue bioassay, suggesting that this low affinity form may be the physiologically relevant receptor.

The fact that δ- and κ-antagonist ligands have been used to suppress binding to these sites probably rules out any involvement of low affinity δ- or κ-sites in the observed heterogeneity of μ-binding.

Following on from these discussions the high levels of [^{3}H]diprenorphine binding previously reported (78, 117) can be explained on the basis of the presence of different states of opioid receptors. Thus the hypothesis can be proposed that [^{3}H]diprenorphine labels more sites than other ligands such as [^{3}H]bremazocine because it recognises all affinity states of opioid receptors whilst other [^{3}H]ligands do not. This may mean a re-estimate of receptor site number determined using [^{3}H]agonist ligands is necessary. The role of G proteins in controlling opioid receptor function is more fully discussed in chapter eight.

CHAPTER 6: COMPARISON OF AGONIST AND ANTAGONIST BINDING IN GUINEA-PIG BRAIN HOMOGENATES

Introduction

In chapter five the problem that [^{3}H]diprenorphine is labelling a greater number of sites than other ligands is raised. The hypothesis that this is due to different affinity states is considered. Certainly the presence of multiple affinity states of opioid binding sites has been demonstrated in rat brain membranes for both δ-(100) and μ-(52) opioid receptors. Recently Werling and co-workers (59) have shown multiple agonist affinity states which can be observed in the presence of Na^+, Mg^{++} and GTP analogues or on ADP-ribosylation by pertussis toxin which inactivates G protein. These experiments have been performed in both μ- and δ-opioid receptor containing cell lines 7315C and NG108-15 respectively and also guinea-pig cortical membranes. The results have been explained as different forms of receptor-G protein complexes proposed by the cyclic scheme of Gilman (99, see introduction). However such different affinity states should not be recognised by antagonists (58), although it has been pointed out in chapter four that certain antagonists do appear to be able to distinguish different affinity states. Importantly however, such compounds do not lose affinity for the low agonist affinity state of the receptor.

The present study has employed the antagonist [^{3}H]diprenorphine to label opioid binding sites in guinea-pig brain homogenates, in order to determine if receptor heterogeneity is a true phenomenon. The guinea-pig was chosen due to the large numbers of all three binding sites, comprising 25% μ-, 45% δ- and 30% κ-sites (49). Competition and saturation assays were performed in buffers of differing ionic strength using selective opioid agonists and antagonists.

Materials and Methods

Homogenates of guinea-pig brain minus cerebellum were prepared and binding assays carried out as described in chapter two. Assays were performed in Tris.HCl buffer (50mM, pH 7.4) in the absence and presence of 100mM NaCl and 50μM GppNHp.

[^{3}H]Diprenorphine and [^{3}H]U-69593 were used to label opioid binding sites. Details of suppression at μ- and δ-sites are described in relevant results sections. Non-specific binding was defined using 10μM naloxone. Scatchard analysis of saturation assays was performed as described in chapter three.

Results

Displacement of [^{3}H]diprenorphine in Tris.HCl by the μ-agonist DAGOL, δ-agonist DPDPE and κ-agonist U50488H confirmed the presence of μ-, δ- and κ-sites (figure 6.1). However, each of the antagonists CTOP, naltrindole and NorBNI displaced a greater proportion of specifically bound [^{3}H]diprenorphine than the corresponding agonists (figure 6.1). The sum of the displacements by the antagonists accounted for most of the bound [^{3}H]diprenorphine whereas this was not the case for the agonists DAGOL, DPDPE and U50488H (figure 6.1). The most marked difference between agonist and antagonist was observed in the displacement of [^{3}H]diprenorphine by μ-ligands where DAGOL displaced only 15-20% of the specifically bound radioligand while CTOP reduced binding by 40% in the same homogenate preparation. A similar difference was observed between the δ-agonist DPDPE and antagonist naltrindole (figure 6.1). For the κ-compounds U50488H and NorBNI the different proportions of

[^{3}H]diprenorphine binding displaced in this tissue did not appear to be so marked.

The assays were repeated in Tris.HCl containing 100mM NaCl and 50μM GppNHp. Under these conditions, at least for μ– and κ–sites the agonists and antagonists appear to displace similar amounts of specifically bound [^{3}H]diprenorphine (figure 6.2). This could not be confirmed a δ–sites since the δ–agonist DPDPE (10μM) was able to displace only 16% of the bound radioligand under these low agonist affinity conditions.

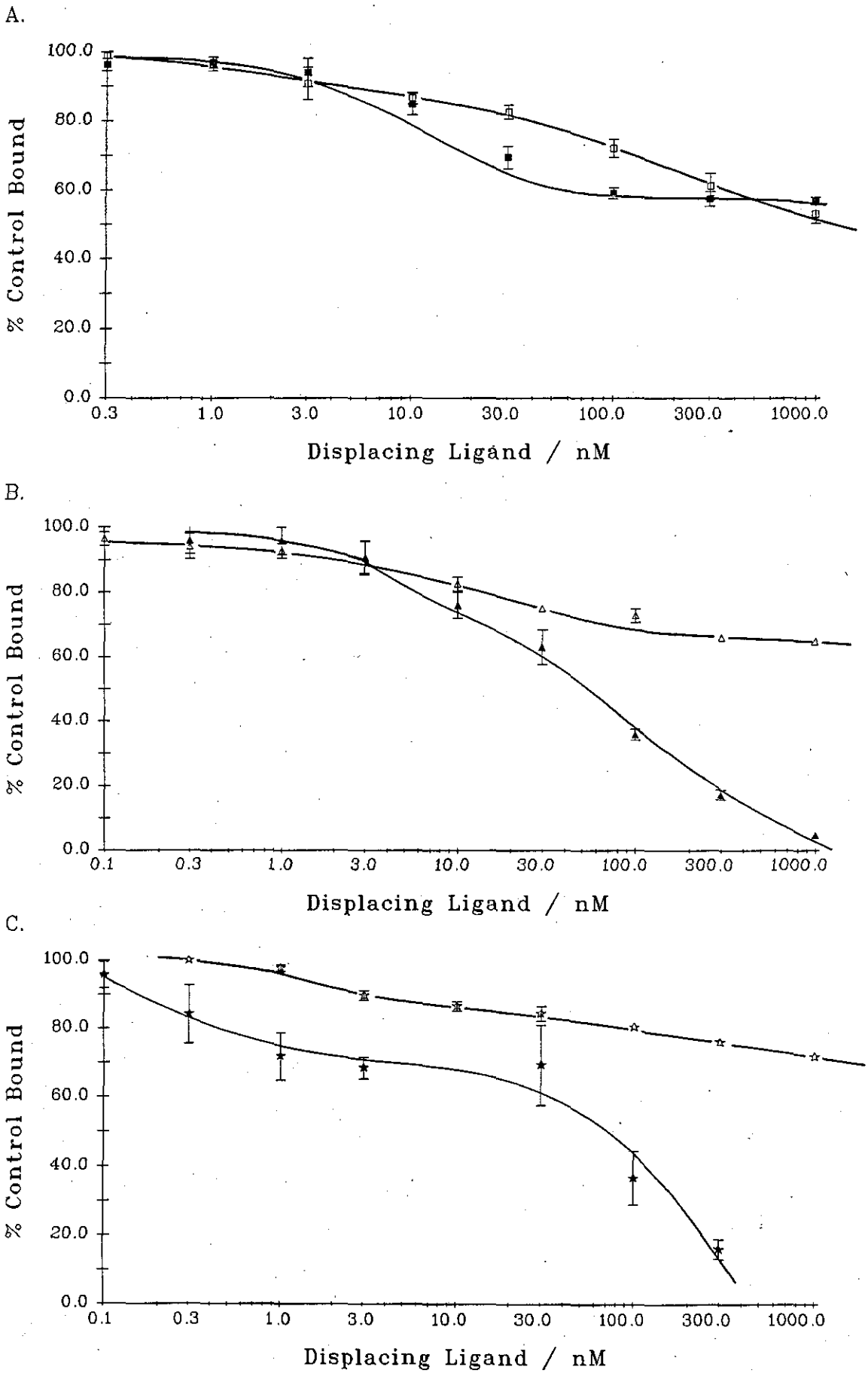

Figure 6.1: Displacement of [^{3}H]Diprenorphine (1.13 ± 0.1nM) from guinea-pig brain homogenates in Tris.HCl (50mM, pH 7.4) by:

A. DAGOL (open squares) and CTOP (closed squares)
B. U-50488H (open triangles) and NorBNI (closed triangles)
C. DPDPE (open stars) and Naltrindole (closed stars)

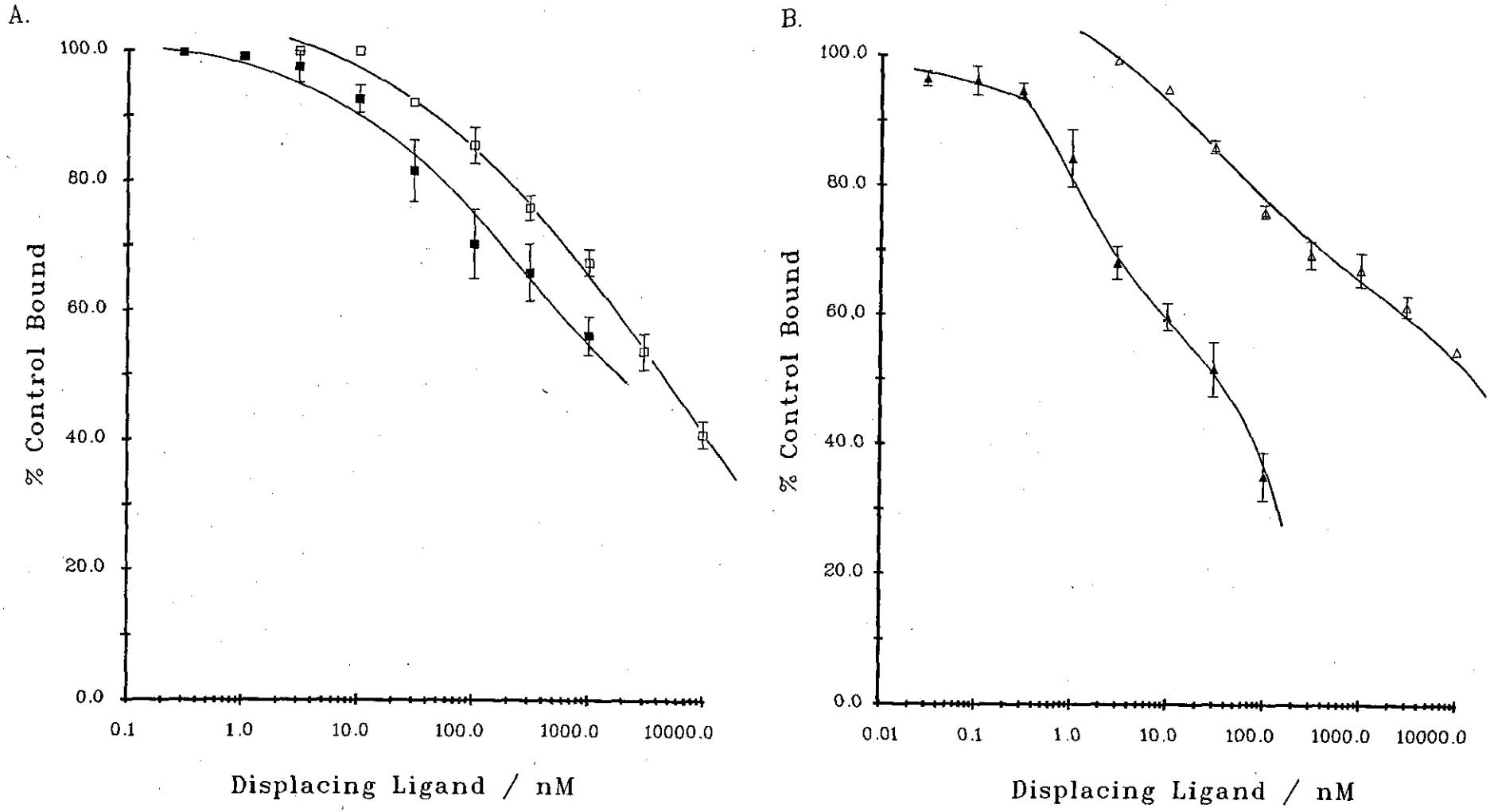

Figure 6.2: Displacement of [^{3}H]Diprenorphine (1.01 ± 0.02nM) from guinea-pig brain homogenates in Tris.HCl (50mM, pH 7.4) containing 100mM NaCl and 50μM GppNHp by:

A. DAGOL (open squares) and CTOP (closed squares)

B. U-50488H (open triangles) and NorBNI (closed triangles)

From the displacement curves shown in figure 6.1 concentrations of the antagonists CTOP (300nM) and naltrindole (30nM) were used in subsequent assays to suppress binding of [^{3}H]diprenorphine at μ– and δ–sites respectively in Tris.HCl . Under these conditions displacement of the remaining specifically bound [^{3}H]diprenorphine by the κ–agonist U–50488H and antagonist NorBNI afforded IC_{50} values of 26.4±0.6nM and 2.8±0.6nM respectively (figure 6.3). The displacement profiles were consistent with binding to a single population of sites, with Hill coefficients not significantly different from unity (1.10±0.05 and 1.20±0.15 respectively). However there was a proportion of undisplaced radioligand.

In order to determine if the undisplaced radioligand was due to a σ–component, the σ–agonist (+)SKF10,047 was assayed. Figure 6.4 shows this ligand to displace approximately 10% of the specifically bound [^{3}H]diprenorphine. From this curve (figure 6.4), it can be seen that 300nM (+)SKF 10,047 should be sufficient to occlude any labelled σ–sites. The displacements by κ–ligands were therefore reassessed in the presence of CTOP (300nM), naltrindole (30nM) and (+)SKF10,047 (300nM). Both U–50488H and NorBNI were then able to fully displace the [^{3}H]diprenorphine in a manner corresponding to binding to a homogeneous population of binding sites (Hill coefficients 0.96±0.15 and 1.16±0.17 respectively). The profiles are depicted in figure 6.5, U–50488H affording an IC_{50} of 32.1±12.0nM and NorBNI 2.4±0.6nM.

κ–Opioid binding sites can be labelled as above using suppression of unwanted binding, or alternatively by employing the selective κ–agonist [^{3}H]U–69593. In order to compare these two means of characterising the κ–site saturation analysis was performed both with [^{3}H]U–69593 and [^{3}H]diprenorphine in the presence of μ–, δ– and σ–suppression. In order to ensure that <10% of total added [^{3}H]diprenorphine was bound, the assays involving

[^{3}H]diprenorphine were carried out in 250x w/v homogenate. Suppression of [^{3}H]diprenorphine binding to the non-κ component was achieved by the addition of 300nM CTOP, 30nM naltrindole and 300nM (+)SKF10,047 per 1nM labelled ligand. However these conditions seemed inadequate at lower (<0.3nM) concentrations of radioligand. Based on the reported affinities of both labelled ligand (107) and unlabelled ligands as determined in chapter four, and use of equation 8 determining receptor occupancy outlined in chapter three, supplied on a spreadsheet (152), the ratio of suppressing ligand : radioligand does not follow a linear progression. The relationship breaks down below the K_D of the radioligand (i.e. at approximately 0.3nM). To compensate therefore at lower concentrations of [^{3}H]diprenorphine common suppressing conditions of 100nM CTOP, 10nM naltrindole and 100nM (+)SKF10,047 were employed. Theoretical curves of μ- and δ-suppression are shown in figures 6.8 and 6.9 respectively.

Figure 6.6 shows that the binding of [^{3}H]U-69593 is saturable. Scatchard transformation of this data yields a Bmax of 3.9±0.3 pmol/g wet weight of brain and a K_D of 1.1±0.1nM. In comparison figure 6.7 represents the saturated binding curve and Scatchard plot for [^{3}H]diprenorphine in the presence of CTOP, naltrindole and (+)SKF10,047 affording a Bmax of 3.6±0.2 pmol/g wet weight and a K_D of 0.21±0.08nM. The saturation data is summarised in table 6.1.

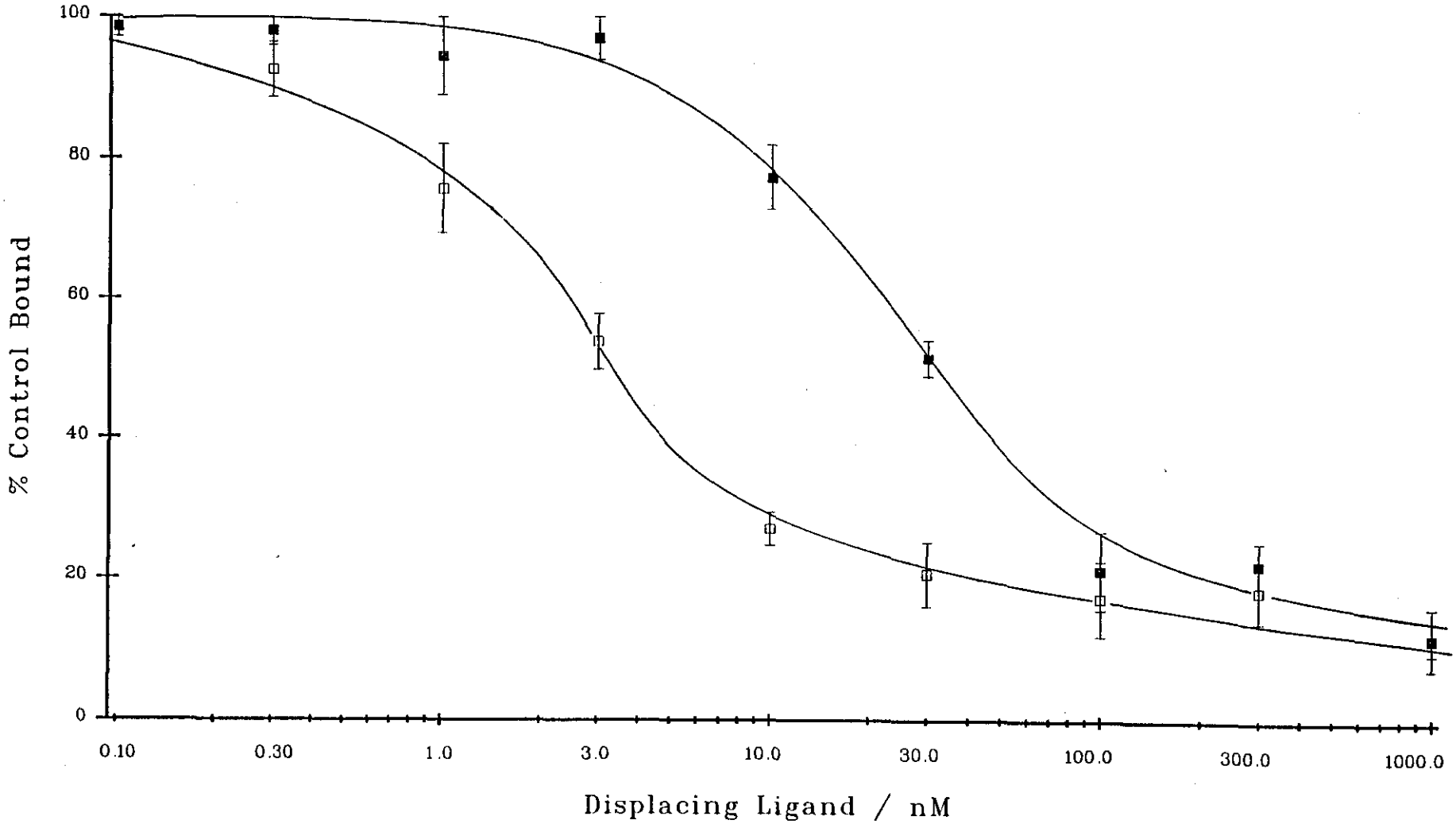

Figure 6.3: Displacement of [^{3}H]diprenorphine (1.17 ± 0.1nM) from guinea-pig brain homogenates in Tris.HCl (50mM, pH 7.4) in the presence of 300nM CTOP and 30nM naltrindole by U-50488H (closed symbols) and NorBNI (open symbols).

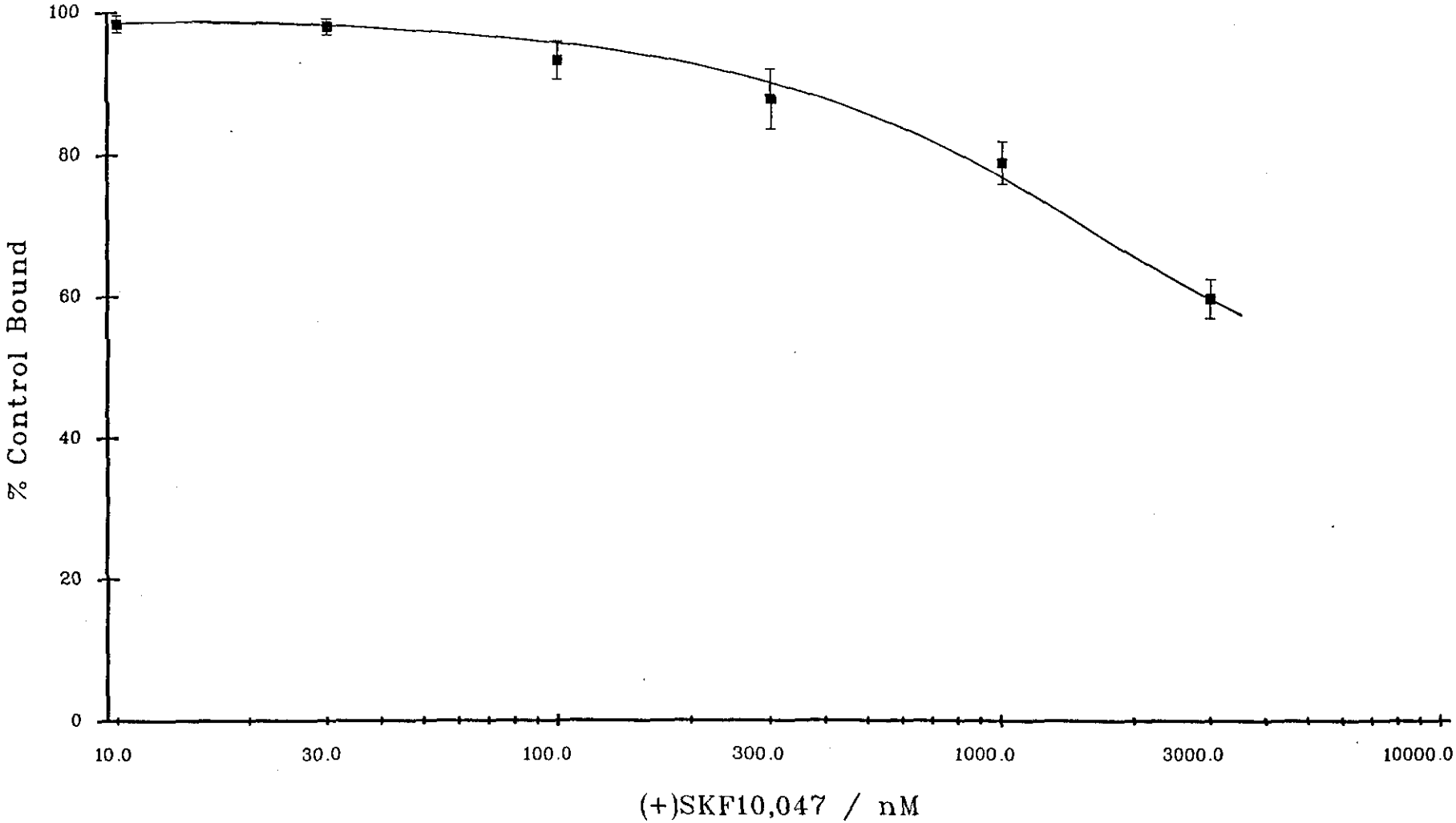

Figure 6.4: Displacement of [^{3}H]diprenorphine (0.9 ± 0.05nM) from guinea-pig brain homogenates in Tris.HCl (50mM, pH 7.4) by (+)SKF10,047.

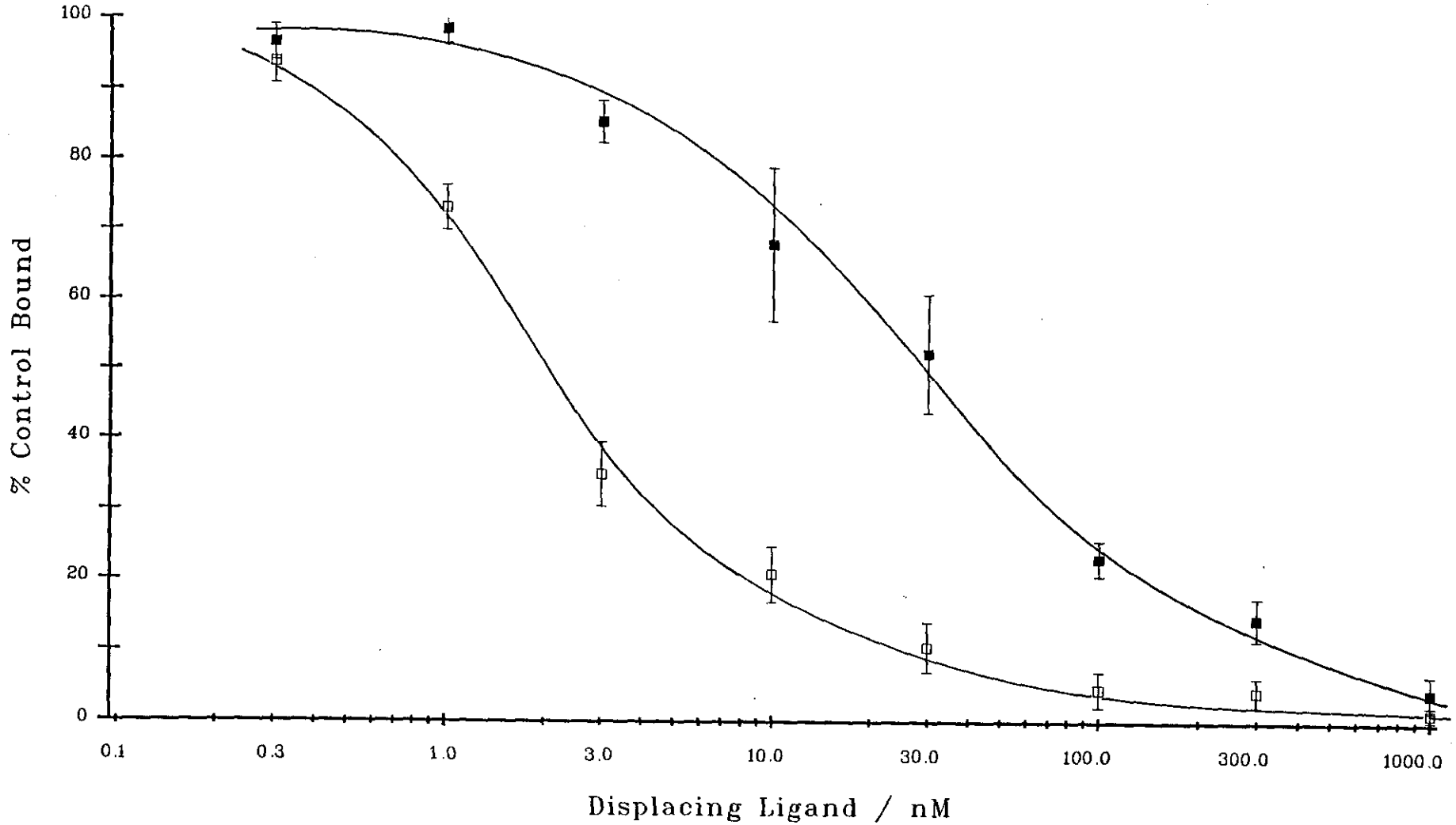

Figure 6.5: Displacement of [^{3}H]diprenorphine (0.86 ± 0.05nM) from guinea-pig brain homogenates in Tris.HCl (50mM, pH 7.4) in the presence of 300nM CTOP, 30nM naltrindole and 300nM (+)SKF10,047 by U-50488H (closed symbols) and NorBNI (open symbols).

Table 6.1: Saturation analysis of [^{3}H]U-69593 and [^{3}H]diprenorphine binding to Guinea-pig brain homogentes.

Compound	Bmax (pmol/g$^+$)	r	K_D (nM)
[^{3}H]U-69593	3.9 ± 0.3*	0.94 ± 0.01	1.1 ± 0.1
[^{3}H]diprenorphine	3.6 ± 0.2*	0.9 ± 0.04	0.21 ± 0.08

* The two Bmax values do not significantly differ as compared by a t-test ($P<0.05$).

r = correlation coefficient of Scatchard plot

+ 1g of brain = 57±13.1 mg protein

[^{3}H]diprenorphine binding was suppressed by the addition of 300nM CTOP, 30nM naltrindole and 300nM (+)SKF10,047 per 1nM labelled ligand to a concentration of 0.3nM radioligand. At all concentrations below this 100nM CTOP, 10nM naltrindole and 100nM (+)SKF10,047 were used.

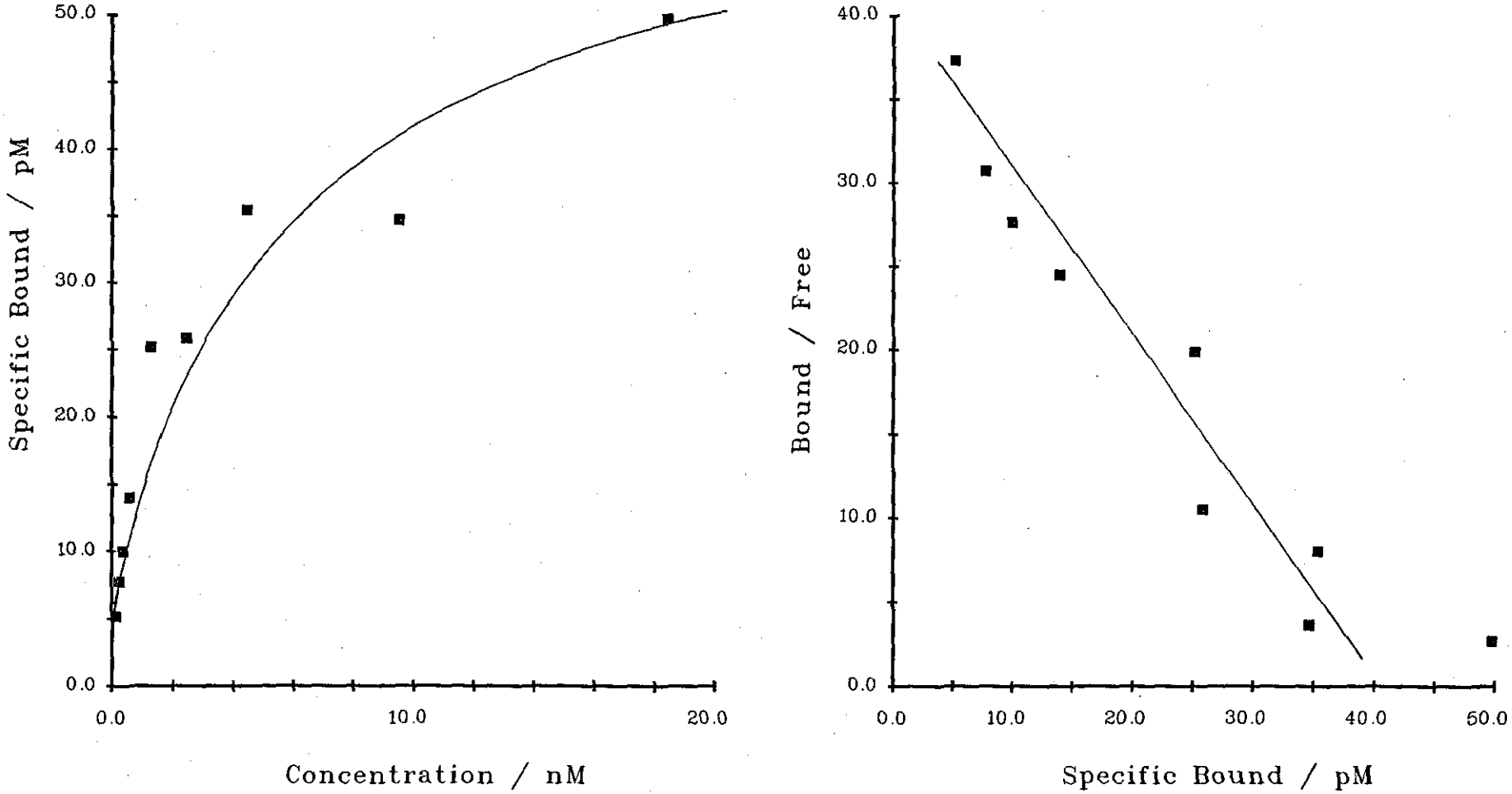

Figure 6.6: Saturation analysis and Scatchard transformation for [^{3}H]U-69593 in guinea-pig brain homogenates prepared in Tris.HCl (50mM, pH 7.4). Representative plot from 3 experiments.

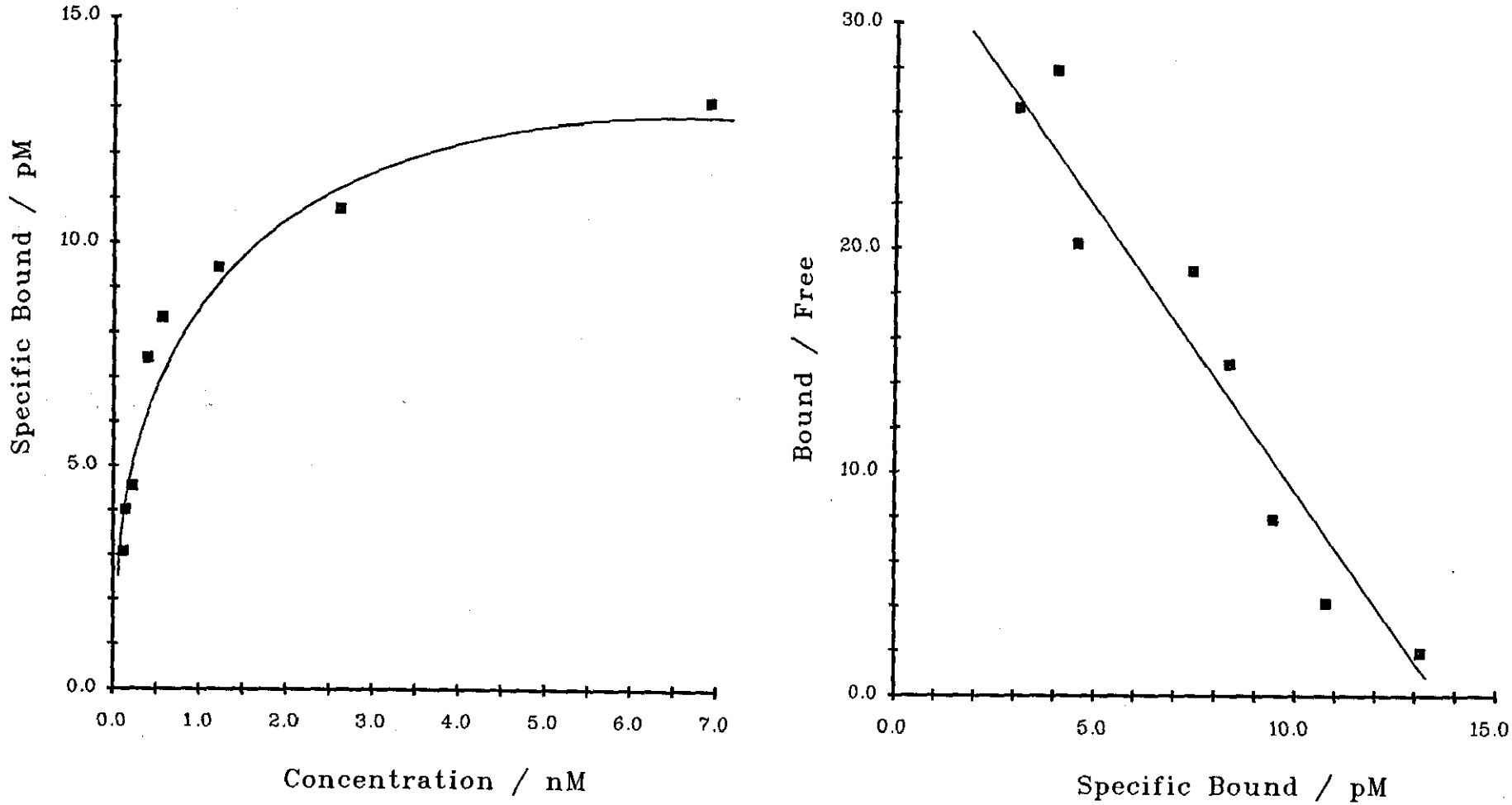

Figure 6.7: Saturation analysis and Scatchard transformation for [^{3}H]Diprenorphine in guinea-pig brain homogenates in the presence of μ-, δ-, and σ-suppression prepared in Tris.HCl (50mM, pH 7.4). Representative plot from 3 experiments.

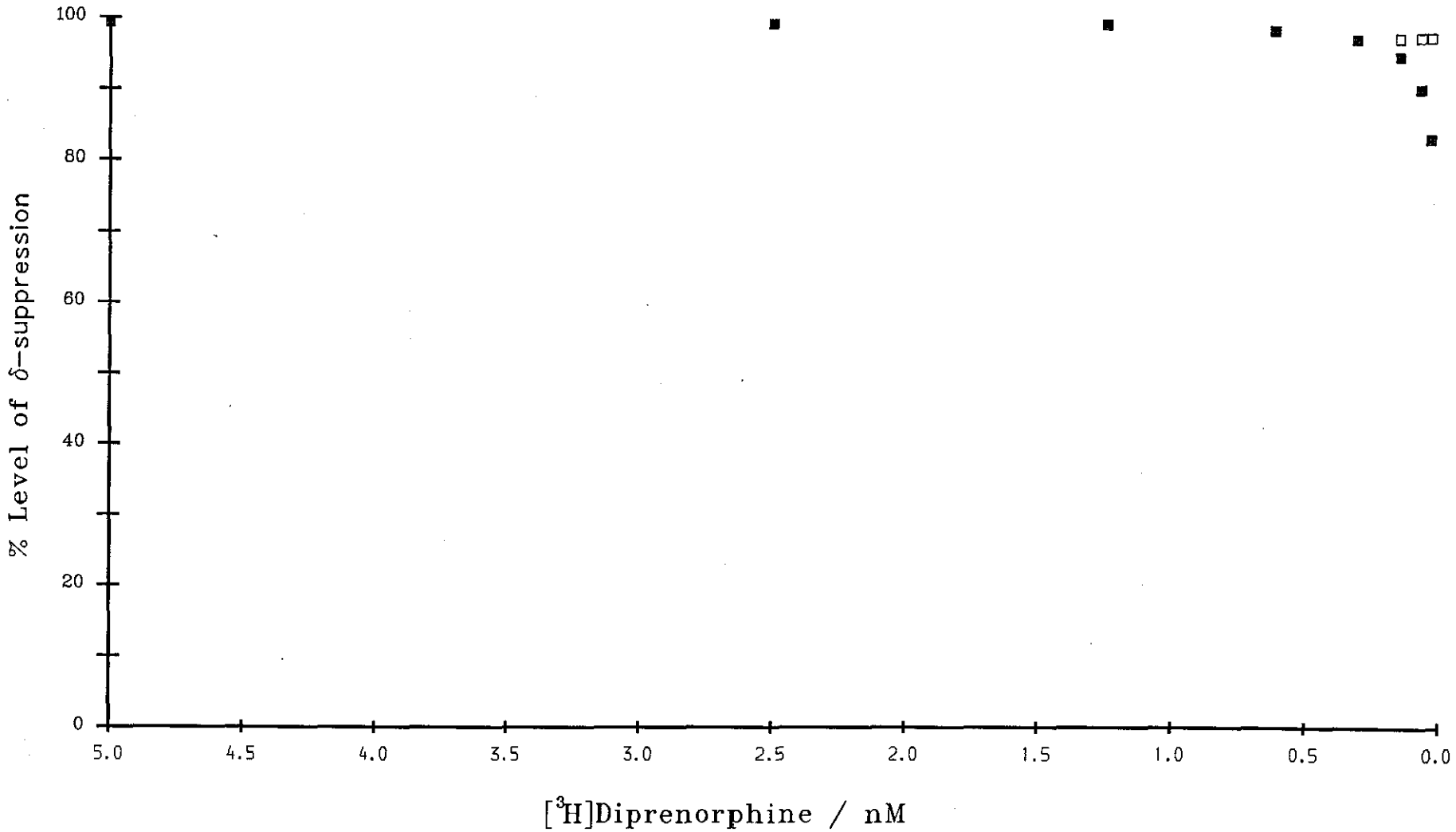

Figure 6.8: Theoretical plot of δ-suppression in guinea-pig brain based on 30nM naltrindole per 1nM radioligand (filled squares). Open squares show actual suppression achieved at lower concentrations of radioligand.

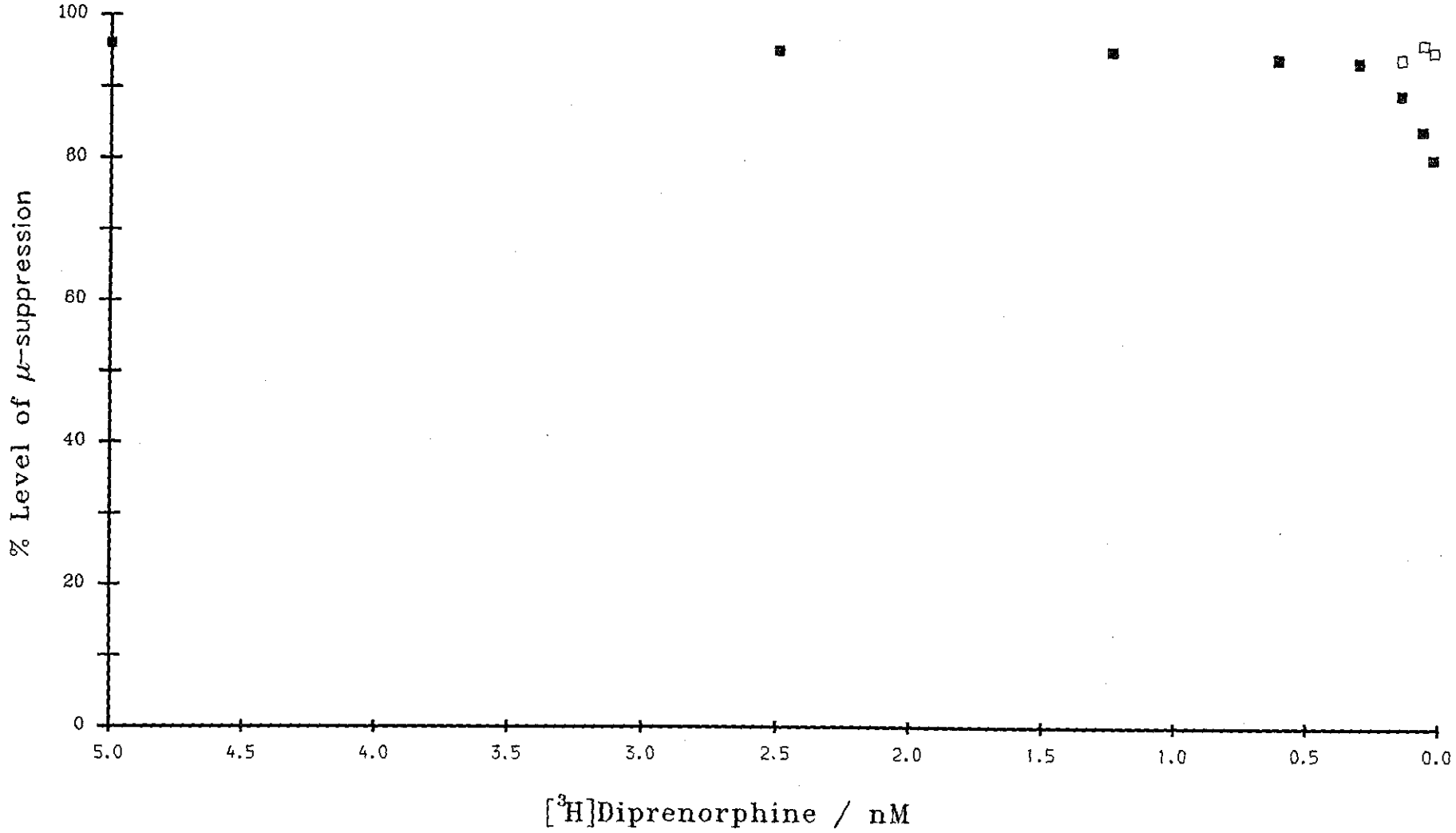

Figure 6.9: Theoretical plot of μ-suppression in guinea-pig brain based on 300nM CTOP per 1nM radioligand (filled squares). Open squares show actual suppression achieved at lower concentrations of radioligand.

Discussion

The proportion of [^{3}H]diprenorphine binding in guinea-pig brain homogenates that can be attributed to a μ-component differs depending on whether the agonist DAGOL or antagonist CTOP is used. Since both compounds are highly selective ligands for the μ-opioid receptor with selectivity profiles greater than 100-fold (39, 53) it is unlikely that the involvment of other opioid sites can account for this difference.

The fact that DAGOL displaces less [^{3}H]diprenorphine than CTOP in Tris.HCl buffer suggests that binding sites in the low agonist affinity form exist under these conditions and are susceptible to CTOP but not to DAGOL. Although previuos work (chapter four) shows CTOP to shift in affinity this is only 6-fold and unlikely to prevent CTOP from recognising both high and low affinity components (52). Such different affinity states of μ-opioid binding sites have been reported previously (58, 59). However in the presence of NaCl and GppNHp the differences in amount of displacement by agonist and antagonist become much less noticable, suggesting that under these conditions the majority of binding sites are in the same (or very similar) affinity states, i.e. low agonist affinity states. The apparent different affinity states of the μ-opioid binding site presumably represent differently coupled forms of the receptor-G protein complex, controlled by metal ions and guanine nucleotides (59), as schematically represented in the introduction. This is further considered in chapter eight.

Similar arguments apply to the highly selective δ-ligands DPDPE (41) and naltrindole (56). Multiple affinity states of δ-opioid binding sites have been reported both in NG108-15 cells (141) and rat brain membranes (100). Unfortunately using DPDPE it was not possible to confirm that in the

presence of NaCl and GppNHp the agonist would displace the same number of δ-sites due to its inability to bind under such conditions. However the fact that the affinity of DPDPE shifts to such a low value implies a change in the affinity state of the binding site. The differences in binding of the κ-preferring compounds U-50488H (140) and NorBNI (51) appears to be much less notable. The presence of high and low affinity [^{3}H]ethylketocyclazocine sites in rat brain and a high affinity site in guinea-pig brain has been described by Zukin and colleagues (79). However the authors assign these as k_1 and k_2 subtypes, rather than affinity states of the same receptor protein.

The observation that even in low ionic strength buffer agonists recognise a smaller population of binding sites than antagonists raises doubt over assays employing agonists as suppressing ligands. The present study has examined the displacement of [^{3}H]diprenorphine by U-50488H (a κ-selective agonist) and NorBNI (a κ-selective antagonist) in the presence of CTOP and naltrindole to occlude binding to μ-and δ-sites respectively. Under these conditions of antagonist suppression, profiles consistent with binding to a single site are obtained. However, a small population of undisplaced sites remain which are removed on the inclusion of (+)SKF10,047 in the suppressing conditions. This suggests that previous reports of κ-heterogeneity in this tissue actually represent under suppression of other binding sites due to the use of agonists as occluding ligands.

Many investigators have inferred the possibility of subtypes, particularly of the κ-opioid receptor (74, 79, 142, 143). However, in terms of binding, these claims have been based upon differences seen in competition and saturation assays between selective κ-agonists such as U-69593 (50) and PD117302 (74) and non-selective agonists such as ethylketocyclazocine, bremazocine or etorphine in the absence and presence of selective μ- and δ-agonists for suppression of the pertinent binding sites (50, 74, 142, 143).

In support of this proposal that different affinity states exist and only part for example of the μ-population can be occluded by DAGOL, saturation analysis comparing [^{3}H]U-69593 and [^{3}H]diprenorphine in the presence of CTOP, naltrindole and (+)SKF10,047 has been performed. The Bmax obtained for [^{3}H]U-69593 of 3.9±0.3pmol/g wet weight compares favourably with that reported by Lahti and colleagues of 3.3pmol/g (50). The structurally similar compound [^{3}H]PD117302 also shows a Bmax of 3.4pmol/g (74). The Bmax obtained for [^{3}H]diprenorphine in the presence of CTOP, naltrindole and (+)SKF10,047 of 3.6±0.2pmol/g does not differ from those obtained with selective ligands. This confirms a lack of difference between the selective κ-agonist and an unselective ligand using antagonists for suppression of non-κ binding, and contrasts with previous reports of apparent κ-heterogeneity (50, 74, 117).

Therefore it appears that under the conditions employed in the present experiments no heterogeneity of the κ-site is evident in guinea-pig brain. Furthermore it implies the possibility that previous reports of κ-subtypes may simply comprise the κ-site and a mixture of other binding sites in low agonist affinity states that are not adequately suppressed. Pasternak has recently suugested the existence of four κ-receptors (161). This conclusion has been based on biphasic binding profiles of dynorphin B and α-neoendorphin in various membrane preparations, such as the guinea-pig cerebellum and calf striatum. However, neither of these opioid peptides are particularly selective κ- ligands (107). One possible reason why κ-subtypes are not seen in the present study could be suppression of one or more subtype by the antagonists used to occlude μ- and δ-binding sites. However the high selectivity of both CTOP and naltrindole for μ- and δ-sites respectively suggests that neither of these compounds have high affinity for a possible κ-subtype. In support of this naltrindole and the peptide ICI 174864 recognise a similar number of such defined δ-sites, in displacement assays.

In conclusion, these results offer further evidence for the presence of high and low agonist affinity states in binmding assay homogenates. It appears that in addition the present study has highlighted a need to carefully calculate concentrations of suppressing ligands in saturation analyses, as shown in the theoretical plots of μ– and δ–suppression.The assumption of a simple linear relationship between radioligand and inhibiting unlabelled ligand could result in under suppression of binding at lower concentrations of labelled ligand. This would manifest in false estimations of both K_D and Bmax.

CHAPTER 7: AGONIST ACTIVITY OF A SERIES OF K-AGONISTS ON THE GUINEA-PIG ILEUM MYENTERIC PLEXUS LONGITUDINAL MUSCLE PREPARATION

Introduction

The guinea-pig ileum myenteric plexus longitudinal muscle preparation is known to contain μ- and κ-opioid receptors (36, 37). Opioid agonists are able to inhibit the electrically-evoked contraction of this tissue in a dose dependent manner. The addition of naloxone reverses this effect. As outlined in chapter three, the presence of such a competitive antagonist should shift the agonist dose-response curve to the right in a parallel fashion. This allows determination of the affinity of the antagonist for the receptor as the equilibrium dissociation constant (Ke).

The Ke value of an antagonist at a particular receptor should be the same measured against any agonist acting selectively at that receptor, since it is a property of the antagonist not the agonist. Therefore a method to determine whether a group of agonists are acting at the same receptor is to compare Ke values of an antagonist against each agonist.

The generally accepted Ke for naloxone at κ-opioid receptors in the guinea-pig ileum is in the region of 10-15nM (74, 119). However, dynorphin 1-13, a peptide selective for κ-opioid receptors (29), has been reported to afford a naloxone Ke of around 30nM (29). More recently a synthetic κ-agonist ICI 204448 has been claimed to yield a similar value (120). This could imply the presence of κ-opioid receptor subtypes in the guinea-pig ileum, which have been implicated by binding assays as outlined in the introduction and discussed in chapter six. Although the conclusion is made that proposed κ-opioid receptor subtypes probably represent different affinity states this is not fully proven. Thus since this bioassay

would represent a physiologically relevant assay for such subtypes it is important to analyse the reported results more closely as the absence of such assays has greatly hampered the understanding of possible κ-subtypes.

The present study has therefore compared four agonists namely ethylketocyclazocine, U-69593, ICI 204448 and dynorphin 1-13 in this system and determined naloxone Ke values for each agonist to try to resolve the apparent anomaly.

Materials and Methods

Isolated tissue preparations were set up for assay and Schild analysis of results performed as outlined in chapter two. Inhibition curves were plotted by eye and subsequently transformed to Schild plots for calculation of Ke values (see chapter three).

Results

The agonist potency of a series of κ-opioid agonists was determined on the guinea-pig ileum longitudinal muscle myenteric-plexus preparation (Table 7.1). Following this the agonist potencies were redetermined after 30 minutes preincubation of the antagonist naloxone.

Figures 7.1-7.4 show the mean Schild plots calculated for the antagonism by naloxone of U-69593, ICI 204448, dynorphin (1-13) and ethylketocyclazocine (EKC) respectively. The Ke values and slopes obtained from the plots are given in Table 7.1. There is no significant deviation from unity for any of the Schild slopes (t-test, $P<0.005$), and with the exception of dynorphin (1-13) the Ke values are similar. To check if the naloxone

was reaching equilibrium the assay was repeated for ICI 204448 using a 10 minute preincubation of the antagonist. The Ke value for naloxone versus ICI 204448 obtained after 10 minutes (16.4± 2.9nM, n=5) and 30 minutes (13.3± 1.6nM, n=4) do not significantly differ (t test, P<0.005).

Table 7.1 Schild Analysis of k-agonists.

Compound	IC_{50} (nM)	naloxone Ke/nM	slope	n
Dynorphin 1-13	2.71± 0.7	34.3± 2.9	0.99± 0.03	4
U69593	6.47± 1.6	13.7± 0.5	1.04± 0.02	4
ICI204448	0.68± 0.1	13.3± 1.6	0.99± 0.02	4
EKC	1.39	12.1	0.93	2

Unless otherwise indicated values represent mean± sem from determinations using tissues from at least three separate animals. Schild analysis was performed using 100nM, 300nM and 1000nM concentrations of naloxone, incubated for 30 minutes prior to addition of agonist.

No Schild slope significantly less than unity ($P<0.05$) as measured by Student's t-test.

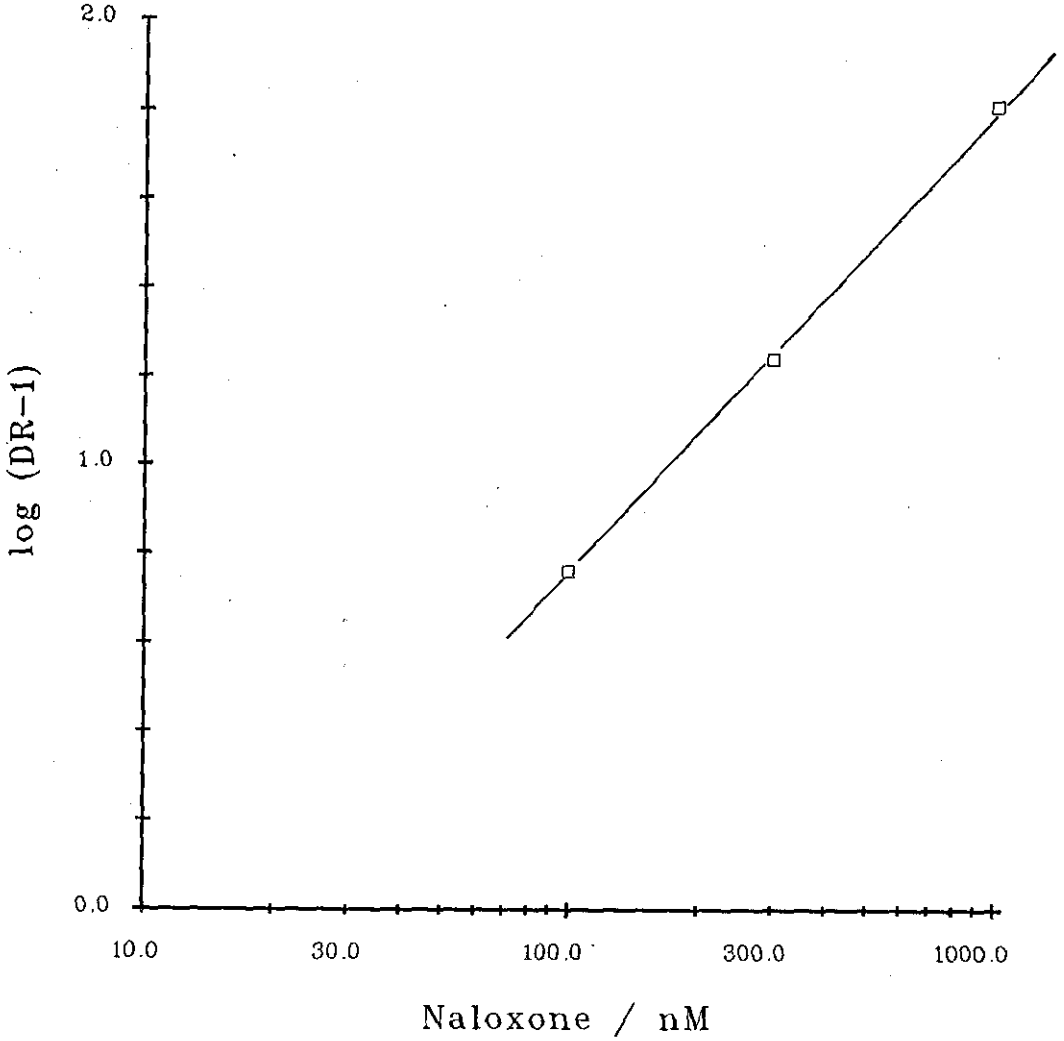

Figure 7.1: Schild plot representing the antagonism of U-69593 by naloxone in guinea-pig ileum myenteric plexus longitudinal muscle.

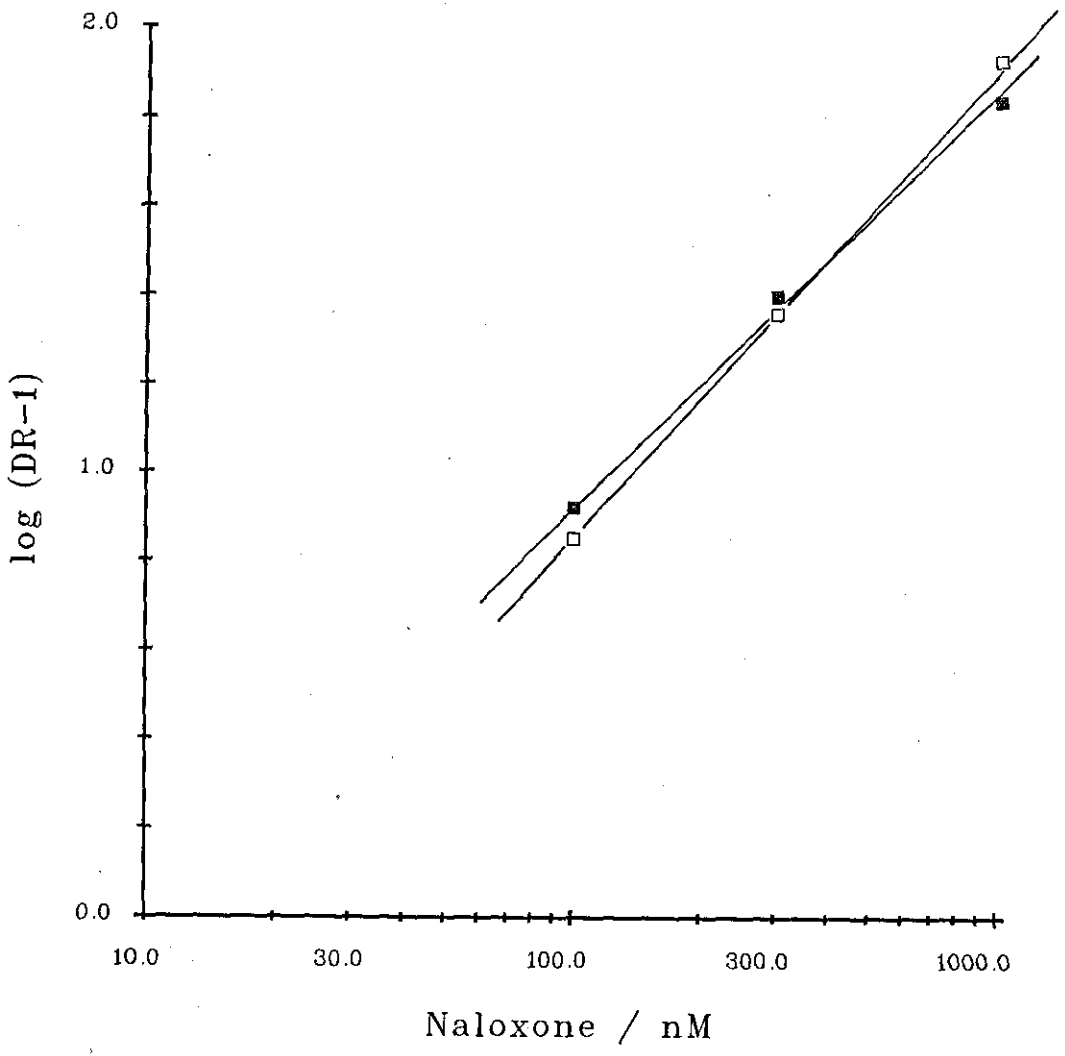

Figure 7.2: Schild plot representing the antagonism of ICI204448 by naloxone after 30 minutes (closed symbols) and 10 minutes (open symbols) in guinea-pig ileum myenteric plexus longitudinal muscle.

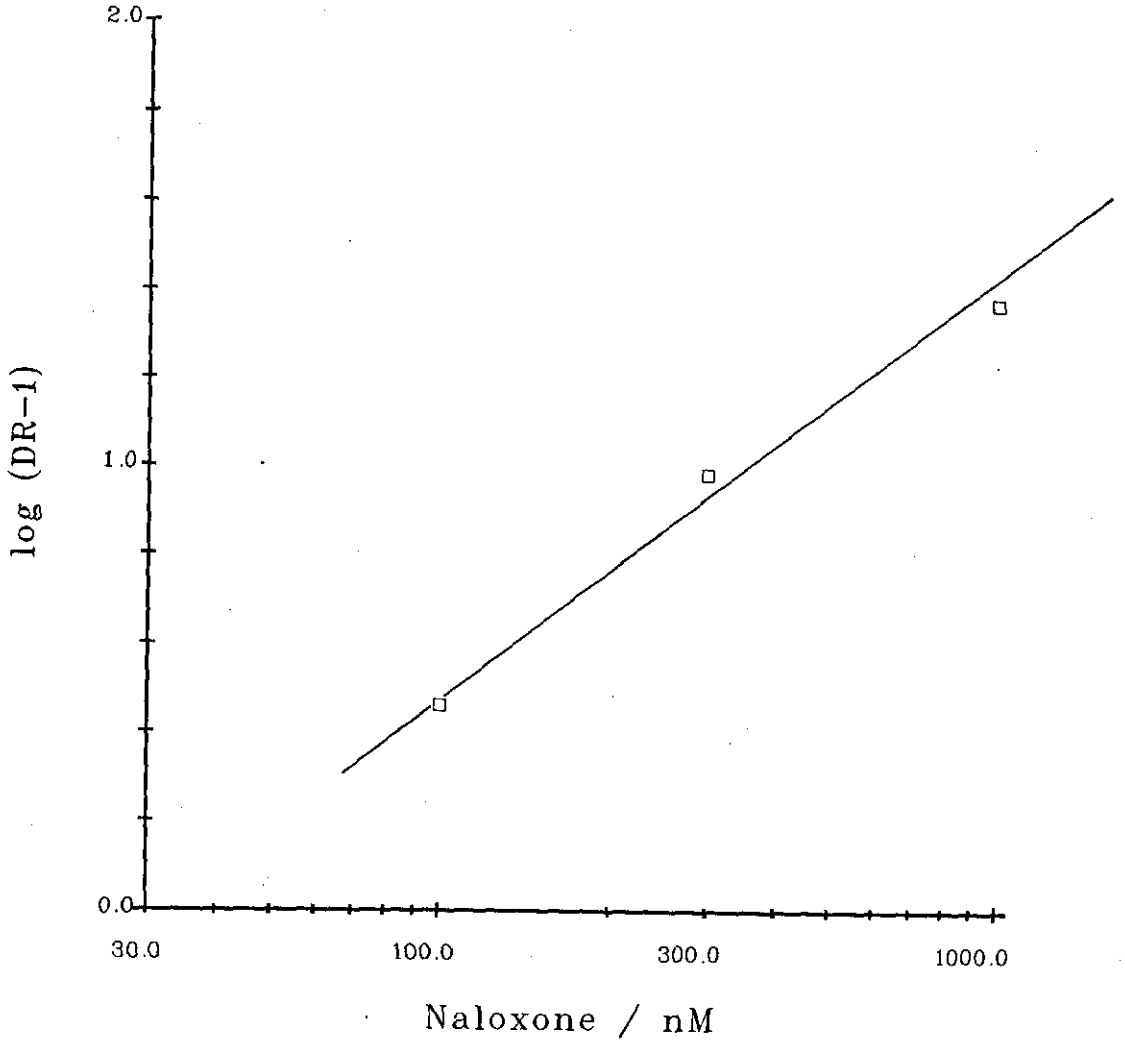

Figure 7.3: Schild plot representing the antagonism of dynorphin A(1–13) by naloxone in guinea–pig ileum myenteric plexus longitudinal muscle.

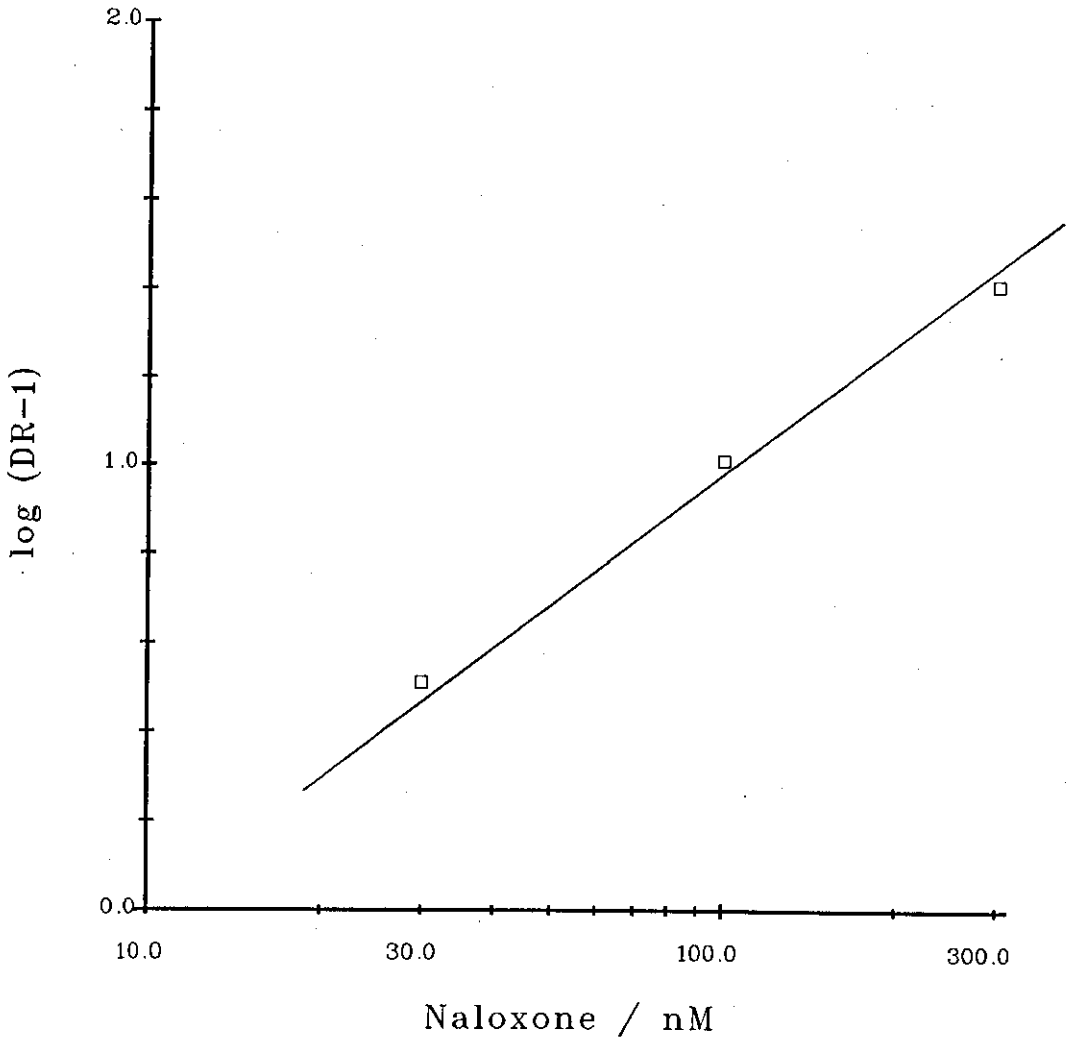

Figure 7.4: Schild plot representing the antagonism of ethylketocyclazocine (EKC) by naloxone in guinea-pig ileum myenteric plexus longitudinal muscle.

Discussion

As expected all of the compounds acted as potent agonists in the guinea-pig ileum, in agreement with previous reports (29, 74).Fundamental to the theory behind the bioassays is the fact that the Ke for an antagonist acting at a particular receptor does not vary on varying agonist at that receptor (109), since it is a function of the antagonist not the agonist. Bearing this in mind the results presented suggest that in the tissues studied dynorphin A(1-13) is acting at a different receptor than EKC, U-69593 and ICI 204448. This could imply the presence of an endogenous peptide receptor, receptor subtypes or subsites on the κ-receptor.

However, in guinea-pig ileum, dynorphin 1-13 and 1-17 exhibit extremely high potency acting as agonists at the κ-receptor (29, 147). The Ke obtained of 34.3±2.9nM for the antagonism of dynorphin 1-13 by naloxone compares favourably with previous reports by Goldstein and coworkers (29). The agonist ICI 204448 has been claimed to afford a similar Ke value for naloxone antagonism (119), however in this study a Ke of 13.3± 1.6nM was obtained, with a Schild slope of 0.99±0.02. This value was unaltered when the assay was repeated with a 10 minute naloxone incubation, ruling out the possibility of non-equilibration of the antagonist. Both EKC and U-69593 gave similar results, and other κ-agonists such as U-50488H and PD117302 have been shown to be antagonised by naloxone affording Ke values in this region (74).

Kenakin (151) has described situations where anomalous Ke values can be obtained from apparently sound assays. For example in a study of β-adrenoceptors on isolated guinea-pig ileum and trachea it was shown that non-equilibration of the antagonist can, upon Schild analysis yield a slope

of unity, although an incorrect estimate of antagonist potency is obtained. This results in misleading indications of receptor heterogeneity. However, in the present study this situation does not apply since the same concentrations and incubation times of antagonist were used throughout.

Although the difference in Ke for dynorphin (1–13) is not great it does appear to be a consistent finding and perhaps does suggest that dynorphin (1–13) is acting differently to the other κ–ligands. However it is notable that the difference is seen only with dynorphin (1–13), resulting in a Ke value for naloxone more in line with that measured at δ–receptors. A problem with this ligand is metabolism to [Leu^5]enkephalin (158). This however is not important in these experiments since [Leu^5]enkephalin would be expected to interact with μ–receptors in this tissue, for which naloxone has an affinity of 1–2nM (107).

There are reports that dynorphins may act differently from other κ–agonists. Thus, studies on the mechanism of spinal analgesia have shown dynorphin 1–13 to have a different profile compared to U–50488H, suggesting action through different receptors (144). These conclusions were made on observation of a major problem with dynorphin 1–13, that is on intrathecal administration the peptide induces severe motor dysfunction characterised by hind–limb paralysis. However this effect cannot be reversed by naloxone suggesting a lack of involvement of opiate receptors. Furthermore, at doses below those which produce motor dysfunction, dynorphin 1–13 is ineffective in behavioural tests of the nociceptive response. Indeed, some investigators have indicated that dynorphin is not interacting with any of the three major opioid receptor types in this system (145).

In binding assays Smith and colleagues (145) report that [^{3}H]dynorphin is only fully displaced from brain membranes by unlabelled dynorphin,

but not by other opioid ligands. From this observation it was postulated that dynorphin may act at another, as yet undefined site. However, this binding could be non-opioid in nature, depending on how the non-specific binding was determined. Further discrepancies have arisen around the binding of dynorphin. Zukin (79) has claimed dynorphin 1-17 to compete for [^{3}H]EKC binding in a different manner to both U-50488H and U-69593. Thus the affinity of dynorphin 1-17 was shown to be the same in rat and guinea-pig brain whereas U-50488H and U-69593 had high affinity in guinea-pig brain but very low affinity in rat brain. In guinea-pig cerebellum a dynorphin resistant site that does not have properties of μ- or δ- sites has been reported in the competition for [^{3}H]EKC and [^{3}H]bremazocine labelled binding (146).

Thus, it is tempting to suggest that the difference observed between dynorphin and the other agonists suggests possible subtypes of the κ-opioid receptor. This is a distinct possibility and the guinea-pig ileum may therefore represent a bioassay distinguishing these subtypes. However, naloxone is a non-selective antagonist and further work must be performed using other antagonists, particularly NorBNI which is highly selective for the opioid κ-receptor (51, 57).

CHAPTER 8: GENERAL CONCLUSIONS

The present study has confirmed early observations about the effects of sodium ions and guanine nucleotides on opioid binding (20). A distinct difference is noticable between agonists and antagonists, namely the attenuation of agonist affinity compared to the lack of effect on, or even potentiation of, antagonist affinity. No similarity between the antagonists that shift in the opposite direction to agonists in the presence of sodium ions and/or guanine nucleotide is reported for other systems including dopaminergic (120), β-adrenergic (121) and α-noradrenergic (122).The closest similarity occurs at benzodiazepine receptors (123), where "inverse" agonists oppose the effect of "true" agonists on the GABA receptor complex. However, these compounds are still agonists since they elicit a response, whereas the action of antagonists is characterised by their inability to cause a response (109). The opioids that shift to higher affinity are all reported to act as pure antagonists in isolated tissue systems and *in vivo* (51, 55, 56, 57, 97, 148). Therefore, a possible explanation of this property of certain opioid antagonists maybe the molecular and stereochemical reasons outlined in chapter four, and may not relate to the actual conditions seen under the true physiological state. However it will be interesting to see if such compounds have some form of intrinsic activity.

The data reported also adds to evidence for the involvement of G proteins with opioid receptors. The early ideas based on the β-adrenergic receptor (98) appear to be applicable to opioid systems. DeLean and colleagues stated that the major effect of adding guanine nucleotides is to destabilise the agonist–receptor–G protein complex, from which both agonist and G protein can dissociate. This reasoning accounted for shallow agonist displacement curves, representing different affinty states of the receptor to which antagonists were insensitive.

Gilman (137) proposed that the interaction between receptor and G protein is driven by the agonist, leading to formation of a high affinity agonist–receptor–G protein complex. This complex is a prerequisite for effector activation which occurs upon binding of the nucleotide. This cycle of events is controlled by the nucleotide which antagonises the receptor–G protein interaction by causing dissociation of both the agonist and also the G protein into its various subunits (see introduction).

In the case of the β–adrenergic receptor the effector has been shown to be adenylyl cyclase (98, 99, 137). Opioid receptors have been demonstrated to be linked to adenylyl cyclase in NG108–15 and 7315C cell–lines (141, 59). Electrophysiological evidence (149) supports the involvement of GTP in coupling between opioid receptors and K^+ ion channels in guinea–pig cortex. However, the mechanisms by which G protein activation is achieved in ion channel–coupled receptors in cortex or adenylyl cyclase–coupled receptors in cell cultures cannot be distinguished on the basis of effects of nucleotides on agonist binding affinity.

Using the models proposed by DeLean (98) and Gilman (99), many investigators have invoked the existence of multiple affinity states of opioid receptors, in terms of different receptor–G protien–nucleotide complexes (59, 100, 141). Opioid agonist effects are believed to be mediated via receptor–G protein interactions (59). The high agonist affinity state is seen with either a coupling of the receptor and G protein (nucleotide dissociated) (137), or by allowing an action of a precoupled G protein on the receptor–ligand complex (138). The low affinity state on this basis would represent a situation where the receptor and G protein are uncoupled, implying that the G protein is associated to nucleotide. It is known that receptor and G protein can interact in the absence of agonist but the presence of an agonist greatly facilitates this interaction, and guanine nucleotides antagonise this process (137). Spain and Coscia (100) have suggested at δ–sites, on the

basis of guanine nucleotide effects on agonist dissociation rate, that GTP may act at more than one regulatory site to influence agonist–receptor–G protein interactions. Thus, it is possible that more than one affinity state may be related to the formation of the agonist–receptor–G protein–nucleotide complex.

The present study supports these notions as detailed in discussion sections, and furthermore, suggests that previous claims of the existence of receptor subtypes (50, 62, 74, 79, 117, 142, 143) can be explained on the basis of such affinity states. This is particularly relevant in the case of the controversy surrounding the possible existence of κ–subtypes. The observation that [^{3}H]diprenorphine in the presence of CTOP, naltrindole and (+)SKF10,047 affords the same Bmax as [^{3}H]U–69593 in guinea–pig brain, suggests that κ–opioid subtypes do not exist in these animals, but that different affinity states may exist. This implication highlights the difference between the use of agonists and antagonists for suppressing unwanted binding. It is distinctly possible that previous investigators using agonists to suppress μ– and δ–binding (79, 117, 143) have not accounted for the fact that μ– and δ–sites may be present in low agonist affinity conformations. These low affinity sites would not be occluded by agonists and show up in subsequent assays possibly as subtypes. However such sites would be suppressed by antagonists that bind well to low agonist affinity states. Furthermore, this may mean that data generated on binding site numbers using agonists such as DAGOL only refers to high agonist affinity states and may not represent the total receptor number. Problems also arise when correlating a binding site to a physiologically relevant receptor. The findings of Carroll (58) suggest the physiological μ–receptor is of low agonist affinity. However, the receptor is unlikely to be a totally uncoupled form of the G protein and most likely correlates to an intermediate state as shown on the scheme in figure 8.1.

Figure 8.1: Extension of the DeLean model (98), allowing for a range of agonist affinity states. Taken from Werling et al. (59).

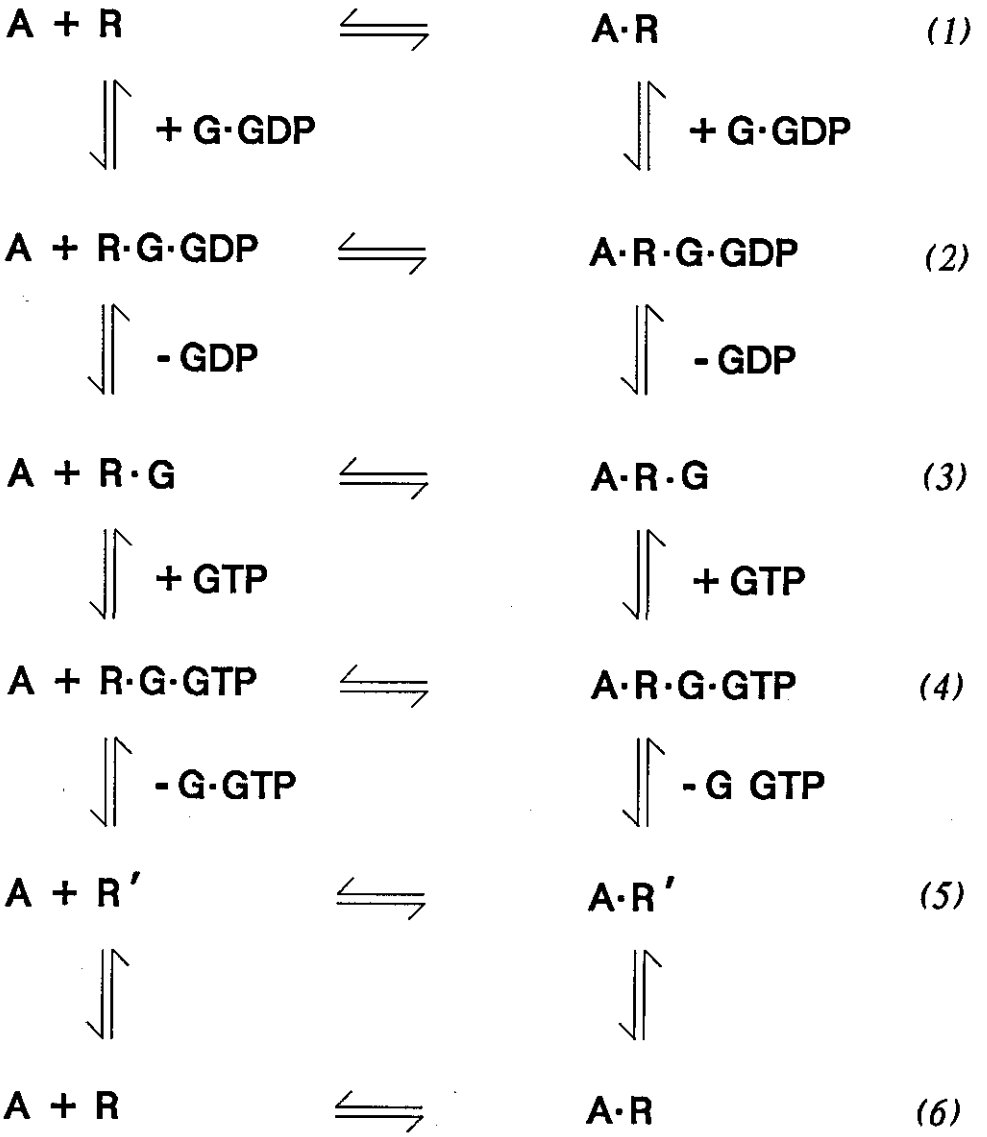

Despite these findings, the possibilty of κ-receptor heterogeneity cannot be discounted since evidence from functional studies exists. Thus the isolated tissue data presented suggests that in the guinea-pig ileum myenteric plexus dynorphin 1-13 may be acting at a different receptor to synthetic κ-agonists such as U-69593, EKC and ICI 204448. To determine if this is

in fact the case, studies using the selective antagonists, particularly norbinaltorphimine (57) are necessary. Work in this laboratory has found dynorphin 1–8 (in the presence of enzyme inhibitors) and U–69593 to be antagonised by NorBNI affording similar Ke values, although in this instance they showed no difference upon antagonism by naloxone. Thus, a definite conclusion cannot be made regarding differences between peptide and non–peptide κ– agonists based on the results of this study.

In summary, the research performed has provided binding profiles of a number of selective opioid antagonists and used these compounds to probe the nature of opioid binding sites. Continued use of such antagonists should enable a better understanding of opioid receptor systems to be achieved, and perhaps answer some fundamental questions such as the existence or otherwise of opioid receptor subtypes. Furthermore visualisation of the distribution of opioid receptors will be greatly aided by compounds which can recognise all affinity states.

REFERENCES.

1. McCawley E.L., Hart E.R. and Marsh D.F., *J. Amer. Chem. Soc.*, *63*, 314, **1941.**
2. Blumberg H., Dayton H.B., George M. and Rapaport D.N., *Fed. Proc.*, *20*, 311, **1961.**
3. Hart E.R., *J. Pharmacol. Exp. Ther.*, *72*, 19, **1941.**
4. Foldes F.F., Lunn J.N., Moore J. and Brown I.M., *Amer. J. Med. Sci.*, *245*, 25–30, **1963.**
5. Lasagna L. and Beecher H.K., *J. Pharmacol. Exp. Ther.*, *112*, 356–363, **1954.**
6. Martin W.R., *Pharmacol. Rev.*, *19*, 463–521, **1967.**
7. Portoghese P.S., *J. Med. Chem.*, *8*, 609–616, **1965.**
8. Beckett A.H. and Casy A.F., *J. Pharm. Pharmacol.*, *6*, 986–1001, **1954.**
9. Martin W.R., Eades C.G., Thompson J.A., Huppler R.E. and Gilbert P.E., *J. Pharmacol. Exp. Ther.*, *197*, 517–532, **1976.**
10. Martin W.R., Bell J.A., Gilbert P.E., Sloan J.W. and Thompson J.A., *NIDA Res. Monogr. Sept.*, 27–30, **1976.**
11. Gilbert P.E. and Martin W.R., *Drug Alcohol Depend.*, *1*, 373–376, **1976.**
12. Gilbert P.E. and Martin W.R., *J. Pharmacol. Exp. Ther.*, *198*, 66–82, **1976.**
13. Hutchinson M., Kosterlitz H.W., Leslie F.M., Waterfield A.A. and Terenius L., *Br. J. Pharmacol.*, *55*, 541–546, **1975.**
14. Goldstein A., Lowney L.I. and Pal B.K., *Proc. Natl. Acad. Sci.*, *68*, 1742–1747, **1971.**
15. Simon E.J., Hiller J.M. and Edelman I., *Proc. Natl. Acad. Sci.*, *70*, 1947–1949, **1973.**
16. Pert C.B. and Snyder S.H., *Proc. Natl. Acad. Sci.*, *70*, 2243–2247, **1973.**

17. Pert C.B., and Snyder S.H., *Science, 179*, 1011–1014, **1973.**
18. Wong D.T. and Horng J.S., *Life Sci., 13*, 1543–1553, **1973.**
19. Terenius L., *Acta Pharmacol. Toxicol., 37*, 211–221, **1975.**
20. Pert C.B., Pasternak G.W. and Snyder S.H., *Science, 182*, 1359–1361, **1973.**
21. Appelmans N., Carroll J.A., Rance M.J., Simon E.J., Traynor J.R., *Neuropeptides, 7*, 139–143, **1986.**
22. Pert C.B., Snowman A.M. and Snyder S.H., *Brain Res., 70*, 184–188, **1974.**
23. Kosterlitz H.W. and Hughes *J., Life Sci., 17*, 91–96, **1975.**
24. Hughes J., Smith T.W., Kosterlitz H.W., Fothergill L.A., Morgan B.A. and Morris H.R., *Nature, 258*, 577–579, **1975.**
25. Bradbury A.F., Smyth D.G. and Snell C.R., In: *The Peptide Hormones: Molecular and Cellular Aspects, CIBA Found. Symp.* No.41, pp61–75 (Churhill, London **1976**).
26. Bradbury A.F., Smyth D.G., and Snell C.R., In: *Peptides, Chemistry, Structure and Biology, Proc. IV American Peptide Symp.* (Meinhofer J., Ed.), pp 609–615, (Ann Arbor Science Inc., Ann Arbor, **1975**).
27. Bradbury A.F., Smyth D.G., Snell C.R., Birdsall N.J. and Hulme E.C., *Nature, 260*, 793–795, **1976.**
28. Li C.H. and Chung D., *Proc. Natl. Acad. Sci., 73*, 1145–1148, **1976.**
29. Goldstein A., Tachibana S., Lowney L.I., Hunkapillar M. and Hood L., *Proc. Natl. Acad. Sci., 76*, 6666–6671, **1979.**
30. Hughes J., *Br. Med. Bull., 39*, 17–24, **1983.**
31. Smyth D.G., *Br. Med. Bull., 39*, 25–30, **1983.**
32. Hughes J., Neurosci. *Res. Prog. Bull., 13*, 55–58, **1975.**
33. Pert C.B., Bowie D.L., Fong B.T.W. and Chang J-K., In: *Opiates and Endogenous Opioid Peptides* (Kosterlitz H.W., Ed.) pp79–86, (Elsevier/North Holland biomedical Press, **1976**).

34. Kosterlitz H.W., Lord J.A.H., Paterson S.J. and Waterfield A.A., *Br. J. Pharmacol., 68*, 333–342, **1980.**
35. Corbett A.D., Paterson S.J., McKnight A.T., Magnan J. and Kosterlitz H.W., *Nature, 299*, 79–81, **1982.**
36. Lord J.A.H., Waterfield A.A., Hughes J. and Kosterlitz H.W., In: *Opiates and Endogenous Opioid Peptides* (Kosterlitz H.W., Ed.) pp 275–280, (Elsevier/North Holland Biomedical Press, **1976**).
37. Lord J.A.H., Waterfield A.A., Hughes J. and Kosterlitz H.W., *Nature, 267*, 495–499, **1977.**
38. Wuster M., Rubini P. and Schulz R., *Life Sci., 29*, 1219–1227, **1981.**
39. Handa B.K., Lane A.C., Lord J.A.H., Morgan B.A., Rance M.J. and Smith C.F.C., *Eur. J. Pharmacol., 70*, 531–540, **1981.**
40. Kosterlitz H.W. and Paterson S.J., *Br. J. Pharmacol., 73*, proc. suppl. 299P, **1981.**
41. Mosberg H.I., Hurst R., Hruby V.J., Gee K., Yamamura H.I., Galligan J.J. and Burks T.F., *Proc. Natl. Acad. Sci., 80*, 5871–5874, **1983.**
42. Kosterlitz H.W. and Paterson S.J., *Proc. R. Soc. Lond., B210*, 113–122, **1980.**
43. Kosterlitz H.W., Paterson S.J. and Robson L.E., *Br. J. Pharmacol., 73*, 939–949, **1981.**
44. Magnan J., Paterson S.J., Tavani A. and Kosterlitz H.W., *Naunyn–Schmiedeberg's Arch. Pharmacol., 319*, 197–205, **1982.**
45. Gillan M.G.C. and Kosterlitz H.W., *Br. J. Pharmacol., 77*, 461–469, **1982.**
46. Chang J–K., Hazum E. and Cuatrecases P., *Proc. Natl. Acad. Sci., 78*, 4141–4145, **1981.**
47. Hiller J.M. and Simon E.J., *J. Pharmacol. Exp. Ther., 214*, 516–519, **1980.**
48. Piercey M.F., Lahti R.A., Schroder L.A., Einsphar F.J. and Barsuhn C., *Life Sci., 31*, 1197–1200, **1983.**

49. Gillan M.G.C., Jin W-Q, Kosterlitz H.W. and Paterson S.J., *Br. J. Pharmacol.*, 79 proc. suppl., 275P, **1983.**
50. Lahti R.A., Mickelson M.M., McCall J.M. and Von Voigtlander P.F., *Eur. J. Pharmacol., 109*, 281–284, **1985.**
51. Takemori A.E., Begonia H.Y., Naeseth J.S. and Portoghese P.S., *J. Pharmacol. Exp. Ther., 246*, 255–258, **1988.**
52. Hawkins K.N., Knapp R.J., Lui G.K., Gulya K., Kazmierski W., Wan Y–P., Pelton J.P., Hruby V.J. and Yamamura H.I., *J. Pharmacol. Exp. Ther., 248*, 73–80, **1989.**
53. Gulya K., Pelton J.T., Hruby V.J. and Yamamura H.I., *Life Sci., 38*, 2221–2229, **1986.**
54. Schmidhammer H., Burkard W.P., Eggstein–Aeppli L. and Smith C.F.C., *J. Med. Chem., 32*, 418–421, **1989.**
55. Cotton R., Giles M.G., Miller L., Shaw J.S. and Timms D., *Eur. J. Pharmacol., 97*, 331–332, **1984.**
56. Portoghese P.S., Sultana M., Nagase H. and Takemori A.E., *J. Med. Chem., 31*, 281–282, **1988.**
57. Portoghese P.S., Lipowski A.W. and Takemori A.E., *Life Sci., 4*, 1287–1292, **1987.**
58. Carroll J.A., Shaw J.S. and Wickenden A.D., *Br. J. Pharmacol., 94*, 625–631, **1988.**
59. Werling L.L., Puttfarcken P.S. and Cox B.M., *Mol. Pharmacol., 33*, 423–431, **1988.**
60. Passarelli F. and Costa T., *J. Pharmacol. Exp. Ther., 248*, 299–305, **1988.**
61. Pasternak G.W. and Snyder S.H., *Nature, 253*, 563–565, **1975.**
62. Wolozin B.L. and Pasternak G.W., *Proc. Natl. Acad. Sci., 78*, 6181–6185, **1981.**
63. Pasternak G.W. and Hahn E.F., *J. Med. Chem., 23*, 674–676, **1980.**
64. Hahn E.F., Carroll–Buatti M. and Pasternak G.W., *J. Neurosci., 2*, 572–576, **1982.**

65. Pasternak G.W., *Proc. Natl. Acad. Sci., 77*, 3691–3694, **1980.**
66. Hahn E.F. and Pasternak G.W., *Life Sci., 31*, 1385–1388, **1982.**
67. Ling G.S.F. and Pasternak G.W., *Brain Res., 271*, 152–156, **1983.**
68. Ling G.S.F., Spiegel K., Nishimura S. and Pasternak G.W., *Eur. J. Pharmacol., 86*, 487–488, **1983.**
69. Ling G.S.F., Spiegel K., Lockhart S.H. and Pasternak G.W., *J. Pharmacol. Exp. Ther., 232*, 149–155, **1985.**
70. Ling G.S.F., MacLeod J.M., Lee S., Lockhart S.H. and Pasternak G.W., *Science, 226*, 462–464, **1984.**
71. Pfeiffer A., Brantl V., Herz A. and Emrich M.H., *Science, 233*, 774–7776, **1986.**
72. Attali B., Gouarderes C., Mazarguil H., Audigier Y. and Cros J., *Neuropeptides, 3*, 53–64, **1982.**
73. Traynor J.R., Wood M.S., Carroll J.A. and Rance M.J., In: *Progress in Opioid Research* (NIDA Monogr. 75), (Holaday J.W., Law P–Y. and Herz A., Eds.) pp 73–76, US Department of Health and Human Sciences, **1986.**
74. Clarke C.R., Birchmore B., Sharif N.A., Hunter J.C., Hill R.G. and Hughes J., *Br. J. Pharmacol., 93*, 618–626, **1988.**
75. Pfeiffer A., Pasi A., Mehraein P. and Herz A., *Neuropeptides, 2*, 89–97, **1981.**
76. Morre M., Bachy A., Grant B., Bioigegrain R., Arnone M. and Roncucci R., *Life Sci., 33*(1), 179–182, **1983.**
77. Su T–P., *J. Pharmacol. Exp. Ther., 223*, 284–290, **1982.**
78. Morris B.J. and Herz A., *Brain Res. 384*, 362–366, **1986.**
79. Zukin R.S., Eghbali M., Olive D., Unterwald E.M. and Tempel A., *Proc. Natl. Acad. Sci., 85*, 4061–4065, **1988.**
80. Wuster M., Schultz R. and Herz A., *Biochem. Pharmacol., 30*, 1883–1887, **1981.**
81. Tam S.W., *Proc. Natl. Acad. Sci., 80*, 6703–6707, **1983.**

82. Simon E.J., Hiller J.M., Groth J. and Edelman I., *J. Pharmacol. Exp. Ther.*, *192*, 531–537, **1975.**
83. Blume A.J., *Life Sci.*, *22*, 1843–1852, **1978.**
84. Childers S.R. and Snyder S.H., *Life Sci.*, *23*, 759–762, **1979.**
85. Childer S.R. and Snyder S.H., *J. Neurochem.*, *34*, 583–593, **1980.**
86. Blume A.J., *Proc. Natl. Acad. Sci.*, *75*, 1713–1717, **1978.**
87. Pert C.B. and Snyder S.H., *Mol. Pharmacol.*, *10*, 868–879, **1974.**
88. Harden T.K., Meeker R.B. and Martin H.W., *J. Pharmacol. Exp. Ther.*, *227*, 570–577, **1983.**
89. Childers S.R. *J. Pharmacol.* Exp. *Ther.*, *230*, 684–691, **1984.**
90. Mack K.J., Lee M.F. and Wehenmeyer J.A., *Brain Res. Bull.*, *14*, 301–306, **1985.**
91. Gilman A.G., *Trends Neurosci.*, *9*, 460–463, **1986.**
92. Rodbell M., Birnbaumer L., Pohl S.L. and Krans H.M.J., *J. Biol. Chem.*, *246*, 1877–1882, **1971.**
93. Blume A.J., Lichtstein D. and Boone G., *Proc. Natl. Acad. Sci.*, *76*, 5626–5630, **1979.**
94. Rodbell M., *Nature*, *284*, 17–22, **1980.**
95. Katada T., and Ui M., *J. Biol. Chem.*, *257*, 7210–7216, **1982.**
96. Katada T. and Ui M., *Proc. Natl. Acad. Sci.*, *79*, 3129–3133, **1982.**
97. Smith C.F.C., *Life Sci.*, *40*, 267–274, **1987.**
98. DeLean A., Stadel J.M., Lefkowitz R.J., *J. Biol. Chem.*, *255*, 7108–7117, **1980.**
99. Gilman A.G., *Trends Neurosci.*, *9*, 460–461, **1986.**
100. Spain J.W. and Coscia C.J., *J. Biol. Chem.*, *262*, 8948–8951, **1987.**
101. Paton W.D.M. and Zar A.B., *J. Physiol.*, *194*, 13–33, **1968.**
102. Lowry O.H., Rosebrough N.J., Farr A.L. and Randall R.J., *J. Biol. Chem.*, *193*, 265–275, **1951.**
103. Schacterle G.R. and Pollack R.L., *Anal. Biochem.*, *51*, 654–655, **1973.**

104. Scatchard G., *Ann. N. Y. Acad. Sci., 51*, 660–672, **1949.**
105. Munson P.J. and Rodbard D., *Anal. Biochem., 107*, 220–239, **1980**
106. Hill A.V., *J. Physiol., 40*, iv–vii, **1910.**
107. Leslie F.M., *Pharmacol. Rev., 39*, 197–249, **1987.**
108. Cheng Y.–C. and Prusoff W.H., *Biochem. Pharmacol., 22*, 3099–3108, **1973.**
109. Arunlakshana O. and Schild H.O., *Br. J. Pharmacol., 14*, 48–58, **1959.**
110. Robson L.E., Foote R.W., Maurer R. and Kosterlitz H.W., *Neurosci., 12*, 621–627, **1984.**
111. Klee W.A. and Nirenberg M., *Proc. Natl. Acad. Sci., 71*, 3474–3477,**1974.**
112. Traynor J.R., Corbett A.D. and Kosterlitz H.W., *Eur. J. Pharmacol. 137*, 85–89, **1987.**
113. Bloomfield S.S., Mitchell J., Sinkfield A., Cissell G.B. and Barden T.P., *IUPHAR 9th International Congress of Pharmacology, Abst.*, 1737P, **1984.**
114. Nelson E.D., Bloomfield S.S., Barden T.P., Mitchell J., Cissell G.B. and Sinkfield A., *Curr. Ther. Res. Clin. Exp., 41*, 276–289, **1987.**
115. Kent R.S., DeLean A. and Lefkowitz R.J., *Mol. Pharmacol., 17*, 14–23, **1979.**
116. Paterson S.J., Robson L.E. and Kosterlitz H.W., *Br. Med. Bull., 39*, 31–36, **1983.**
117. Wood M.S. and Traynor J.R., *J. Neurochem. 53*, 173–178, **1989.**
118. Frost J.J., Smith A.C. and Wagner Jr. H.N., *Life Sci., 38*, 1597–1606, **1986.**
119. Shaw J.S., Carroll J.A., Alcock P. and Main B.G., Br. *J. Pharmacol., 96*, 986–992, **1989.**
120. Creese I., Prosser T. and Snyder S.H., *Life Sci., 23*, 495–500, **1978.**

121. Lucas M. and Bockaert J., *Mol. Pharmacol., 13*, 314–329, **1977.**
122. U'Prichard D.C. and Snyder S.H., *J. Biol. Chem., 253*, 3444–3452, **1978.**
123. Fryer R.I., Cook. C., Gilman N.W. and Walser A., *Life Sci., 39*, 1947–1957, **1986.**
124. Loew G.H. and Berkowitz D.S., *J. Med. Chem., 22*, 603–607, **1979.**
125. Hutchins C.W., Cooper G.K., Purro S. and Rapoport H., *J. Med. Chem., 24*, 773–777, **1981.**
126. Hutchins H.W. and Rapoport H., *J. Med. Chem., 27*, 521–527, **1984.**
127. Feinberg A.P., Creese I. and Snyder S.H., *Proc. Natl. Acad. Sci., 73*, 4215–4219, **1976.**
128. Tyers M.B., Hayes A.G. and Sheehan M.J., *NIDA Res. Monogr., 75*, 698, **1986.**
129. Oka T., Negishi K., Suda M., Matsumiya T., Inazu T. and Ueki M., *Eur. J. Pharmacol., 73*, 235–236, **1981.**
130. Howes J.F., Villarreal J.E., Harris L.S., Essigmann E.M. and Cowan A., *Drug Alcohol Depend., 14*, 373–380, **1985.**
131. Sheehan M.J., Hayes A.G. and Tyers M.B., *Eur. J.* Pharmacol., *130*, 57–64, **1986.**
132. Corbett A.D., Kosterlitz H.W., McKnight A.T. and Marcoli M., *J. Physiol., 357*, 128P, **1984.**
133. Pfeiffer A. and Herz A., *Biochem. Biophys. Res. Comm., 101*, 38–44, **1981.**
134. Rosenbaum J.S., Holford N.H.G., Richards M.L., Aman R.A. and Sadee W., *Mol. Pharmacol., 25*, 242–248, **1984.**
135. Sadee W., Perry D.C., Rosenbaum J.S. and Herz A., *Eur. J. Pharmacol., 81*, 431–440, **1982.**
136. Kurowski M., Rosenbaum J.S., Perry D.C. and Sadee W., *Brain Res., 249*, 345–352, **1982.**

137. Gilman A.G., *Ann. Rev. Biochem., 56*, 615–649, **1987.**
138. Rodbell M., *Trends Biochem. Sci., 10*, 461–464, **1985.**
139. Kosterlitz H.W., Paterson S.J. and Robson L.E., *J. Receptor Res., 8*, 363–373, **1988.**
140. Vonvoigtlander P.F., Lahti R.A. and Ludens J.H., *J. Pharmacol. Exp.* Ther., *224*, 7–12, **1983.**
141. Law P.Y., Hom D.S. and Loh H.H., *J. Biol. Chem., 260*, 3561–3569, **1985.**
142. Nock B., Rajpara A., O'Connor L.H. and Cicero T.J., Eur. *J. Pharmacol., 154*, 27–34, **1988.**
143. Nock B., Rajpara A., O'Connor L.H. and Cicero T.J., *Life. Sci., 42*, 2403, **1988.**
144. Stevens C.W. and Yaksh T.L., *J. Pharmacol. Exp. Ther., 238*, 833–838, **1986.**
145. Smith A.P. and Lee N.M., *Ann. Rev. Pharmacol. Toxicol., 28*, 123–140, **1988.**
146. Carroll J.A. and Shaw J.S., *Br. J. Pharmacol., 95*, 904P, **1988.**
147. Hurlbut D.E., Evans C.J., Barchas J.D. and Leslie F.M., Eur. *J. Pharmacol., 138*, 359–366, **1987.**
148. Portoghese P.S., Sultana M. and Takemori A.E., Eur. *J. Pharmacol., 146*, 185–186, **1988.**
149. North R.A., Williams J.T., Surprenant A. and Christie M.J., *Proc. Natl. Acad. Sci., 84*, 5487–5491, **1987.**
150. Traynor J.R., Hayes A.G. and Lawrence A.J., *Adv. in the Biosci., 75*, 109–113, **1989.**
151. Kenakin T.P., *Eur. J. Pharmacol., 66*, 295–306, **1980.**
152. Personal communication, Dr. J. Shaw, ICI Pharmaceuticals.
153. Costa T. and Herz A., *Proc. Natl. Acad. Sci., 86*, 7321–7325, **1989.**
154. Kelly P.D., Rance M.J. and Traynor J.R., *Neuropeptides, 2*, 319–324, **1982.**

155. Barnard E.A. and Demoliou-Mason C., *Br. Med. Bull., 39*, 37-45, **1983.**

156. Wood M.S., Rodriguez F.D. and Traynor J.R., *Neuropharmacol., 28*, 1041-1046, **1989.**

157. Cotton R., Kosterlitz H.W., Paterson S.J., Rance M.J. and Traynor J.R., *Br. J. Pharmacol., 84*, 927-932, **1985.**

158. Jones A.K.P., Hume S., Myers R., Manjil L.G. and Cremer J.E. *Br. Opioid Coll., P12*, **1990.**

159. Dixon D.M. and Traynor J.R., *J. Neurochem.*, in press.

160. Iyengar S., Kim H.S. and Wood P.L., *Life Sci., 39*, 637-644, **1986.**

161. Clark J.A., Liu L., Price M., Hersh B., Edelson M. and Pasternak G.W., *J. Pharmacol. Exp. Ther., 251*, 461-468, **1989.**

162. Michne W.F., Lewis R.T., Michalec S.J., Pierson A.K. and Rosenberg F.J., *J. Med. Chem., 22*, 1158, **1979.**

163. Frost J.J., Wagner Jr. H.N., Dannals R.F., Ravert H.T., Links J.M., Wilson A.A., Burns H.D., Wong D.F., McPherson R.W., Rosenbaum A.E., Kuhar M.J. and Snyder S.H., *J. Comp. Asst. Tom., 9*, 231-236, **1985.**

164. Paterson S.J. and Kosterlitz H.W., *Br. Opioid Coll., P23*, **1990.**

165. Wood M.S. and Traynor J.R., *Neuropeptides, 10*, 313-320, **1987.**

All Text and Graphics

Created

By

LAZERGRAFIX

146 Bottleacre Lane

Loughborough

Leicestershire

LE11 1JQ

TEL: (0509) 267679